# Investigation of Preventive Tamoxifen Resistance Mechanisms in the Normal Breast

A thesis submitted to The University of Manchester for the degree of Doctor of Philosophy in the Faculty of Biology, Medicine and Health

**2022**

**Suad A Alghamdi**

**School of Medical Sciences**

## Table of Contents

*List of Figures* ..... *5*

*List of Tables* ..... *9*

*Abbreviation* ..... *10*

*Abstract* ..... *13*

*Declaration* ..... *14*

*Copyright Statement* ..... *15*

*Acknowledgement* ..... *16*

*Dedication* ..... *17*

*1 Introduction* ..... *19*

**1.1 Breast cancer epidemiology** ..... **19**

**1.2 Breast cancer subtypes** ..... **19**

**1.3 The normal human mammary gland** ..... **22**

1.3.1 Human mammary gland structure ..... 22

1.3.2 Cellular composition of the mammary gland ..... 23

1.3.3 Mammary Epithelial cells Hierarchy ..... 25

**1.4 Mammary gland development** ..... **28**

1.4.1 Embryonic development of human mammary gland. ..... 29

1.4.2 Pubertal Mammary Development ..... 30

1.4.3 Development in Pregnancy and Lactation ..... 32

**1.5 Molecular mechanisms of steroid receptor signalling in the normal breast** ..... **33**

1.5.1 Estrogen Receptors ..... 33

1.5.2 Progesterone Receptors ..... 37

**1.6 The regulation of paracrine signalling in normal breast development** **38**

1.6.1 Local paracrine mediator ..... 38

**1.7 Physiology of Menopause** ..... **42**

**1.8 Breast cancer risk factors** ..... **42**

1.8.1 Age and Gender ..... 44

1.8.2 Family history of breast cancer ..... 45

1.8.3 Reproductive History ..... 46

1.8.4 Hormones up-regulation and Hormone Replacement Therapy ..... 48

1.8.5 Mammographic Density ..... 48

**1.9 Breast cancer prevention** ..... **55**

1.9.1 Tamoxifen ..... 56

**1.10 Tissue culture systems** ..... **61**

1.10.1 Cell culture characteristics ..... 62

1.10.2 The use of cell cultures to study breast biology ..... 64

**1.11 Hypotheses and Objectives** ..... **67**

*Chapter 2* ..... *68*

Table of Contents

*2 Materials and Methods ..... 69*

**2.1 Materials ..... 69**

2.1.1 Antibodies ..... 69
2.1.2 List of General Reagents ..... 69
2.1.3 Buffers Formulation ..... 71
2.1.4 Kits ..... 73
2.1.5 Breast Tissue Samples ..... 73

**2.2 Methods ..... 75**

2.2.1 Tissue Processing and *in vitro* Tissue Culture ..... 75
2.2.2 Hydrogel culture system ..... 76
2.2.3 Dissociation of normal human mammary tissue - vacuum-assisted biopsy (VAB) 77
2.2.4 Mammosphere Formation Assay ..... 78
2.2.5 Morphometric analysis ..... 79
2.2.6 Immunohistochemistry (IHC) ..... 80
2.2.7 Analysis of IHC staining by automated HALO™ Image Analysis software ... 82
2.2.8 Gene Expression Analysis ..... 83
2.2.9 Preparation of LCM captured tissue for mass spectrometry ..... 87
2.2.10 Bioinformatics and Statistical Analysis ..... 95

***Chapter 3 ..... 98***

***3 The effects of tamoxifen on breast tissue of women at increased risk of breast cancer. ..... 99***

**3.1 Introduction ..... 99**

**3.2 Results ..... 102**

3.2.1 Breast Biomarkers Chemoprevention trial ..... 102

**FFTP= First full-term pregnancy. OCP= Oral contraceptive pills. FDR= First degree relatives. SDR= Second degree relatives. BiRads= Breast Imaging-Reporting and Data System. Nil= none ..... 103**

3.2.2 Tamoxifen significantly increases serum estradiol levels ..... 104
3.2.3 Ki67 expression is reduced after tamoxifen treatment ..... 105
3.2.4 Tamoxifen treatment reduces intralobular epithelial and acinar areas ..... 108
3.2.5 Tamoxifen treatment reduces both estrogen and progesterone receptor expression ..... 111
3.2.6 Mammosphere forming efficiency was not affected by tamoxifen treatment 115
3.2.7 Participants with higher baseline Mammographic Density show greater proportional reduction with treatment ..... 116

**3.3 Discussion ..... 119**

***Chapter 4 ..... 126***

***4 Investigating Mechanisms of Tamoxifen Resistance in Breast Cancer Preventive Therapy Using Genomic and Proteomic Analyses. ..... 127***

**4.1 Introduction ..... 127**

**4.2 Results ..... 129**

4.2.1 Unsupervised transcriptomic analysis ..... 129
4.2.2 Identification of differentially expressed genes in women receiving tamoxifen treatment. ..... 131

4.2.3 Tamoxifen treatment modulation of luminal hormone receptor positive cell gene expression. ..... 136
4.2.4 Tamoxifen mediated expression of proliferation associated genes..... 141
4.2.5 Tamoxifen effects on ER and PR protein and related gene expression..... 146
4.2.6 Proteomic analysis of breast lobules reveals differences between RG1 and RG2. 148
4.2.7 Potential biomarkers associated with poor response to tamoxifen ..... 154
4.2.8 Functional protein associated networks modified by tamoxifen therapy ..... 157

**4.3 Discussion ..... 161**

***Chapter 5 ..... 169***

***5 Can In vitro Tissue Culture Systems Replicate In vivo Response to Tamoxifen? ..... 170***

**5.1 Introduction ..... 170**

**5.2 Results ..... 173**
5.2.1 Morphometric analysis ..... 173
5.2.2 Proliferation assessment of *in vitro* tissue culture of normal breast tissue samples 177
5.2.3 Estrogen receptor expression of normal breast tissue cultured *in vitro*..... 179
5.2.4 PR expression of *in vitro* tissue culture of normal breast tissue slices..... 181
5.2.5 Gene Expression of normal breast tissue samples cultured *in vitro*..... 183
5.2.6 Hydrogel culture system..... 189

**5.3 Discussion ..... 193**

***Chapter 6 ..... 202***

***6 Discussion and Future Directions ..... 203***

**Final Word Count: 34,014**

## List of Figures

Figure 1.1 Schematic representation of the anatomy of female human breast……..……22

Figure 1.2 Schematic representation of different cell types of mammary gland microenvironment…….…..…24

Figure 1.3 Putative map of mammary epithelial cell differentiation hierarchy…….…..…25

Figure 1.4 Hormone regulation during the menstrual cycle…….……....31

Figure 1.5 The three-dimensional structure of the estrogen receptor-α LBD…….……34

Figure 1.6 Genomic signalling activity of ERα…….……35

Figure 1.7 An illustration of coregulators selective recruitment mechanism that regulate tamoxifen activity…….……36

Figure 1.8 An illustrated view of paracrine interactions in mammary development…..……39

Figure 1.9 Most common risk factors for development of breast cancer…….……..43

Figure 1.10 Age-specific incidence rate for female breast cancer…….……45

Figure 1.11 Reproductive cycle and breast cancer risk…….……47

Figure 1.12 Biological differences in breast tissue composition with high mammographic density (HMD) and low mammographic density (LMD).…….……52

Figure 1.13 The forest plot demonstrates the effects of tamoxifen on breast cancers…..……58

Figure 1.14 The 3D conformational structure of Erα is altered differently by estrogen and tamoxifen…….……60

Figure 2.1 Image analysis of normal breast tissue……80

Figure 2.2 Quantification of epithelial cells was performed using HALOTM Image Analysis software (v3.2.1851)……...83

Figure 2.3 Illustration of good and bad RNA quality samples using the 2100 Bioanalyzer….86

Figure 2.4: A diagram of samples preparation and computational analysis of LCM-MS data for peptides Identification……88

Figure 2.5 Laser captured micro-dissected tissue ……...89

Figure 3.1 The study design of breast cancer prevention trial BBCP……102

Figure 3.2 Serum hormones level in premenopausal women at baseline and after 3 months TAM treatment……..……105

List of Figures

Figure 3.3 The percentage of Ki67 positive cells and representative images of nuclear staining in normal breast tissue…….107

Figure 3.4 Tissue morphology in normal breast biopsies of women before and after receiving tamoxifen treatment……..……109

Figure 3.5 Acini average area and numbers in normal breast biopsies of women after receiving tamoxifen treatment…….……110

Figure 3.6 The percentage of ER positive cells and representative images of nuclear staining in normal breast tissue……..……...113

Figure 3.7 The percentage of PR positive cells and representative images of nuclear staining in normal breast tissue……..……...115

Figure 3.8 Mammosphere forming efficiency of normal breast biopsies of women after receiving tamoxifen treatment……..……...116

Figure 3.9 Breast density change at the baseline and one year follow-up after receiving tamoxifen treatment…….…118

Figure 4.1 The unsupervised analysis of the normal breast biopsies shows the changes in post-treatment versus baseline in gene expression in women who received preventive TAM therapy for 12 weeks……..…….130

Figure 4.2 Heatmap displaying the 54 differentially expressed genes……..……132

Figure 4.3 Principal component analysis (PCA) shows samples cluster according to their response to TAM treatment…….……135

Figure 4.4 Heatmap displaying the gene set signature associated with mammary epithelial cells…….…137

Figure 4.5 Heatmap displaying the gene set signature associated with Luminal hormone positive cells……..138

Figure 4.6 Analysis of pathway enrichment using Gene Ontology……..……..140

Figure 4.7 Heatmap displaying the gene set signature associated with proliferation…..…..141

Figure 4.8 Ki67 protein and *MIK67* gene as biomarkers for TAM response in premenopausal women……143

Figure 4.9 Scatter plots showing the correlation between Ki67 protein, *MKI67* gene expression and acinar area after 12 weeks of tamoxifen treatment……..145

List of Figures

Figure 4.10 Waterfall and scatter plots showing the correlation between change in protein and gene expression of steroid receptors with TAM treatment……..147

Figure 4.11 Differentially expressed proteins in the lobular compartment of RG1 samples after TAM treatment……..……151

Figure 4.12 Differentially expressed proteins in the lobular compartment of RG1 samples after TAM treatment……..……155

Figure 4.13 Functional protein association networks within breast lobules in RG1……..…..157

Figure 4.14 Functional protein association networks within breast lobules in RG2……....158

Figure 4.15 Differentially regulated pathways in the different responsive groups as predicted by IPA approach……160

Figure 5.1 Illustration of 3D tissue culture systems…….……174

Figure 5.2 Quantification of the mean acini area of normal breast tissues from healthy women cultured *in vitro* for 3 weeks……176

Figure 5.3 The percentage of Ki67 positive cells and nuclear staining in normal breast tissue in three different culture conditions with different serum constituents at Day 0, 7, 14, and 21 days, respectively……..……..178

Figure 5.4 The percentage of ER positive cells and nuclear staining of normal breast tissue slices cultured in three different culture conditions with different serum constituents at Day 0, 7, 14, and 21 days……..……..180

Figure 5.5 The percentage of PR positive cells and nuclear staining of normal breast tissue cultured in 3 different culture conditions with different serum constituents at Day 0, 7, 14, and 21 days…….……..182

Figure 5.6 Heatmap of the top 150 significant differentially expressed genes in patients' samples cultured *in vitro* at D0 and week1……...184

Figure 5.7 Principal component analysis…….188

Figure 5.8 Quantification of the mean average of acini area of normal breast tissues from healthy women cultured *in vitro* for 7 days using hydrogel culture system…….190

Figure 5.9 Fold change of Ki67 positive cells in normal breast tissue slices cultured in the hydrogel with FBS and B27 constituents at D0, 3, 7, and 14 days……..191

List of Figures

Figure 5.10 Fold change of cells positive for ER and PR expression in normal breast tissue slices cultured in the hydrogel with FBS and B27 constituents at D0, 3, 7, and 14 days, respectively……....192

## List of Tables

Table 1.1 BiRADS Atlas 5th edition. Categories for mammographic density……49

Table 2.1 Primary antibodies used in IHC……69

Table 2.2 List of reagents, suppliers and catalogue numbers……69

Table 2.3 LCM-MS buffer formulation……71

Table 2.4 BenchMark Ultra Medical System bulk reagents……72

Table 2.5 General kits……73

Table 2.6 Patient characteristics……74

Table 3.1 BBCP participant characteristics……103

Table 4.1 Down-regulated genes identified in the normal breast tissue of pairs of samples from 10 women who received TAM treatment……133

Table 4.2 .Up-regulated genes identified in the normal breast tissue of pairs of samples from 10 women who received TAM treatment……133

Table 4.3 Pathway enrichment analysis for differentially expressed genes in Response Group 1 after TAM treatment……139

Table 4.4 Up-regulated proteins identified in the lobular compartment of pairs of samples from 6 participants……149

Table 4.5 Down-regulated proteins identified in the lobular compartment of pairs of samples from 6 participants……149

Table 4.6 Up-regulated proteins identified in the lobular compartment of pairs of samples from participants included in RG1……152

Table 4.7 Down-regulated proteins identified in the lobular compartment of pairs of samples from participants included in RG1……153

Table 4.8 Up-regulated proteins identified in the lobular compartment of pairs of samples from participants included in RG2……156

Table 4.7 Down-regulated proteins identified in the lobular compartment of pairs of samples from participants included in RG2……156

Table 5.1 Pathway enrichment analysis for differentially expressed genes in patients' samples cultured *in vitro* at D0 and week 1……186

## Abbreviation

| | |
|---|---|
| **2D** | Two dimensional |
| **3D** | Three dimensional |
| **AF-1** | Amino-terminal activation function-1 |
| **Ais** | Aromatase inhibitors |
| **AKT** | Ak strain transforming |
| **AR** | Androgen receptor |
| **AREG** | Amphiregulin |
| **ATCC** | American Type Culture Collection |
| **BC** | Breast Cancer |
| **BiRADS** | Breast Imaging Reporting and Data System |
| **BM** | Basement membrane |
| **BRCA1** | Breast cancer gene 1 |
| **BRCA2** | Breast cancer gene 2 |
| **BSA** | Bovine serum albumin |
| **CXCL-12** | C-X-C motif chemokine ligand 12 |
| **CXCR-4** | C-X-C motif chemokine receptor 4 |
| **DBD** | DNA-binding domain |
| **DNA** | Deoxyribonuclic acid |
| **E2** | Estrogen |
| **ECM** | Extracellular Matrix |
| **EGF** | Epidermal growth factor |
| **EGFR** | Epidermal growth factor receptor |
| **ERα** | Estrogen receptors Alpha |
| **Erβ** | Estrogen receptors beta |
| **ESR1** | Estrogen receptor gene 1 |
| **ESR2** | Estrogen receptor gene 2 |

Abbreviation

| | |
|---|---|
| **FAK** | Focal Adhesion kinase |
| **FDA** | Food and drug administration |
| **FFDM** | Full-field digital mammograms |
| **FFTP** | First-full-term pregnancy |
| **FSH** | Follicle-stimulating hormone |
| **HCP** | Hormone contraceptive pill |
| **HRT** | Hormone replacement therapy |
| **H&E** | Haematoxylin and eosin |
| **HER2** | Human epidermal growth factor receptor2 |
| **HMD** | High mammographic density |
| **HR** | Hormone receptor |
| **IBIS** | International Breast Cancer Intervention Study |
| **ICC** | Intraclass correlation coefficient |
| **Ki67** | The Ki67 nuclear antigen |
| **LBD** | Ligand binding domain |
| **LCIS** | Lobular carcinoma in situ |
| **LCM-MS** | Laser capture microdissection coupled mass spectrometry |
| **LH** | Luteinizing hormone |
| **LMD** | Low mammographic density |
| **MAPK** | Mitogen-activated protein kinase |
| **MaSC** | Mammary stem cell |
| **MCRC** | Manchester Cancer Research Centre |
| **MD** | Mammographic density |
| **MKI67** | Ki67 gene coding |
| **MRI** | Magnetic resonance imaging |
| **OCP** | Oral contraceptive pill |
| **PBS** | Phosphate-buffered saline |
| **PCA** | Principal component analysis |

Abbreviation

| | |
|---|---|
| **PGR** | Progesterone receptor gene |
| **PI3K** | Phosphoinositide 3-kinases |
| **PIF** | Prolactin inhibiting factor |
| **PARA** | Progesterone receptor Alpha |
| **PRB** | Progesterone receptor beta |
| **PRLR** | Prolactin receptor |
| **RANKL** | Receptor activator of nuclear factor kappa-B ligand |
| **RNA** | Ribonucleic Acid |
| **SDS** | Sodium dodecyl sulphate |
| **SEER** | Surveillance, Epidemiology, and End Results |
| **SERDs** | Selective estrogen receptor degraders |
| **SERMs** | Selective estrogen receptor modulators |
| **SNPs** | Single nucleotide polymorphisms |
| **TAM** | Tamoxifen |
| **TDLU** | Terminal duct-lobular unit |
| **TEAB** | Triethylammonium bicarbonate |
| **TEBs** | Terminal end buds |
| **TEMED** | Tetramethylethylenediamine |
| **TGF-α** | Transforming growth factor alpha |
| **TNBC** | Triple negative breast cancer |
| **TNFR** | Tumour necrosis factor receptor |
| **VAS** | Visual Analogue Scale |

## Abstract

**Background:** Breast cancer (BC) is the most common cancer in women worldwide and there is a need for more targeted BC prevention strategies. The selective estrogen receptor modulator tamoxifen (TAM) has been shown to reduce the risk of estrogen receptor (ER) positive but not ER negative BC. Furthermore, TAM does not reduce BC mortality but can induce troublesome side effects. Predictive biomarkers for preventive TAM therapy are required.

**Methods:** A clinical trial was set up in which premenopausal women at increased risk of BC, due to start taking TAM, had a biopsy of one breast in the luteal phase of the menstrual cycle and then a biopsy of the contralateral breast after 3 months of TAM treatment. Biopsy samples were subjected to multiple analytical techniques including immunohistochemistry, RNA sequencing (RNAseq) and Laser Capture Microdissection coupled to Mass Spectrometry (LCM-MS). The principal hypothesis was that examining interpatient variation in response could lead to the development of predictive biomarkers of TAM prevention. We also sought to develop in vitro culture of normal breast tissue that could help to test novel preventive approaches.

**Results:** 12 weeks of TAM treatment significantly reduced the average epithelial proliferation, normal breast acinar area and estrogen and progesterone receptor expression levels in 10 paired samples. However, there was clear interindividual variation in response with some participants showing increases in certain parameters. TAM induced changes in gene expression (RNAseq) in particular in a luminal hormone receptor positive cell signature identified two broad groups of response (RG1 and RG2). RG2 was characterized by an increase in gene expression in a set of estrogen and androgen responsive genes. Similar findings were observed in a subset of these samples subjected to LCM-MS. In vitro culture of intact breast tissue without a supporting matrix revealed massive disruption of gene expression by RNAseq, not previously reported. Encouraging results were obtained with hydrogel culture but more optimization work is required.

**Conclusions:** Alterations in ER and/or AR signaling in response to TAM may define mechanisms of normal tissue resistance to TAM. Further work is ongoing to increase the sample size and to analyse blood from all participants to determine whether circulating biomarkers that correlate with the changes in breast tissue can be identified. Personalised BC prevention may be one step closer.

## Declaration

No portion of the work referred to in this thesis has been submitted in support of an application for another degree or qualification of this or any other university or other institute of learning.

## Copyright Statement

**Acknowledgement**

First and foremost, praise and thanks to Allah, the Almighty, for his support throughout my research work.

Each of my Dissertation Committee members has provided me with extensive personal and professional guidance and taught me a great deal about both scientific research and life in general. I would like to express my deep and sincere gratitude to my research supervisors, Dr. Sacha Howell and Prof. Robert Clarke for their supervision, continuous guidance, un-failing help, unending kindness and cooperation. Dr. Howell has provided me with great support and pieces of advice throughout the laboratory work, kept telling me ‘it is okay to struggle in the lab’, and taught me how I should learn from these mistakes. I will never forget that Prof. Clarke was ‘Big Brother” to every Breast Biology group member and myself and made us more than a family. I would also like to thank Dr. Bruno Simões, my lab supervisor, for helping me since day one, even though he was not one of my supervisory team during my first year.

My deep appreciation and gratitude go to Dr. Robert Pedley, who generously impacted my work and for constantly reminding me that we, as scientists, our work is dedicated to society for helping cure diseases. I am incredibly grateful for what he has offered me. Special thanks to Dr.Hannah Harrison, and Matthew Roberts and my sister, Dalia, for their unconditional help and support in the laboratory. A special thanks for our lab manager, Katherine Spence for creating a great organized working atmosphere.

## Dedication

I want to dedicate this work to all women who agreed to join me in this project and breast cancer patients “fighters” who dream of beating this disease; without their support, we would not accomplish this research work.

This work is also dedicated to my family. My husband, whose love and guidance are with me in whatever I pursue and believed in me even though I was a dependent woman standing behind his back asking for his protection. Most importantly, my three little heroes who went through this journey with me and became little scientists discussed scientific problems with me during dinner time. Finally, I want to thank my parents and siblings for their support, encouragement and prayers throughout my study. They are the ultimate role models.

After all, this work is dedicated to all scientists and healthcare professionals who are carrying these pure goals in life to support and build up a healthy society.

# CHAPTER 1

# General Introduction

# 1 Introduction

## 1.1 Breast cancer epidemiology

Breast cancer (BC) is the most common cancer in women worldwide, with 2.26 million new cases diagnosed per year, (Ferlay et al., 2021; Torre et al., 2016). At least 1 in every 8 UK women will develop breast cancer in their lifetime (Bray et al., 2018). Breast cancer survival rates are improving but it remains the fourth highest cause of female deaths in the UK and the most common of any cause of death in women aged 30-55 (Office of National Statistics, 2018). Despite improvements in mortality there were more than 11,500 breast cancer deaths per year in the UK between 2016-2018, demonstrating the need for more effective approaches in prevention, early detection and treatment of the disease (Cancer Research UK, 2021).

## 1.2 Breast cancer subtypes

Breast cancer tumours arise from the epithelial cells of the breast and can be subdivided into multiple types based on receptor expression or transcriptional profiling. This has important implications for therapy as it allows interventions to be tailored to the tumour subtype. The estrogen receptor (ER) is expressed in approximately 70% of breast cancers (Masood et al., 1992) and is the target of anti-estrogens such as tamoxifen. Currently, drugs such as tamoxifen are recommended in almost all women with ER-expressing early breast cancers to reduce the chance of recurrence and to improve survival rates. The progesterone receptor (PR) is also co-expressed in the majority of ER-positive tumours, (Niemeier et al., 2010). Lack of PR expression in an ER-positive tumour is a poor prognostic factor (Work et al., 2014). Human epidermal

growth factor receptor 2 (HER2) is expressed in approximately 15% of tumours and is also an adverse prognostic factor. However, HER2 is the target of drugs such as trastuzumab (Herceptin) and pertuzumab (Perjeta), which are valuable tools in the treatment of such breast cancers (Work et al., 2014). Tumours that lack ER, PR and HER2 are termed triple negative breast cancers (TNBC). TNBCs have poor prognosis, tending to relapse earlier then ER expressing BC, and treatment is largely limited to chemotherapy in the majority of cases.

At the turn of the century, transcriptional profiling and unsupervised clustering was used to see how breast tumours segregate, (Sorlie et al., 2001). Five subtypes were derived from this approach, namely luminal A, luminal B, basal, HER2-enriched (HER2E) and normal-like. ER is usually expressed by the luminal subtypes, with particularly high expression in luminal A tumours. In contrast, basal tumours usually lack ER and HER2, and approximately 60–90% of basal-like tumours are considered TNBC, (Fan et al., 2006). HER2 protein expression is seen predominantly in luminal B and HER2E subtypes, with luminal B tumours also co-expressing ER.

Importantly, from the perspective of breast cancer prevention, variation in subtype may be related to the cell of origin of the cancer. In order to determine whether this is the case an understanding of normal human breast gland biology is required.

In this chapter, the following will be discussed:

1. Human mammary gland structure, development and maintenance with a particular focus on the impact of steroid hormones during reproductive cycles and menopause.
2. The current understanding of the cancer cell of origin in different types of breast cancers.
3. Breast cancer risk factors, including mammographic density, and how they may promote the incidence of different subtypes of breast cancer.
4. Current preventive therapy focussing on tamoxifen
5. Normal breast culture techniques and whether they accurately reflect *in vivo* breast tissue characteristics and responses to therapy, such that they could be used to screen for novel preventive agents in future studies.

## 1.3 The normal human mammary gland

### 1.3.1 Human mammary gland structure

The primary role of the mammary gland is the production of milk. Milk production occurs in the breast lobules and is excreted through ducts via the nipple, (Figure 1.1). The gland is divided into approximately 12-20 lobular units each supplying one branched duct. Each of these ductal lobes is made up of many more smaller lobules consisting of bi-layered epithelial acini, (Deome et al., 1959). The inner layer is composed of luminal cells while the outer layer is composed of a basal myoepithelial layer. Luminal cells are responsible for milk production while myoepithelial cells are responsible for propelling milk forward to the nipple.

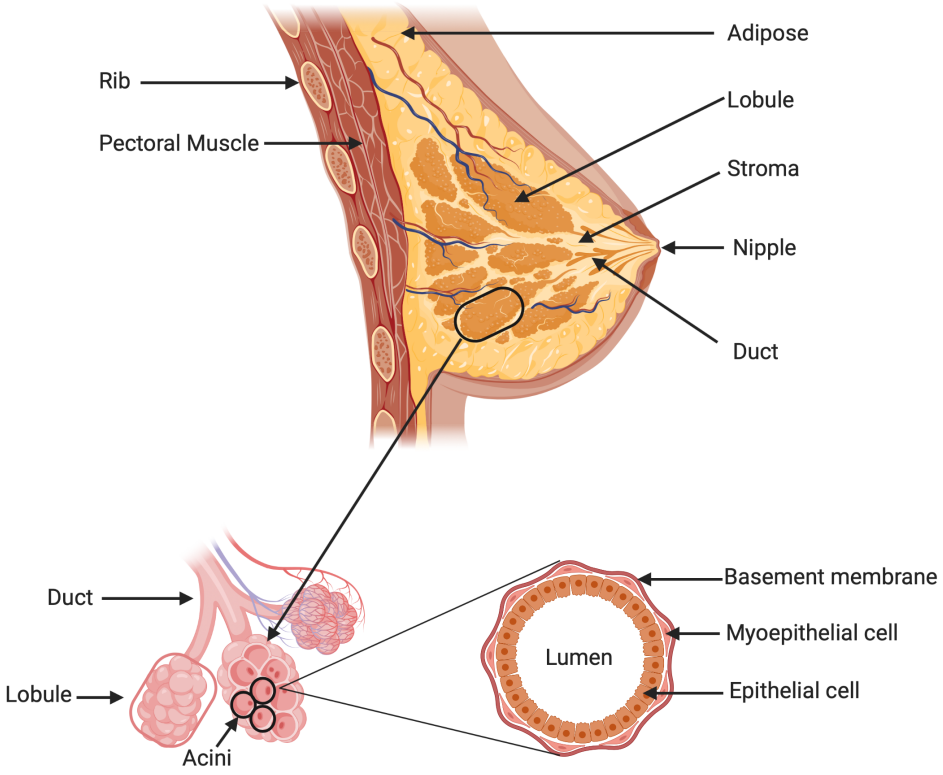


**Figure 1.1 Schematic representation of the anatomy of female human breast.** The general architecture is starting from the acini connected to the nipple through the ducts. The figure also shows the structure of a cross section of an acinus, including luminal cells, myoepithelial cells and the basement membrane. Figure was created with BioRender.com.

Lobules have been divided into four types based on their size and appearance. Type 1 lobules have from 1-15 acini, type 2 from 16-50, and type 3 have more than 50 acini (Boyer et al., 2014; Milanese et al., 2006). Type 4 lobules are characterized based on their development to allow secretions: the acini have lumen swollen with secreted substance. This type of lobule is the most common in the mammary glands when lactation is ongoing, and it is known as a terminally differentiated milk-secreting lobule, (Lyons et al., 2009).

In humans, smaller lobules of types 1 and 2 are the most common before pregnancy. Larger type 3 lobules become the most common in pregnant women before maturing into type 4 lobules during lactation, (Russo et al., 2004). As lobules grow more complex, the area they take up increases. Type 4 lobules have the biggest area when producing and secreting milk, before regressing into type 3 lobules when lactation finishes by a process called involution. The epithelial cells within a lobule are contained within the basement membrane (BM). In contrast to other tissue types in the human body, the breast epithelium retains a unique behaviour since the development does not stop after birth, (Sternlicht et al., 2005). A layer of adipose tissue surrounds the gland and extends throughout the breast.

### 1.3.2 Cellular composition of the mammary gland

In response to distinct hormones and growth factors during puberty, the mammary gland begins to develop, transforming from a simple underdeveloped tree to a branch-like network of epithelial ducts, which are surrounded by various types of stromal cells, (Howlin et al., 2006), (Figure 1.2). The extracellular matrix (ECM) provides structural support and is thought to be

the key regulator of normal homeostasis and tissue phenotype (Lee et al., 2007). ECM contains varied stromal cells, fibrous connective tissues and blood vessels, (Zhu et al., 2013). The vital function of the breast ECM is that it significantly contributes to provide the majority of soluble factors contributing to the epithelial microenvironment.

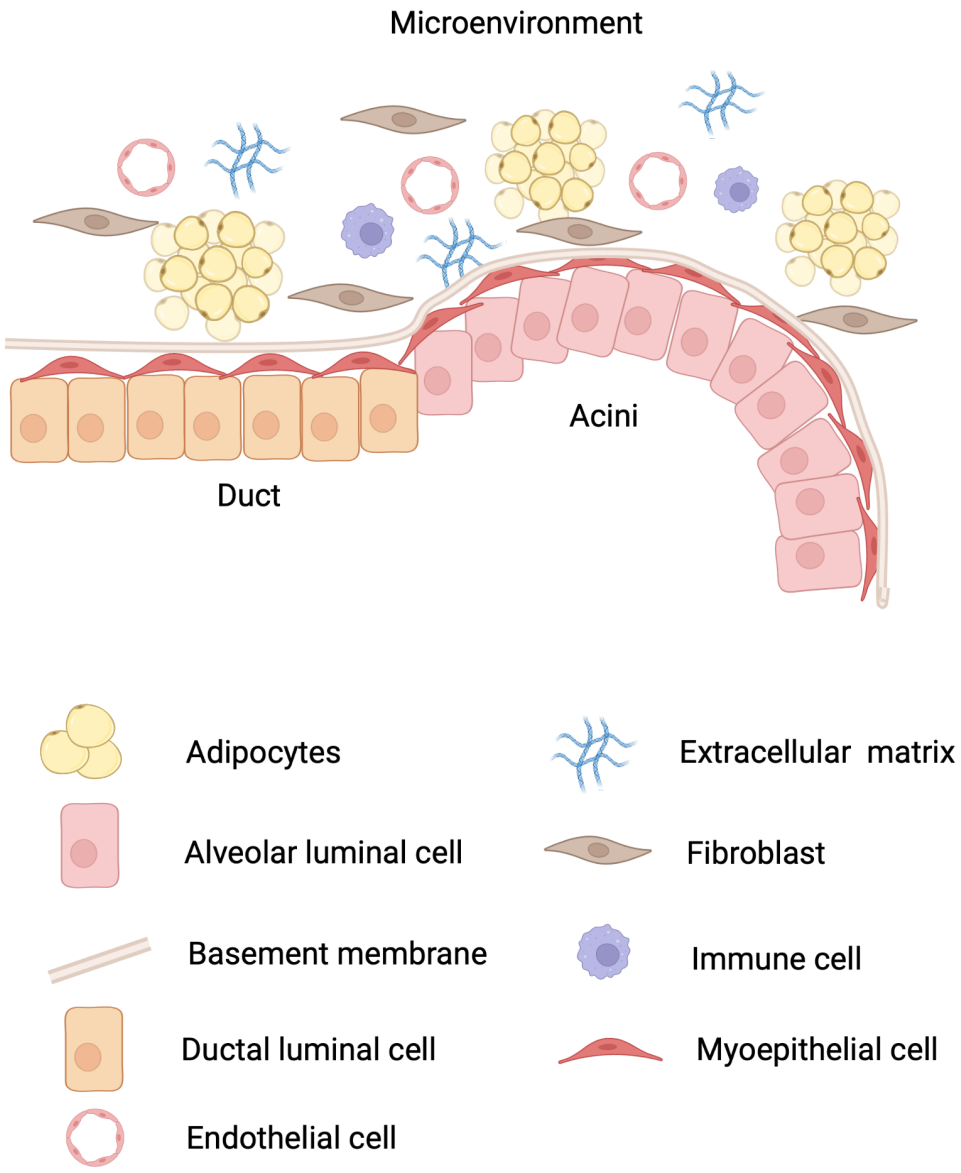


**Figure 1.2 Schematic representation of different cell types of mammary gland microenvironment.** The major cellular composition of the terminal ductal lobular units is separated from stromal compartment by a basement membrane. Figure was created with BioRender.com

### 1.3.3 Mammary Epithelial cells Hierarchy

The profound dynamics of the mammary gland, particularly during reproduction, demonstrate the remarkable ability of the tissue to undergo vast remodeling and regeneration throughout life. These changes are primarily adapted by the activities of distinct populations of adult mammary stem cells (MaSCs) and lineage-restricted progenitor cells, (Visvader et al., 2014).The epithelial cells include the $Krt8^{+}/18^{+}$ luminal cells, which can be further subdivided into hormone-responsive and secretory cell subpopulations based on expression of the hormone receptors estrogen alpha (ERα) and progesterone (PR). The basal myoepithelial cells typically express cytokeratins Krt5 and Krt14, p63 and smooth muscle actin (SMA), (Figure 1.3).

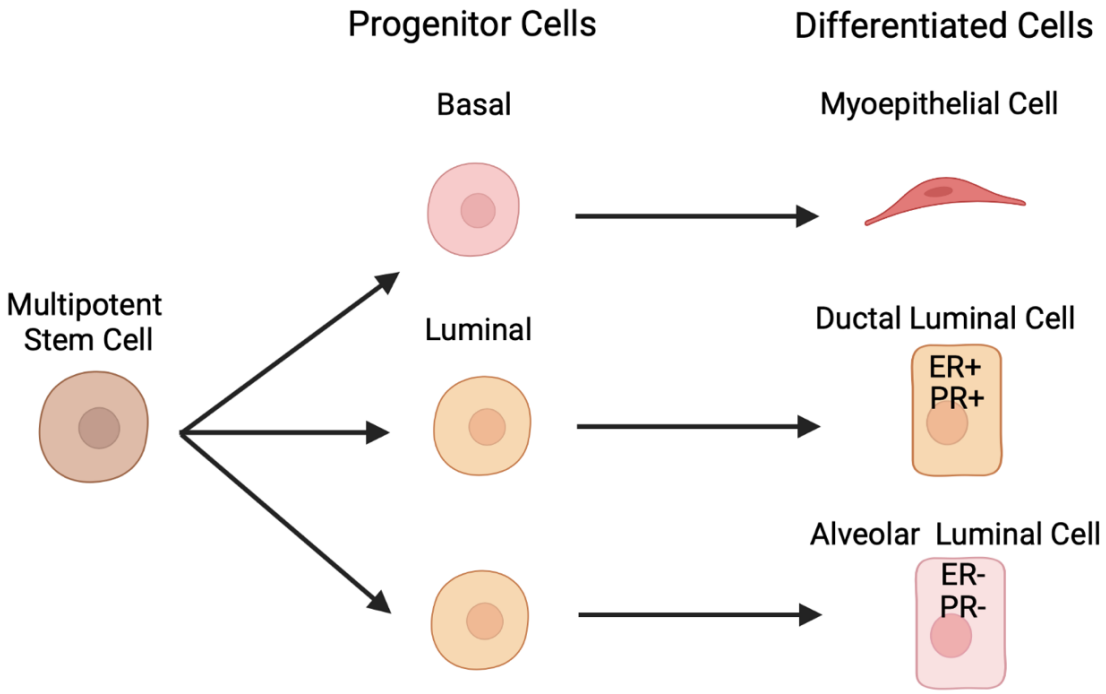


**Figure 1.3 A putative map of mammary epithelial cell differentiation hierarchy.** During development, a multipotent stem cell gives rise to both luminal epithelial and basal progenitor cells which further differentiate into myoepithelial, ductal luminal and alveolar luminal cells. Figure was created with BioRender.com

#### 1.3.3.1 Identification and properties of the luminal mammary lineage

In mice, mammary luminal cells can be enriched and purified based on the positive expression of CD61 (Integrin-β3), which is expressed in luminal progenitors and absent in differentiated cells, (Asselin-Labat et al., 2007). As mentioned previously, the luminal compartment of the mammary gland can be resolved into distinct subpopulations. These include the hormone-responsive ERα$^{+}$ lineages, which express high levels of transcription factors required for ductal morphogenesis, (Bernardo et al., 2010), and ERα$^{-}$ secretory alveolar progenitor cells, which express Integrin-β3 and the transcription factor Elf5, which coordinate the mammary alveolar cell program, (Oakes et al., 2008). Additionally, other markers such as Sca1 and CD49b (Integrin-α2) can also be used to refine the mammary luminal compartment, (Shehata et al., 2012; Sleeman et al., 2007).

In mice, genetic recombination studies have demonstrated the existence of both long- and short-lived luminal progenitor cells that display unipotency *in vivo*. Clonal analyses using two distinct *Krt8* driver mouse models have shown that Krt8$^{+}$ cells contribute to luminal cell maintenance and propagation after consecutive cycles of pregnancy and that luminal cells can be sustained by dedicated long-lived luminal progenitors,(Van Keymeulen et al., 2011; Wuidart et al., 2016). However, while another lineage tracing model examining labelled Elf5$^{+}$ cells (which also expressed Krt8 and Krt18) indicated their considerable contribution to mammary gland morphogenesis, labelled cells were relatively short lived, (Rios et al., 2014).

#### 1.3.3.2 Luminal progenitors as the cancer cells-of-origin

While the genetic mutational landscape plays a key role in shaping the tumor phenotype, there is mounting evidence that different cancers, particularly heterogeneous subtypes, can also be founded from cancer "cells-of-origin". In many cancers, stem cells and progenitors are described as the cell-of-origin, owing to their unique capabilities for long-term self-renewal and susceptibility to genome damage, (Visvader et al., 2011). In breast cancers, expression profiling analyses have indicated that distinct MaSC and progenitor populations correlate with the different breast cancer subtypes, which include luminal A, luminal B, HER2-enriched, and basal-like breast cancers. For example, luminal-type tumors often express luminal-associated genes such as *Krt8, Krt18* and *Krt19,* as well as luminal differentiation genes *CD24*, *ESR1*, *MUC1* and *GATA3*. Similarly, basal-like breast cancers express basal cell expression signatures including *Krt5, Krt14,* p63 and CD49f, (Prat et al., 2011).

Yet, experimental assays that functionally tested the cellular origins of breast cancer indicated that when human mammary luminal cells underwent oncogenic transformation, they could give rise to both $ERα^+$ luminal-like tumors and $ERα^-$ basal-like tumors when transplanted into immunocompromised mice hosts, (Keller et al., 2012). In this regard, it is becoming increasingly clear that mammary luminal cells can serve as the cell-of-origin for basal-like breast cancers. In support of this, the knockdown of BRCA1 or activation of PI3K in luminal cells, but not basal cells, was shown to give rise to basal-like tumors in mice, (Hein et al., 2016; Keymeulen et al., 2015; Koren et al. ,2015;

Molyneux et al., 2010). Interestingly, TNBC patients carrying the *BRCA1* mutation appeared to harbor an expanded pool of luminal progenitor cells, while their gene expression profiles correlated strongly with the luminal progenitor signature, (Lim et al., 2009).

These studies, amongst others, suggest that dedifferentiation or reprogramming of adult cells may reactivate embryonic developmental programs and revert cells back to a primitive multipotent stem cell state, (Breindel et al., 2017; Dhawan et al., 2016; Wang et al., 2016).

## 1.4 Mammary gland development

The human mammary gland serves as a unique and highly specialized organ, which undergoes drastic remodeling at various stages of life including puberty, pregnancy, lactation, and involution. In the new-born breast, there are very primitive structures, composed of ducts ending in short ductules. The main spurt of growth occurs with lobule formation at puberty, but the development and differentiation of the breast are completed only by the end of the first full term pregnancy, (Russo and Russo 2004).

These stages of development are hormones dependent, (Cowin et al., 2010). The mammary gland is unique amongst branching organs in that the majority of branching takes place after birth (during adolescence) rather than before (Sternlicht et al., 2005). The early stage of human mammary gland development is a process initiated during embryonic life which is hormones independent, (Cowin et al., 2010).

### 1.4.1 Embryonic development of human mammary gland.

The human mammary glands begin to develop during the embryonic development from a single epithelial ectodermal bud known as the mammary ridge, (Dabelow 1957). The nipple primordium is shown as a thin cluster of ectodermal cells in 7 to 8 mm embryos and has a single layer of tightly applied mesenchyme cells by 10 mm, (Hughes 1950). By 14 mm, the nipple shifted from a dorsal to ventral position. The mammary epithelium at this stage has proliferated to form a nodule which keep expanding to form breast buds that are completely surrounded in the mesenchyme, (Tobon and Salazar 1975). According to Howard and Gusterson (2000), the buds extend and penetrate the mesenchymal tissue causing remodelling of ducts, (Howard and Gusterson 2000).

Although the development of mammary gland during the embryonic phase is hormone-independent, it does involve regulatory mechanisms. Studies of proteins involved in signalling and extracellular matrix formation have shown a role of these proteins in the development, maturation, and differentiation in the early stage of human breast proliferation. For instance, the basal cells which are positive for keratin 14 and smooth muscle actin have been identified at 28 weeks, (Anbazhagan et al. 1998). These cells have high expression of epidermal growth factor receptors (EGFR) and transforming growth factor alpha (TGF$\alpha$), implying the role of autocrine signalling on proliferation stimulation. The expression of TGF beta, tenascin, and type IV collagen was observed in the extracellular matrix in the developing embryo, (Osin et al. 1998).

### 1.4.2 Pubertal Mammary Development

The mammary gland undergoes lateral branching during the menstrual cycle, (Ramakrishnan et al., 2002). Estrogen is required to activate ER for the development and proliferation in the mammary gland, (Clarke et al., 1997; Petersen et al., 1987). When ER-/- cells were transplanted into inguinal fat pads of ER-/- mice, they were unable to undergo ductal elongation, but when combined with wild-type cells, they participated in ductal elongation, (Feng et al., 2007; Mallepell et al., 2006). Mature epithelial cells that express ER also express PR, (Russo et al., 1999) and estrogen stimulates PR expression in the mature mammary gland (Schultz et al., 2003). Progesterone is required for side-branching and lobuloalveolar development, (Brisken et al., 1998).

#### 1.4.2.1 The menstrual cycle

Puberty is a hormone-dependent stage at which menstrual cycles and ovulation begin. The function of puberty is to develop sexual function including both uterine and breast development to facilitate pregnancy and breast feeding respectively. At this stage, mature mammary gland cells go through a cycle of proliferation and apoptosis during each menstrual cycle due to the circulating hormones, (Figure 1.4). Between days 4 and 14 of the cycle (the follicular stage), the estrogen level rises, stimulating proliferation of the epithelial tissues and higher rates of mitosis, (Hovey et al., 2002). Between days 15 and 28 (the luteal phase), there is a fall in estrogen levels but a rise in progesterone levels. The proliferation of mammary epithelial cells peaks in this phase. ERα expression was reported to be expressed at the lowest level in the luteal phase while PR expression had limited expression throughout the early follicular

phase yet increased throughout the late follicular and luteal stages, (Shaw et al., 2002). Li et al., (2010) have reported that ERα and PR are primarily expressed in the inner layer of acini, (Li et al., 2010).

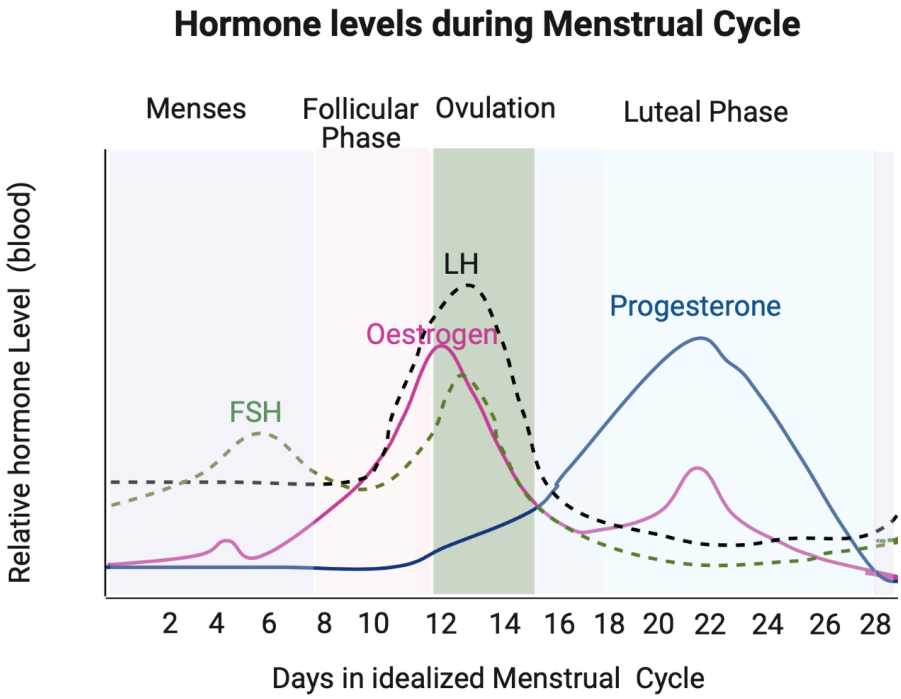


**Figure 1.4 Hormone regulation during the menstrual cycle.** There are three phases of the menstrual cycle. The follicular phase begins at day 8. Estrogen and progesterone hormones are low which trigger the pituitary gland to produce follicle-stimulating hormone. The process of follicle maturation begins in the ovaries and estrogen hormone level increases. Ovulation phase starts around days 12-14. Luteinizing-hormone level increase and stimulate egg release from the follicle. During the Luteal phase, ruptured follicle forms the corpus luteum which produce progesterone. If the egg is not fertilised, the corpus luteum degrades and progesterone hormone levels decreases. (Information adapted from (Mihm et al., 2011). Figure was created with BioRender.com

Further changes occur, including the growth of the existing ducts that branch into secondary ducts. Following puberty, the breast comprises stroma, fat, type I and type II lobules and lactiferous ducts.

Hormonal changes through the menstrual cycle significantly affect the types of lobules seen in the mammary gland. Notably, type I lobules have the highest

level of ER and PR expression, (Russo et al., 1999) and are observed more frequently in the follicular phase of the menstrual cycle. In contrast, type II lobules are observed more frequently in the luteal phase, (Ramakrishnan et al. 2004).

### 1.4.3 Development in Pregnancy and Lactation

During pregnancy, mammary epithelial cells become fully matured and the mammary gland becomes a functional organ. Fibrous stroma is reduced while new acini and lobules are formed. At the early stage of pregnancy, the proliferation of mammary epithelial cells results in duct elongation with a rise in estrogen levels, (Russo et al., 2004). The development of lobules into type 3 lobules, which typically have around 80 acini, along with the sprouting and branching of ducts, is also triggered during the second trimester (Aydiner et al., 2016). With the second trimester comes a rise in progesterone which stimulates side-branching and lobule formation, (Lydon et al., 1995). Progesterone also plays a role in mammary epithelial alveologenesis, (Brisken et al., 2002), a process where acini clusters dilated as a result of the pressure of the fluids generated by the epithelial cells. However, prolactin, a pituitary polypeptide hormone, is the primary regulator of alveologenesis differentiation, (Brisken et al., 2006).

The final trimester sees the completion of the processes of epithelial cell differentiation and secretory cell formation. These cells are responsible for producing and secreting milk proteins. During this phase, elevated levels of prolactin stimulates mammary epithelial morphogenesis, (Brisken et al., 2002), and oxytocin stimulates myoepithelial cells contraction around ducts in order

to push milk onto the nipple-areolar complex, (Britt et al., 2007; Yu et al., 2013). In the breast, prolactin is essential for alveologenesis because it stimulates the proliferation and differentiation of mammary cells. In addition, insulin, EGF and TGF-α play roles in promoting milk composition and mammary gland development, (Brisken et al., 2002; Sternlicht et al., 2005). Taken together, both progesterone and prolactin play a fundamental role in mammary gland maturation, beginning with duct elongation and followed by alveologenesis.

During postpartum, placenta lactogen, estrogen and progesterone levels immediately drop, while prolactin levels rise, causing milk to be both produced and secreted, (Macias et al., 2013).

## 1.5 Molecular mechanisms of steroid receptor signalling in the normal breast

### 1.5.1 Estrogen Receptors

#### 1.5.1.1 Estrogen Receptor Structure

Estrogen receptors (ERs) are a group of ligand-activated nuclear receptors that bind to 17β-oestradiol, Estrone and Estriol, (Figure 1.5). They include ERα and ERβ which are nuclear receptors. GPER (GPR30), ER-X, and Gq-mER are membrane receptors. ERs act mainly as DNA transcription factors, but they also exert some effects independent of DNA binding, (Levin et al., 2005). The two forms of the nuclear ERs, ERα and ERβ, are encoded by two separate genes, *ESR1* and *ESR2* which are found on the sixth and fourteenth chromosomes (6q25.1 and 14q23.2) respectively.

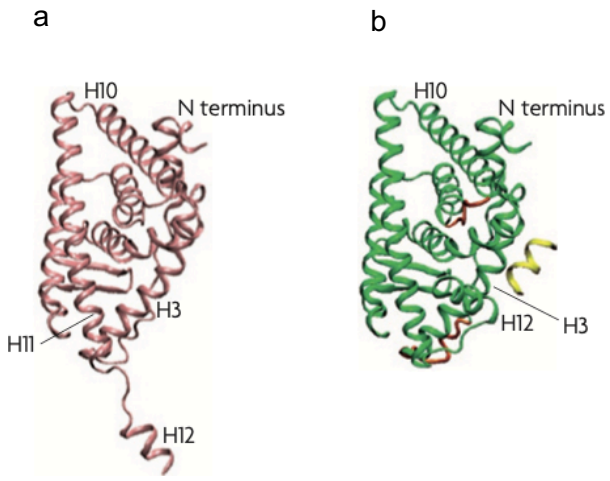


**Figure 1.5 The three-dimensional structure of the ER-α LBD.** (a) unbound estrogen receptor. (b) Estrogen binds LBD in the ERα activating interaction with the co-activators at AF-1 and AF-2. A docking site within the AF-2 domain interacts with the LXXLL motif of proteins in the p160 co-activator family. This interaction causes conformational change to the ERα protein allows for correct structural positioning for interactions with other co-factors and stimulates gene transcription, (Green et al., 2007).

Around 10-15% of the cells express the ERs in the mammary gland, (Clarke, et al., 1997) while stromal cells are estrogen negative, (Clarke et al., 2004; Petersen et al., 1987). The expression of the receptor was found to be mutually exclusive with the proliferation-associated marker Ki67. Co-expression of $ER_{\alpha}$ and Ki67 marker is usually observed in breast cancer (Shoker et al., 1999).

The four main functional domains of ER-α are the activation function-1 and 2 (AF-1 and AF-2) domains, a central DNA-binding domain (DBD) and a carboxyl-terminal ligand binding domain (LBD), (Figure 1.6). Within the interior of the LBD is a hydrophobic ligand binding cavity that binds estrogen with high affinity and specificity, (Q. Feng and O'Malley 2014). Estrogen binding to the LBD results in a conformational change in the DBD which is formed by two C4-type zinc fingers. The DBD then recognises estrogen-responsive elements (ERE), which are DNA sequences found in the enhancer or promoter regions of target genes. Estrogen binding to the LBD results in conformational changes that expose co-activator binding sequences in AF2. The end result is thus a

dimerised receptor complexed with co-activators and interacting with EREs on DNA to stimulate ER mediated gene transcription conformation. The linear structure of $ER_{\alpha}$ binding to oestradiol is shown in Figure 1.6.

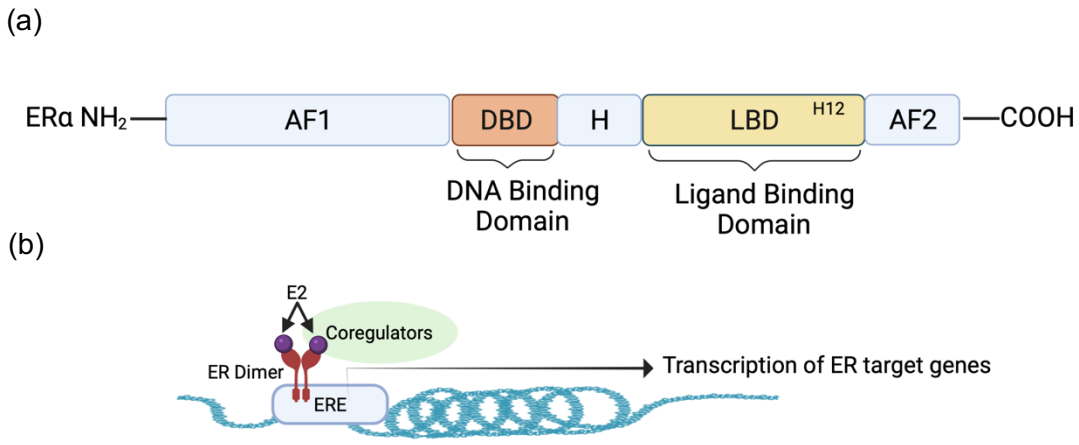


**Figure 1.6 Genomic signalling activity of ERα. (a) ER protein structure. (b)** Oestradiol (E2) effect is mediated by the translocation of (ER-E2) complex into nucleus, binding with ERE along with coregulators to start the transcription of an independent set of genes and other downstream pathways. Active ER protein stimulates cells proliferation. AF-1: an N-terminal transcriptional activation function domain-1, DBD: a DNA-binding domain, H: a hinge region, LBD: the ligand-binding domain, AF-2: A C-terminal activation function domain-2. Figure was created with BioRender.com.

### 1.5.1.2 The mechanism of estrogen action on the ER

The fundamental role of selective recruitment of coregulators in estrogen and Selective Estrogen Receptor Modulator (SERM) functions had been well explained, (Feng et al., 2014). Because the ER protein lacks intrinsic enzymatic activity, it recruits coregulators with a variety of enzymatic functions; these coregulators are lacking DBD and therefore unable to bind directly to genomic DNA, (Figure 1.7). The SRC/p160 family of coactivators are the most recognized coactivators for steroid hormone receptors, including the ER. Upon estrogen binding, the carboxyl-terminal alpha helix 12 of ER

folds back toward the ER LBD and, forming a hydrophobic cleft with helix 3 and 5, which interacts with the hydrophobic surface of LxxLL motifs of SRCs.

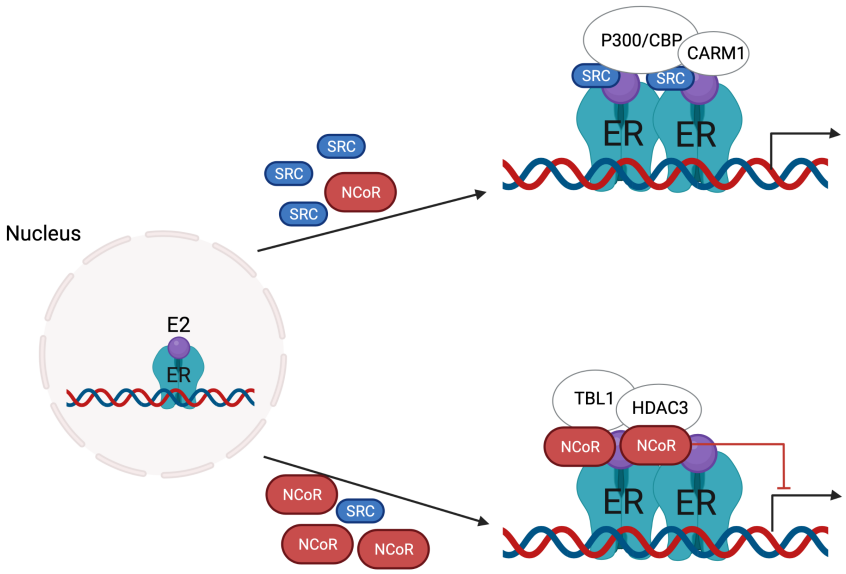


**Figure 1.7 An illustration of coregulators selective recruitment mechanism that regulate estrogen receptor activity.** Figure was adapted from (Feng et al., 2014) and created with BioRender.com

Corepressors are a transcriptional group that opposes the activity of coactivators in nuclear receptor-mediated transcriptional regulation. NCoR1 and SMRT are nuclear receptor corepressors, they bind with nuclear receptors in the absence of hormone and their interaction is disrupted by agonist binding. As NCoR1 and SMRT have no intrinsic enzymatic activity, NCoR1 and SMRT function as scaffold proteins, and they recruit histone deacetylases such as HDAC3 via several repression domains (RD1, RD2 and RD3). Recent investigations have demonstrated that NCoR1/SMRT may operate as corepressors for steroid receptors and reduce target gene transcription.

### 1.5.2 Progesterone Receptors

#### 1.5.2.1 Progesterone effects on lobular-alveolar structures development

ER signalling is required to induce PR expression. The activity of ER molecules has an impact on PR downstream signalling mediators that have an impact on mammary gland development. Progesterone receptor (PR) is a member of a family of ligand-activated nuclear transcription regulators, (Mehasseb et al., 2011). The receptor has two isoforms known as PRA and PRB. Both isoforms are encoded by the same gene known as *PGR* found on chromosome 11q22, (Gadkar-Sable et al., 2005). The receptor's structure can be divided into a regulatory domain at the N-terminus, a DNA binding domain, a hinge section and a hormone-binding domain at the C-terminus (Horwitz et al., 1992; Leonhardt et al., 2003).

Progesterone acts in balance with estrogen to stimulate the growth of the mammary glands which depends on the combined action of both hormones. The role of progesterone on the breast development is also affected by the balance between the two isoforms of the receptor. It has been noticed that PRB acts as a stronger activator of the progesterone target genes while PRA acts as a dominant repressor of the receptor, (Conneely et al., 2003; Graham et al., 1997).

Progesterone action on PR is essential in the development of lobular-acinar structures in the breast during pregnancy. The hormone is also important in controlling the breast epithelium's cyclical proliferation, including the increased proliferation of the cells during the late luteal phase, (Masters et al., 1977). The proliferative effect of progesterone on the cells is mediated by inducing

progression through the cell cycle by stimulating the expression of cell cycle-regulatory genes, such as cyclins and cyclin-dependent kinases. Additionally, the hormone potentiates the insulin-mediated increase in cyclin D1 mRNA levels, (Musgrove et al., 1993; Musgrove et al., 1991). Additionally, progesterone may also inhibit the expression of genes responsible for suppression of cell growth including p53 tumour suppressor protein, (Hurd et al., 1995). Progesterone induces the production of several growth factors and growth factor receptors including epidermal growth factor (EGF) and EGF receptors, TGFα and TGFβ.

## 1.6 The regulation of paracrine signalling in normal breast development

### 1.6.1 Local paracrine mediator

In both humans and mice, the majority of cells that express ER and PR do not co-localize with proliferation markers suggesting that estrogen acts in a paracrine manner to induce the expansion of surrounding cells, (Clarke et al., 1997; Russo et al., 1999). A variety of paracrine mediators that may contribute as downstream signals of steroid hormones have been identified including receptor activator of nuclear factor Kappa-B ligand (RANKL), WNT4, IGF-II, CXCL-12, amphiregulin (AREG), calcitonin, and inhibitor of DNA binding 4 (Id4), (Ciarloni et al., 2007; Rosen et al., 2014) (Figure 1.8).

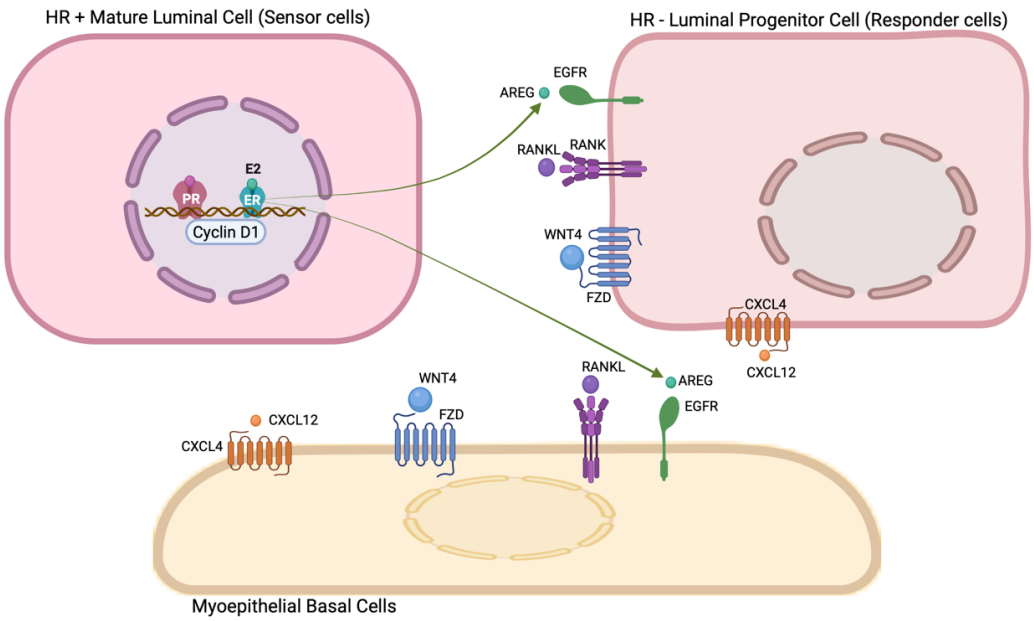


**Figure 1.8 An illustrated view of paracrine interactions in mammary development.** Estrogen receptor alpha/progesterone receptor-positive ($ER_{\alpha}$+/PR+) cells directly drive $ER_{\alpha}$-/PR− cells proliferation via paracrine signalling. Hormone-specific paracrine mediators involve amphiregulin (AREG), which acts downstream of estrogen, and receptor activator of nuclear factor kappa-B ligand (RANKL), CXCL12 and WNT4, which act downstream of progesterone signalling. Figure was adapted from (Tharmapalan et al. 2019) and created with BioRender.com

### 1.6.1.1 AREG signalling

Amphiregulin (AREG) is a paracrine ERα signalling mediator. AREG is a member of the epidermal growth factor (EGF) family. It is a paracrine growth factor stimulated by estrogen in the mammary gland of pubertal mice throughout the ductal system's development, (Ciarloni et al., 2007). They stimulated prepuberal ER-α negative mice to test if ER-α mediates 17-β-oestradiol-induced expression of amphiregulin. At this stage, ER-α negative and wild-type (WT) glands are phenotypically indistinguishable. Amphiregulin mRNA did not increase in the absence of ER-α. Therefore, 17-β- oestradiol regulate amphiregulin expression in the puberal mammary gland through ER-α dependent transcriptional activation. In another study, it has been

demonstrated that the expression of amphiregulin significantly increases during puberty while its expression decreases through pregnancy and lactation. Amphiregulin knockout (AREG KO) mice were created and examined their mammary gland maturation to better understand the amphiregulin function in normal mammary gland development. Mammary glands of AREG KO mice, when compared to wild type control glands, showed a delayed in the development of ducts throughout adolescence, (McBryan et al. 2008).

#### 1.6.1.2 RANKL, WNT-4 and CXCL12 signalling

Nuclear factor kappa-B ligand (RANKL), WNT-4 and CXC chemokine (CXCL12) proteins are significant paracrine PR signalling mediators in the mammary epithelium and during early pregnancy. Progesterone binds to its receptor in PR-positive breast luminal cell, leading to an increase in RANKL, WNT-4 and CXCL12 protein levels mainly through stabilization of its mRNA. RANKL binds to its signalling receptor RANK, a member of the tumour necrosis factor receptor (TNFR) family located on the surface of surrounding PR-negative breast luminal cells; stimulating downstream signalling pathways that promote cell proliferation, expansion and survival, (Infante et al., 2019). The RANKL protein is found in 11% of human breast tumours and stromal cells, (Rajaram et al., 2012). Several pre-clinical investigations have shown that the RANKL/RANK system promotes breast carcinogenesis, indicating that this system may be responsible for the increased incidence of breast cancer linked to progesterone and progestin use, (Infante et al., 2019).

Localized WNT signalling is essential in the mammary gland for regulating cell division orientation and cellular fate throughout development, (Rosen et al., 2014). *Brisken et al.* examined the mammary epithelium of mice without both copies of the WNT4 gene. The group were able to determine the particular role of WNT4 in mammary morphogenesis. At day 12 of pregnancy, the epithelium fails to induce side-branching. With a more normal branching pattern, engrafted $WNT4^{+}$ epithelia began to resemble wild-type epithelial grafts later in pregnancy. Because WNT4 is a direct target of PR signalling, in situ hybridization revealed that PR and WNT4 mRNAs had comparable expression patterns in luminal epithelial cells, (Brisken et al., 2000).

CXCL12 and its receptor CXCR4 have been shown to play a key role in mammary epithelial cell fate and tissue regeneration in previous studies, (Shiah et al., 2015). Shiah et al. identified CXCL12- CXCR4 as a possible progesterone-initiated paracrine signalling pathway. They demonstrated that CXCR4 and CXCL12 are well-positioned for autocrine and paracrine signalling in luminal and basal cells, respectively. This study confirms CXCL12 as a crucial progesterone-stimulated effector whose signalling is facilitated by PR-dependent overexpression of its corresponding receptor, CXCR4, resulting in the generation of progenitors required for alveolar formation.

In xenograft animal models, overexpression of CXCL12 stimulates the formation of robust gland-like structures in mammary epithelial cells. Overall, the findings imply that CXCL12 promotes epithelial cell reprogramming into non-luminal cell-derived stem cells, which aid gland development, (Jung et al., 2020).

## 1.7 Physiology of Menopause

Menopause triggers regression of the breast parenchyma, with fatty tissue coming in its place, as ducts, glands, stroma and connective tissues become involuted, and lymphatic channels are reduced in number. Atresia occurs in the ducts, which remain, and lobular units collapse. At this stage, similar to the breast before childbearing, type 1 lobules predominate. Estradiol is no longer secreted by the ovaries; instead, adrenal and androstenedione is converted into estrone, (Qureshi et al., 2020). However, estradiol is still produced in menopausal women from aromatization of testosterone. In addition, the level of serum follicle-stimulating hormone is increased, and more luteinizing hormone is also present, due to the lack of negative feedback from estradiol, (Pritchard et al., 2001). The reduction in glandular tissues is thought to occur because of the estrogen level drop, (Den Tonkelaar et al., 2004). Post-menopause, breast adipocytes show decreased lipolysis, (Den Tonkelaar, et al., 2004).

## 1.8 Breast cancer risk factors

In order to efficiently prevent breast cancer, we must first understand who is at increased risk of the disease. Multiple breast cancer risk factors have been identified, including female sex, age, inherited gene mutations, weight gain, presence of benign breast disease and high mammographic density (Figure 1.9), (Howell et al., 2014).

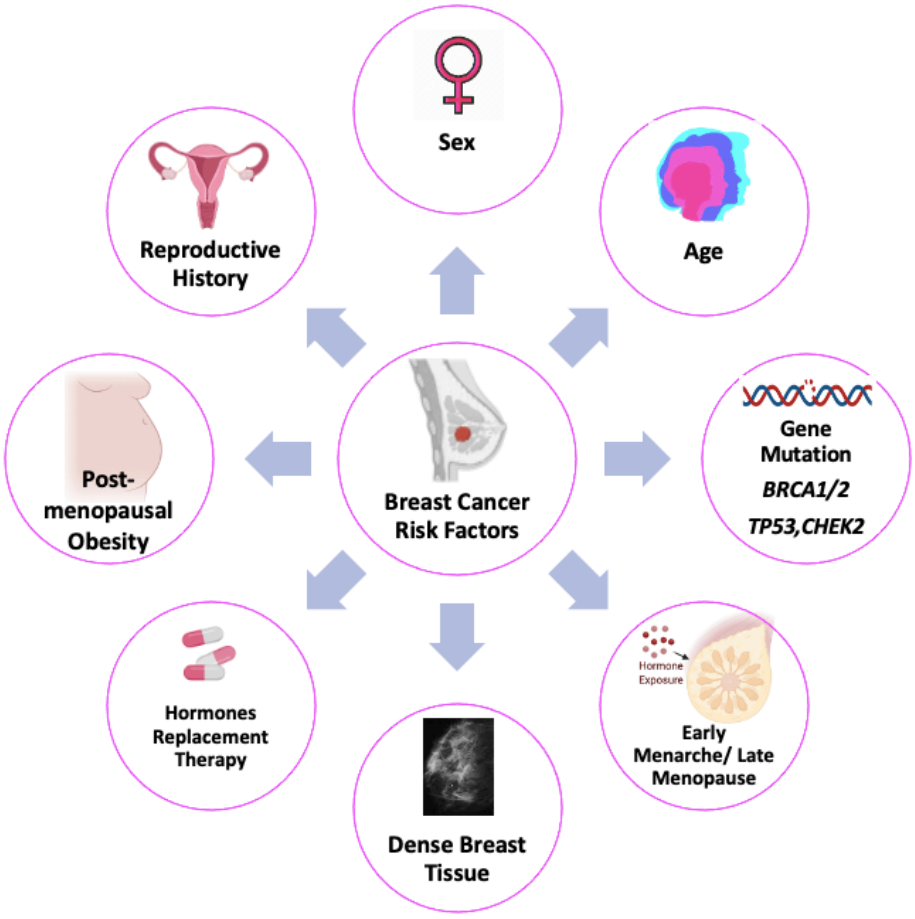


**Figure 1.9 Most common risk factors for development of breast cancer,** (Information adapted from (Britt et al., 2020). Figure was created with BioRender.com

Similar to other types of tumours, breast cancer arises due to mutations in DNA, particularly in the coding sequence of an oncogene or tumour suppressor gene. Mutations can cause inhibition of apoptotic processes, resulting in cells becoming 'immortal' or replicating without the normal controls. Some individuals have uncommon inherited mutations in DNA repair genes that predispose them to breast cancer although this does not explain the majority of cases. Single nucleotide polymorphisms (SNPs) are single base-pair differences in DNA sequences that are more frequent than inherited mutations but individually have a small impact on risk. More than 300 breast

cancer SNPs have now been identified and, in combination, can predict significantly more breast cancers than single gene mutations, (Woodward et al., 2021). In addition, certain hormonal factors, both extrinsic and intrinsic are intimately related to the risk of breast cancer. These factors will be discussed below.

### 1.8.1 Age and Gender

The incidence rate of breast cancer increases with age reaching a peak at 90 years of age or older, (Figure 1.10), (Cancer Research UK, 2021). Breast cancer is rare in those under the age of 30, but the incidence rises exponentially through the 30s and 40s. Breast cancer is diagnosed in 1 in 8 females and 1 in 870 males giving a male: female ratio of over 1:100, (Parks et al., 2018). The main reasons for this gender predominance are likely to be the presence of significantly more breast tissue in females and the differences in the hormonal milieu between the sexes. This suggests that hormones also play a significant role in somatic mutation-induced carcinogenesis.

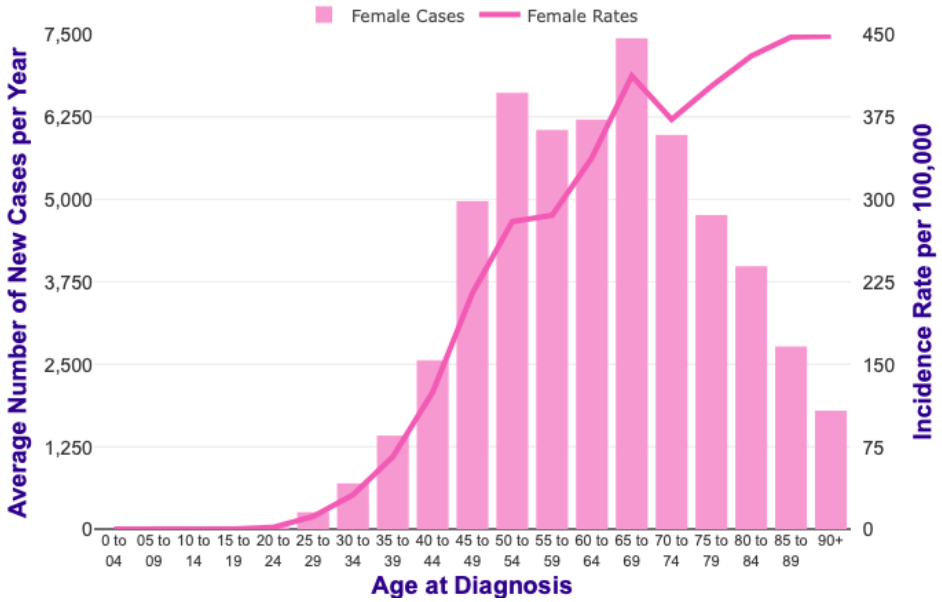


**Figure 1.10 Age-specific incidence rate for female breast cancer. (Adapted from (Cancer Research UK, 2021).**

### 1.8.2 Family history of breast cancer

The existence of a relative who had been diagnosed with breast cancer increases the risk of breast cancer for the individual. The risk increases more significantly when relatives are diagnosed at younger ages, (Claus et al., 1990). The stronger a family history, the more likely the family carries a germline pathogenic variant in one of several genes known to associate with an increased BC risk such as *BRCA1*, *BRCA2,* or *PALB2*. This can be quantified in a scoring system that determines the chance of a mutation and thus the women in whom gene testing should be performed, (Evans et al., 2004).

In addition, a personal history of 'benign' abnormalities in the breast tissue, such as lobular carcinoma in situ (LCIS) and atypical hyperplasia, convey a

significant increase in breast cancer risk. Such factors have also been fashioned into a scoring system based on precise histological appearances, (Pankratz et al., 2015). In addition, an individual with a previous diagnosis of breast cancer in one breast is more likely to have breast cancer diagnosed in the other, (Michowitz et al., 1985).

### 1.8.3 Reproductive History

Several endogenous factors are associated with breast cancer risk; shown in Figure 1.11. Early menarche (<12 years old) and late menopause (>55 years) raise the likelihood of breast cancer. This is thought to be due to the increase in the number of menstrual cycles in which epithelial cells divide and thus are exposed to potential gene mutations. In one study, for every year of delay in menarche, the relative risk of breast cancer fell by 9%, (Li et al., 2013). In contrast, in a second study, breast cancer risk increased by 5% for each year younger at menarche and by 3.5% with each year older at menopause (Britt et al., 2020).

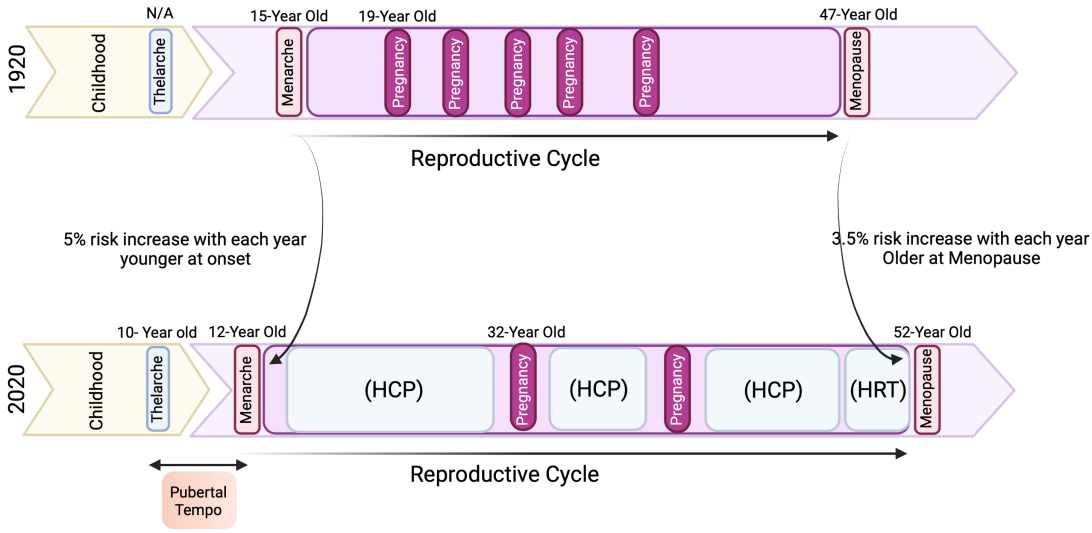


**Figure 1.11 Reproductive cycle and breast cancer risk.** Schematic representation of changes in reproductive hormones in females over the last 100 years. Age at thelarche and menarche declined while age at first full-term pregnancy and menopause has increased. The rate of nulliparity and parity after the age of 30 had increased. All these factors led to increase exposure to estrogen for a longer time and increased breast cancer risk. HCP= Hormone contraceptive pills. HRT= Hormone replacement therapy. N/A= not available. Figure was created with BioRender.com.

Parity, particularly the age at first full-term pregnancy (FFTP), also influences breast cancer risk. In general, an early FFTP (<25) reduces risk while nulliparity or a late FFTP (>29) increases risk. Breastfeeding, if undertaken for at least six months also reduces breast cancer risk, (Britt et al., 2020). Although these factors have been described for many years, several studies have now considered the potential relation between reproductive variables and the various subtypes of breast cancer. These studies show concordant results that early FFTP is predominantly associated with a reduction in the risk of ER positive (luminal A) breast cancer, whereas the beneficial effect of breastfeeding is most strongly associated with a reduction in the risk of TNBC, (Gaudet et al., 2011; Holm et al., 2017). These factors may thus become useful in subtype-specific risk prediction models, which will be vital to personalise cancer prevention approaches.

### 1.8.4 Hormones up-regulation and Hormone Replacement Therapy

Lifestyle factors can influence health in different ways. Gaining weight during late pre- and post-menopause is identified as a risk factor for breast cancer, potentially through the increase in estrogen levels by the adipose tissue itself, (Howell et al., 2014). Conversely, being overweight in younger women is protective, potentially due to reduced progesterone levels, (Gaudet et al., 2011; Poole et al., 2011). Exogenous hormones in the form of oral contraceptive pills (OCP) and Hormone replacement therapy (HRT) have also been shown to increase the risk of breast cancer. This is particularly the case for combined estrogen and progesterone HRT which has been shown to increase the risk of postmenopausal breast cancer in both observational and randomised studies, (Collaborative Group on Hormonal Factors in Breast Cancer, 2019). In contrast, breast cancer risk was seen to be less with estrogen alone HRT in these studies. Molecular analysis of breast tissue from women taking HRT vs. those who were not, shows that estrogen plus progesterone therapy increases proliferation in the terminal ductal lobular units (TDLUs) whereas estrogen alone did not, potentially providing a rationale for the disparity in risk, (Hofseth et al., 1999).

### 1.8.5 Mammographic Density

The proportion of radio-dense fibroglandular tissue in the breast, known as mammographic density (MD). The degree of MD is positively associated with an increased risk for breast cancer with those in the highest vs lowest quartile having 4-6 fold excess risks, (Archer et al., 2022). Initially, quantification of MD used categorical approaches and the most frequently used categorical system in the USA forms part of the Breast Imaging Reporting and Data System

(BiRADS® Atlas, 5th edition). The categories in the latest BiRADS range from 'almost entirely fatty' to 'extremely dense with very little fat, as shown in (Table 1.1). Although it is helpful in determining risk and in assigning the possibility of masking a cancer, the 4 category-nature of BiRADS means that some accuracy and differentiation between women is lost. Several approaches to assess MD as a continuous variable have now been described for full-field digital mammograms (FFDM).

**Table 1.1 BiRADS Atlas 5th edition. Categories for mammographic density, adapted from (www.acr.org)**

| Category | Breast composition |
|---|---|
| **A** | The breast is almost fatty |
| **B** | Scattered areas of dense glandular and fibrous tissue |
| **C** | Breast is made of dense glandular and fibrous tissue |
| **D** | Extremely dense breast tissue that makes it difficult to see tumours |

#### 1.8.5.1 Visual Analogue Scale (VAS)

Visual Analogue Scale (VAS) scoring of MD relies on the subjective estimation of percent density by providing the assessor with a form depicting a horizontal VAS labelled 0% and 100% at the two ends of the scale. VAS readings are frequently read by two or more radiologists and averaged to provide a final score. Using this approach both intra and inter-observer agreement have been calculated to be excellent (intraclass correlation coefficient (ICC) > 0.80 and 0.82 respectively), (Astley et al., 2018). VAS outperforms risk measurement in breast cancer patients on the contralateral breast and in the average of bilateral mammographic views prior to the detection of cancer, (Astley et al., 2018). However, this is a time-consuming method, and the ICCs highlight some inconsistency between observers. Automated methods for quantifying both percent area and percent volumetric density have been developed to

reduce this inconsistency and make the process less time-consuming and costly.

#### 1.8.5.2 Automated MD assessment

There are currently four commercial programmes for MD assessment from FFDM. These are Cumulus™, Densitas™, Quantra™ and Volpara™. Cumulus is semi-automated and uses an interactive thresholding technique to guide the operator in the production of an overall MD assessment, (Byng et al. 1994). It is more time consuming than the full VAS scoring and has not gained widespread use. The other three techniques use fully automated algorithms to define either the percent area (Densitas) or percent volume (Quantra and Volpara) of MD. In two UK based case control studies assessing the three techniques, Volpara showed the greatest correlation between density and breast cancer risk, (Astley et al., 2018; Eng et al., 2014). In one of the studies Quantra showed no predictive power at all. Importantly, all of the approaches need to be corrected for BMI and age as both have been shown in multiple studies to be inversely associated with %MD, (reviewed in Astley et al., 2018). There are also technical issues with these approaches, including the need to ensure that breast positioning is as accurate and reproducible as possible, as small changes in breast position can result in wide variations in reported MD.

#### 1.8.5.3 Tissue composition of MD

Dense areas of the breast consist predominantly of extracellular matrix (ECM) and cellular areas, in a ratio of approximately 15:1, whereas non dense areas are mainly fat, (Ghosh et al., 2012; Li et al., 2005). Collagen is the major component of the ECM. Breast stroma contains a high proportion of fibrillar collagens and, as with other connective tissues, these show around three

times more stiffness in comparison to elastin and other ECM elements, (Zhu et al., 2014). Recently the periductal collagen from areas of high MD was shown to be arranged in fibrillar form as compared to the disorganised collagen in ducts from non-dense areas, (McConnell et al., 2016). The collagen abundance in the mammary glands of parous mice is less linearized and linked with a reduction in stromal rigidity, implying that collagen organization and rigidity play a significant role in parity-induced breast cancer protection, (Maller et al., 2013). This leads to the hypothesis that stiffness in areas of high MD may lead to cellular transformation, a phenotype seen in animal models of mammary tumorigenesies.

ECM stiffness is detected and signalled to epithelial cells through transmembrane receptors called integrins. These receptors are contained in adhesomes, or multiprotein agglomerations, (Gilmore et al., 2009; Streuli et al., 2016). Integrins connect the cell's external environment to internal signalling and cytoskeleton. As the ECM stiffens, the adhesomes structure and link to the cytoskeleton is reorganised, and cell signalling is altered, along with nuclear response (Mohammadi et al., 2018). A mechanism for MD to promote cancer could potentially be based on the response of signalling proteins to the degree of stiffness in the ECM. Integrins responding to altered ECM interaction target focal adhesion kinase (FAK), the Rho pathway and p130Cas, resulting in stimulation of proliferative activity. Such proliferation could then result in DNA mutations and ultimately tumorigenesis, (Tomasek et al., 2002).

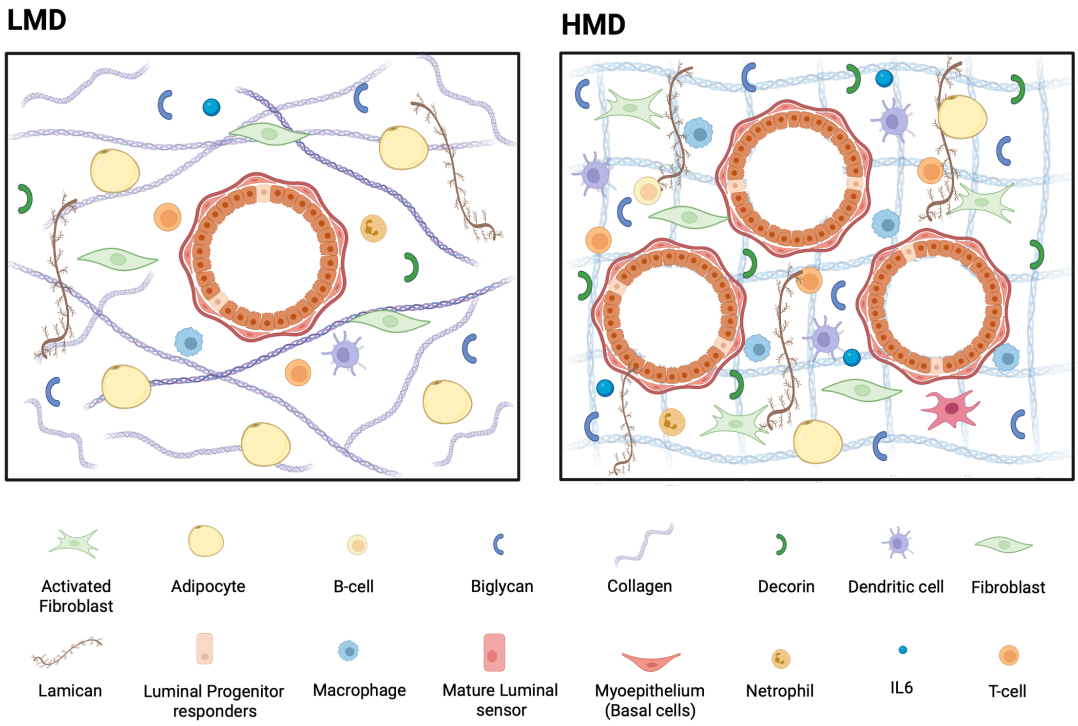


**Figure 1.12 Biological differences in breast tissue composition with high mammographic density (HMD) and low mammographic density (LMD).** Dense tissue has stiffened ECM and epithelium content compared to LMD. There is no evidence that HMD promotes stem or progenitor cell proliferation. Collagen fibers in HMD breast tissue are arranged in fibrillar form compared to the disorganized collagen in LMD breast tissue. Collagen-binding proteoglycans lumican, decorin, fibromodulin and biglycan are associated with HMD. Lumican is strongly associated with tumorigenesis by promoting angiogenesis, epithelial cell proliferation, migration and invasion. Cellular immune components have also been shown to be increased in dense areas: innate cells, adaptive cells and interleukin-6 (IL-6). Stromal fibroblasts in dense areas have also been shown to exhibit gene expression signatures associated with cancer-stimulating pathways, such as stress response, inflammation, stemness and signal transduction, reviewed by (Britt et al., 2020). Figure was created with BioRender.com

Although the precise molecular mechanisms of stiffness-induced increase in proliferation have not been identified, an increase in epithelial cell proliferation in areas of high vs. low density has been observed, (Harvey et al., 2008). In addition, the use of estrogen and progesterone HRT increases both epithelial proliferation and MD, suggesting that the two processes are linked (Greendale et al., 2003).

#### 1.8.5.4 Genetic Factors associated with MD

Twin studies have been used to investigate the heritability of MD, (Boyd et al., 2002, 2005, 2011; Kaprio et al., 1987; Stone et al., 2006, 2007; Ursin et al., 2009). The first two studies gathered questionnaire data from twins between 40 and 70 years old in the USA, Canada and Australia, including data related to factors previously identified as associated with MD. Mammographic data was also measured for each participant and %MD was assessed using automated techniques. Observers were blinded to pairing and zygosity, (Boyd et al., 2002). Once data were adjusted for participant age, parous status, age at first menstrual period, number of live births, BMI and whether pre- or post-menopause, there was a substantial conformity in density between twins. Monozygotic twins were twice as closely correlated as dizygotic, and this supports the theory of an additive genetic effect. There is no genetic difference between monozygotic twins, so variation in density can only be related to environmental variables or measurement error. In contrast, dizygotic twins typically have around half of their twins' genes, so where twins are the same sex, variations can be either genetic, environmental or due to measurement error.

In non-twin families, the probability of having dense breasts is 17% greater for women with an affected 1$^{st}$-degree relative than women with no family history, (Crest et al., 2006; Ziv et al., 2003). This probability also increased with more affected 1st degree relatives a woman had. For example, the probability increased to 46% with three or more first-degree relatives affected, (Crest et al., 2006). Despite extensive study, most of genetic variants that can be attributed to the inheritance of MD have not been identified.

An individual SNP is one variation within one DNA nucleotide, and such variations typically occur at a frequency of 1 per 300 nucleotides, totalling roughly 10 million across the genome, (Ghoussaini et al., 2012; Lindström et al., 2014). SNPs have the potential to be used as biological markers for locating genes linked to various conditions. In general, the more recent research points to a common genetic element between breast cancer and MD, further showing that certain density-associated genes also contribute to excessive proliferative activity.

#### 1.8.5.5 The activity of paracrine markers in high-risk women

The RANK/RANKL signalling pathway may explain its correlation to the breast cancer risk due to its role in proliferation, differentiation, and migration of mammary epithelial cells as demonstrated in mouse models, (Moran et al., 2018). *Kiechl et al.* indicate that higher progesterone and RANKL serum levels identify a subset of postmenopausal women without known recognized genetic predispositions who have a 5-fold greater risk of breast cancer 12-24 months, (Kiechl et al., 2017).

## 1.9 Breast cancer prevention

As discussed above, estrogen either directly or through the stimulation of PR, promotes breast epithelial cells division. In addition, ER positive breast cancers are treated by approaches to antagonise estrogen activity. Such anti-estrogenic drugs are classified into three major classes namely selective ER modulators (SERM), selective ER degraders (SERD) and aromatase inhibitors (AI). These classes of drugs have been used for the treatment of advanced and localised disease. In early breast cancer tamoxifen treatment was noted to result in 50% reduction of contralateral breast cancers, (Cuzick et al., 2005). This then led to the initiation of large scale breast cancer prevention studies, (Cuzick et al., 2013). Tamoxifen was shown to be more effective than raloxifene whilst raloxifene was found to be safer in postmenopausal women as it does not stimulate the endometrium and induce endometrial cancer, (Nazarali et al., 2014).

Breast cancer prevention is currently viewed as an important medical goal taking into the consideration the number of new cases and breast cancer-related deaths each year. The principle focus of this thesis is the effects of tamoxifen on the normal breast tissues of women at increased risk of breast cancer.

In the UK the SERMs tamoxifen and raloxifene and the AI anastrozole are approved for use in primary BC prevention by the National Institute for Health and Care Excellence, (NICE Guidelines committee, 2019) Women are eligible if they are at moderate (17-30%) or high (>30%) lifetime risk of breast cancer. The SERMs are also approved for this indication in the USA and other

developed countries. In all countries the standard recommendation is for five years' treatment duration, (Jones et al., 2021).

### 1.9.1 Tamoxifen

Subsequent studies have been performed to evaluate the mechanism of action of tamoxifen in the normal breast. In the International Breast Cancer Intervention Study (IBIS1), the effect of tamoxifen on MD was studied, (Cuzick et al., 2011). A single reader using a VAS method analysed the baseline mammogram and that performed after approximately 1 year of tamoxifen. A reduction in breast cancer incidence was only seen in women who had a fall in absolute MD by >10% and in these women breast cancer incidence was reduced by 70%, (Cuzick et al., 2011). However, in a more recent study using multiple MD analytical techniques including VAS from the same reader used in IBIS-1, Brentnall and his colleagues showed that tamoxifen treatment in premenopausal women resulted in large reductions in the majority of women but more importantly that the reduction in MD at 1 year could not predict the reduction at 2 years, (Brentnall et al., 2020). This may be due to technical factors such as the variability in breast positioning from one year to the next, but the observation has effectively ruled out the use of density change at 1 year as a predictive biomarker for tamoxifen.

Tamoxifen was the first drug to be approved by the FDA in 1998 for prevention of breast cancer in high risk women (Fisher et al., 1998). The compound, initially known as Compound ICI 46,474, was developed as a contraceptive pill. However, it was found to stimulate ovulation rather than suppressing it. The drug was then tested as a palliative treatment for late stage breast cancer,

(Harvey et al., 1982). The tamoxifen market was boosted in the late 1980s when clinical trials showed it to be effective as an adjuvant treatment after breast surgery in early-stage breast cancer, reducing recurrence and improving mortality, (Fisher et al., 1986). Several primary prevention trials were then initiated in the 1980s and 1990s to test whether tamoxifen reduced breast cancer incidence in women without a personal history of the disease. For example, the IBIS study tested the use of tamoxifen on 4536 women at increased risk of breast cancer who were randomised to receive tamoxifen or placebo. In the first report, after 3.5 years of median follow up, tamoxifen reduced the incidence of breast cancer by 45%, but this was associated with increased incidence of endometrial cancer (EC) and thromboembolism, although the increase in EC was only seen in post-menopausal women, (Cuzick et al., 2002). Subsequently analysis of the same study after a median follow up of 16 years showed a continued reduction in the incidence of breast cancer, (Cuzick et al., 2015).

In a meta-analysis of all SERM prevention trials; (Figure 1.13), tamoxifen was shown to reduce the incidence of ER positive breast cancer by approximately 50%. However, no reduction in ER negative breast cancer was seen (Cuzick et al 2013). Of concern the incidence of ER- breast cancer was higher in those treated with tamoxifen vs placebo, although this did not achieve statistical significance. In further analysis, and disappointingly, tamoxifen did not reduce breast cancer or all-cause mortality.

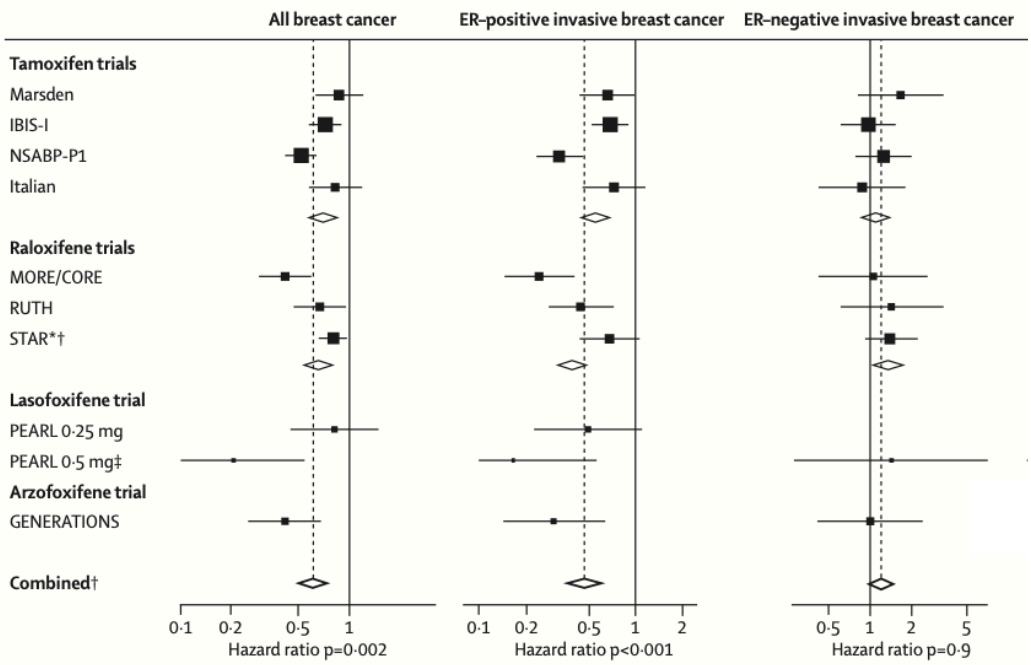


**Figure 1.13 The Forest plot demonstrates the effects of tamoxifen on breast cancers.** The left panel is for breast cancer overall. The middle panel is for ER+ breast cancer and the right panel is for ER- breast cancer. Square: odd ratio. Diamond: summary measurement at the centre line with confidence intervals at lateral tops of the diamond. (*) Adjusted by overall tamoxifen effect to give raloxifene versus placebo comparisons. † STAR data not included in comparisons. ‡Data for ER-invasive cancer are pooled. Figure adapted from (Cuzick et al., 2013).

The effects of tamoxifen on the normal breasts of women at increased risk of breast cancer were studied by Euhus et al, (Euhus et al., 2011). In this study 73 pre and post-menopausal women were randomised to tamoxifen (n=40) or placebo (n=33) and had core biopsies of the normal breasts at baseline and after 3 months of treatment. The primary analysis sought to identify homogenous changes in gene expression across all women receiving tamoxifen. Only in the 29 premenopausal women (n=14 tamoxifen and n=15 placebo) was there a uniform regulation of genes (n=18) by tamoxifen not seen in the placebo group. The majority of the genes were known estrogen regulated genes and were down-regulated by tamoxifen, including *ETV4* and

*ETV5*, members of the Ets-oncogene family, known to be important in stem/progenitor regulation and normal murine mammary gland development, (Kurpios et al., 2009). Tamoxifen also regulated the expression of genes linked to epithelial-stromal interaction and tissue remodelling such as *PTHLH, PLAT, SERPINA3, SERPINA5, SERPING1, DBC1,* and *EXTL1*.

Hattar and colleagues investigated the effects of tamoxifen on mouse normal mammary glands (Hattar et al., 2009). They found that tamoxifen acted to inhibit mammary alveoli from developing and prevented mammary epithelial cells from proliferating. Furthermore, they suggested that tamoxifen can have an impact on stromal cells and ECM.

In the absence of hormone, ER recruits NCoR1 to the pS2 gene promoter, and tamoxifen therapy enhances NCoR recruitment. The existence of both coactivators and corepressors indicates a complementary interaction for regulation of gene transcription. Tamoxifen treatment can induce growth signalling pathways which phosphorylate SRC-3 and enhances its coactivator activity in the endometrium. This mechanism leads to stimulate cell growth and tamoxifen resistance.

17β-estradiol (E2) causes the helix (H) 12 in ER-LBD (ligand binding domain) to relocate, allowing ER to react with certain coactivators and so initiate transcriptional activation, as per X-ray crystal structure analysis. Tamoxifen instead displaces H12 from its normal position, which prevents formation of the surface for recruitment of numerous coactivators and excludes AF2, (Figure 1.14), (Okamoto et al., 2019). Tamoxifen functions identified in the mammary gland involve induction of corepressors to target gene promoters;

instead it resembles estrogen through recruiting the coactivators to a subset of genes in the endometrium. According to Shang et al., (2002), the high level of steroid receptor coactivator (SRC-1) expression is required for the agonist impacts of tamoxifen in the uterus, (Shang et al., 2002).

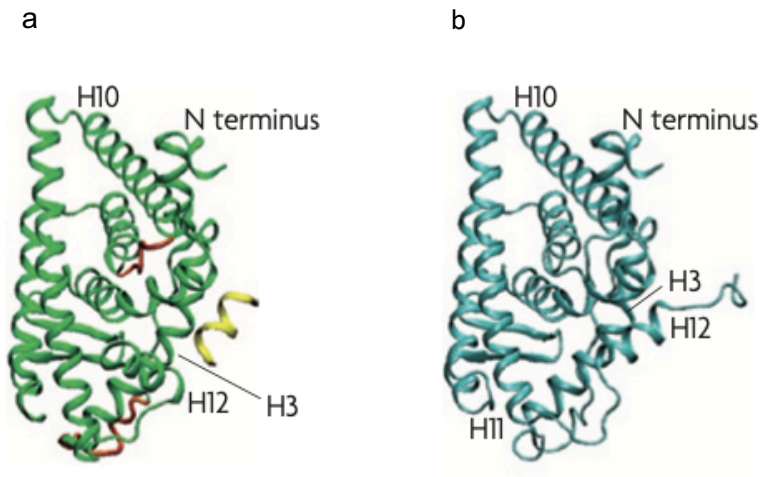


**Figure 1.14 The 3D conformational structure of ERα LBD is altered differently by estrogen and tamoxifen.** (a) Estrogen binds LBD in the ERα. (b) The active metabolite of tamoxifen, 4-hydroxytamoxifen, binds to the LBD and stimulates structural rearrangement of helix 12 and interacts with LXXML. This interaction inhibits the access to p160 co-activators family and recruits the co-repressors such as NCOR1 and SMART, (Green et al., 2007).

Tamoxifen is metabolized into active metabolites by different cytochrome P450 enzymes. The primary enzyme which metabolizes tamoxifen is CYP2D6, and others include CYP3A4, CYP3A5, CYP2C9 and CYP2C19, (Cronin-Fenton., 2014). These enzymes are encoded by polymorphic genes and metabolize tamoxifen into metabolites with specific binding affinities for the ER, (Lim et al., 2005). For example, tamoxifen metabolites with hydroxyl groups attached to their C4 atom, such as endoxifen, show highest binding affinities. Subsequently, these tamoxifen metabolites are converted into excretable forms through the activity of UDP-glucuronosyltransferase and sulfotransferase enzymes, (Gjerde et al., 2008; Lazarus et al., 2009). Enzymes

in this metabolic pathway are generally polymorphic, meaning that individuals express different variants, which can differ in their activities and can therefore impact tamoxifen metabolism and effectiveness of the drug, (De Vries Schultink et al., 2015). This phenomen is best described for CYP2D6 polymorphisms, which are known to impact tamoxifen efficacy in premenopausal breast cancer patients, (Saladores et al., 2015). More than 46 different major polymorphic CYP2D6 alleles were identified, (Ingelman-Sundberg., 2005). For some SNPs in CYP2D6, their impact on enzyme activity and expression is known. For example, the most common allele in the Asian population is CYP2D6*10.24, which encodes the CYP2D6.10 enzyme carrying the deleterious P34S mutation, which impairs folding of the enzyme and reduces its affinity for its substrates,(Johansson et al., 1994). Another major variant is the CYP2D6*17 allele, which endodes the CYP2D6.17 enzyme carrying three deleterious mutations, T107I, R296C and S486T, which alter the active site of the enzyme and therefore its substrate specificity, (Oscarson et al., 1997). Additional differences in tamoxifen metabolism can be attributed to polymorphisms in CYP3A4, CYP2C9, CYP3D6, CYP2C19, SULT1A1 and SULT1A2, among others.

## 1.10 Tissue culture systems

The use of *in vitro* models including cell culture is an essential step to understand biological processes or develop new treatments. The first documented cell culture was reported in 1907 by Ross Harrison who studied the development of neuronal cells, (Harrison et al., 1907). Since then, cell cultures became an essential research tool in the medical and biological fields.

### 1.10.1 Cell culture characteristics

Controlling cell culture characteristics depends on various factors including the growth medium, supplements, induced mutations or culture conditions. For general purposes as cytotoxicity or cellular uptake testing, cancer cells are commonly used as they grow easily and for indefinite number of passages. However, testing of tissue specific properties requires the use of specific cells from the corresponding tissues or organs. For example, testing the effects of various drugs on the normal growth of breast tissues and mammary glands require the use of normal breast cells. Additionally, it is sometimes needed to co-culture multiple cell types to study the interactions between cells during biological responses or processes.

Several types of cell cultures have been established for *in vitro* experiments intended for various purposes. Cell cultures can be based on primary cells isolated directly from living organisms. These cultures usually include multiple types of cells and represent more accurately the genetic profile of the living organism. They are useful for several purposes including the preparation and testing of personalized therapies for patients as the case with targeted cancer therapy. However, primary cell cultures are difficult to isolate and have short life span.

Cell cultures can be classified into 2D or 3D cell cultures. The most commonly used type is 2D cell cultures where cells are cultured as a monolayer adhering to a culture flask or petri dish. In general cells are more easily grown in monolayer resulting in greater experimental efficiency and lower cost. However, there are several limitations for the use of 2D cell cultures as they

do not reflect accurately the cellular interactions, cellular microenvironment, cell morphology, polarity and methods of cellular division, (Pampaloni, et al., 2007). Growing cells in 2D cultures also result in loss of the phenotype diversity which can affect significantly the cell functions. Another limitation of 2D cultures is that cells have uncontrolled access to nutrients, oxygen, metabolites or signalling molecules. On the contrary, normal tissue and organ tissues have variable access to these supplies as cells, for example, in the core of a tumour are subject to relative hypoxia. This hypoxia results in significant changes in the characteristics of the cells and responses to external factors including drugs, (Pavlacky et al., 2020).

The limitations of 2D cell cultures motivated the search for more realistic *in vitro* models that can resemble more closely the human tissues and organs. Hamburger and Salmon reported in 1977 the use of soft agar to support the growth of tumour stem cells allowing the study of growth characteristics and cell colony morphology. The technique was proposed to study the effects of anti-cancer agents and irradiation on various types of tumours, (Hamburger et al., 1977). Preparation of 3D culture models can be achieved using various approaches. Cells can be grown in the form of a suspension grown on non-adherent plates, (Krishnamurthy et al., 2013). They can also be grown in concentrated medium or gel-like substances, (Sodunke et al., 2007), or they can be grown on scaffolds prepared to mimic the structure of certain tissues as the bones or neurons, (Uebersax et al., 2006). Spheroid models can have cavity at the core of the structure which is normally formed through cell apoptosis. This cavity at the core resembles the structure of acinar glands in the body as the sweat glands and the salivary glands. Additionally, 3D models

have variable cell growth rate with cells at the periphery growing at higher rate as they have better access to nutrients, oxygen and signalling molecules, (Pradhan-Bhatt et al., 2014).

In general, the use of 2D or 3D culture models depends on the purpose of the *in vitro* testing and the availability of required facilities. However, in general the use of 3D is expected to be more common in the future with the improvement of automation techniques and the reduction of costs.

### 1.10.2 The use of cell cultures to study breast biology

The human female breast has a complex structure and develops through several stages that involves interactions with multiple hormones and other signalling molecules. Several cell lines have been established to study the normal breast tissue. The most common cell line currently used for studying normal breast is MCF10A which was derived from non-tumorigenic proliferative breast tissue that spontaneously became immortal, (Qu et al., 2015). However, this cell line does not express the ER which is an important limitation for studying the biology of the breast. Another less commonly used cell line is 48R which are non-cancerous cells with finite life-span in cell culture, (Meadows et al., 2008). Several cells with progenitor/stem characteristics are also available to study the development of the breast and mammary glands. For example, D492 progenitor cells can differentiate *in vitro* into both luminal and myoepithelial cells, (Briem et al., 2019).

Despite the availability of normal breast cell lines, the simplicity of these models does not accurately reflect the normal structure of female human breast. The female breast is a complex structure consisting of multiple types

of cells arranged into glands, ducts and alveoli. 3D co-cultures that more closely resembles the normal human breast tissue have been developed to try and recapitulate some of this complexity. Huss and Kratz reported in 2001 the co-culture of mammary epithelial cells and adipocytes in a matrix of collagen gel, (Huss et al., 2001). *Meng et al.* used 3D culture of primary cells derived from normal breast tissue to study the propagation of progenitor cells and ER positive cells in the tissue. Results of this study showed that it is possible for 3D culture to overcome the disadvantages of 2D cultures by maintaining the endocrine functions of the normal tissue and the growth control of the cells, (Meng et al., 2019). Wang et al. developed a co-culture of the MCF10A human mammary epithelial cell line with human fibroblasts and adipocytes on 3D scaffold of porous silk protein. The 3D culture resembled normal breast tissue in that alveolar and ductal structures formed and α- and β-casein expression was seen, (Wang et al., 2010).

*In vitro* models in which different cellular components are admixed go some way to replicate the complexity of normal tissues but cannot do so fully. Xenograft models of human tissue can also be used for preclinical testing to overcome some of these limitations, (Byrne et al., 2017). This type of model involves the direct transplantation of the human tissue in immunodeficient mice. This method regardless of the inoculation method (i.e. orthotopically or subcutaneously) has resulted in more accurate and predictive models compared to *in vitro* 2D and 3D cell cultures, (Ruggeri et al., 2014). Xenograft models have commonly been used for studying the breast structure and development. For example, Chew and colleagues studied in 2013 the changes occurring to the breast tissue in a xenograft model of low- and high-density

human breast tissue in SCID mice which were either pregnant, nulliparous, or undergoing lactation or post-partum involution. The model helped to demonstrate the dynamic changes occurring in the glandular tissue area, stromal areas, and adipose areas as well as changes in the MD observed by radiographic measurements, (Chew et al., 2013). In 2014, Chew et. al used the same model to study the effects of estrogen and tamoxifen on human breast tissues. The low-density tissue did not show any differences between the treatment groups while the high-density tissue showed significant differences observed by histopathology and radiographic examination, (Chew et al., 2014). Another similar study was published in 2015 to evaluate the correlation between COX-2 expression and increased MD of breast tissue. The study showed that COX-2 is highly expressed in the epithelial and stromal cells of breast tissues with increased MD. The expression was also increased by estrogen treatment, (Chew et al., 2015). However, the xenograft approach does not lend itself to high-throughput screening and novel in vitro approaches are required to facilitate this to drive forward breast cancer prevention research.

## 1.11 Hypotheses and Objectives

The initial hypothesis of this thesis was that the mechanisms of resistance to preventive tamoxifen could be defined by serial biopsy of women starting tamoxifen and subsequently supervising molecular analyses by change in percentage MD (greater or less than 10% reduction). However, the emerging data described above show MD reduction at 1 year is not a reliable biomarker. The hypotheses of the thesis is now that:

1. changes in molecular analyses in response to tamoxifen treatment can be used to predict response/resistance to tamoxifen and
2. that in vitro whole tissue culture systems can be developed to replicate the in vivo findings to further prevention research.

The aims of the project are:

1) to investigate the effects of tamoxifen on epithelial and stromal compartments of the normal breast in patients commencing preventive therapy

2) to identify patterns of response and resistance in gene expression and proteomic analyses that can be tested as predictive biomarkers in future studies.

3) To develop an *in vitro* culture model of intact human breast tissue that replicates the *in vivo* effects of tamoxifen.

# Chapter 2

# Materials and Methods

# 2 Materials and Methods

## 2.1 Materials

### 2.1.1 Antibodies

**Table 2.1: Primary antibodies used in IHC**

| Primary antibody | Host Species | Supplier | Catalogue number | Dilution | Clonality | Clone |
|---|---|---|---|---|---|---|
| **CONFIRM anti-Ki67** | Rabbit | Roche,Ventana | 790-4286 | Ready to use | Monoclonal | 30-9 |
| **CONFIRM anti-PR** | Rabbit | Roche,Ventana | 790-2223 | Ready to use | Monoclonal | 1E2 |
| **ER** | Rabbit | ThermoFisher | RM-9101-S1 | 1:100 | Monoclonal | SP1 |

### 2.1.2 List of General Reagents

**Table 2.2: List of reagents, suppliers and catalogue numbers**

| Reagents | Supplier | Catalogue Numbers |
|---|---|---|
| **0.05% Trypsin** | Gibco | 25300054 |
| **2-Mercaptoethanol (99%)** | Sigma-Aldrich | M7522 |
| **6 $cm^2$ culture petri dish** | Corning | CLS430166 |
| **Amphotericin B** | Gibco | 15290018 |
| **B-27 Supplement** | Gibco | 12587-010 |
| **96-well collection plate** | ABgene | Ab2800 |
| **96-well Elution plate** | Agilent | 5043-9311 |
| **FiltrEX$^{TM}$96-well White Filter plate membrane plate (0.2µm PVDF membrane, Sterile)** | Corning | 3505 |
| **BAMBANKER serum free freezing media** | ThermoFisher | NC9582225 |
| **Collagenase 1A/Hylauronidase** | Sigma-Aldrich | C2674 |

| | | |
|---|---|---|
| **Dispase 5U/ml** | Stem Cell Technologies | 07913 |
| **DMEM F12 (1X) + L-Glutamine, phenol red free** | Sigma | 21041 025 |
| **Ethanol Absolute** | VWR Chemicals | UN1170 |
| **Falcon cell culture insert for 24 well plate with 8.0 µm pore transparent PET membrane** | Scientific laboratory supplies | 353097 |
| **Foetal Bovine Serum (FBS)** | Gibco | 10270-106 |
| **Hank's Balanced salt solution (HBSS) 10X** | Sigma-Aldrich | H1641 |
| **Hank's Balanced salt solution (HBSS) liquid with calcium Chloride and magnesium chloride** | Gibco | 14025 |
| **Hepes Buffer Sloution** | Gibco | 15630-056 |
| **Human EGF** | MACS Miltenyi Biotec | 130-097-751 |
| **Insulin** | Sigma Aldrich | I9278 |
| **Methanol Absolute** | VWR Chemical | 67561 |
| **OLIGO$^{TM}$ R3.** | ThermoScientific | 1-1339-03 |
| **Penicillin-Streptomycin** | ThermoFisher | 15140122 |
| **Poly (2 hydroxyethylmethacrylate) (poly-HEMA** | Sigma-Aldrich | 25249-16-5 |
| **Sodium dodecyl sulfate (SDS)** | Sigma-Aldrich | 75746-250G |
| **S-Trap micro columns (<100µg)** | ProtiFi | C02-micro-10 |
| **Triethylammonium Bicarbonate (TEAB)** | Sigma | T7408-100ML |
| **Trypsin-EDTA (0.05%)** | Gibco | 25300-054 |
| **UltraPure Distilled Water DNase/RNase free** | Invitrogen | 10977-035 |
| **Urea** | Fisher | 57-13-6 |
| **VitroGel-RGD hydrogel (10mL)** | Tebu-Bio Ltd | TWG002 |

### 2.1.3 Buffers Formulation

**Table 2.3 LCM-MS buffer formulation**

| Buffers | Composition |
|---|---|
| **0.1% Formic Acid in water** | Add 1 mL of 88-100% formic acid to a 1000 mL graduated cylinder. Dilute to final volume of 1000 mL with deionized water and mix well. |
| **0.1% Formic Acid, 5% CAN** | Add 1 mL of 88-100% formic acid and 50 mL of Acetonitrile to a 1000 mL graduated cylinder. Dilute to final volume of 1000 mL with deionized water and mix well. |
| **0.1% Formic Acid,30% Acetonitrile (ACN) in water** | Add 1 mL of 88-100% formic acid and 300 mL of Acetonitrile to a 1000 mL graduated cylinder. Dilute to final volume of 1000 mL with deionized water and mix well. |
| **10% Formic Acid** | Add 100 mL of 88-100% formic acid to a 1000 mL graduated cylinder. Dilute to final volume of 1000 mL with deionized water and mix well. |
| **12% phosphoric acid** | Add 120 mL of 100% phosphoric acid to a 1000 mL graduated cylinder. Dilute to final volume of 1000 mL with deionized water and mix well. |
| **50% Acetonitrile (ACN)** | Add 500 mL of Acetonitrile to a 1000 mL graduated cylinder. Dilute to final volume of 1000 mL with deionized water and mix well. |
| **500mM stocks of DTT** | Mw of DTT is 155g/mol$^{-1}$, weight a small amount on a microbalance and add relevant volume of LC/MS grade water. |
| **500mM stocks of Iodoacetamide** | Mw of Iodoacetamide is 184g/mol$^{-1}$ and it was kept in darkness. Weight a small amount on a microbalance and add relevant volume of LC/MS grade water. |

| | |
|---|---|
| **B1** | 5% SDS (0.5g in 10ml), 50mM TEAB pH 8.5 (0.5ml 1M stock in 10ml), total composition of up to 10ml with Milli-Q water and a pH value of 7.5 with HCl (~10μl in 10ml). |
| **B2** | 5% SDS (0.5g in 10ml), 10M Urea (6g in 10ml), 50mM TEAB pH 8.5 (0.5ml 1M stock in 10ml), composition of up to 10ml with Milli-Q water and pH value of 7.5 with HCl (~10μl in 10ml). |
| **Hydrochloric Acid** | Ready to use |
| **S-Trap binding buffer** | 100mM TEAB, pH 7.1, 90% Methanol (LC-MS grade). 5mL of TEAB at pH 7.1with 45mL of LC-MS grade 100% methanol |
| **S-Trap digestion buffer** | 50 mM TEAB, pH 8.5. 100µL of 1M TEAB stock (pH8.5). Diluted in 1.9mL dd$H_2O$ will give 2 mL of 50mM TEAB at pH 8.5 |

**Table 2.4 BenchMark Ultra Medical System bulk reagents**

| Buffers | Company | Catalogue number |
|---|---|---|
| **Antibody Dilution Buffer** | Ventana | ADB250 |
| **EZ Prep Concentrate (10X)** | Ventana | 950-102 |
| **Reaction Buffer (10X)** | Ventana | 950-300 |
| **ULTRA Cell Conditioning (ULTRA CC1)** | Ventana | 950-224 |
| **ULTRA LCS (Predilute)** | Ventana | 650-210 |
| **SSC (10X)** | Ventana | 950-110 |
| **Bluing reagent** | Ventana | 760-2037 |
| **Haematoxylin** | Ventana | 760-2021 |

### 2.1.4 Kits

**Table 2.5 General kits**

| Kit | Company | Catalogue number |
|---|---|---|
| **RNAeasy Mini Plus** | Qiagen | 74104 |
| **UltraView Universal DAB Detection Kit** | Roche | 760-500 |

### 2.1.5 Breast Tissue Samples

#### 2.1.5.1 Manchester Cancer Research Centre (MCRC) biobank breast tissue samples

Normal breast tissue used to investigate *in vitro* tissue culture systems was obtained from women at high risk of breast cancer undergoing reduction mammoplasty at Wythenshawe Hospital, Manchester, UK with no previous history of breast cancer. Samples were reviewed by consultant breast pathologist. All patients provided written informed consent and some basic endocrine information (i.e., family history of breast cancer, whether oral contraception was being taken, number of children and whether they were breast-fed). Clinical data of patients participating in my study is explained in table 6. Samples were coded with a unique numerical identifier to ensure patient confidentiality. The procedures were approved by biobank research ethical guidelines. Samples were kept in 4°C environment; transported fresh on the day of surgery and immediately processed as described in chapter 5, (Figure 5.1). Patient characteristics is shown in (Table 2.6).

**Table 2.6 Patient characteristics. BC= Breast cancer. N/A= not applicable**

| Patient ID | Age | No. of children | No. of children breast-fed | Use of contraceptive | BC personal history | BC Family history | BRCA-1/2 Mutation Carrier |
|---|---|---|---|---|---|---|---|
| **BB7069N** | 35 | Unknown | Unknown | Unknown | No | Unknown | Unknown |
| **BB7071N** | 57 | 1 | Unknown | Unknown | Yes | Yes | Yes |
| **BB7074N** | 35 | 2 | Unknown | Unknown | No | Yes | Unknown |
| **BB7075N** | 48 | 3 | Unknown | Unknown | Unknown | Yes | Unknown |
| **BB7078N** | 55 | 0 | 0 | Unknown | Unknown | Yes | No |
| **BB7087N** | 36 | 2 | 2 | MIRENA | Unknown | Unknown | YES |
| **BB7088N** | 46 | Unknown | Unknown | Unknown | YES | YES | Unknown |
| **BB7089N** | 27 | 1 | 0 | Unknown | Unknown | Unknown | YES |
| **BB7129T1N** | 44 | Unknown | 0 | Unknown | YES | YES | Unknown |
| **BB7130T1N** | 39 | 2 | 1 | Unknown | NO | YES | Unknown |
| **BB7136T1N** | 45 | Unknown | 2 | Unknown | NO | YES | YES |
| **BB7145T1N** | 49 | Unknown | 2 | Yes | Unknown | NO | Unknown |
| **BB7149T1N** | 45 | Unknown | 1 | Unknown | NO | YES | Unknown |

#### 2.1.5.2 Breast Biomarker Chemoprevention (BBCP) Trial Normal Breast Tissue Samples

Premenopausal women at high risk of breast cancer were recruited to a pilot trial and received 20mg tamoxifen daily. Mammography must have been performed within 6 months of recruitment and was repeated 9-15 months thereafter as per standard of care. Sampling procedure was performed using 9G or 10G Vacuum Assisted Biopsy (VAB) under local anaesthesia and ultrasound guidance to obtain sufficient dense tissue for all planned analyses.

VAB samples were collected before and after 12 weeks of treatment and were coded with a unique numerical identifier to ensure patient confidentiality. Two biopsy cores were formalin-fixed and two snap-frozen biopsy cores were stored in -80°C. An additional 6 VAB cores were placed in DMEM media for transport to the lab at 4°C to be digested into single cells suspensions or cultured as intact tissue *in vitro*. Images, weights and total cells yield were recorded.

## 2.2 Methods

### 2.2.1 Tissue Processing and *in vitro* Tissue Culture

Fresh normal breast tissues were subjected to manual tissue slicing under sterile conditions in a flow hood to avoid contaminations. Excess fat tissue was discarded using surgical tools and tissue slices of approximately 0.5 mm thickness were used. Tissue slices were cultured in DMEM/F-12 medium (Gibco® life Technology™) supplemented with different serum constituents; 100 IU/ml penicillin-100 µg/ml streptomycin, 2.5 µg/ml Amphotericin B (Gibco® life Technology™), 10µg/ml Insulin (Sigma Aldrich), 10µg/ml Hydrocortisone (Sigma Aldrich) and 5µg/ml Epidermal Growth Factor EGF (Sigma Aldrich) at 5% $CO_2$ at 37°C and at atmospheric oxygen levels. Medium was replaced every 2 days to provide fresh nutrients.

Tissue slices were cultured in three different culture systems, 6 $cm^2$ plastic petri dish (PD), falcon cell culture insert for 24 well plate with 8.0 µm pore transparent PET membrane (PI) and the dynamic 3D Rotary Cell Culture System (RCCS™) (Synthecon Inc., Houston TX, USA). In both static conditions, tissue slices were cultured in DMEM/F-12 medium with different serum constituents; medium alone, 10% foetal bovine serum (FBS)

supplemented media and 10% charcoal (Sigma) stripped-FBS supplemented media, while explants cultured in the 50 ml-HARV RCCSTM culture vessels (Synthecon Inc., Houston TX, USA) were cultured in FBS supplemented media. Tissue slices were fixed at Day 0, 7,14 and 21 in 10% neutral buffered formalin for 24 hours at room temperature. Subsequently, tissue slices were embedded in paraffin and 4 µm sections were generated for histological and immunohistochemical analysis.

### 2.2.2 Hydrogel culture system

Tissue slices were embedded between two layers of Xeno-free tunable hydrogel modified with Arginylglycylaspartic acid (RGD) peptide hydrogel, (VitroGel®-RGD hydrogel, TWG002). Falcon cell culture insert for 24 well plate with 8.0 µm pore transparent PET membrane was used in this system. To prepare the bottom layer of gel, equal volumes of 0.5x PBS, VitroGel 3D-RGD gel and DMEM medium supplemented with B27+LGlu (1:1:1) were mixed gently to avoid bubbles. 100µl of hydrogel mix was added in each insert and 700µl medium to each well. The culture plate with inserts were then incubated for 1-2 hours at 37°C until set. 1$mm^3$ tissue chunk was added to the top of the gel. Top layer of hydrogel was then prepared. The top layer of gel was prepared by mixing equal volumes of 0.5x PBS with the gel and Medium (1:1:1). The hydrogel was mixed gently and 150 µl of hydrogel was added on top of tissue. Plate was incubated overnight at 37°C to set fully. 200µl of medium was added to the set gel. Tissue slices were collected at Day 3, 7 and 14 using tweezers and placed in formalin. Medium in the well was exchanged

every 2 days. 50% of medium from the well was exchanged every 3-4 days and 200 µl medium was added to the top of the hydrogel.

### 2.2.3 Dissociation of normal human mammary tissue - vacuum-assisted biopsy (VAB)

Normal breast tissues were obtained via VABs from women before and after they had received Tamoxifen treatment. Each VAB sample was given a trial unique identification code to ensure patient privacy confidentiality. Human mammary tissue was transported from the operating room on ice in sterile tubes in DMEM/F12 + 1% penicillin-streptomycin and immediately processed. Under sterilized conditions, breast material was manually minced into small fragments (approximately 2mm cubes) by using a scalpel and incubated in Dissociation media: 9.75 mL of phenol red free DMEM medium supplemented with 3.75 ml of 7.5% Bovine Albumin Fraction V (BSA Fraction V) solution, 1.5 mL of 1mg/mL collagenase/hyaluronidase, 7.5 µl of 5µg/mL insulin and 0.5% penicillin-streptomycin. The breast tissue was digested overnight at 37$^{o}$C with shaking at 100 rpm. After enzyme digestion, the dissociated breast cell suspension was transferred into 50mL centrifuge tubes to be centrifuged at 450 x g for 5 minutes at 4°C. The fat layer was discarded and the epithelial pellet was resuspended in 30-40mL of DMEM/F12 medium to be washed and centrifuged at 450 x g for 5 minutes at 4°C. After the wash, the cells were resuspended in 10 mL of DMEM/F12 and centrifuged for 4 minutes at 200 x g at 4°C. The pellet from this centrifugation is enriched (but is not pure) for epithelial cells. The supernatant from this slow centrifugation is enriched for human mammary fibroblasts. The pellet was washed until the supernatant became clear. Then, 1 mL of pre-warmed 0.05% Trypsin-EDTA was added to

the enriched epithelial pellet pipetting it up and down gently with a P1000 pipette for 2 - 3 minutes. The sample may become stringy due to lysis of dead cells and the release of DNA. Next, 10mL of cold Hank's Balanced salt solution liquid with calcium chloride and magnesium chloride (Gibco) supplemented with 10mM Hepes (Gibco) and 2% FBS (HF) were added to stop the digestion and centrifuged at 450 x g for 5 minutes at 4°C. The supernatant was removed carefully with a pipette. Pre-warmed 5 mg/mL dispase (StemCell Technologies) was added to the sample and pipetted for 1 minute with a P1000 pipette to further dissociate cell clumps. Then, 5 mL of cold HF was added and the pellet was filtered using 70µm and 40µm sieves to yield a single cell suspension and spun at 450 x g for 5 minutes at 4°C. The supernatant was discarded carefully, and the pellet was resuspended in 1 mL of HF. Total cell concentration was determined using modified Fuchs Rosenthal-counting chamber.

### 2.2.4 Mammosphere Formation Assay

Normal breast epithelial cells with a concentration of 10,000 cells/well in 2 ml of mammosphere media were plated in 6-well plates coated with poly (2 hydroxyethylmethacrylate) (poly-HEMA,Sigma). PolyHEMA (Sigma) was prepared by adding 6g of PolyHEMA (Sigma, Cat# P3932) to 500ml of 95% ethanol and stirring constantly on a heated plate until complete dissolution. 1 ml of polyHEMA was added to each well of a six-well plate and left in an oven at 40°C for 48hours. The plates are then ready to use for mammosphere forming assays. Cells were plated in phenol red free DMEM/F-12 medium with GlutaMAX, supplemented with B27 (Gibco, 12587-010), 20 ng/ml EGF, and 100IU/mL penicillin-100 µg/mL streptomycin in a humidified atmosphere at

37°C in 5% $CO_2$. After 9–11 days, mammospheres with ≥50μm diameter were counted microscopically at x40 magnification. Mammosphere forming efficiency was calculated by dividing the number of mammospheres in each well by the number of cells seeded and expressing this as percentage.

### 2.2.5 Morphometric analysis

To investigate morphological alterations in normal breast tissues, a semi-automated method using Hematoxylin and Eosin (H&E) stained sections was applied. Slides stained with H&E were scanned using Aperio Digital Pathology Scanner (Leica Biosystems Aperio) at 20X. Aperio ImageScope was then used to view digital images and the different tissue compartments were manually annotated as shown in (Figure 2.1-a). Each annotation layer was labelled and then numerical information was exported to XML files to be processed for further calculations. Total tissue area, ductal area, lobular area, stromal area and adipose area were identified and measured. Five lobules of the same size were chosen randomly and the number and the area of each acinus (blue) as well as intralobular terminal duct epithelium (green) within each lobule (red) was measured, (Figure 2.1-b). The percentage of area of each breast tissue compartments at the baseline and post-treatment were calculated.

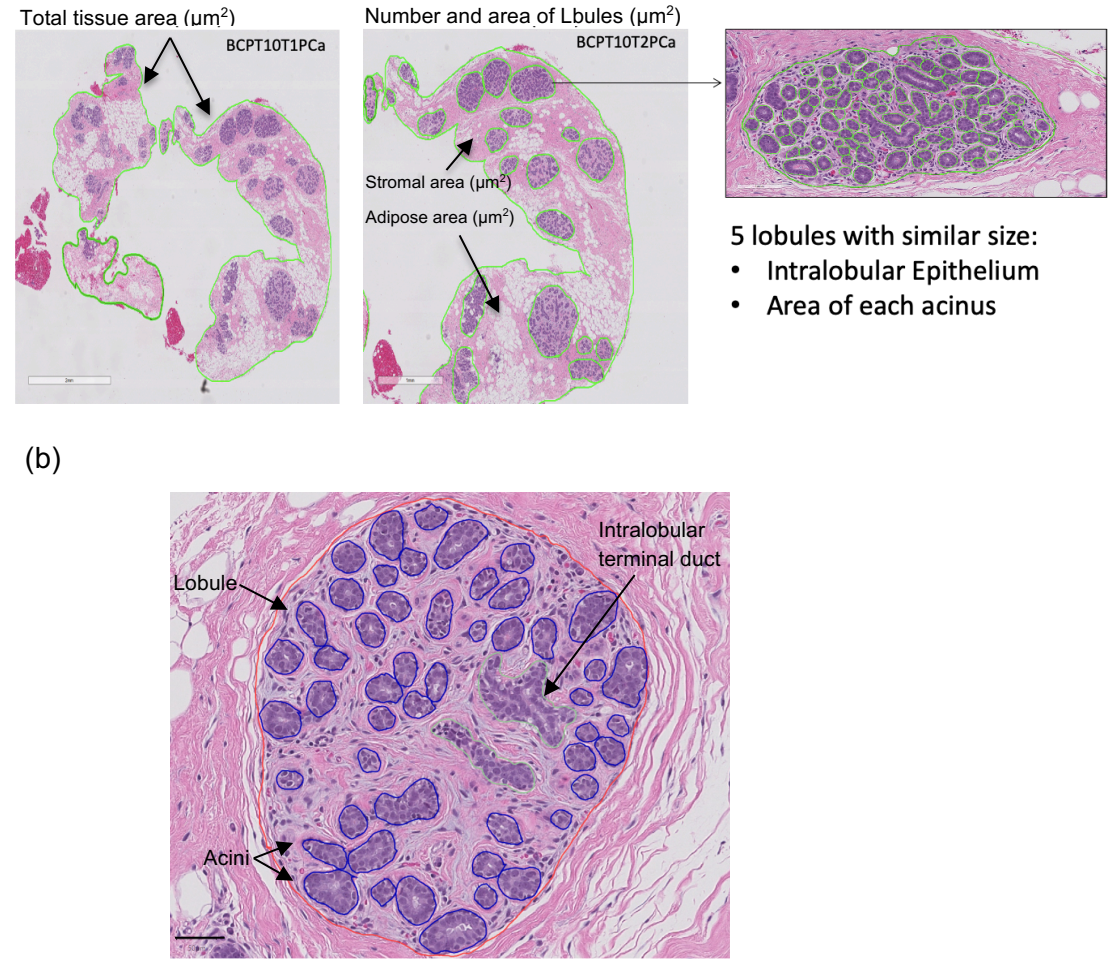


**Figure 2.1 Image analysis of normal breast tissue**. Normal breast tissue biopsies were fixed in 10% formalin and embedded in paraffin. 4μm sections were then prepared and stained with H&E. (a) Total tissue area; lobular area; stromal area and adipose areas were identified and measured. (b) Five lobules of the same size were chosen randomly and the number and the area of each acinus (blue) as well as intraductal epithelium (green) within each lobule (red) was measured. The percentage of area of each breast tissue compartments at the baseline and post-treatment were calculated. Slides were scanned using Aperio Digital Pathology Scanner (Leica Biosystems Aperio) at 20X. Aperio ImageScope was then used to view digital images and the different tissue compartments were manually annotated. Scale bar: 50 μm.

### 2.2.6 Immunohistochemistry (IHC)

#### 2.2.6.1 Hematoxilyn and Eosin Staining

The sections were dewaxed by submerging them into fresh xylene three times for 10 minutes each time. Then, they were rehydrated by submerging them into absolute ethanol for 5 minutes. This step was repeated twice. Sections

were then submerged into 70% ethanol for 10 minutes. The slides were washed for 1 minute under running tap water. Slides were then submerged into Gills twice for 3 minutes and then washed under running water for 2 minutes. Next, counter-staining with hematoxylin for 1 minute to visualise the nuclei and the overall structure of the tissue. Next, they were washed in running tap water for 1 minute. The sections were dehydrated by submerging the slides into a graded ethanol: 70% alcohol for 1 minute, followed by 1 minute in 95% ethanol and then absolute alcohol twice for 1 minute. Slides were kept on the bench to dry out at room temperature for 10 minutes. The slides were submerged into fresh xylene for 1 minute before coverslips were added using Ralmount glue.

#### 2.2.6.2 Automated immunostaining using Ventana medical system

Immunohistochemistry was performed using an automated method (BenchMark Ultra, Ventana medical system 790-2223) to ensure consistent staining quality. Confirm Anti-Ki67 (30-9) and Confirm Anti-PR (1E2) antibodies were ready to use. ER (RM-9101-S1) antibody was diluted in antibody dilution buffer, (1:100). Staining was done using UltraVIEW universal DAB detection kit. Slides were de-paraffinized under standardized conditions. Then, antibodies were used at defined concentration as described in (Table 2.1.1) at 37°C. Incubation periods were different for each antibody. Confirm Anti-Ki67 (30-9), was incubated for 32 minutes while ER and Confirm Anti-PR (1E2) antibodies were incubated for 16 minutes. Sections were blocked by A/B block (Biotin Blocking). Sections were counter-stained with haematoxylin II for 4 minutes followed by bluing reagent for 4 minutes. Next, they were

submerged in soap for 10 minutes to get rid of the oil and washed in running tap water. The sections were dehydrated to prepare them for coverslip. The slides were scanned using a Leica SCN400 slide scanner and visualised using Aperio ImageScope Digital Pathology Slide viewer (Leica Biosystems).

### 2.2.7 Analysis of IHC staining by automated HALO™ Image Analysis software

Quantification of epithelial cells was performed using the automated HALO™ Image Analysis software (v3.2.1851). We used the annotation tool to quantify epithelial cells in lobules (Green annotation) and duct (Yellow annotation) separately, (Figure 2.2, a-b). The software was able to detect the epithelial and stromal regions. Tissue Classifier add-on utilizes algorithm to identify different regions in the tissue section, depending on region colour, texture, and region's specific features. For example, we had trained Classifier add-on tool by highlighting several stromal regions with green colour while highlighting the acinar area with red colour. Glass and adipose regions were highlighted in yellow and were excluded as well. After labelling both regions, we excluded stromal regions from our analysis as shown in (Figure 2.2, c-d). HALO™ labelled positive nuclear staining of protein of interest with red, orange and yellow while negative cells were labelled with blue colour. Total epithelial cells, positive cells and negative cells were quantified by HALO™, (Figure 2.2 e-f). Each paired-sample was represented by two cores at the baseline and post-treatment. Where possible, I counted a minimum of 1000 epithelial cells per sample.

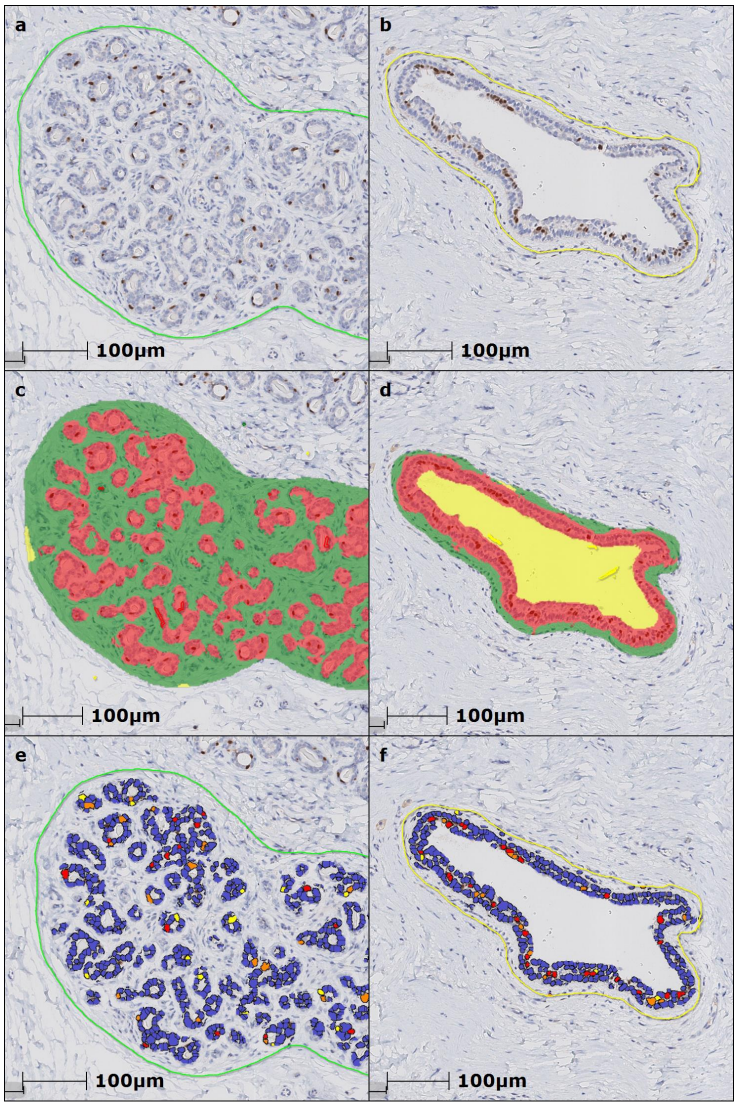


**Figure 2.2 Quantification of epithelial cells was performed using HALO™ Image Analysis software (v3.2.1851).** Lobules (a) and duct (b) were annotated and analysed separately. Stroma was detected in green and excluded from our analysis. Epithelial cells were detected in red and glass area was detected in yellow, (c-d). (e-f) Halo identifies negative epithelial cells in blue and positive strong nuclear staining in red, moderate nuclear staining in orange and weak nuclear staining in yellow. Each paired-sample was represented by two cores at the baseline and post-treatment. Where possible, a minimum of 1000 epithelial cells per sample were counted.

### 2.2.8 Gene Expression Analysis

#### 2.2.8.1 Total RNA extraction

Snap-frozen patients' core samples from BBCP trial and MCRC biobank were obtained for RNA sequence approach. Total RNA purification was done by using RNeasy® Mini kit, (Qiagen®). In brief, 10µl of β-Mercaptoethanol (β-ME)

was added to 1ml of lysis buffer (RLT) before use. Frozen tissue was placed in liquid nitrogen and ground thoroughly with a RNase-free mortar and pestle. Liquid nitrogen was allowed to evaporate, without allowing the tissue to thaw. 600µl of RLT Buffer was added to tissue powder and the lysate was directly transferred into a QIAshredder spin column placed in a 2 ml collection tube and centrifuged for 2 min at full speed. Using the micropipette, the supernatant (lysate) was carefully transferred into a new microcentrifuge tube and 600µl of 70% ethanol was added into the cleared lysate and mixed immediately by pipetting. The sample was transferred to a RNeasy spin column placed in a 2 ml collection tube and centrifuged for 15 seconds at ≥ 8000 x g. The flow-through was discarded. 700µl of RW1 Buffer was added to the RNeasy spin column and centrifuged for 15 s at ≥8000 x g (≥10,000 rpm) to wash the spin column membrane. The flow-through was discarded. 500µl of Buffer RPE were added to the RNeasy spin column and centrifuged for 15 s at ≥8000 x g to wash the spin column membrane and the flow-through was discarded. This step was then repeated; however, the centrifugation was done for 2 minutes. To eliminate RPE buffer, RNeasy spin column was then placed in a new 2 ml collection tube and centrifuged at full speed for 1 min. Finally, RNeasy spin column was placed in a new 1.5 ml collection tube and 30–50µl RNase-free water was added directly to the spin column membrane. The lid of the column was gently closed and centrifuged for 1 min at ≥ 8000 x g to elute the RNA sample. RNA samples were stored at -80°C.

#### 2.2.8.2 RNA Quality Control

To investigate the quantity and quality of the total RNA extracted from the samples before performing RNA sequencing, the 2100 Bioanalyzer (Agilent 2100 Bioanalyzer system, Agilent Technologies) and the Qubit (Thermofisher Scientific) were used. The 2100 Bioanalyzer is a chip-based nucleic acid system that performs electrophoresis analysis of DNA, RNA, and protein samples. The system was used to evaluate RNA quality by looking at the ribosomal RNA (rRNA) peaks (18S and 28S for eukaryotic rRNA). (Figure 2.3-a) shows an electrophoresis summary of the two integral rRNA subunits. To calculate the RNA concentration, the area under the RNA electropherogram and the intensity of the bands are measured and compared to that from the ladder. The upper band (28s rRNA) intensity is stronger than the lower rRNA band (18s rRNA) and this is a good sign of lack of degradation. In general, the ratio of 28s rRNA subunits to 18s rRNA subunits derived from mammalian cells should be present at a ratio of 2:1. Since those 2 bands appear as distinct entities without smearing between or below those subunits, RNA is sufficiently intact and not degraded, and therefore, it will work in functional assays.

RNA Integrity Number (RIN) value was also calculated. It is an important value to assure an accurate quantitative measurement of gene expression of the sample. It shows how intact and undegraded the RNA is. RIN values range from 1, which considered highly degraded, to 10 which means that RNA is entirely intact. RIN ≥7 is considered optimal for downstream applications. (Figure 2.3, b-i) presents an example of good RNA integrity for one of the BBCP samples and (Figure 2.3b-ii) shows an example of a degraded RNA sample.

(a)

[i] [ii]

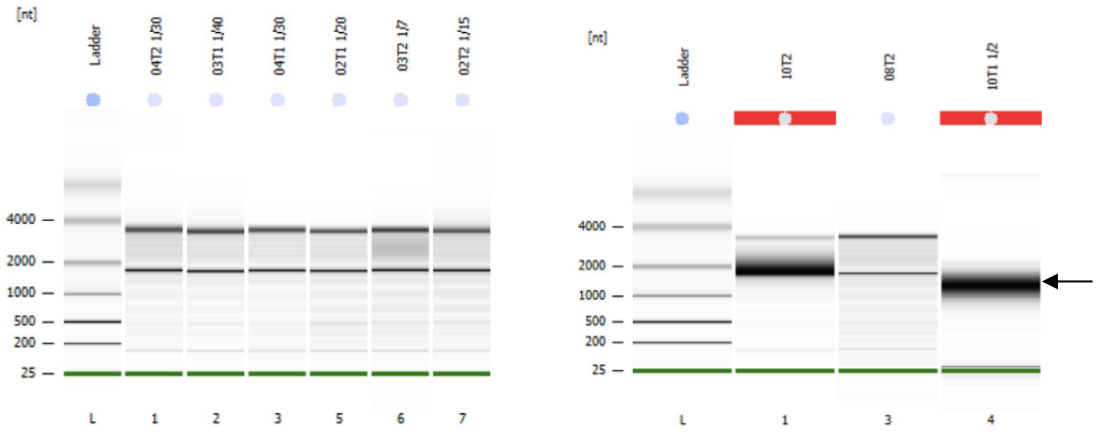


(b)

[i] [ii]

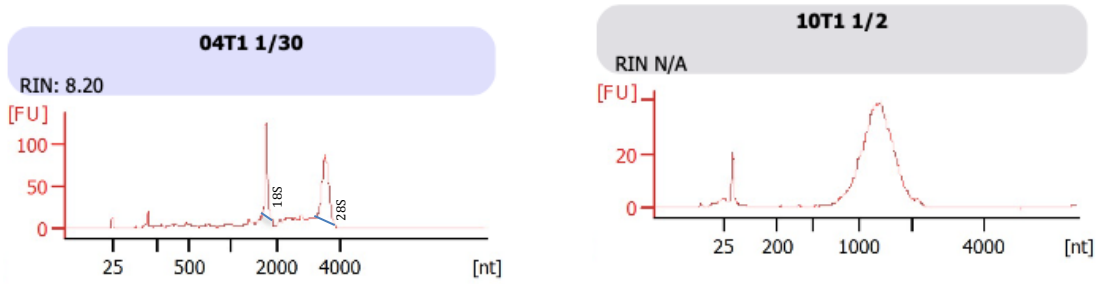


**Figure 2.3 Illustration of good and bad RNA quality samples using the 2100 Bioanalyzer.** Electrophoresis was used to measure RNA concentration. The area under the RNA electropherogram and the intensity of the bands are measured and compared to that from the ladder. (a-i) The upper band (28s rRNA) intensity is stronger than the lower rRNA band (18s rRNA). (a-ii) Smeared bands indicates RNA samples degradation. (b-i) Electropherogram graph shows a perfect distinguished peaks for both 18s and 28s rRNA and therefore RIN value of 8.20 is assigned to the sample. (b-ii) Graph did not show distinguished peaks which indicate that RNA sample is degraded.

#### 2.2.8.3 RNA-Sequencing

##### 2.2.8.3.1 Library preparation

Library preparation was performed through the CRUK Manchester Institute Molecular Biology Core Facility. Indexed polyA libraries were prepared using the Agilent SureSelect Automated Strand-Specific RNA Library Prep for Illumina (G9691B). An input of 200ng of total RNA was used with 14 cycles of amplification. Libraries were quantified by qPCR using Kapa Library Quantification kit for Illumina (Roche, cat no. 07960336001). Paired-end 100bp sequencing was performed by loading 500pM equimolar by clustering 40 million reads per sample of the library pool on a NovaSeq 6000 sequencer with standard loading (Illumina inc.).

### 2.2.9 Preparation of LCM captured tissue for mass spectrometry

#### 2.2.9.1 Sample preparation

Six pairs of patients' samples from BBCP trial were used for mass spectrometry analysis. Three pairs of samples were grouped in Responsive Group 1 including BCPT03, BCPT06 and BCPT08. The second three pairs were included in Responsive Group 2. These samples were BCPT04, BCPT07 and BCPT11. Blocks of tissue biopsies were used in this approach. Tissue sections of 5µm were generated and mounted in (Microdissection-Micromanipulation-Imaging) MMI membrane slides, RNase free slides. These sections were dewaxed and stained with hematoxilyn and eosin staining as described in section (2.2.6.1). The methed was illustrated in (Figure 2.4).

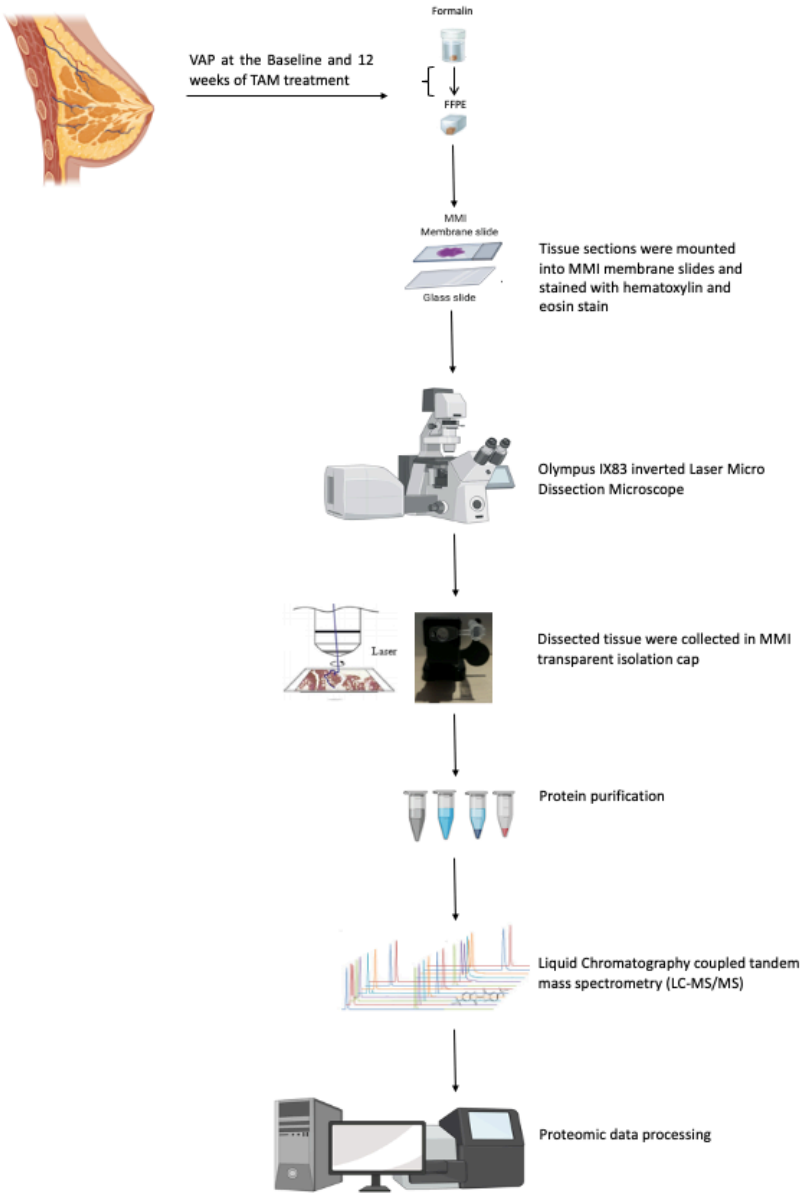


**Figure 2.4: A diagram of samples preparation and computational analysis of LCM-MS data for peptides Identification.** 5 µm sections of FFPE tissue were mounted onto MMI Membrane Slides (MMI), stained with H&E. From tissue sections mounted on MMI slides, equal volumes of lobular epithelium & peri-lobular stroma and were dissected using a MMI CellCut Laser Microdissection system. Tissue was collected using MMI transparent isolation caps and pooled with dissected tissue from the same region to a final volume of 0.05mm$^3$. Formalin-mediated protein cross-linking was reversed by resuspending the dissected tissue in 50mM TEAB (triethyl ammonium bicarbonate) containing 5% SDS (w/v) and heating at 95˚C for 20mins, then 60°C for 2 hours. To assist the solubilisation of extracellular matrix (ECM) proteins, urea and DTT (dithiothreitol) was added to the samples to a final concentration of 8M and 5mM respectively. Samples were then sonicated in a LE220-Plus focused ultrasonicator (Covaris) for 10 mins. Samples were reduced and alkylated, then proteins were isolated and digested with trypsin using S-Trap™ spin columns (Protifi) as per the manufacturer's instructions. Peptides were desalted using POROS Oligo R3 beads (Thermo fisher) and analysed by LC-MS/MS (liquid chromatography - tandem mass spectrometry) using an UltiMate 3000 Rapid Separation LC system (RSLC, Dionex Corporation) coupled to a Q Exactive HF™ mass spectrometer (Thermo Fisher).

Using MMI CellCut Laser Microdissection system and MMI CellCut software, slides were scanned at 4X magnification to visualize total tissue morphology. Manually, we used drawing tool to select area of interest. Laser was used to dissect region of interest, (Figure 2.5 a-d) and micro-dissected areas were collected in MMI Isolation caps, (Figure 2.5e) Approximately, 6,813,462 $\mu m^2$ of Lobules compartments were collected from each sample at baseline and after-treatment separately. Samples were proceeded to peptide extraction.

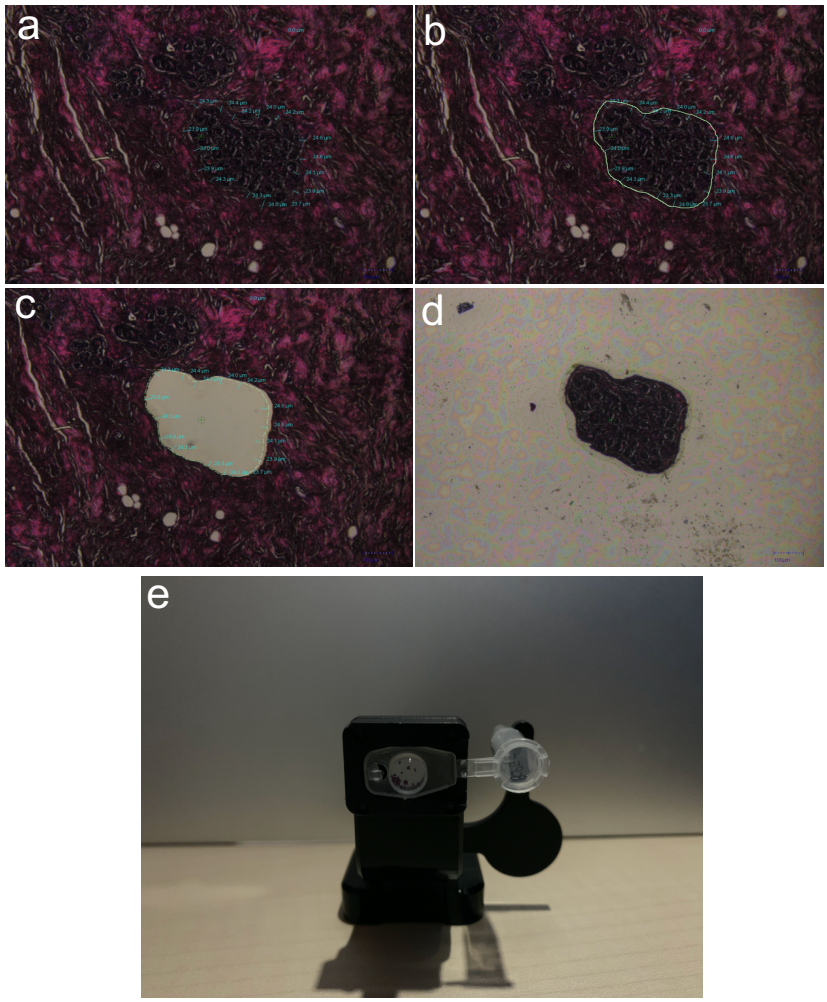


**Figure 2.5 Laser captured micro-dissected tissue.** From tissue sections mounted on MMI slides, equal volumes of lobular epithelium and peri-lobular stroma, (a-d) were dissected using a MMI CellCut Laser Microdissection system. Dissected tissues were collected using MMI transparent isolation caps (e) and pooled to a final volume of 0.05$mm^3$.

#### 2.2.9.1.1 Crosslink reversal and ECM solubilisation

Equipment required for the method to be completed includes 1.5ml “Safe-Lock” Eppendorf tubes and Covaris LE220, sonicator and 130μl Covaris tubes. Buffers B1 and B2 contain 5% SDS; a protein solvent that dissolves proteins. Firstly, the heat block was set to 95°C. Once the block is heated, 25μl of B1 was poured into a 1.5ml LoBind Eppendorf tube. Yellow pipette tip was cut at an angle of 45°, dipped in the buffer B1 to moisten the tip and used to scoop/scrape tissue from tissue capture tube cap. After this, tissue was transferred into the decanted buffer B1. To ensure that all of the tissue is transferred to the liquid a fresh needle was used.

The samples were incubated at 95°C shaking at 1,400 rpm for 20 min, then 60°C shaking at 1,400 rpm for 2 hours was progressed. Then, 75μl of buffer B2 was added to samples with 1μl of 500mM DTT (fc is 5mM) and they were incubated at 60°C for 10 min. DTT is a strong reducing agent and it was used to breakdown protein disulfide bonds. It also promotes enzymes and proteins stabilization.

B2 contains Urea which enhances protein unfolding indirectly by altering water structure and dynamics, it introduces nonpolar groups to water. This will minimize the hydrophobic effect and enable the exposure of the hydrophobic core residues. After incubation, samples were transferred to 130μl Covaris tube. Samples were sonicated in covaris LE220 Plus ultrasonicator running “130μl” programme. The programme was set up for two rounds of 600s time, 500w power, 20% duty factor, 200 cycle/burst and 100w average power. Finally, samples were transferred into new 1.5ml LoBind Eppendrof tubes. The

samples can be frozen until they are required or can be directly used towards the alkylation and reduction processes.

For the reduction and alkylation, 500mM DTT was added to samples, increasing final concentration by 5mM. After this, the samples were incubated at 60°C for 10 minutes on a covered heat block (to avoid evaporation/condensation) to reduce cysteine bonds. The samples were allowed to return cool to RT and then the Iodoacetamide was added to give a final concentration of 30mM (3x DTT concentration). Alkylation with iodoacetamide after cysteine reduction prevents the formation of disulfide bonds. Samples were incubated in the darkness for about 30 min at RT. the iodoacetamide was quenched by adding enough DTT to increase final concentration by 10mM. The samples were clarified from salt particles by centrifugation at 14000 RCF for 10 min and the supernatant was poured into fresh tube. The samples can be frozen at this point or used directly towards the S-trap clean up.

#### 2.2.9.2 S-Trap clean up and digestion

The materials which are required for the S-trap clean up along with its digestion includes S-Trap micro (ProtiFi) recommended for <100μg protein. The process of proteins denaturation was performed by acidification followed by exposure to high methanol concentration.

In the beginning, the samples were acidified with the help of 12% $H_3PO_4$ (1:10 dilution in sample to give a 1.2% final concentration). After acidifying the samples, 6x S-trap binding buffer was added to the samples and the S-trap columns were placed into the clean tubes having a length of 2 ml. Later on,

the columns were loaded to 150μl at a time and were centrifuged at 4000 RCF for 1 min. Multiple loads were performed and the flow through was discarded after every spin. The liquid coming into contact with binding matrix will detrimentally affect peptide yield. After this, the proteins were washed with 150μl S-Trap binding buffer, spun at 4000RCF for 1 min. The process was repeated for a total of 10 washes. S-trap column were placed into the fresh 1.5ml collection tubes and 2μg trypsin in 25μl of digestion buffer was added to the columns, then, columns were incubated for 1 hour at 47°C without shaking.

Samples can be digested overnight if it is required, this will significantly contribute toward the decline in the missing cleavages from 20-30% to 10-15%. Whilst it must be ensured that column do not dry by adding more digestion buffer. After incubation, the columns were moved to the fresh collection tubes of 2ml. 65μl of digestion buffer was added to columns and they were centrifuged at 4000RCF for 2 min for the elution of peptides. Further elution was brought up by the addition of 65μl 0.1% formic acid in water, spun at 4000RCF for 2 min.

For the final elution 30μl of 0.1% formic acid, 30% ACN were added and column were spun at 4000RCF for 2 min. The peptides can be stored overnight at a temperature of 4°C in this buffer. For prolonged period of storage peptides samples were lyophilized in a speedvac and stored at 4°C.

#### 2.2.9.3 Peptide desalting

The peptide desalting requires POROS R3 beads. Lyophilized peptides were re-suspended in 200μl of 5% acetonitrile (ACN), 0.1% formic acid. The pH of the samples was checked with the help of Whatman indicator strips and was

adjusted to ~pH 3 with 10% formic acid. Usually, the addition of 10μl 10% formic acid will adjust pH close to 3. After preparing 10mg/ml solution of POROS R3 beads in 50% ACN, 100μl of 10mg/ml POROS R3 bead solution was added into the single well of a 96-well filtration membrane plate (0.2μM PVDF membrane).

A collection plate was placed beneath the membrane plate and both plates were gyrated in centrifuge at 200g 1min, which allows the separation of liquid phase from the beads. Further, the collection plate was emptied and beads were washed once in 0.1% formic acid in ACN, re-suspend gently via pipetting and spun out liquid phase and collection plate was emptied again like before. The beads were washed for 2 times in 0.1% formic acid in water. After washing, beads were re-suspended in 200μl of sample and were placed on shaking block at 800rpm for 2 min for centrifugation.

After this, the beads were washed twice in 0.1% formic acid in water by the use of shaking block at 800rpm for 2 min to mix. Then, the collection plated was changed with the elution plate and beads were re-suspended in 50μl of 30% ACN, 0.1% formic acid, spinning was performed for the separation of liquid phase but it was not discarded. The step including 30% ACN, 0.1% formic acid elution was repeated pooling both fractions and finally the pooled elution fractions were transferred to the injection vial and was lyophilized in the speed vacuum. To check the concentration of the peptides, peptides were resuspended in 10μl 5% ACN, 0.1% formic acid in water; 1μl was used to spot on Direct Detect cards and assay peptide concentration with the Direct Detect spectrometer. System has poor precision/accuracy, however values above

0.2ng/µl are reassuring. Finally, peptides were lyophilized and dried peptides were stored at 4°C at dark place.

#### 2.2.9.4 Liquid chromatography coupled tandem mass spectrometry (LC-MS/MS)

Dried peptide samples were submitted to Biological Mass Spectrometry facility for analysis using an ultiMate® 3000 Rapid Separation LC system (RSLC, Dionex Corporation) coupled to a Thermo Q-Exactive HF (QE) Quadrupole-Obitrap mass spectrometer. Briefly, 10 µL 0.1% formic acid in 5% acetonitrile (ACN) was used to resuspend the dried peptides. The formic acid was 0.1% in water at mobile phase A, while at the mobile phase B, the formic acid was 0.1% in ACN. By employing a flow rate of 300 nL/min and a 75 mm x 250 µm inner diameter CSH C18 analytical column (Waters), the solvent gradient was modified to be as following: 95% A and 5% B to 18% B at 58 min, 27% at 72 min, and 60% at 74 min. By using data dependent acquisition (DDA), peptides were randomly selected for fragmentation, and data was collected for 90 minutes in the positive mode.

#### 2.2.9.5 Mass spectrometry data analysis

MaxQuant (v1.6.14.0, available from Max Planck Institute of Biochemistry, Tyanova, Temu and Cox, 2016) was used to assess raw mass data. Features were identified using MaxQuant default parameters and afterwards scanned against the human proteome (UniProt database, August 2020). Oxidation of methionine (M) & proline (P) and Acetylation of protein N-terminus were set as variable modifications, whereas Carbamidomethyl (C) was set as a fixed modification. Un-modified, unique and with ‘match between runs’ enabled

peptides were used for peptide quantitation analysis using label-free quantification (LFQ) method. For laser capture microdissection experiments, the lobular tissue regions at baseline and post-treatment, were analysed independently.

### 2.2.10 Bioinformatics and Statistical Analysis

#### 2.2.10.1 RNA-Seq Analysis

Unmapped paired-end sequence from NovaSeq 6000 sequencer were tested by FASTQC, (http://www.bioinformatics.babraham.ac.uk/projects/fastqc). Files were processed with Nextflow (19.10.0), nf-core/rnaseq (1.3) pipeline, (Baylis et al., 2020; DI Tommaso et al., 2017). The analysis was performed in RStudio Workbench (1.4.1717.3) running R (4.0.3), and deployed as a shiny app on a server running R (3.6.0) and shiny (1.6.0). Differentially expressed gene analysis was performed with DESeq2 (1.26.0). Additional gene IDs were retrieved from Ensembl BioMart website (https://www.ensembl.org/biomart/martview/) with Ensembl Genes 101 dataset and Human Genes to map Ensembl Gene IDs to gene symbols and Entrez IDs for downstream analyses using the following attributes: 'Gene Stable ID', 'Gene name' and 'NCBI gene (formerly Entrezgene) ID'. Gene set enrichment analysis and pathway analysis was performed using ideal (1.10.0), fgsea (1.14) with MSigDB gene set collections, https://www.gsea-msigdb.org/gsea/msigdb/collections.jsp. limma (3.42.2), pathview (1.26.0), ggplot2 (3.3.3), pheatmap (1.0.12) were used for making plots. Tidyr (1.1.3), tibble (3.1.2), dplyr (2.0.6) and magrittr (2.0.1) were used for general data processing and formatting. Analysis was performed by Matthew Roberts at Cancer Research UK (CRUK) Manchester Institute.

#### 2.2.10.2 Ingenuity Pathway Analysis

Ingenuity Pathway Analysis (IPA) was performed for all differentially expressed genes. Ensemble gene IDs were submitted as identifiers and Log2 Fold change, p-value, p-adj were used as observation. Filters such as (Homo sapiens/Human) were applied to acquire relevant information. Submitting Log2 Fold change was applied since it is linked to the activation Z-score, which help understanding and predicting the directionality of enriched pathways independently from p-value, based on significant pattern match of up/down regulation.

#### 2.2.10.3 Principal components Analysis

Principal component analysis (PCA) is an unsupervised statistical technique that have been used to compare variability and relationship between different samples. It reduces the dimensionality of large dataset such as RNA seq and identify patterns between samples. It transforms large dataset into significant smaller dataset without losing important information, (Abid et al., 2018). PCA tool was used as exploratory data analysis to visualize samples clustering.

#### 2.2.10.4 Heatmaps of the fold change of genes

Heatmap figures of the fold change of genes were generated using R function (heatmap) from the ggplot2 package by Dalia Alghamdi at University of British Columbia (UBC).

#### 2.2.10.5 Absolute fold change heatmap of 300 genes

For *in vitro* culture systems experiments, two groups of tissue explants; Day 0 (D0) samples and tissue explant cultured for one week (W1), were compared, (n=5). The Log2 fold change, p-value and false discovery rate (FDR) was generated from DeSeq2. Genes with p value > 0.05 were removed. The top 300 differentially expressed genes were visualized on heatmaps. Analysis was performed by Matthew Roberts at Cancer Research UK (CRUK) Manchester Institute.

#### 2.2.10.6 Statistics

Statistical analysis for IHC, morphometry and MFE experiments was performed using GraphPad Prism. Data was assessed using non-parametric Wilcoxon matched pairs signed rank test. All P values were two sided and P values less than 0.05 were considered significant. $P<0.05$ (*), $P<0.01$ (**), $P<0.001$(***). Error bars were generated using standard error of mean (SEM).

Statistical analysis was performed using MSqRob, (Goeminne et al., 2016; Goeminne et al., 2020). The median of peptide intensities was used to normalise LFQ data. Core or edge sample regions were considered as fixed effects. Run, peptide sequence, and replication (depending on the experiment, biological or technical) were all considered as random effects. Peptides from contaminating proteins as identified by MaxQuant or proteins with less than two peptides were disregarded from statistical analysis. Analysis was performed by Robert Pedley at Wellcome Centre for Cell-Matrix Research, The University of Manchester.

# Chapter 3

# The Effects of Tamoxifen on Breast Tissue of Women at Increased Risk of Breast Cancer

# 3 The effects of tamoxifen on breast tissue of women at increased risk of breast cancer.

## 3.1 Introduction

Primary prevention (before cancers develop) is a highly attractive goal as it save the physical, psychological and financial burdens of cancer diagnosis, (Anthis et al.,2020).

Chemoprevention is defined as the application of pharmacological agents which aim to inhibit carcinogenesis, thus lower the risk of developing a cancer. In breast cancer, tamoxifen, which functions by blocking the effects of estrogen, was the first medication approved for prevention in both pre- and post-menopausal women, (Fisher et al., 1998). According to the Food and Drug Administration (FDA), women aged 35 years or older, that have a 5-year risk of invasive breast cancer of at least 1.67%, are eligible for tamoxifen therapy, (Freedman et al., 2003). Other authorities, such as The National Institute for Health and Care Excellence (NICE) in the United Kingdom, have approved the use of tamoxifen for pre- and post-menopausal women, although anastrozole is the preferred option in postmenopausal women due to its favourable toxicity profile. NICE guidance suggests chemoprevention should be recommended for women at high lifetime risk (>30%) of breast cancer and considered for those at moderate lifetime risk (17-30%). The recommended duration of breast cancer chemoprevention is five years, (Jones et al., 2021).

Meta-analysis of tamoxifen prevention trials shows a significant reduction in ER positive breast cancer but no impact on ER negative breast cancer or indeed breast cancer mortality, (Cuzick et al., 2013). A previous study has shown that the preventive efficacy of tamoxifen is only seen in women with

>10% reduction in mammographic density, (Cuzick et al., 2011). However, more recent studies suggest that most women experience density reductions with tamoxifen therapy, (Brentnall et al., 2020). Of concern, the meta-analysis of tamoxifen studies showed an increase in the number of ER negative breast cancers in tamoxifen vs placebo treated women indicating a need to identify women at increased risk of such cancers, in whom tamoxifen should perhaps be avoided.

One important and currently unmet clinical need is to identify primary factors that predict response to chemoprevention of breast cancer. A clinical trial was set up in Manchester, in which women at increased risk of breast cancer had breast biopsy immediately prior to commencing preventive tamoxifen and again after three months of therapy. Initially, the plan was to investigate the degree of change in mammographic density at the 1-year mark and determine whether we can categorize participants in our cohort into those who respond and those who are resistant to tamoxifen treatment. Subsequently, we wanted to correlate the molecular analysis to the degree of change in mammographic density at the 1-year mark. However, data were subsequently published showing that density reduction at 1 year is not a good predictor of ongoing reduction, (Brentnall et al., 2020). The focus of this study is thus to try to identify participants with differential response characteristics to preventive tamoxifen that might lead to a biomarker driven approach to personalise preventive therapy in future.

The effect of tamoxifen on proliferation, through changes in Ki67 expression, was the primary endpoint of the study. Additional analyses included expression of steroid hormone receptors (HRs), lobular morphology and serum hormone

levels. These data are presented in the following chapter before transcriptomic and proteomic data are presented in chapter 4.

## 3.2 Results

### 3.2.1 Breast Biomarkers Chemoprevention trial

Normal breast tissues were obtained from premenopausal women at increased risk but no previous diagnosis of breast cancer. Moderate or high risk of BC was defined by Tyrer-Cuzick 10-year risk, (Cuzick et al., 2013). The median age of participants at first biopsy was 43 years (range 35-47). Participants' characteristics are shown in (Table 3.1). The study design is shown in (Figure 3.1)

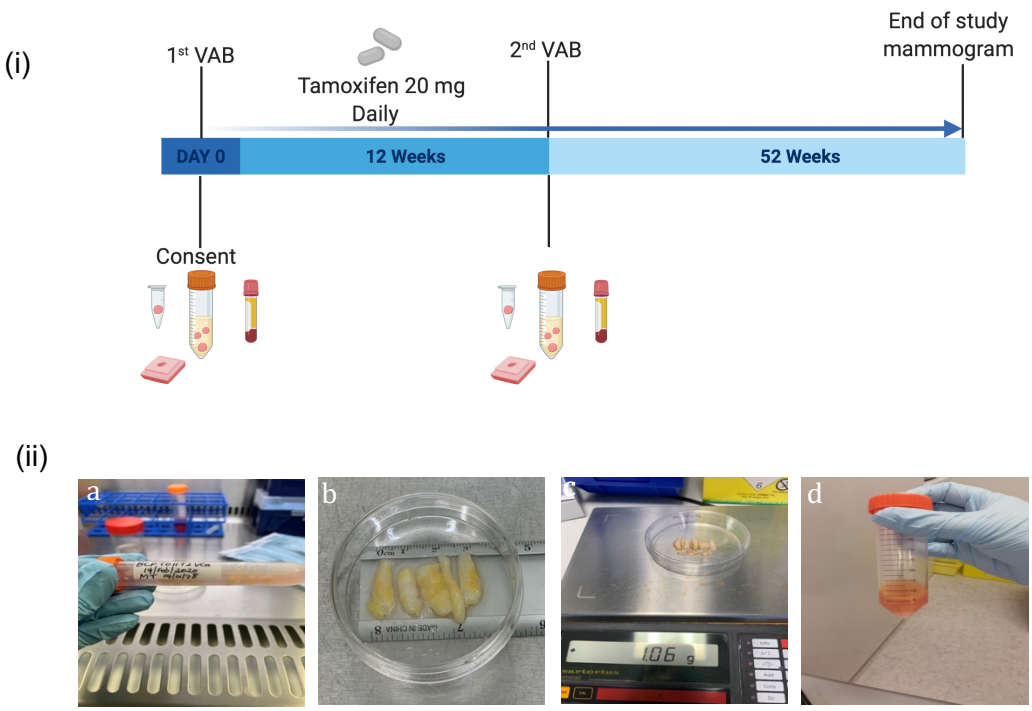


**Figure 3.1 The study design of breast cancer prevention trial BBCP. (**i) Eligible premenopausal women recruited to the prevention pilot trial. VAB samples were collected before and after 12 weeks of TAM treatment. For downstream analysis, 2 VAB cores were snap frozen in liquid nitrogen and 2 VAB cores were formalin-fixed. Breast Magnetic Resonance Imaging (MRI) screening is being performed at the baseline and at the final time point to analyse differences in breast density after treatment. (ii,a). VAB cores were coded with a unique numerical identifier. VAB cores were received in DMEM media to be digested and cultured *in vitro*. (ii,b-d) Images, weight and total cells yield with clear description of the samples were recorded.

**Table 3.1 BBCP Participant characteristics**

| Patient ID | Age at 1st VAB | Menarche | FFTP | Parity | OCP | FDR | SDR | Lifetime Risk | BiRads |
|---|---|---|---|---|---|---|---|---|---|
| **BCPT02** | 43 | 13 | Unknown | Unknown | Unknown | 1 | 4 | 1 in 3 | C |
| **BCPT03** | 38 | 13 | 30 | 2 | COCP: 17Y-29Y<br>Mirena: 34-current | 1 | 1 | 1 in 3 | C |
| **BCPT04** | 37 | 13 | Nil | 0 | COCP: 15Y-30Y | 1 | 0 | 1 in 3 | B |
| **BCPT05** | 40 | 13 | 35 | 1 | COCP: 17Y-27Y | 0 | 2 | 1 in 4 | C |
| **BCPT06** | 46 | 13 | Nil | 0 | Mirena current | 0 | 0 | 1 in 3 | C |
| **BCPT07** | 46 | 13 | 33 | 3 | COCP: 23Y-31Y<br>Mirena current | 2 | 0 | 1 in 3 | C |
| **BCPT08** | 47 | 13 | Nil | 0 | COCP: 16Y-28Y | 1 | 0 | 1 in 4 | C |
| **BCPT09** | 42 | 13 | 26 | 2 | COCP: 19Y-25Y<br>Mirena: 37Y-current | 1 | 1 | 1 in 4 | C |
| **BCPT10** | 35 | Unknown | Unknown | Unknown | Unknown | 2 | 1 | 1 in 2-3 | C |
| **BCPT11** | 41 | 10 | 18 | 3 | COCP: 16Y-25Y | 2 | 0 | 1 in 4 | B |
| **BCPT12** | 47 | 12 | 29 | 2 | COCP: 10Y-28Y | 1 | 1 | 1 in 4 | B |
| **BCPT13** | 44 | 12 | Nil | 0 | COCP: 16Y-35Y | 1 | 0 | 1 in 3 | C |
| **BCPT14** | 40 | 13 | 36 | 2 | Prior | 1 | 1 | 1 in 3 | C |
| **BCPT15** | 43 | 13 | 38 | 1 | Unknown | 1 | 1 | 1 in 4 | B |
| **BCPT16** | 48 | 15 | 31 | 11 | OCP: 18Y-24Y | 1 | 0 | 1 in 4 | C |
| **BCPT17** | 37 | 13 | 18 | 2 | None | 1 | 1 | 1 in 3 | B |
| **BCPT18** | 41 | 14 | 30 | 3 | OCP: 16Y-27Y | 0 | 2 | 1 in 4 | D |

FFTP= First full-term pregnancy. OCP= Oral contraceptive pills. FDR= First degree relatives. SDR= Second degree relatives. BiRads= Breast Imaging-Reporting and Data System. Nil= none

### 3.2.2 Tamoxifen significantly increases serum estradiol levels

As a first step, changes in steroid hormones (estradiol and progesterone) levels in serum were measured to investigate the response of pre-menopausal women to tamoxifen treatment. Data was obtained from the Biochemistry Department at Manchester University NHS Foundation Trust, Wythenshawe Hospital – a UKAS (United Kingdom Accreditation Service) accredited clinical laboratory. A significant increase in median estradiol levels from baseline (378.5pmol/L; IQR [307pmol/L-410pmol/L]) to 3 months (1060pmol/L; IQR [824pmol/L-1327pmol/L]; p=0.0039) was observed in the group overall, (Figure 3.2a-i). In contrast, no significant change in median serum progesterone levels were seen with tamoxifen treatment although a numerical increase in median levels was seen from baseline (23.05nmol/L; IQR [0.5nmol/L-36.5nmol/L]) to 3 months (27.05nmol/L; IQR [1.7nmol/L-81.1nmol/L]; p=0.1435); (Figure 3.2b-i). There was a great deal of variation in both the baseline and on treatment progesterone levels but with no clear pattern seen. Of note two participants with the progestin (levonorgestrel) releasing Mirena coil in situ (BBCPT03 and BBCPT07) had undetectable levels of progesterone at baseline but the implications of this are not clear.

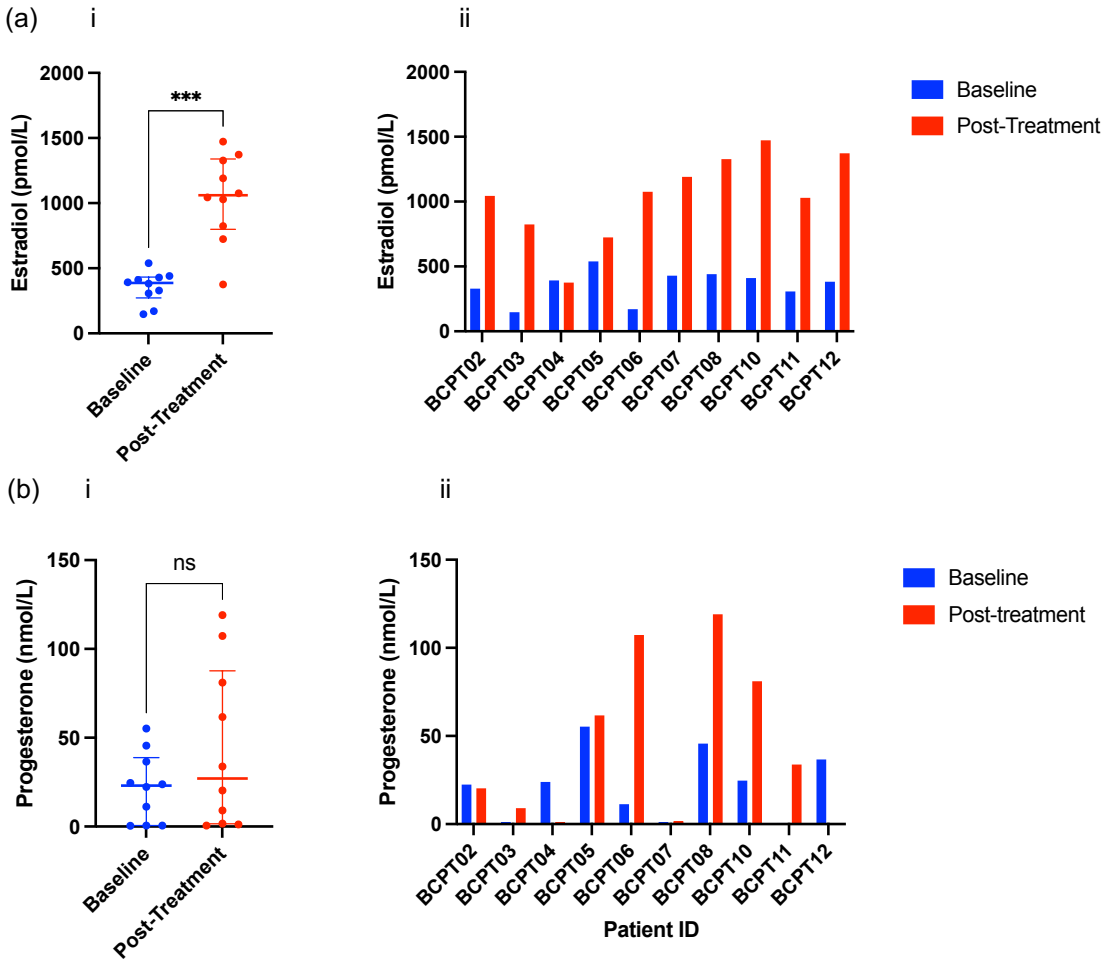


**Figure 3.2 Serum hormones level in premenopausal women at baseline and after 3 months TAM treatment.** (a-i) A significant increase in median estradiol serum levels. (a-ii) An increase in estradiol level in serum was seen in all Participants treated with TAM except for Participants BCPT04 and BCPT05 (b-i) No significant change in median progesterone serum level is seen after TAM treatment. (a-ii) Progesterone level in serum among Participants after TAM treatment. Data in scatter plot indicates individual values. Median is shown by horizontal line and interquartile range by the whiskers. Statistical significance was determined by Wilcoxon matched pairs signed rank test. N=10. *** $p \leq 0.001$.

### 3.2.3 Ki67 expression is reduced after tamoxifen treatment

To investigate proliferation in epithelial cells, the proliferation marker Ki67 was determined by immunohistochemistry (IHC). Formalin-fixed paraffin-embedded (FFPE) biopsies of participants' samples at the baseline and after treatment were sectioned and stained with Ki67 antibody and positive cell nuclei counted as a percentage of all epithelial nuclei. The median percentage of total epithelial Ki67 reduced with treatment from baseline 4.4% (IQR [3.8%-

7.4%]) to 3 months 2.9% (IQR [2.1%-5.4%]; p=0.0181); (Figure 3.3a-i). A similar pattern was seen in the acinar epithelium from baseline 4.3% (IQR [2.7%-5.9%]) to 3 months 2.1% (IQR [1.3%-3.05]; p=0.0125); (Figure 3.3b-i) and the ductal epithelium baseline 4.3% (IQR [4.1%-6.4%]) to 3 months 2.1% (IQR; [0.9%-4.7%]; p=0.058); (Figure 3.3c-i) although the latter did not reach statistical significance, (Figure 3.3. The response in the ducts appeared to be more heterogenous across the participants group than that in the acini (Figure 3.3c-ii).

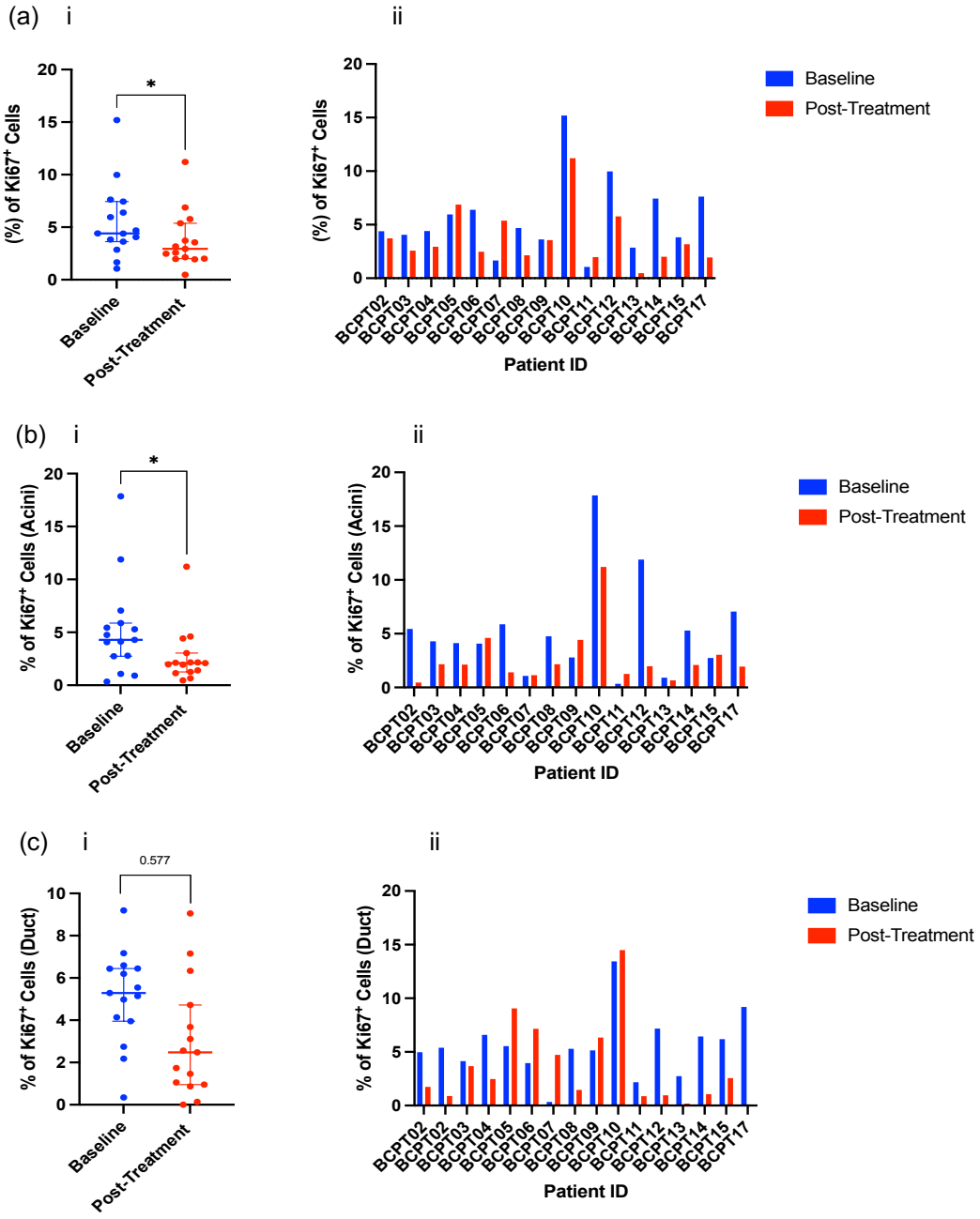

(d)

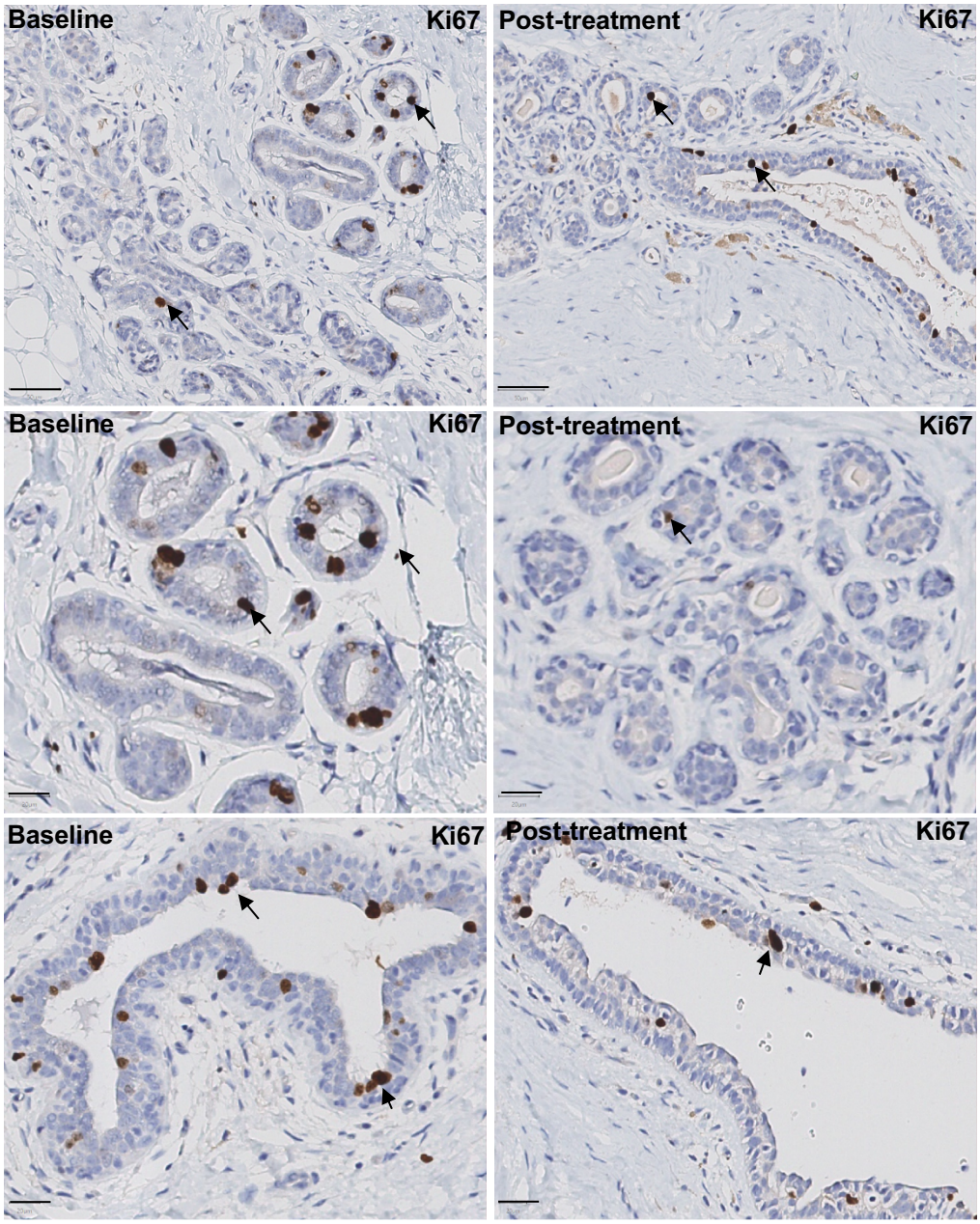


**Figure 3.3: The percentage of Ki67 positive cells and representative images of nuclear staining in normal breast tissue.** Changes in Ki67 expression after 12 weeks of TAM treatment was assessed by immunohistochemistry (IHC). Percentage of Ki67-positive cells in total epithelium (a), acini (b) and ducts (c) as detected by IHC analysis (n=15). (d) Representative images of normal breast sections at the baseline (left column) and after 12 weeks of treatment (right column) stained with Ki67 antibody. Arrows indicate positive (brown) chromogenic staining in the normal breast. Data in scatter blots represent values of individual samples. Median is shown by horizontal line and interquartile range by the whiskers. The statistical significance was determined using by Wilcoxon matched pairs signed rank test.
*p< 0.05. Scale bars for total epithelium, acini and ducts are 50μm, 20μm and 20μm respectively.

### 3.2.4 Tamoxifen treatment reduces intralobular epithelial and acinar areas

Considering the differences in proliferation, we next accessed whether tamoxifen could influence normal breast tissue architecture. For this aim, quantitative morphological analysis was performed on 14 pairs of samples. Five lobules of the same size were chosen randomly and the total number of acini, the area of each acinus as well as the area of intralobular terminal duct epithelium within each lobule were measured, see (Figure 2.1-b) in method section.

We observed a reduction in total epithelial area within the lobules including acini and ductules, (Figure 3.4a-i), however it was not significant. Separately we have analysed acinar epithelial area and a significant decrease in acinar epithelial area was seen with tamoxifen treatment from baseline 38.4% (IQR [31.8%-47.4%]) to 3 months 30.8% (IQR [25.9%-36%]; p=0.02); (Figure 3.4b-i). There was some apparent heterogeneity in response with a reduction in acinar epithelial cells within lobules seen in eight participants with minimal change in four and an apparent increase in two participants, (BBCPT04 and BBCPT13) (Figure 3.4b-ii). The area of each individual acinus and the number of acini were quantified. A significant decrease in median acinar area was observed with tamoxifen treatment from baseline 1241$\mu m^2$ (IQR [1052.2 $\mu m^2$-1655.7 $\mu m^2$) to 3 months 815$\mu m^2$ (IQR [542 $\mu m^2$-958.2 $\mu m^2$; p=0.0006); (Figure 3.5a-i), whereas a non-significant increase in the number of acini was seen (Figure 3.5b-i).

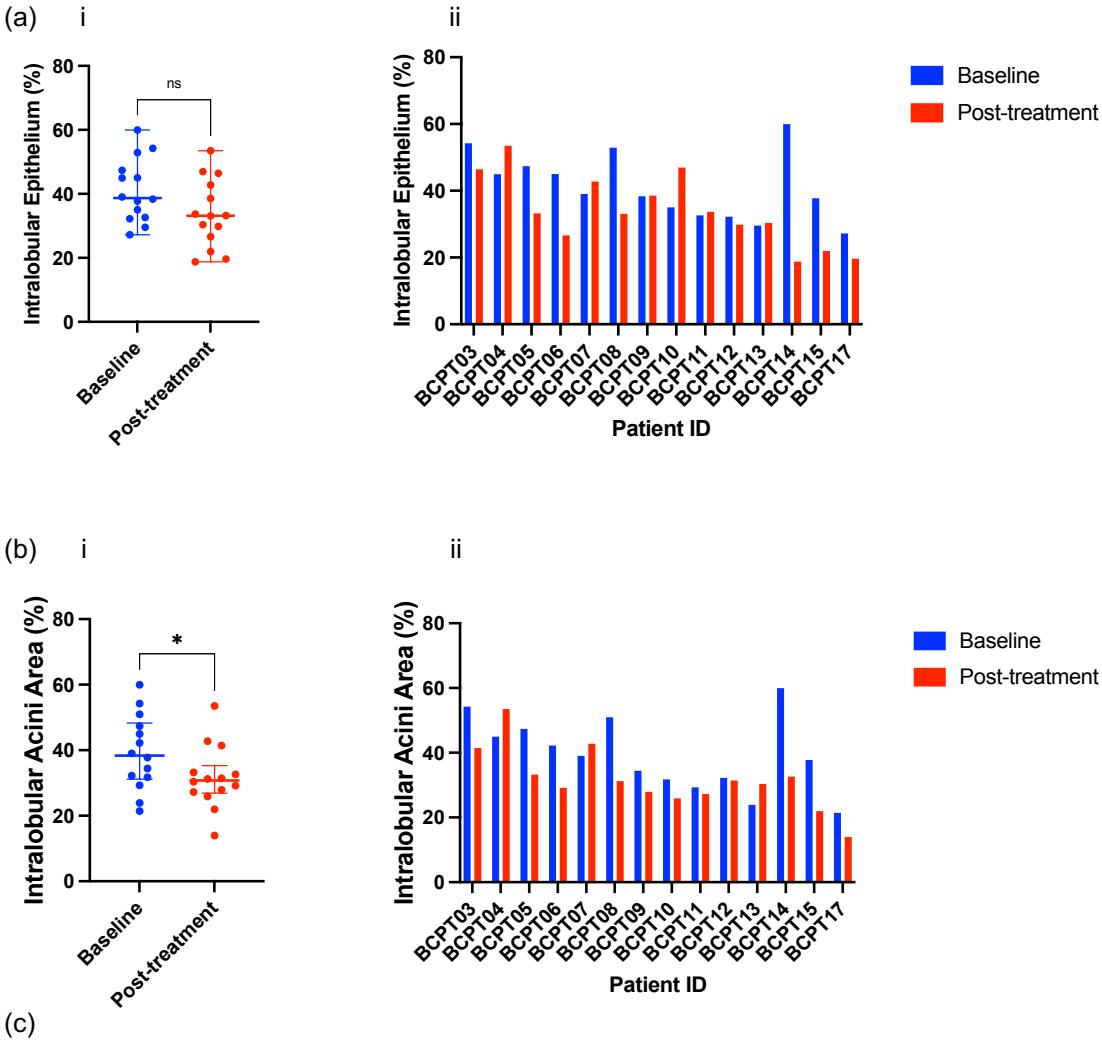


**Figure 3.4: Tissue morphology in normal breast biopsies of women before and after receiving TAM treatment.** The median (a,i) and the percentage of total epithelial area for individuals (a,ii) at the baseline and after 12 weeks of treatment. The median (b,i) and the percentage of acini epithelium for individuals (b,ii) at the baseline and post-treatment. (c) Representative images of FFPE sections stained with H&E at baseline and post-treatment (n=14). Arrows indicate epithelial cells within each acinus in the normal breast. Data in scatter blots represent values of individual samples and median. The statistical significance was determined using Wilcoxon matched pairs signed rank test. * $p < 0.05$. Scale bars are 20μm.

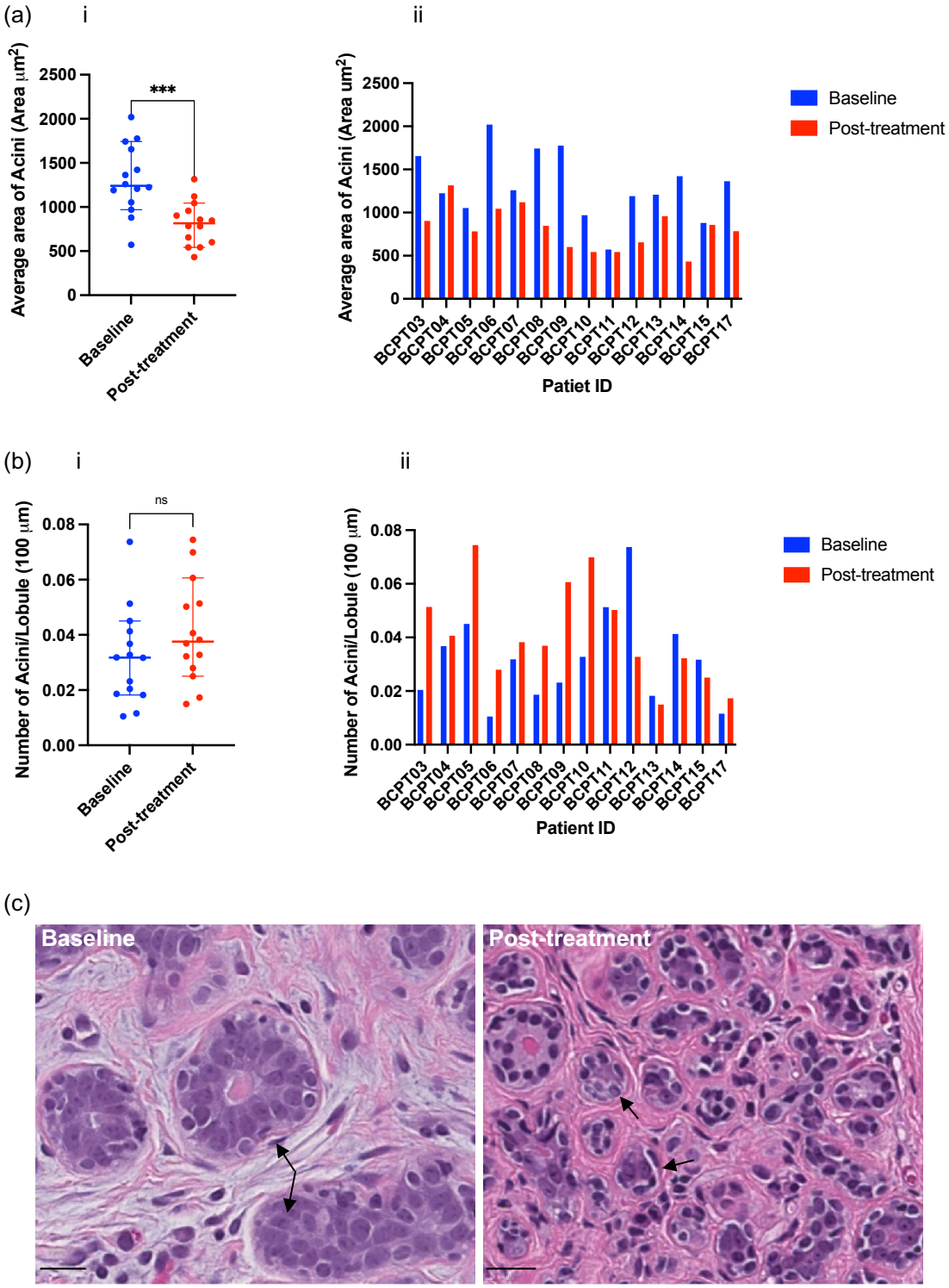


**Figure 3.5: Acini average area and numbers in normal breast biopsies of women after receiving TAM treatment.** The median acini area (a,i) and the median area of acinus in each sample (a,ii) at the baseline and after 12 week of TAM treatment are quantified. The median total number of acini in 100µm$^2$ (b,i) and the median number of acini per 100µm$^2$ of lobule for individuals (b,ii) at the baseline and post-treatment. (c) Representative images of FFPE sections stained with H&E at baseline and post-treatment (n=14). Arrows indicate the area of acinus in the normal breast. Data in scatter blots represent values of individual Participants and median. The statistical significance was determined using Wilcoxon matched pairs signed rank test. *** p< 0.001. Scale bars are 20µm.

### 3.2.5 Tamoxifen treatment reduces both estrogen and progesterone receptor expression

We next sought to understand whether tamoxifen therapy could affect expression of the ER and PR. To this end, we quantified expression of both after 12 weeks of tamoxifen treatment. We observed a significant reduction in ER-positive cells in both acinar baseline 23.2% (IQR [19.1%-40%]) to 3 months 16.1%; (IQR [11.9%-27%]; p=0.02); (Figure 3.6a-i) and ductal epithelium baseline 18.5% (IQR [10.4%-29.5]) to 3 months 12.8% (IQR [4.8%-25.1%];p=0.02); (Figure 3.6b-i). The reduction in acini was seen across all participants except for participants BCPT04 and BCPT10 where there was a slight increase in ER expression, and BCPT08 where there was no appreciable change, (Figure 3.6ii). PR expression was seen to be reduced in participants in acinar epithelial cells in both baseline 33.6% (IQR [20.2%-48.8%] to 3 months 14.5% (IQR [5.8%-20.6]; p<0.0001); (Figure 3.7a-i) and ductal epithelial cells baseline 36.6% (IQR [26.8%-44.4%] to 3 months 13.3% (IQR [4.9%-21.2%]; p<0.0001); (Figure 3.7b-i). This reduction in acini epithelium was seen across almost all participants' samples (Figure 3.7a-ii) although participants BCPT10 and BCPT15 displayed little change with treatment.

(a) i ii

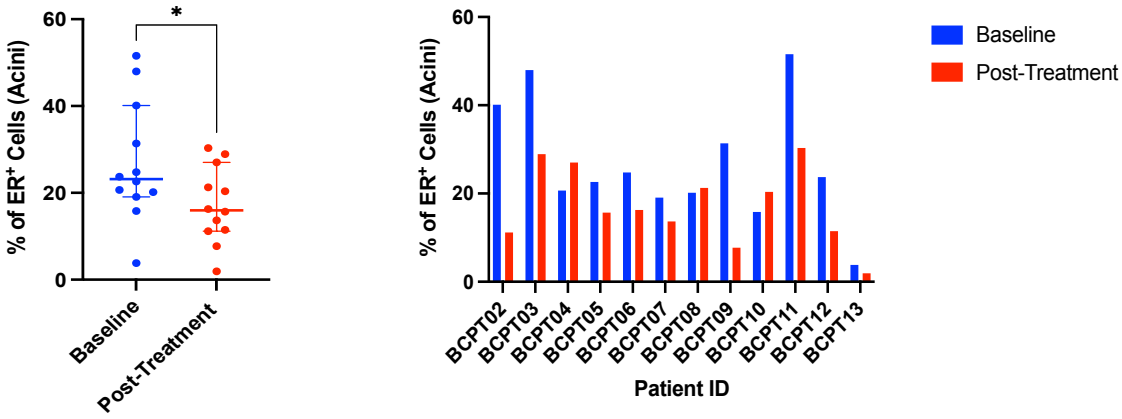
*
% of ER+ Cells (Acini)
60
40
20
0
Baseline
Post-Treatment
% of ER+ Cells (Acini)
BCPT02
BCPT03
BCPT04
BCPT05
BCPT06
BCPT07
BCPT08
BCPT09
BCPT10
BCPT11
BCPT12
BCPT13
Patient ID
Baseline
Post-Treatment

(b) i ii

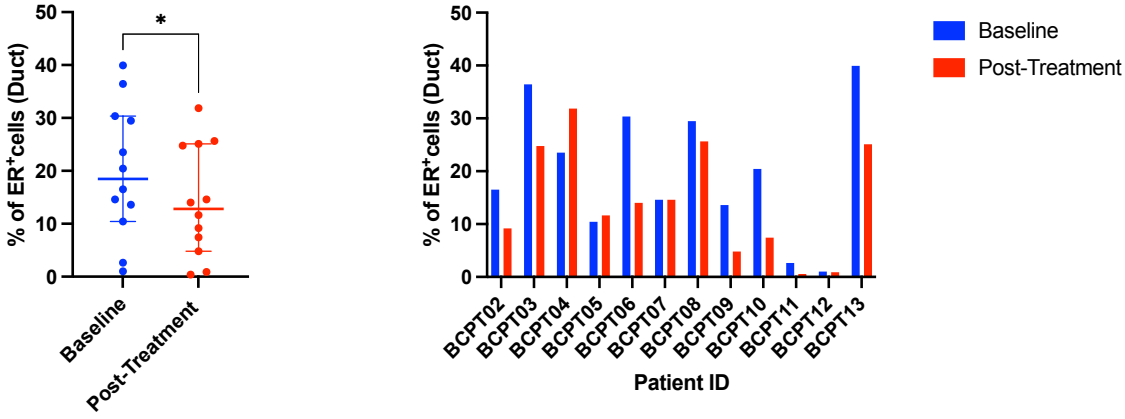
*
% of ER+cells (Duct)
50
40
30
20
10
0
Baseline
Post-Treatment
% of ER+cells (Duct)
BCPT02
BCPT03
BCPT04
BCPT05
BCPT06
BCPT07
BCPT08
BCPT09
BCPT10
BCPT11
BCPT12
BCPT13
Patient ID
Baseline
Post-Treatment

(c)

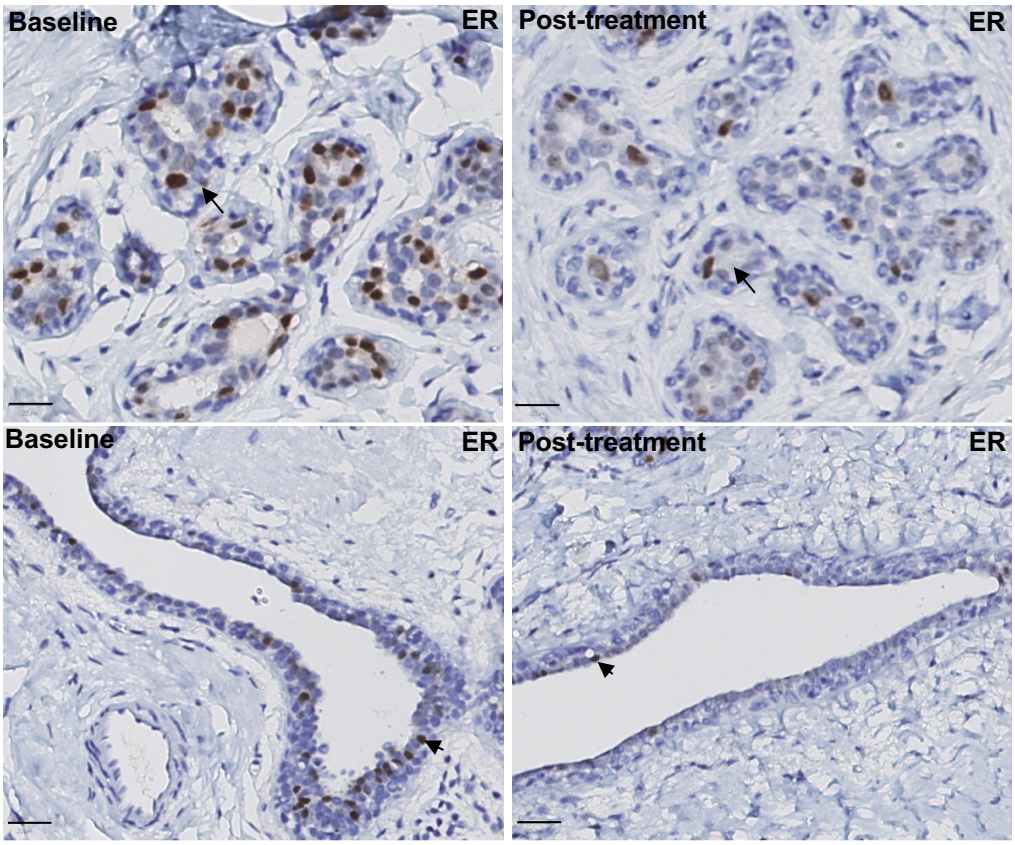


**Figure 3.6: The percentage of ER positive cells and representative images of nuclear staining in normal breast tissue.** Changes in ER expression after 12 weeks of TAM treatment were assessed by immunohistochemistry (IHC). Median ER positive cells in acinar (a) and ductal (b) epithelial cells as detected by IHC analysis (n=12). (c) Representative images of normal breast sections at the baseline (left column) and after 12 weeks of treatment (right column) stained with ER antibody. Arrows indicate positive (brown) chromogenic staining in the normal breast. Data in scatter blots represent values of individual Participants. Median is shown by horizontal line and interquartile range by the whiskers. The statistical significance was determined using Wilcoxon matched pairs signed rank test. * $p<0.05$. Scale bars are 20μm.

(a) i

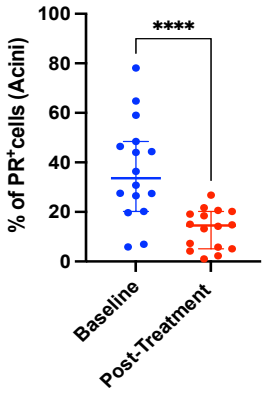
****
% of PR+cells (Acini)
100
80
60
40
20
0
Baseline
Post-Treatment

ii

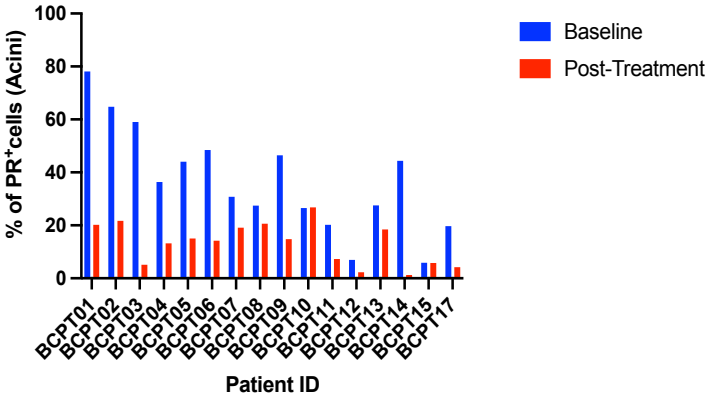
% of PR+cells (Acini)
100
80
60
40
20
0
BCPT01
BCPT02
BCPT03
BCPT04
BCPT05
BCPT06
BCPT07
BCPT08
BCPT09
BCPT10
BCPT11
BCPT12
BCPT13
BCPT14
BCPT15
BCPT17
Patient ID
Baseline
Post-Treatment

(b) i

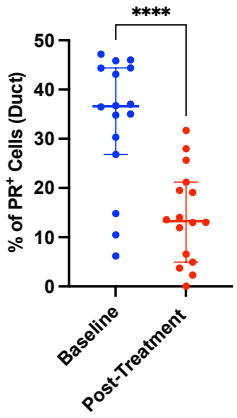
****
% of PR+ Cells (Duct)
50
40
30
20
10
0
Baseline
Post-Treatment

ii

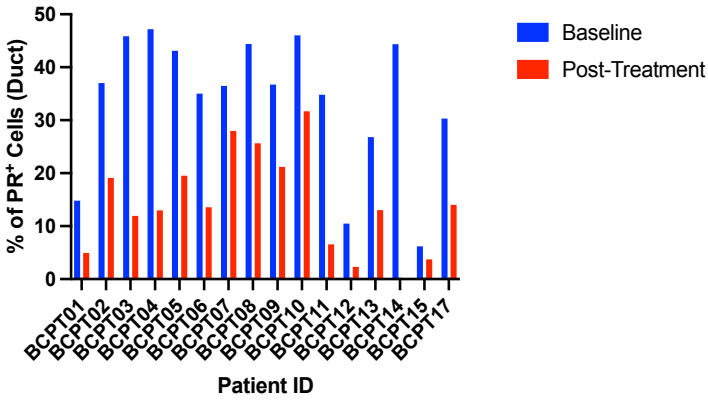
% of PR+ Cells (Duct)
50
40
30
20
10
0
BCPT01
BCPT02
BCPT03
BCPT04
BCPT05
BCPT06
BCPT07
BCPT08
BCPT09
BCPT10
BCPT11
BCPT12
BCPT13
BCPT14
BCPT15
BCPT17
Patient ID
Baseline
Post-Treatment

(c)

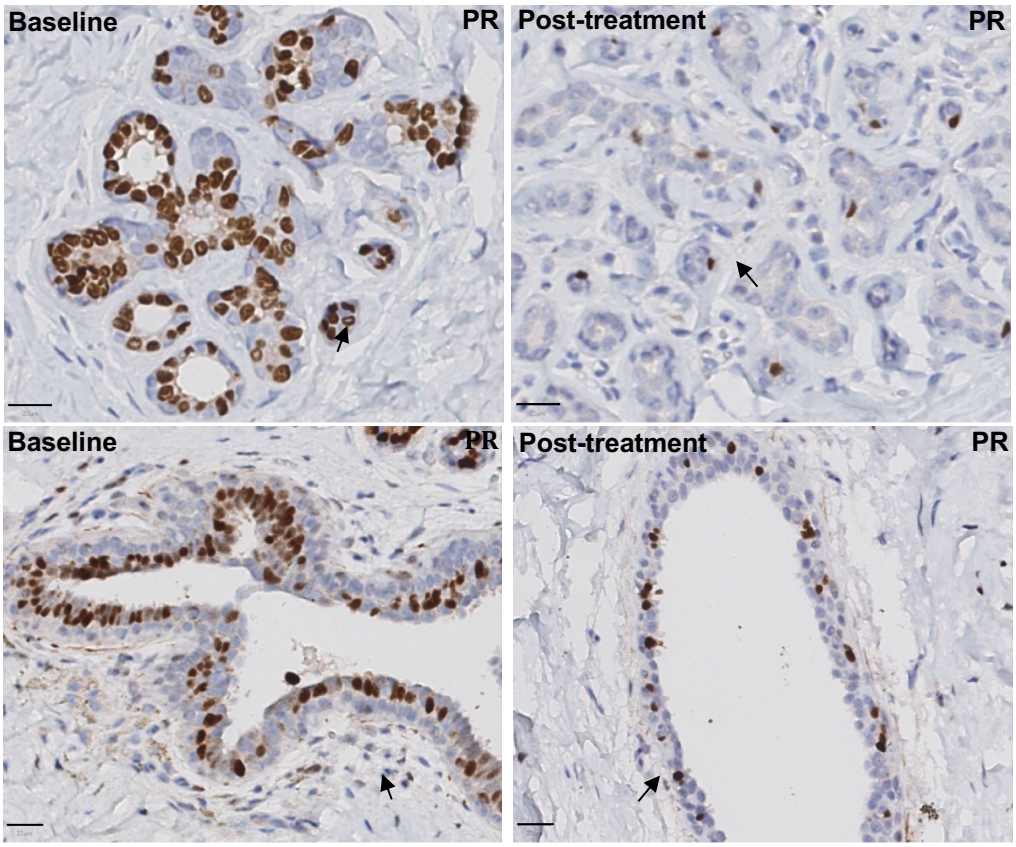


**Figure 3.7: The percentage of PR positive cells and representative images of nuclear staining in normal breast tissue.** The change in PR expression after 12 weeks of TAM treatment was assessed by immunohistochemistry (IHC). Percentage of PR positive cells in acinar (a) and ductal (b) epithelial cells as detected by IHC analysis (n=16). Arrows indicate positive (brown) chromogenic staining in the normal breast. (c) Representative images of normal breast sections at the baseline (left column) and after 12 weeks of treatment (right column) stained with PR antibody. Data in scatter blots represent values of individual Participants. Median is shown by horizontal line and interquartile range by the whiskers. The statistical significance was determined using Wilcoxon matched pairs signed rank test. ****p<0.0001. Scale bars are 20μm.

### 3.2.6 Mammosphere forming efficiency was not affected by tamoxifen treatment

As a next step, we examined the effects of tamoxifen on colony formation using the mammosphere formation efficiency (MFE) assay, (Shaw et al., 2012). MFE was carried out on baseline and post-treatment samples following dissociation into single cell suspensions. In these experiments, no significant difference in MFE was seen with treatment across the whole group (Figure 3.8a-i) due to marked heterogeneity in response between individual participants (Figure 3.8a-ii).

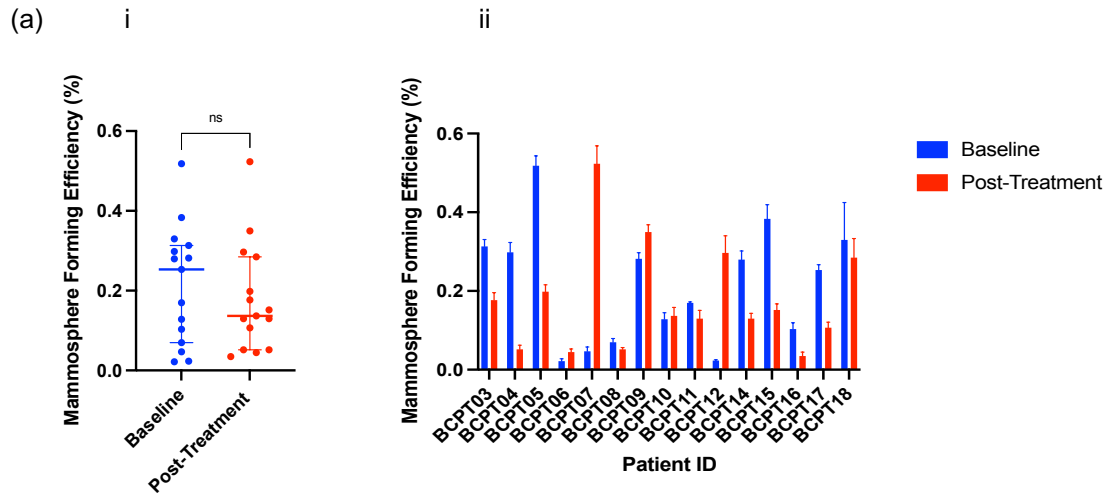


**Figure 3.8: Mammosphere forming efficiency of normal breast biopsies of women after receiving TAM treatment.** Samples were collected before and after TAM treatment and were enzymatically digested into single cell suspensions and plated in non-adherent 6-well plates (10,000 cells/well). Plates were incubated for 10 days. (i) Mammospheres with diameter above 50μm were quantified and data is presented as percentage. (ii) Error bars represent SEM from 6 independent wells (n=15). Data in scatter blots represents values for individuals and the median is shown by horizontal line while the interquartile range by the whiskers. The statistical significance was determined using Wilcoxon matched pairs signed rank test.

### 3.2.7 Participants with higher baseline Mammographic Density show greater proportional reduction with treatment

We next investigated changes in breast density using digital mammography images. To minimise interobserver error we utilised Volpara® Health software for quantitative image analysis (Alonzo-Proulx et al., 2015). We examined the differences in Volpara Breast Density (VBD) read-outs at one year of follow-up, (n=9 only as several participants are yet to reach the one-year timepoint). Overall, there was a significant reduction in median VBD at baseline 12.6% (IQR [9.1%-17%]) to one year follow-up 8.5% (IQR [6.8%-12.5%]; p=0.0039); (Figure 3.9, a-i). Of note all participants showed >10% relative reduction in VBD with treatment except for participant BCPT04 where there was no change in MD after treatment, (Figure 3.9ii). This reduction was not significantly

correlated with the change in Ki67, ER, PR and acinar area. Again, the mammographic data suggests that quantitative reduction in density may not be an appropriate biomarker of tamoxifen response.

(a) i ii

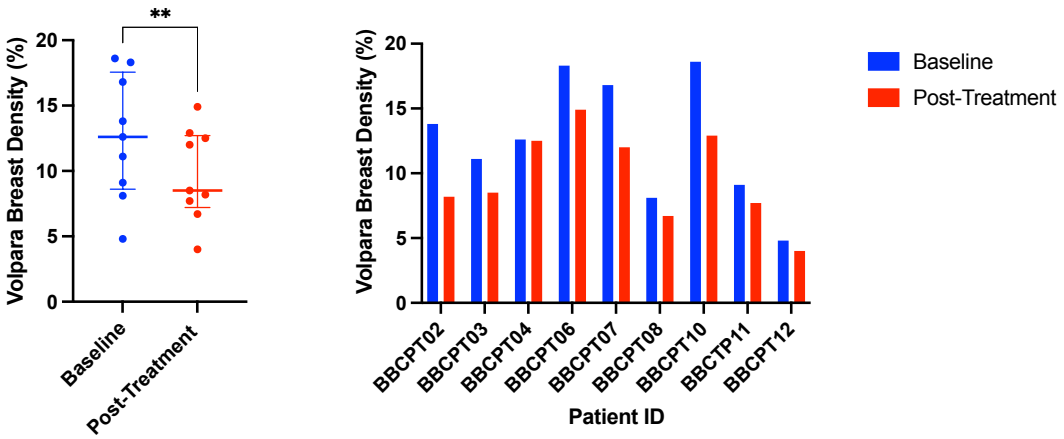


(b) i: Case with high dense tissue at the baseline

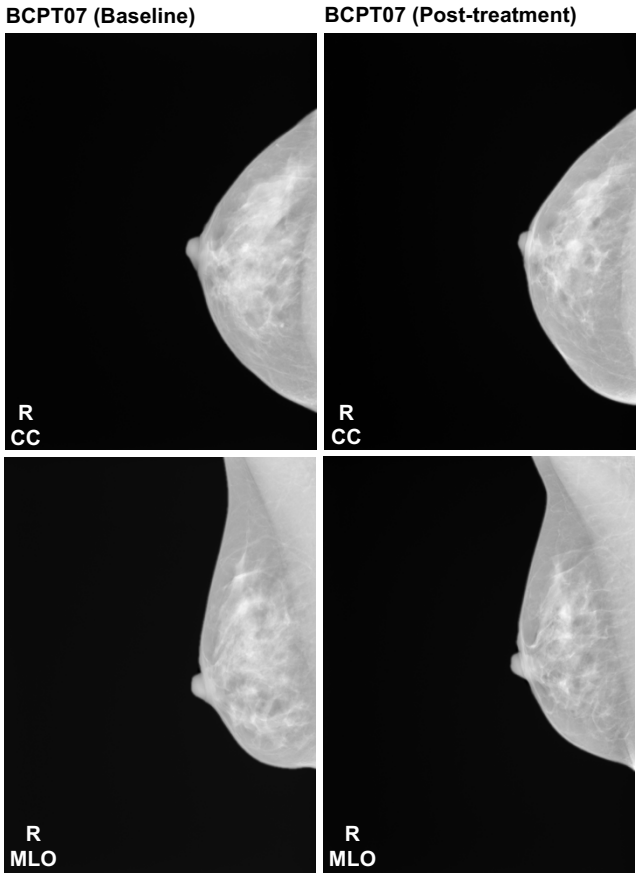

ii: Case with low dense tissue

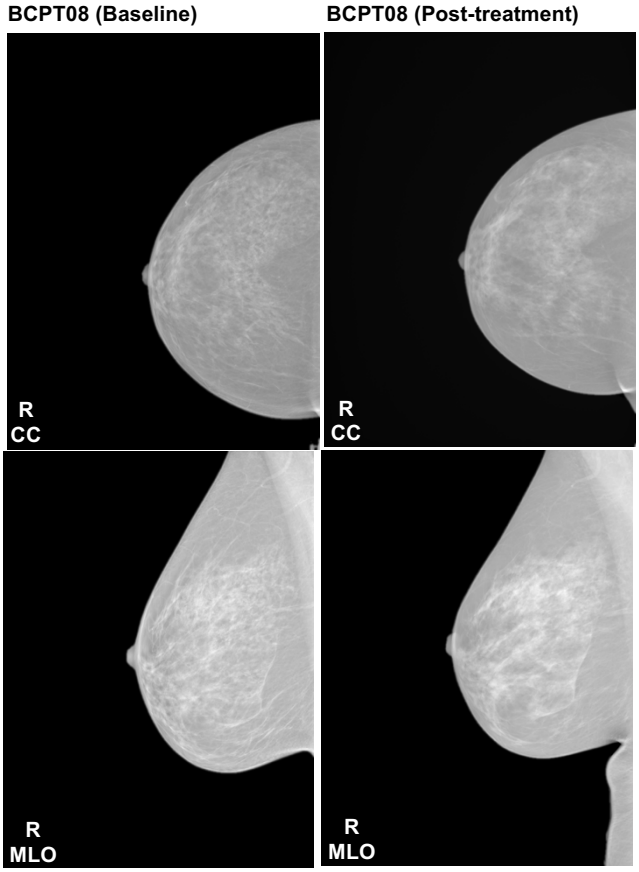


**Figure 3.9: Breast density change at the baseline and one year follow-up after receiving TAM treatment.** Changes in breast density in healthy women after one year of TAM treatment was assessed by using Senographe Essential$^{TM}$ Mammography System from General Electric (GE). (a-i) the median of VBD in all women (n=9). (a-ii): Changes in VBD in each individual. (b) Representative digital mammography images of right (R) side of the woman's breast. Bilateral craniocaudal (CC) and mediolateral oblique (MLO) views are presented. (i) Patient with high dense breast tissue at the baseline and one year follow-up, (ii) Patient with low dense breast tissue at the baseline and one year follow-up. Data in scatter blots represent values of individuals. Median is shown by horizontal line and interquartile range by the whiskers. The statistical significance was determined using Wilcoxon matched pairs signed rank test. * $p<0.05$

## 3.3 Discussion

Identifying predictive biomarkers of preventive tamoxifen efficacy is a significant clinical priority. In our cohort, tissue biopsies and blood samples were collected at luteal phase before treatment began and again in the 12$^{th}$ week of therapy. In our assessments we first determined the level of estradiol and progesterone in blood. The normal range of estradiol in premenopausal women during the luteal phase of the menstrual cycle is 82-1251 pmol/L, whereas it is below 110 pmol/L in postmenopausal women, (Frederiksen et al., 2020). In comparison to the baseline, we noted a considerable increase in the estradiol levels. In our cohort, the baseline median of estradiol blood levels in women was 354.7 pmol/L and considerably raised to 1043.4 pmol/L, representing a nearly three-fold increase. These findings support Groom and Griffiths hypothesis that tamoxifen has direct effects on ovarian function, which cause an elevation of circulating estradiol level, (Groom et al., 1976). The agonist action of tamoxifen can enhance ovarian hyper-stimulation, resulting in higher luteinizing, follicle stimulation, estradiol, progesterone hormones through the hypothalamic-pituitary axis, (Madeddu et al., 2014). In conflict with our data, progesterone blood levels did not increase after tamoxifen treatment. Interestingly, in our investigations two participants (BCPT04 and BCPT05) did not show any change in estradiol blood level. This heterogeneity could potentially identify participants less likely to respond to tamoxifen, with a hypothesis that those exhibiting the greatest increase in serum estradiol levels may have reduced anti-estrogenic effect on the breast tissue. Notably, in cancer treatment, ovarian function suppression (OFS) in combination with tamoxifen has been shown to be superior to tamoxifen alone, potentially as it

counters the effect of increased estrogen with tamoxifen treatment, (Kim et al., 2020). However, we did not observe any correlation between change in estradiol levels and reduction in Ki67, ER, PR and acinar area, (data not shown).

As part of our investigations, patient samples were prepared for IHC and morphometric analysis. These samples displayed a variety of ducts and TDLU structures, which enabled us to analyse these morphological features separately. It was hypothesized that exposing epithelial cells in dense breast tissue and mature TDLU to steroid hormones and growth factors stimulates cell proliferation, accumulation of genetic damage, and increase in the probability of transformation, (Ginsburg et al., 2008).

Ki67 is a nuclear protein that is expressed in cycling cells. It was shown to be a more accurate and predictive marker of cancer cell proliferation than mitotic counts for breast cancer participants, (Brentnall et al., 2020; Cuzick et al., 2011; Viale et al., 2008).

We demonstrated significant reduction in Ki67 expression after treatment with tamoxifen. Reduction in Ki67 was most obvious in acini epithelial cells and was borderline significant in ductal epithelial cells. We determined the Ki67 expression median to be 4.4%, which is similar with a prior studies that indicated $Ki67^{+}$ cells comprises around 4% of total epithelium in normal breast in premenopausal women with high risk of breast cancer, (Huh et al., 2016; Oh et al., 2016).

The hormones estradiol and progesterone can directly and indirectly stimulate the proliferative activity of luminal epithelial cells, (Brisken et al., 2010). Sensor

luminal cells release paracrine growth factors when estradiol and progesterone hormones bind with ER and PR receptors. This influences the downstream activity of responder luminal cells that do not express hormone receptors, (Brisken et al.,2010). Since PR and paracrine signalling are downstream of ER-related signalling pathways, the inhibition of ER via tamoxifen lowers the activity of ER, and thus reduced PR expression and paracrine signalling activity. This may serve as one potential explanation for the decreased proliferation observed in our cohort.

In normal breast tissue, myoepithelial cells do not express hormone receptors. Prior studies have showed that both ER and PR are expressed in less than 15% of the luminal cells in normal breast tissue, (Clarke et al., 1997; Oh et al., 2016). In a study by Oh et al., the expression of ER was inversely related with subsequent risk. PR and Ki67 expression were non-significant, however they were reported to be strongly linked with subsequent risk, (Oh et al., 2016). However, in their study the percentages of ER and PR positive cells were higher than in our data. Moreover, a recent study has revealed that increased stiffness can have an impact on ERα signalling. Munne et al., cultivated patient-derived breast luminal $ERα^{+}$ epithelial cells and breast cancer explant in various three-dimensional matrix scaffolds. They found that the matrix stiffness regulates ERα signalling via stress-mediated p38 activation in breast tissue, (Munne et al., 2021).

In our cohort, both ER and PR receptors were significantly reduced after treatment with tamoxifen. Euhus et al., has reported that tamoxifen suppressed ERα by a median of 27% when evaluated by IHC, however, this was not statistically significant (P= 0.058). However, tamoxifen treatment was shown

to reduce ESR1 gene expression levels by approximately 50%, (Euhus et al., 2011).

Morphometric characteristics of the normal breast were analyzed to visualize changes in TDLU architecture. We performed quantitative measurements of lobules, and quantified acini total number and area within lobules. The results showed a statistically significant reduction in the percentage of total acinar epithelium within lobules area as well as individual acinar area after tamoxifen treatment. This data suggests that reduction in the acinar area could be correlated with reduced epithelial cell proliferation. In contrast, after three months of tamoxifen treatment, Euhus et al. (2011) reported no differences in morphological aspects of benign breast tissue. The researchers utilized computer-assisted tissue component analysis to evaluate the morphologic characteristics of breast tissue, but they manually calculated the number of acini in each lobule and the number of epithelial cells. Furthermore, they did not observe changes in the frequency of cytologic atypia, using Masood scoring approach to access the cell structure, (Euhus et al., 2011).

In a study looking at a longer duration of tamoxifen treatment (12 months) Baker et al. showed that Masood cytology scores, indicating the degree of cellular atypia, were reduced suggesting that longer treatment periods may be necessary to translate into morphologic changes, (Baker et al., 2008).

Some women still go on to develop breast cancer, sometimes even ER+ BC, despite tamoxifen therapy. The reasons for this tamoxifen resistance are yet unknown, however, it is possible that stem-like activity may contribute to tamoxifen resistance since stem/progenitor cells are likely to be the cells that

are transformed into breast cancers, and stem-like activity may contribute to tamoxifen resistance, (Piva et al., 2014). As such, we investigated whether tamoxifen could affect stem cell properties, such as 3D colony formation. For this we employed the MFE assay on single cell suspensions generated from participants' baseline and post-treatment samples. We noticed a differential response to tamoxifen treatment among participants and a statistically non-significant reduction in MFE overall. According to our current findings and earlier reported data results on normal breast tissue, tamoxifen does not significantly change the proportion of stem-like cells following treatment, nor does it appear to affect stem-like cells in the normal breast, (Raffo et al., 2013; Simões et al., 2011). Although tamoxifen could influence paracrine signalling downstream of the targeted ER+ cells, our data do not currently support an effect on stem-like cell activity. It is tempting to speculate that this maybe why there is no reduction in ER- breast cancer with tamoxifen as these tumours are thought to originate from the ER- luminal progenitor cell population, (Hein et al. 2016; Keller et al. 2012; Van Keymeulen et al. 2015; Koren et al. 2015; Molyneux et al. 2010; Pelissier Vatter et al. 2018).

Overall mammographic density in this study was reduced by a median of 22.4% at one year, comparable to a recent study that reported a mean reduction in mammographic density by (17-25%) of the inter-quartile range, (-11: [-21.6-2.6-2.7, -74.2-26.5]), (Brentnall et al., 2020). We sought to understand the variability among our participants. There was an indication that participants with high MD would exhibit a greater reduction after a one year of tamoxifen treatment. Chew et. al found that only human breast tissue of high MD, transplanted into immunosuppressed mice, showed reduced MD in

response to 3 months' tamoxifen treatment, (Chew et al., 2014). Following tamoxifen treatment, the percentage area of adipose tissue in the high MD biochamber tissue was increased, whereas after estrogen treatment, they noticed an increase in MD and a reduction in adipose tissue, (Chew et al., 2014). They did not detect the status of epithelial proliferation markers following tamoxifen treatment, but they did imply that the decrease in MD in dense tissue is linked to the maturation of stromal cells into adipocytes. According to clinical studies, it is suggested that high breast cancer risk is linked with longer steroid hormone exposure using HRT, (Ross et al., 2000; Weiss et al., 2002), while tamoxifen treatment has been linked to a reduction in estrogen impacts on the breast. However, we did not observe a correlation between reduction in density and reduction in other markers; such as Ki67, ER or acinar area. It is possible that this is due to the relatively small number of patients that we have analysed to date. As further participants are recruited and the data analysed, we will be able to determine whether there or not a direct correlation between density reduction and molecular analyses exists.

The conclusions from this chapter are that tamoxifen treatment inhibits ER activity and leads to a reduction in epithelial cell proliferation. The reduction of Ki67 protein expression following tamoxifen treatment is linked to reduced acinar area. Secondly, we conclude from the mammosphere data that tamoxifen therapy exerts no direct or indirect effects on the activity of stem-like cells. Finally, all participants treated with tamoxifen displayed reduction in MD. Accordingly, we speculate that evaluating the reduction in MD could not help us discriminate who responded to tamoxifen treatment and those who are resistant. From the data presented in this chapter, we cannot yet identify those

who will gain benefit from preventive tamoxifen. I have thus gone on to investigate transcriptomic and proteomic approaches to try and uncover signatures of response/resistance to tamoxifen treatment. The following chapter will elaborate further on our gene expression and proteomic analyses.

# Chapter 4

# Investigating Mechanisms of Tamoxifen Resistance in Breast Cancer Preventive Therapy Using Genomic and Proteomic Analyses

# 4 Investigating Mechanisms of Tamoxifen Resistance in Breast Cancer Preventive Therapy Using Genomic and Proteomic Analyses.

## 4.1 Introduction

Our initial hypothesis for the tamoxifen study was that we would be able to correlate the molecular analysis of breast tissue to the mammographic data at 1 year. However, even though earlier studies showed density reduction predicted preventive efficacy, (Cuzick et al., 2011), subsequent studies using automated methods of density assessment suggest that density change at 1 year does not predict density at year 2, (Brentnall et al., 2020). We thus changed our approach and looked for patterns of differential gene and protein expression that may define response vs resistance to tamoxifen prevention.

In Chapter 3 we identified variability in response in terms of changes in proliferation, morphology and steroid receptor expression. Here, we wanted to try and identify mechanisms of resistance to preventive tamoxifen in women at increased risk for breast cancer. By using RNA sequencing and LCM-MS approaches, we sought to identify signalling pathways and proteomic signatures that may be affected by tamoxifen treatment and whether these changes could help discriminate between responders, whom we hypothesise would gain preventive benefit, and resistant participants who would not.

One emerging challenge for the use of tamoxifen in chemoprevention is the development of drug resistance. As such, further research into the molecular and cellular mechanisms underlying tamoxifen resistance will be key in overcoming resistance, uncovering novel therapeutic agents for the prevention of breast cancer, as well as designing more efficacious therapeutic strategies

for the clinic. Moreover, there is an urgent clinical need for biomarkers to identify women who will be resistant to preventive tamoxifen and who can thus be spared the toxicities.

## 4.2 Results

### 4.2.1 Unsupervised transcriptomic analysis

To investigate the effects of tamoxifen on the normal breast transcriptome, 10 paired samples, taken before and after 12 weeks of tamoxifen therapy, were subjected to RNA sequencing (RNAseq) analysis. In RNA sequencing data sets, Principal Components Analysis (PCA) can be used to visualize baseline samples to post-treatment samples distances, highlight variation and capture significant patterns. In a PCA, the data points (samples) are presented on a 2D plane where they spread out in two directions. Principal component 1 (PC1) and PC2 account for the greatest and second greatest variation in gene expression between samples respectively. In the PCA of our 10 paired samples (Figure 4.1a), 45% of the variation was explained by PC1 and 11% by PC2. There was no clear separation of the baseline and post-treatment samples into groups suggesting that both inter-patient variability and tamoxifen treatment effect are both important.

A similar result was found using a heatmap of distance matrix, which can be used to give an overview of similarities and dissimilarities between paired samples, (Figure 4.1b). Overall, it explains how samples at baseline and post-treatment are clustered. The colours in the heatmap indicate similarities across samples. The distance between samples at the baseline and post-treatment indicates that tamoxifen is driving changes in the gene expression profile in all samples apart from BCPT07 where the baseline and post treatment samples cluster together.

(a)

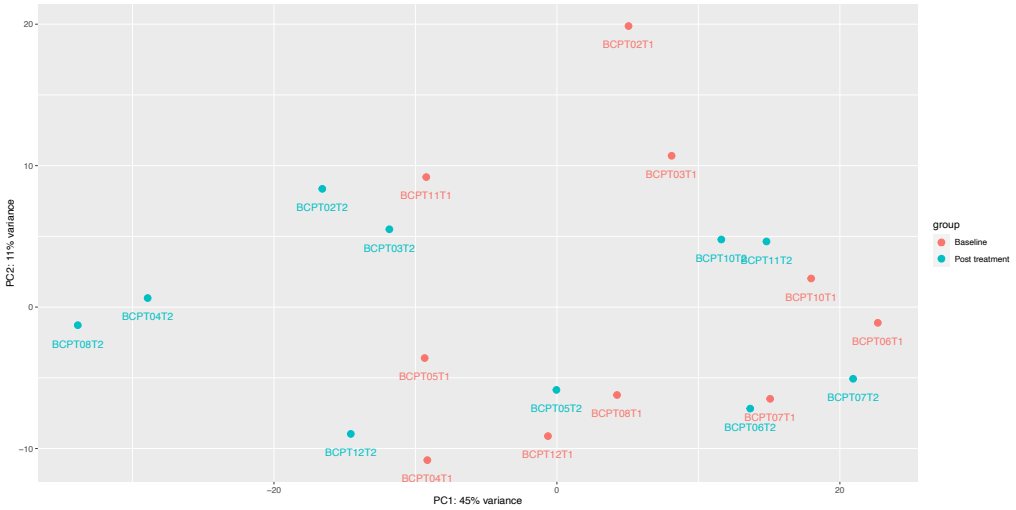


(b)

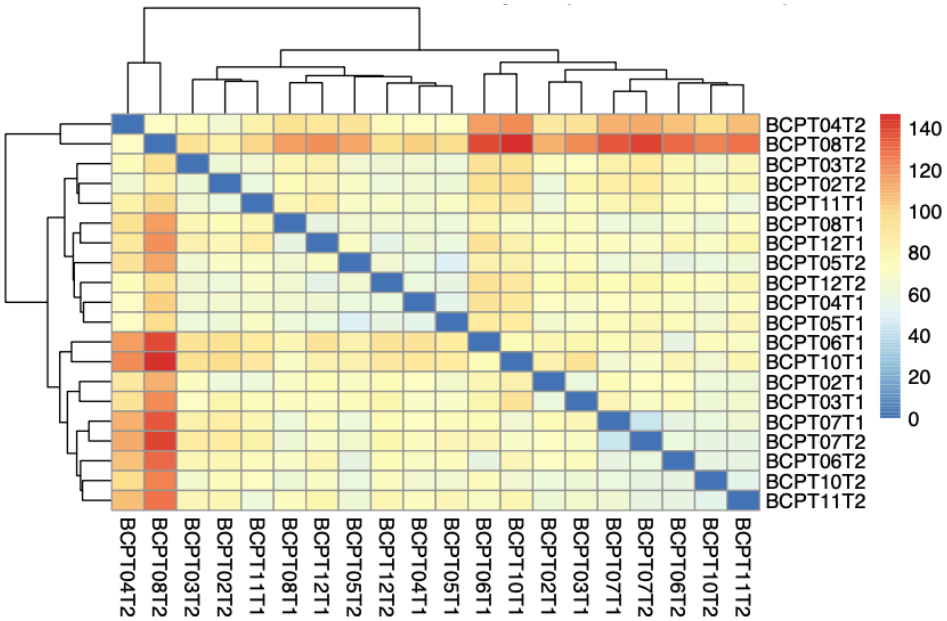


**Figure 4.1 The unsupervised analysis of the normal breast biopsies shows the changes in post-treatment versus baseline in gene expression in women who received preventive TAM therapy for 12 weeks.** (a) A Principal Component Analysis (PCA) plot of the normal breast biopsies at the baseline and 12 weeks of TAM treatment. Sample condition can be seen in the key. PCA plot was generated using the function plotPCA in the DESeq2 package. (b) A heatmap of gene expression shows pair-wise distances across baseline and post-treatment samples using a variance-stabilizing transformation. The heatmap with a hierarchical clustering function was generated based on the sample distances between the rows/columns of the distance matrix. Sample IDs can be found at the bottom and right- hand borders of the heatmap. The scale represents the similarities across samples. Blue colour means short distance and high similarity between samples. Red colour means long distance and low similarity between samples. The diagonal has dark blue colour which represent the distance of each individual sample with itself. To generate the heatmap, a function in R software was used. RNAseq was performed on 10 pairs of normal breast tissues at the baseline and 12 weeks of TAM treatment.

### 4.2.2 Identification of differentially expressed genes in women receiving tamoxifen treatment.

To further explore the effects of tamoxifen on the normal breast transcriptional profiles we performed differentially expressed genes (DEG) analysis of the 10 paired samples. Each participant's post-treatment gene expression profile was compared to the baseline profile in the analysis and DEGs were evaluated. By using the DEseq2 package with an adjusted p-value threshold of <0.05, 54 differentially expressed genes were identified (Figure 4.2; Table 4.1; 4.2). Many of the differently expressed genes are known to be regulated by estrogen signalling and were consistently down-regulated by tamoxifen treatment. Despite the fact that the majority of these genes were uniformly up or down regulated by tamoxifen, unsupervised clustering analysis demonstrated separation of the samples into two broad groups, (Figure 4.2)

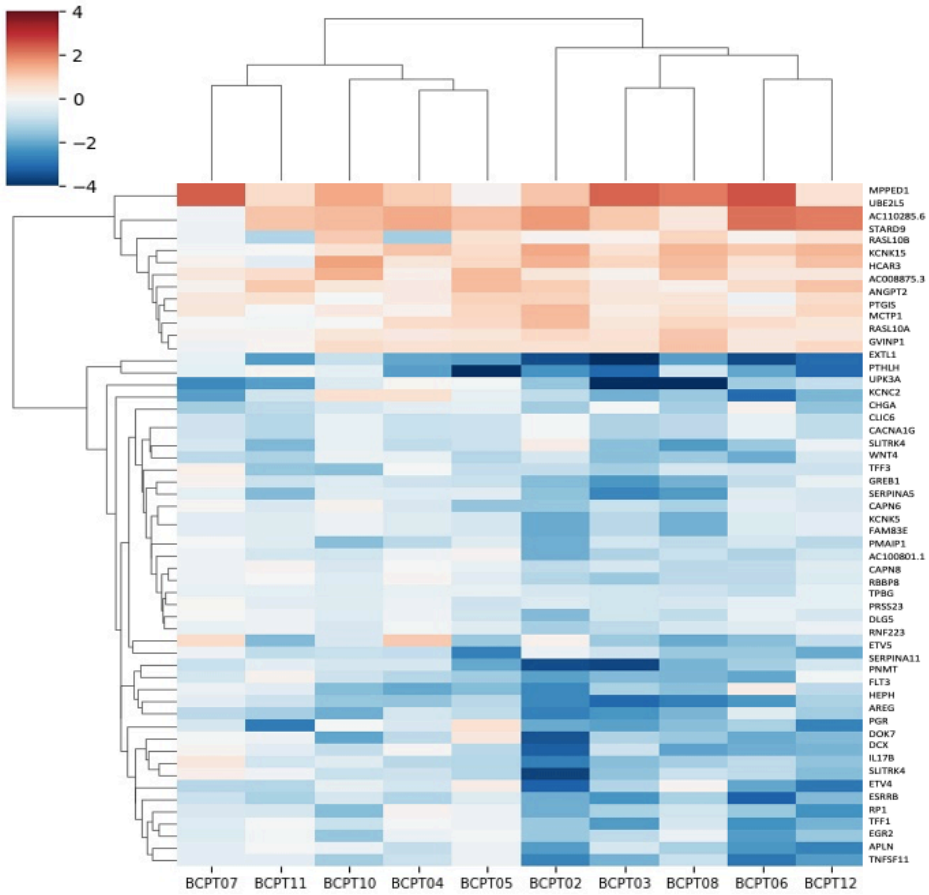


**Figure 4.2 Heatmap displaying the 54 differentially expressed genes.** Genes are displayed as log2 fold change and p of 0.05 was used. Each column on the heatmap represents an individual participant; Red indicates an upregulation and blue a downregulation, the degree to which can be seen on the colour key scale.

**Table 4.1 Down-regulated genes identified in the normal breast tissue of pairs of samples from 10 women who received TAM treatment. $Log_2FC$ = log2 fold change. FDR= False Discovery Rate.**

| GENE NAME | $LOG_2FC$ | P-VALUE | FDR |
|---|---|---|---|
| **PTHLH** | -2.41 | 2.14E-12 | 0.0000004 |
| **AREG** | -1.71 | 6.07E-11 | 0.0000006 |
| **TFF3** | -1.03 | 1.74E-09 | 0.000009 |
| **ESRRB** | -1.42 | 1.89E-09 | 0.000009 |
| **RP1** | -1.51 | 3.18E-09 | 0.00001 |
| **TFF1** | -2.64 | 7.82E-08 | 0.0002 |
| **PRSS23** | -0.52 | 2.52E-07 | 0.0006 |
| **SLITRK4** | -0.75 | 4.34E-07 | 0.0008 |
| **RASL10A** | -0.9 | 4.83E-07 | 0.0008 |
| **PNMT** | -1.21 | 7.79E-07 | 0.001 |
| **DCX** | -1.35 | 1.19E-06 | 0.002 |
| **CACNA1G** | -1.11 | 2.98E-06 | 0.003 |
| **WNT4** | -1.12 | 2.98E-06 | 0.003 |
| **TNFSF11** | -1.85 | 4.59E-06 | 0.005 |
| **SERPINA5** | -1.09 | 5.40E-06 | 0.006 |
| **FLT3** | -1.15 | 5.54E-06 | 0.006 |
| **PGR** | -1.1 | 7.58E-06 | 0.007 |
| **UPK3A** | -1.22 | 9.71E-06 | 0.009 |
| **RNF223** | -1.15 | 1.08E-05 | 0.009 |
| **CAPN8** | -0.84 | 1.10E-05 | 0.009 |
| **GREB1** | -1.12 | 1.34E-05 | 0.01 |
| **DLG5** | -0.44 | 1.49E-05 | 0.01 |
| **FAM83E** | -0.84 | 1.50E-05 | 0.01 |
| **SERPINA11** | -1.51 | 1.71E-05 | 0.01 |
| **ETV5** | -0.53 | 4.01E-05 | 0.02 |
| **DOK7** | -1.41 | 2.03E-05 | 0.01 |
| **CHGA** | -1.32 | 2.74E-05 | 0.01 |
| **CAPN6** | -0.91 | 3.73E-05 | 0.02 |
| **CLIC6** | -0.81 | 6.34E-05 | 0.03 |
| **EGR2** | -1.02 | 4.99E-05 | 0.03 |
| **AC100801.1** | -1.41 | 6.17E-05 | 0.03 |
| **KCNC2** | -1.71 | 6.62E-05 | 0.03 |
| **TPBG** | -0.62 | 6.71E-05 | 0.03 |
| **PMAIP1** | -0.79 | 7.39E-05 | 0.03 |
| **IL17B** | -1.25 | 8.54E-05 | 0.04 |
| **ETV4** | -1.11 | 9.97E-05 | 0.04 |
| **HEPH** | -0.52 | 1.00E-04 | 0.04 |
| **KCNK5** | -0.71 | 1.03E-04 | 0.04 |
| **EXTL1** | -1.25 | 1.04E-04 | 0.04 |
| **AC037198.2** | -1.73 | 1.09E-04 | 0.04 |
| **RBBP8** | -0.61 | 1.23E-04 | 0.05 |
| **APLN** | -1.16 | 1.25E-04 | 0.05 |

**Table 4.2 Up-regulated genes identified in the normal breast tissue of pairs of samples from n=10 women who received TAM treatment. $Log_2FC$ = log 2 fold change. FDR= False Discovery Rate.**

| GENE NAME | $LOG_2FC$ | P-VALUE | FDR |
|---|---|---|---|
| **MPPED1** | 1.42 | 1.43E-07 | 0.0004 |
| **AC110285.6** | 1.22 | 3.12E-07 | 0.0006 |
| **ANGPT2** | 0.67 | 6.10E-07 | 0.0009 |
| **GVINP1** | 0.47 | 3.14E-05 | 0.02 |
| **UBE2L5** | 0.82 | 4.06E-05 | 0.02 |
| **HCAR3** | 0.82 | 5.90E-05 | 0.03 |
| **PTGIS** | 0.5 | 6.06E-05 | 0.03 |
| **KCNK15** | 0.66 | 6.45E-05 | 0.03 |
| **MCTP1** | 0.51 | 1.01E-04 | 0.04 |
| **AC008875.3** | 0.53 | 1.19E-04 | 0.05 |
| **STARD9** | 0.51 | 1.34E-04 | 0.05 |

Using Gene Set Enrichment Analysis (GSEA) of these 54 DEGs, no single pathway was enriched significantly (data not shown), despite the observation that multiple ER targets were down-regulated. We next undertook a PCA using Log2 fold-change (Log2FC) values to further evaluate the spatial separation of the samples with respect to their intrinsic response characteristics. In this PCA (Figure 4.3), PC1 accounts for 45.6% of the variance and PC2 17.2%. Samples BCPT04,7,10 and 11 separate out from BCPT02,3 and 12 on PC1 with the remaining three samples showing variance in PC2 predominantly. Broadly defining the samples into two groups by PC1, acknowledging that samples BCPT5,6 and 8 show minimal variance in PC1, shows consistency with the 2 major clusters in the previous heatmap (Figure 4.2). We have tentatively labelled these as response group 1 (RG1) that includes BCPT02, BCPT03, BCPT06, BCPT08 and BCPT12 and response group 2 (RG2) which includes BCPT04, BCPT05, BCPT07, BCPT10 and BCPT11.

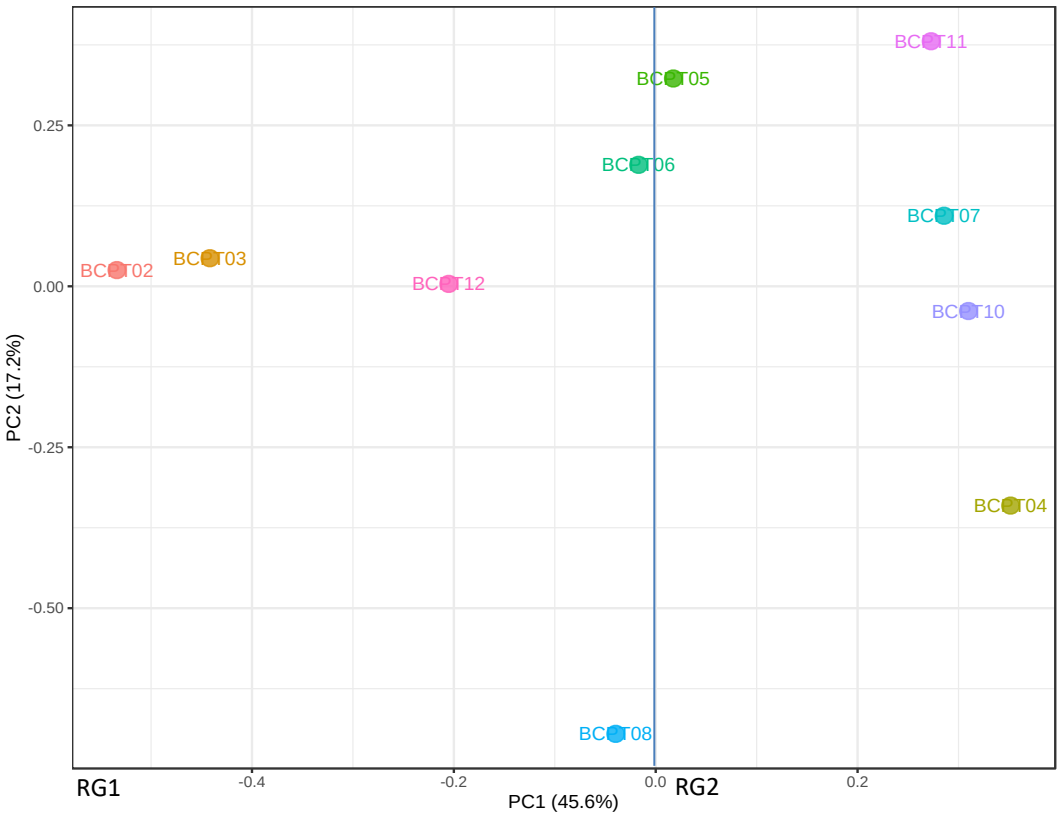


**Figure 4.3 Principal component analysis (PCA) shows samples cluster according to their response to TAM treatment.** Sample IDs are shown on the PCA itself. The PCA is used to define 2 clusters, based on PC1 with the blue line separating participants into response group 1 (RG1) on the left and response group 2 (RG2) on the right. n=10 participants.

### 4.2.3 Tamoxifen treatment modulation of luminal hormone receptor positive cell gene expression.

To further evaluate the patterns of gene expression we next analysed the epithelial and stromal gene set signatures in our cohort. Epithelial and stromal cell gene set signatures were identified from published single cell RNAseq datasets (Bach et al., 2017; Kanaya et al., 2019; Twigger et al., 2020). First, we examined the epithelial cell signatures, including genes expressed predominantly in luminal hormone receptor positive, luminal hormone receptor negative, both luminal subtypes or basal cells, and examined their differential expression in response to tamoxifen (Figure 4.4). In contrast to the initial DEG analysis (Figure 4.2) many of the selected genes showed wide variation in expression in response to tamoxifen, the same gene often showing significant upregulation in some and downregulation in other samples. Although hierarchical clustering showed some separation of samples across all epithelial lineages combined (Figure 4.4), we next looked at the luminal HR+ subset individually as these are the cells on which tamoxifen acts through expressed ER, (Figure 4.5). Several of the genes in this cluster (ESR1, TFF1, TFF3, PGR, and AREG) showed almost uniform down regulation by tamoxifen. However, the other genes (PRLR, AGR2, PIP, AZGP1 and FOXA1) were upregulated in some and downregulated in other samples. Interestingly these two main clusters were concordant with RG1 and RG2 defined from the DEG PCA analysis. We did not observe the same separation among participants in 5 stromal gene set signatures analysed (data not shown).

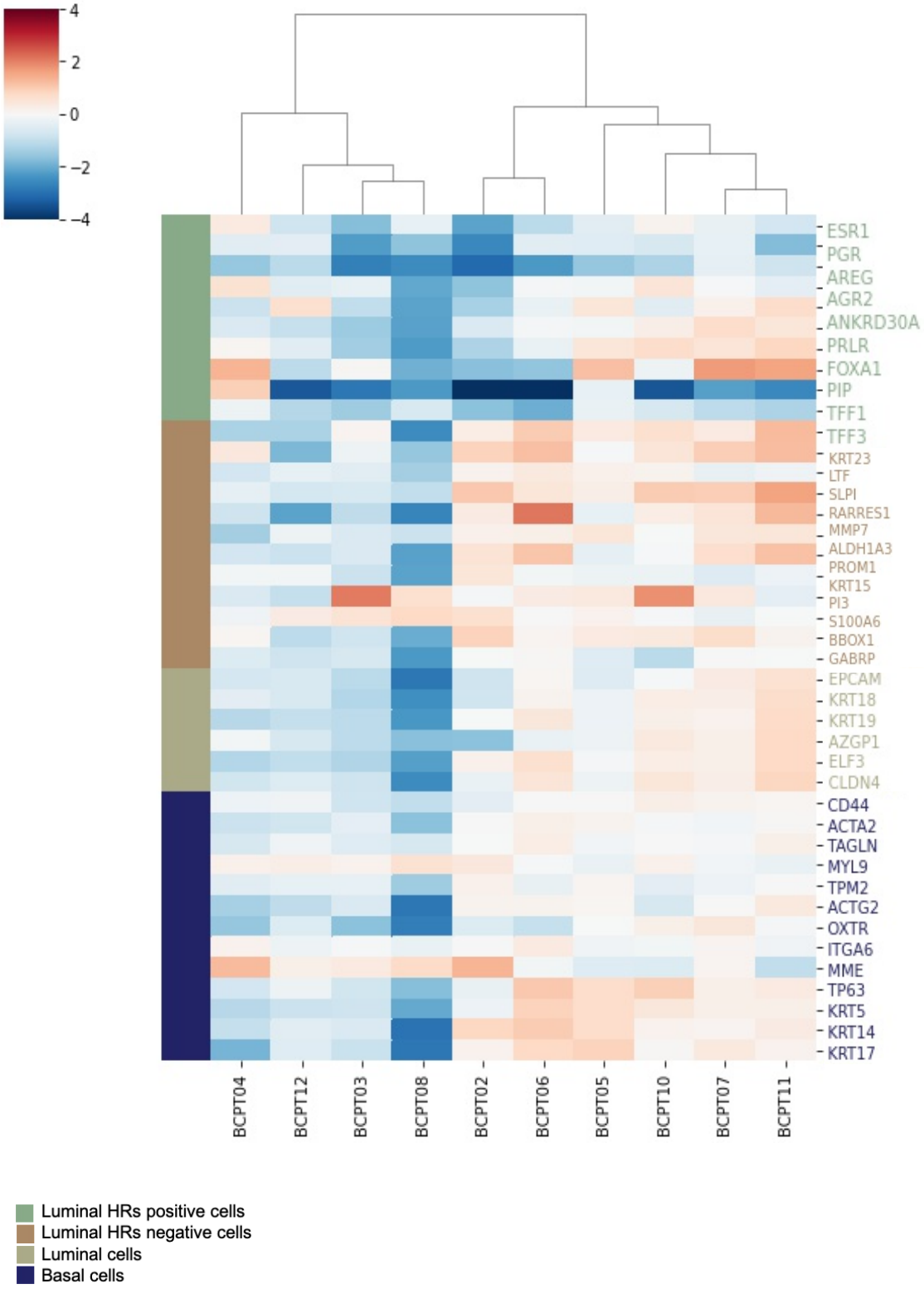


**Figure 4.4 Heatmap displaying the gene set signature associated with mammary epithelial cells.** Genes are displayed as log2 fold change. n=41genes. Each column on the heatmap represents an individual participant; Red indicates an upregulation and blue a downregulation, the degree to which can be seen on the colour key scale**.**

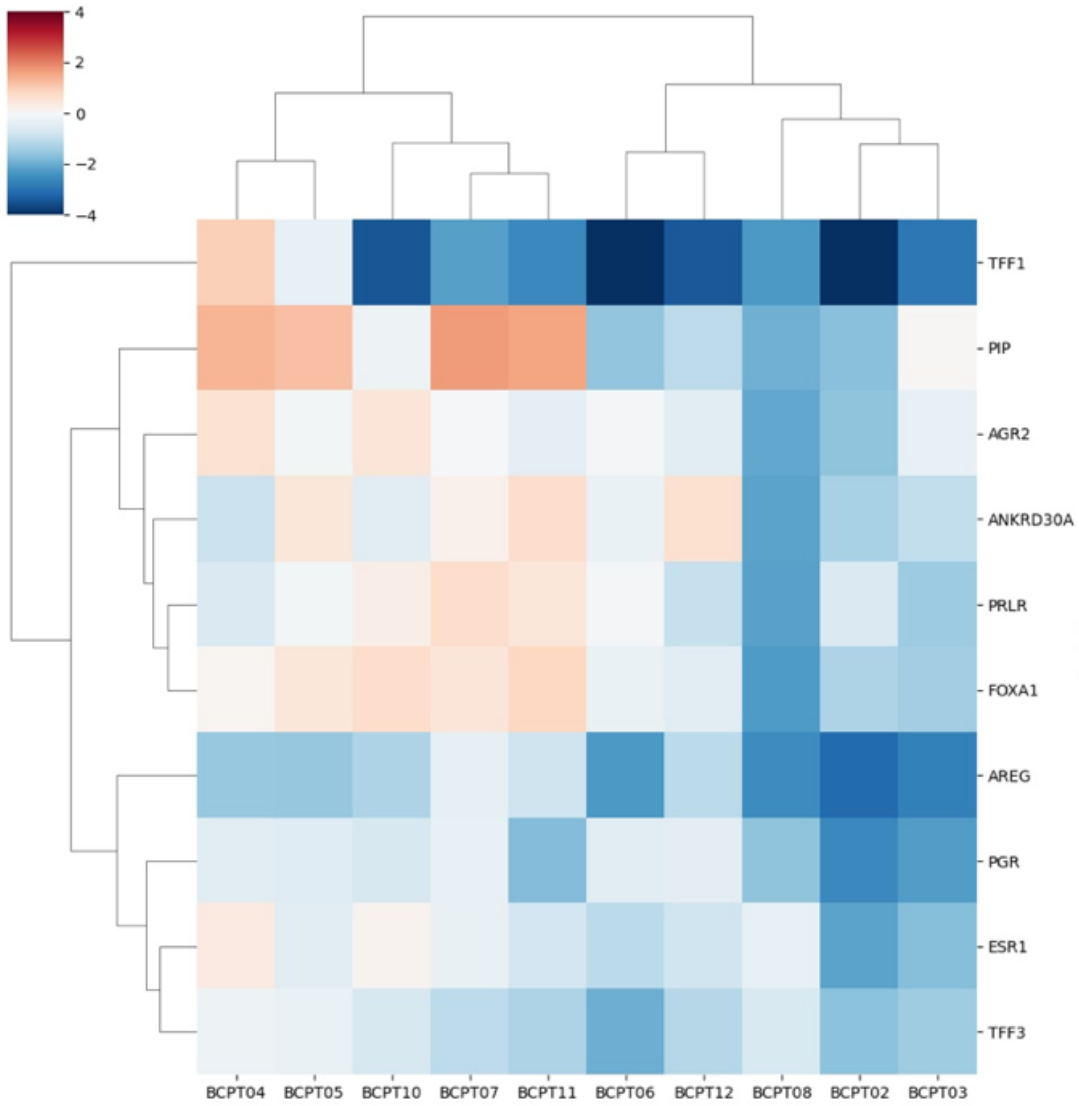


**Figure 4.5 Heatmap displaying the gene set signature associated with Luminal hormone positive cells.** Genes are displayed as Log2 fold change. n=10 genes. Each column on the heatmap represents an individual participant; Red indicates an upregulation and blue indicates a downregulation, the degree to which can be seen on the colour key scale

We next performed pathway enrichment analysis of differentially expressed genes in response to tamoxifen within RG1 and RG2 independently. We found that differentially expressed genes in RG1 were significantly enriched in seven pathways (Table 4.3. and Figure 4.6). Adipogenesis, fatty acid metabolism, myogenesis and oxidative phosphorylation related pathways were upregulated whereas estrogen response, G2M checkpoints and E2F target related pathways were downregulated in this group. In contrast, there were no significantly enriched DEG pathways in RG2 suggesting a lack of 'classical' antiestrogen response.

**Table 4.3: Pathway enrichment analysis for differentially expressed genes in Response Group 1 after TAM treatment. NES = Normalized enrichment score, Padj= adjusted P value. Size = number of genes included in each pathway**

| Pathway | NES | Padj | Size | Biological Process |
|---|---|---|---|---|
| **Adipogenesis** | 4.04 | 0.00 | 62 | Metabolic |
| **Estrogen response early** | -4.06 | 0.00 | 73 | Signalling |
| **Estrogen response late** | -3.64 | 0.00 | 75 | Signalling |
| **Myogenesis** | 2.35 | 0.01 | 46 | Development |
| **G2M checkpoint** | -2.19 | 0.02 | 24 | Proliferation |
| **E2F targets** | -2.09 | 0.02 | 21 | Proliferation |
| **Oxidative phosphorylation** | 2.11 | 0.03 | 20 | Metabolic |
| **Fatty acid metabolism** | 1.99 | 0.05 | 37 | Metabolic |

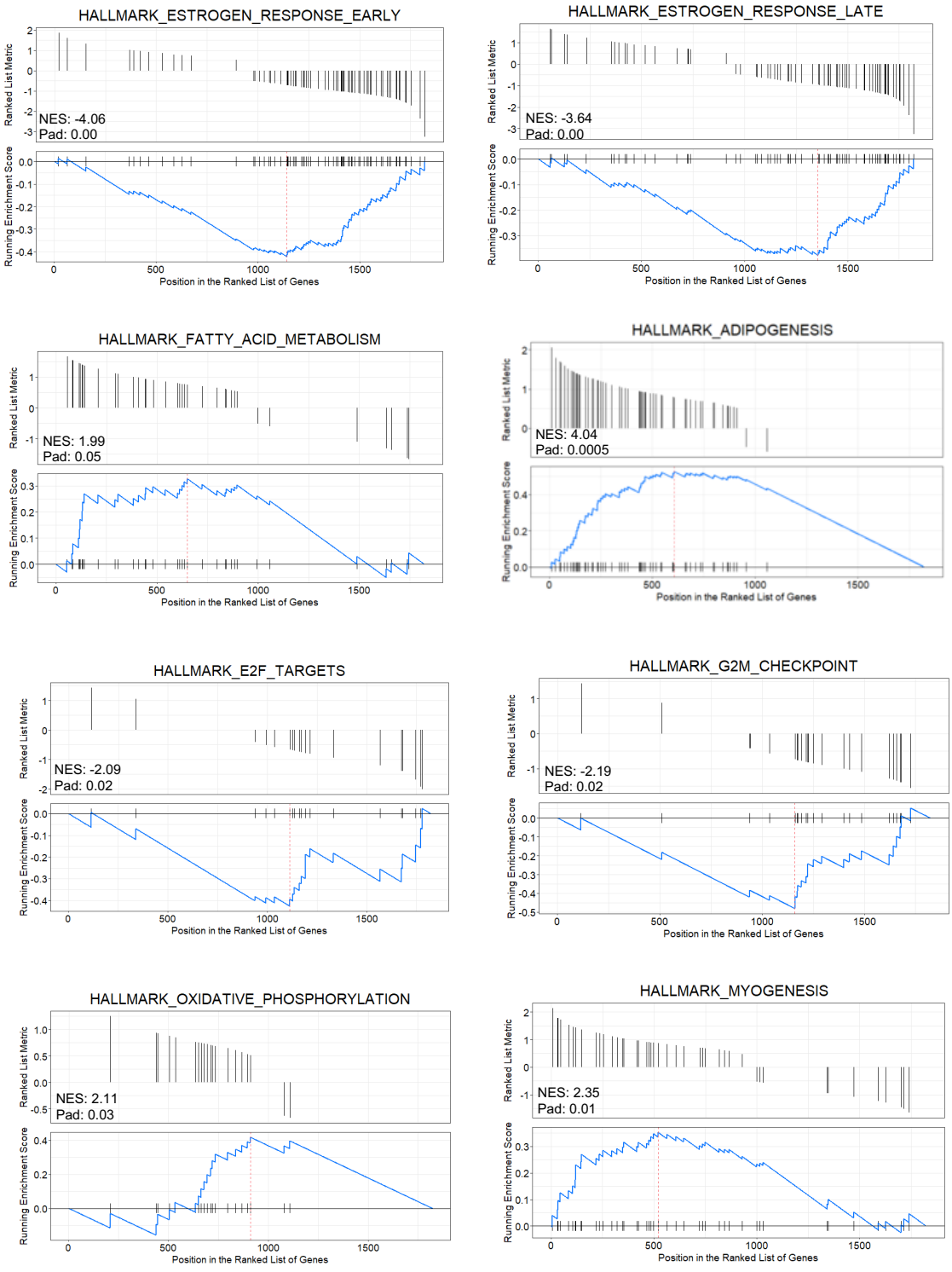


**Figure 4.6 Analysis of pathway enrichment using Gene Ontology.** The pathways enrichment scores for each enriched pathway in RG1. Rank represents the position in the ranked list at which the maximum enrichment score occurred. The most interesting gene sets achieve the maximum enrichment score near the top or bottom of ranked list. For inferring GSEA pathways, MsigDB database was used which contain HALLLMARK pathways. For conducting GSEA analysis R packages FGSEA, MSIGDBR and cluster profiler were used.

### 4.2.4 Tamoxifen mediated expression of proliferation associated genes

We next investigated a proliferation related gene set consisting of *MKI67, BUB1, MYBL2, E2F1* and *PLK1* genes (Figure 4.7). Interestingly three of RG2 (BCPT04,7 and 11) clustered together and showed increase in proliferative gene expression with tamoxifen including *MKI67* which is the gene for the Ki67 protein, regulation of which was the primary endpoint of this prevention clinical trial, (See methods section 2.1.5.2).

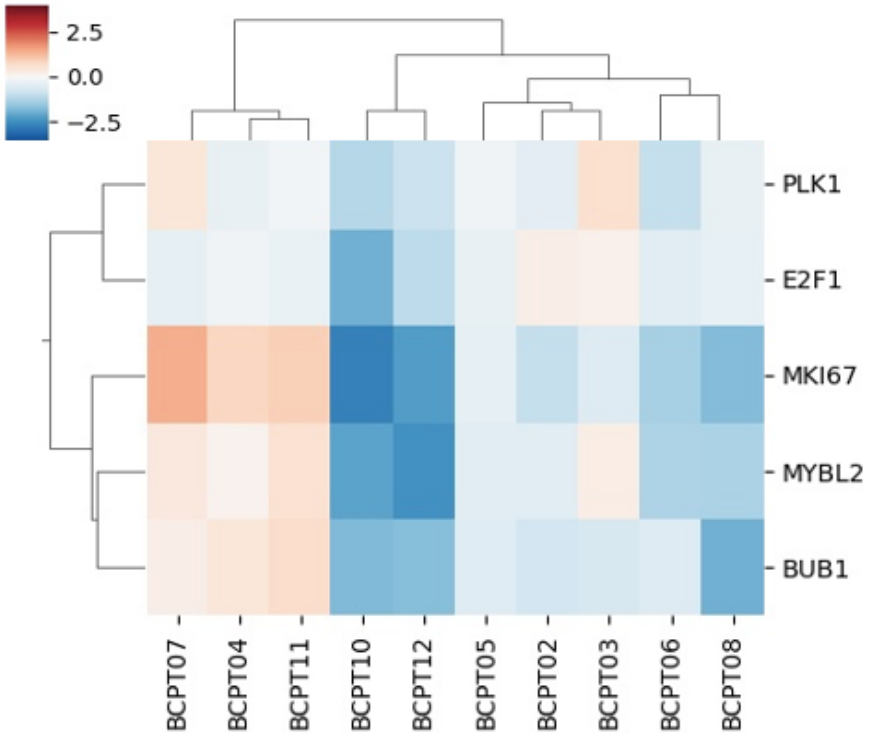


**Figure 4.7 Heatmap displaying the** 5 **gene set signature associated with proliferation.** Genes are displayed as log2 fold change. Each column on the heatmap represents an individual participant; Red indicates an upregulation and blue a downregulation, the degree to which can be seen on the colour key scale.

Interestingly BCPT10 showed marked downregulation of all proliferation genes despite aligning with RG2 samples generally and showing stimulation of expression of the luminal HR+ genes. This suggests there may be a decoupling of proliferative and HR+ cell gene expression in response to tamoxifen in some patients that could have important implications for biomarker selection.

To investigate further we examined the correlation between Ki67 protein expression and *MKI67* gene expression (Figure 4.8c) and showed a moderate correlation (r=0.71; p=0.023). Interestingly the three main outliers in this analysis were from RG2 (BCPT04,7 and 10) suggesting the association between RNA and protein expression, at least for Ki67/*MKI67*, is weaker in the less responsive subgroup. With the exception of *MKI67* expression in BCPT10 waterfall plots of the changes in expression of Ki67 and *MKI67* with treatment separated RG1 and RG2, (Figure 4.8a,b).

(a)

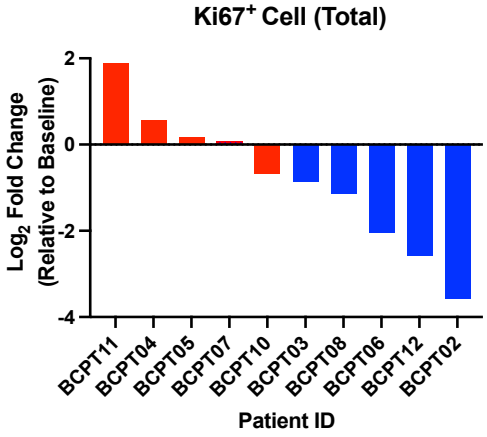


(b)

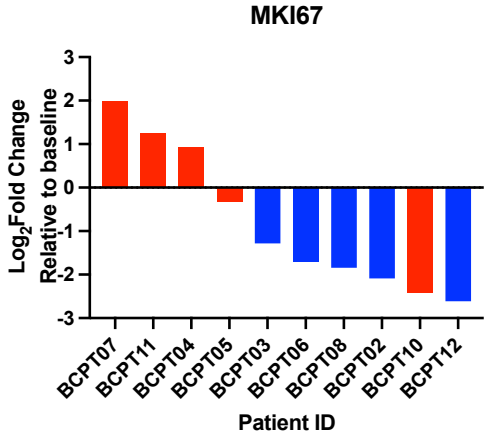


(c)

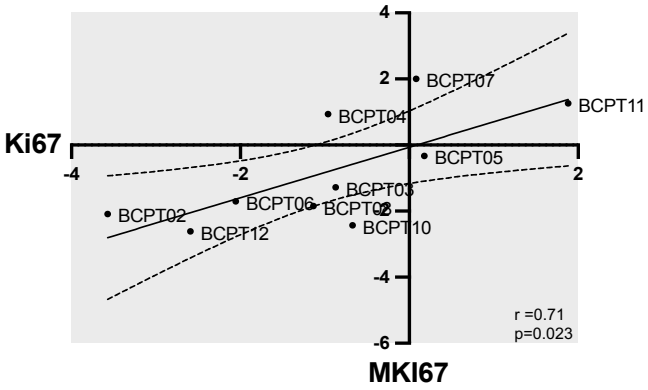


**Figure 4.8 Ki67 protein and *MKI67* gene as biomarkers for TAM response in premenopausal women.** Waterfall plots of fold change differences in (a) Ki67 protein, (b) *MKI67* gene relative to the baseline values. Ki67 protein expression was detected by Immunohistochemical analysis. *MKI67* gene expression was detected by RNAseq analysis. The blue bars represent participants included in RG1 while red bars represent participants included in RG2 (c) Scatter plots showing the correlation between the change in Ki67 expression and *MKI67* gene expression after 12 weeks of TAM treatment. The best-fit linear regression line (solid line) of each scatter plot is shown together with the Pearson correlation coefficient (r). Dotted lines represent 95% confidence intervals (CI). n=10.

We next examined whether changes in either *MKI67* gene or Ki67 protein expression correlated with changes in acinar area. A very strong positive correlation was observed for reduction in *MKI67* gene expression and reduction in acinar area with tamoxifen treatment (r=0.9102; p=0.0003: Figure 4.9c), with a weaker but still significant association between change in %Ki67 and acinar area, (r=0.6542. p=0.0402: Figure 4.9b). Again, the waterfall plot for acinar area reduction broadly separated RG1 and RG2 albeit with BCPT10 exhibiting reductions similar to most RG1 samples (Figure 4.9a), consistent with the more marked reduction in *MKI67* expression.

(a)

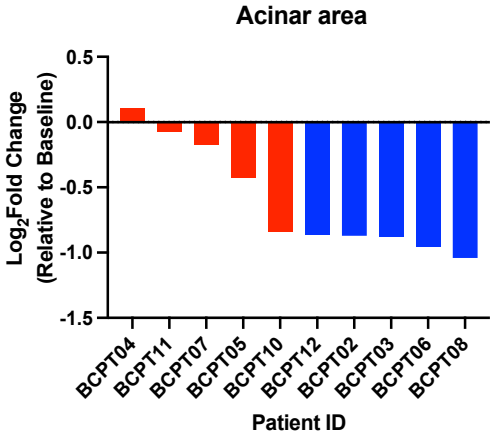


(b)

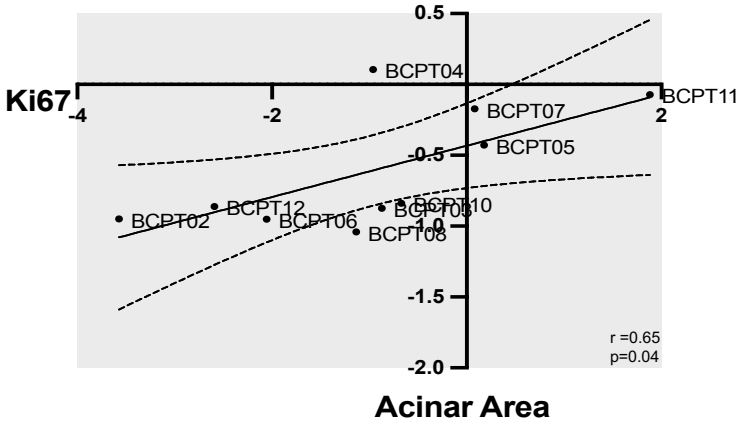


(c)

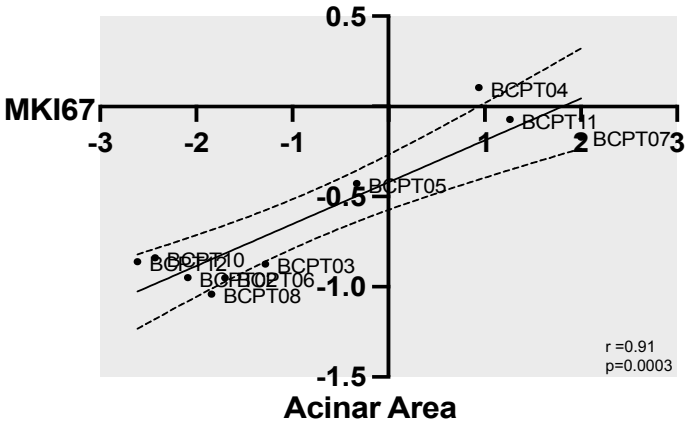


**Figure 4.9 Scatter plots showing the correlation between Ki67 protein and *MKI67* gene expression and acinar area after 12 weeks of tamoxifen treatment.** (a) Waterfall plots of fold change differences in the acinar area. Scatter plots showing the correlation between the change in Ki67 expression and acinar area (b) and the change in MKI67 expression and acinar area (c) after 12 weeks of TAM treatment. The best-fit linear regression line of each scatter plot (solid line) is shown together with the Pearson correlation coefficient (r) Dotted lines represent 95% confidence intervals (CI). n=10.

### 4.2.5 Tamoxifen effects on ER and PR protein and related gene expression

We have previously shown (chapter 3 and Figure 4.5 that both ER protein and ESR1 gene expression are down regulated by tamoxifen in the majority of participants in the tamoxifen study. All participants showed a reduction in PR and PGR expression. Plotting these data as waterfall plots one can see that the majority of RG1 cases group together with more marked responses and RG2 with less marked (PR/PGR) or even stimulatory (ER/ESR1) responses (Figure 4.10 a-d). There are, however, outliers in each analysis. The reduction of ER protein expression was strongly positively correlated with the downregulation of *ESR1* gene expression (r=0.88, p=0.0008: Figure 4.10e). However, there was no comparable correlation between PR and PGR expression (r=0.40, p=0.26: Figure 4.10f).

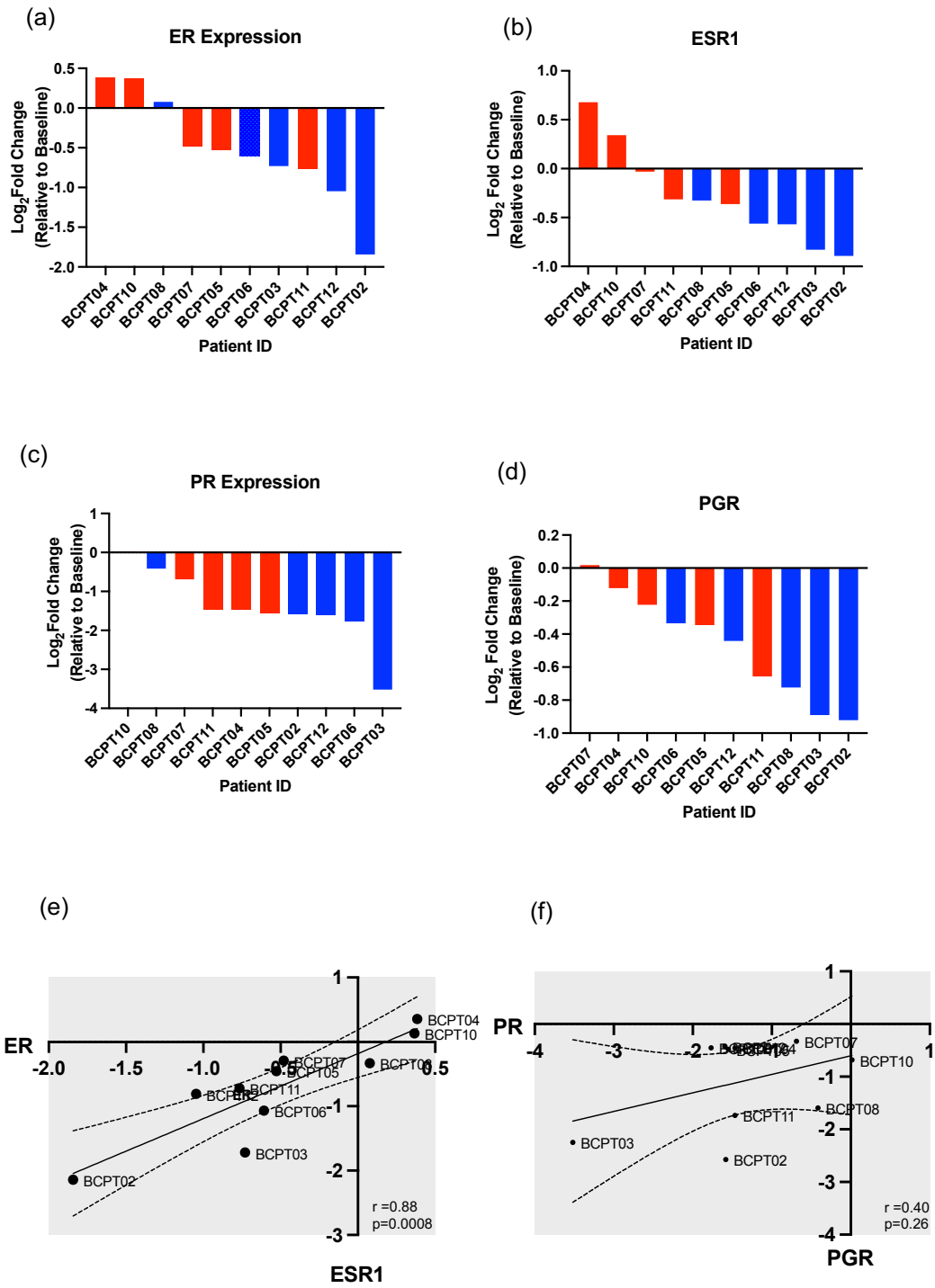


**Figure 4.10 Waterfall and scatter plots showing the correlation between change in protein and gene expression of steroid receptors with TAM treatment.** Waterfall plots of fold differences in ER and PR protein expression and ESR1 and PGR gene expression relative to the baseline values. (a) ER and (c) PR protein expression was detected by Immunohistochemical analysis and the percentage of hormone receptor positive epithelial cells after treatment was compared to the baseline values. ESR1 (b) and PGR gene expression levels (d) were derived from RNAseq data analysis. Blue bars represent participants classified in RG1 while red bars represent participants classified in RG2. The best-fit linear regression line of each scatter plot is shown (e and f) between protein and gene expression, together with Pearson correlation coefficient (r). n=10.

### 4.2.6 Proteomic analysis of breast lobules reveals differences between RG1 and RG2.

We next sought to identify proteins that may have been potentially affected by tamoxifen in the lobular compartment of the normal breast. To this end, we utilized laser capture microdissection -coupled mass spectrometry (LCM-MS). This technology enables distinct tissue regions, including subpopulations or individual cells, to be excised and harvested for downstream proteomic analyses.

For our studies, we utilized only six pairs of samples to reduce cost. Three pairs of samples were analysed from Response Group 1 (BCPT03, BCPT06, BCPT08) and three pairs in Response Group 2 (BCPT04, BCPT07, BCPT11). We first performed LCM to collect equal volumes of the breast lobular compartment from each baseline and 12-week sample. Collected tissues were then processed for proteomic analyses. Volcano plots were generated using a -Log 10 (FDR) and fold change ≥2.

In the lobular compartments of the six pairs of samples, we identified 37 significantly differentially expressed proteins. Among those proteins, 19 proteins were up-regulated (Table 4.4) and 18 proteins were down-regulated (Table 4.5). Using the KEGG method did not reveal any enriched pathways perturbed by tamoxifen across all 6 paired samples (data not shown).

**Table 4.4 Up-regulated proteins identified in the lobular compartment of pair of samples from 6 participants. $Log_2FC$ = log fold change. FDR= False discovery rate. P value ≤ 0.05. N=6.**

| PROTEIN NAMES | $LOG_2FC$ | P-VAL | FDR |
|---|---|---|---|
| **LTF** | 0.82 | 1.46E-12 | 9.00E-10 |
| **COL7A1** | 0.34 | 1.19E-09 | 3.00E-07 |
| **APCS** | 0.61 | 5.68E-09 | 1.20E-06 |
| **HSPA1A** | 0.5 | 2.17E-08 | 4.00E-06 |
| **HSPA1B** | 0.5 | 2.17E-08 | 4.00E-06 |
| **TMEM43** | 0.4 | 6.70E-06 | 0.0009 |
| **LMNB2** | 0.28 | 1.03E-05 | 0.0013 |
| **IGHM** | 0.27 | 1.78E-05 | 0.002 |
| **H1F0** | 0.52 | 2.24E-05 | 0.002 |
| **FTL** | 0.71 | 5.55E-05 | 0.004 |
| **HIST1H4A** | 0.31 | 6.93E-05 | 0.005 |
| **TXNDC5** | 0.41 | 0.00028909 | 0.02 |
| **MFAP4** | 0.63 | 0.00077073 | 0.03 |
| **PGK1** | 0.3 | 0.00090591 | 0.04 |
| **ANXA5** | 0.5 | 0.00099926 | 0.04 |
| **SLC25A11** | 0.26 | 0.00101876 | 0.04 |
| **OGN** | 0.41 | 0.00112449 | 0.04 |
| **ANXA3** | 0.44 | 0.00138336 | 0.05 |
| **MUC1** | 2.11 | 0.00146345 | 0.05 |

**Table 4.5 down-regulated proteins identified in the lobular compartment of pair of samples from 6 participants. $Log_2FC$ = log fold change. FDR= False discovery rate. P value ≤ 0.05. N=6.**

| PROTEIN NAMES | $LOG_2FC$ | P-VAL | FDR |
|---|---|---|---|
| **DSP** | -0.31 | 1.00E-12 | 9.00E-10 |
| **COL14A1** | -0.65 | 7.00E-11 | 2.00E-08 |
| **AZGP1** | -0.91 | 2.00E-06 | 0.00031 |
| **CKAP4** | -0.36 | 1.00E-05 | 0.001 |
| **HAL** | -1.81 | 4.00E-05 | 0.004 |
| **CDSN** | -0.81 | 5.00E-05 | 0.004 |
| **DSC1** | -0.71 | 7.00E-05 | 0.005 |
| **DSG1** | -0.48 | 7.00E-05 | 0.005 |
| **EEF2** | -0.23 | 8.00E-05 | 0.005 |
| **VCL** | -0.15 | 0.0001 | 0.006 |
| **A2ML1** | -1.2 | 0.0003 | 0.02 |
| **JUP** | -0.35 | 0.0005 | 0.02 |
| **PSMA5** | -0.42 | 0.0005 | 0.02 |
| **SERPINB12** | -0.46 | 0.0006 | 0.03 |
| **PKP2** | -0.62 | 0.001 | 0.04 |
| **IDH1** | -0.47 | 0.001 | 0.04 |
| **EMILIN1** | -0.28 | 0.001 | 0.04 |
| **CALML5** | -0.71 | 0.001 | 0.05 |

Our data in chapter three and transcriptomic analysis showed distinctive responses to tamoxifen treatment between RG1 and RG2. Accordingly, the proteomic data from RG1 (n=3) and RG2 (n=3) samples were examined separately. In the lobular compartment of Response Group 1, we identified 66 significantly differentially expressed proteins, (Figure 4.11a; Table 4.6; 4.7). Gene Ontology (GO) analysis indicated that proteins involved in extracellular matrix (ECM) composition, fibrillar collagen trimerization, ECM organization, ECM-receptor interaction and focal adhesion pathways were upregulated. Tamoxifen significantly reduced the expression of fibronectin (FN1) and proteins related to epithelial-stromal interaction and tissue remodelling, such as SERPINA3 and SERPINH, Figure 4.11b).

(a)

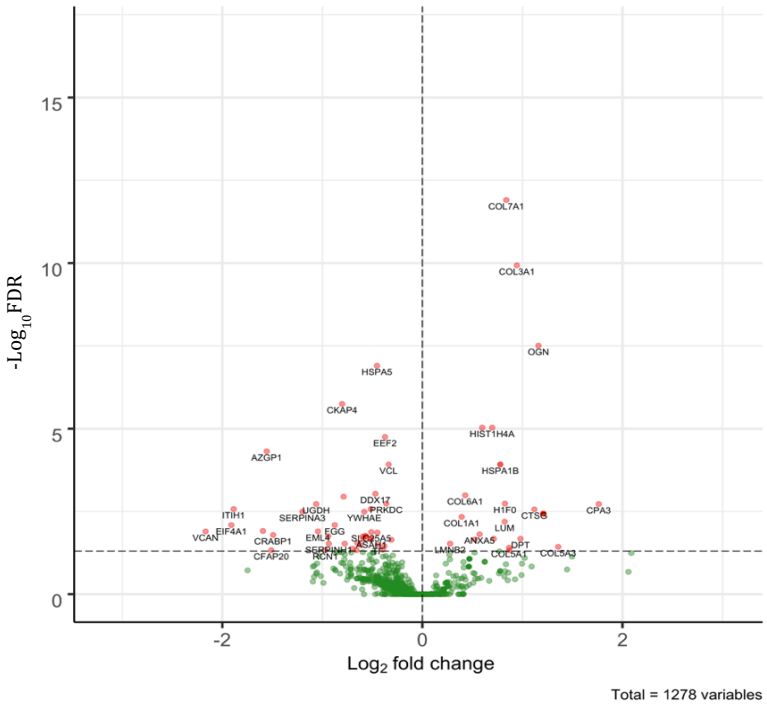


(b)

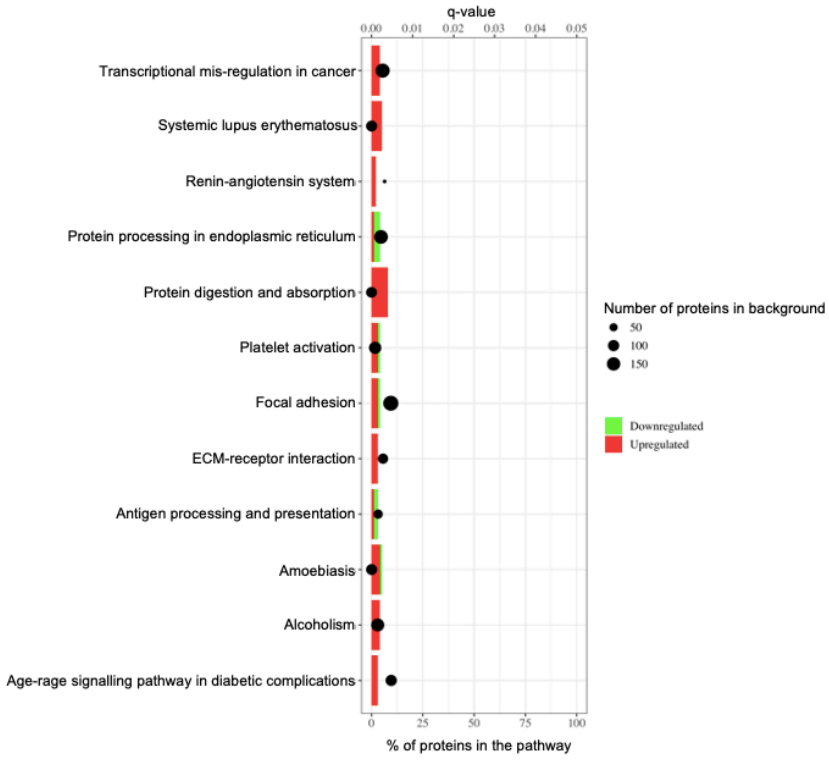


**Figure 4.11: Differentially expressed proteins in the lobular compartment of RG1 samples after TAM treatment.** A total of 1278 proteins were identified. 66 differentially expressed proteins were identified. (a) Volcano plot using a -Log 10 (FDR) and fold change ≥2. Significantly differentially expressed proteins are labelled in red, where q value < 0.05. Proteins that pass the fold change cut-off but not the q-value cut-off are labelled in green. (b) Gene Ontology (GO) analysis of differentially expressed proteins using KEGG database. Bars in green represent the down-regulated pathways while bars in red represent the up-regulated pathways.

**Table 4.6 Up-regulated proteins identified in the lobular compartment of pair of samples from participants included in RG1. $Log_2FC$= log fold change. P value ≤ 0.05. FDR= False discovery rate. N=3**

| Protein names | $LOG_2FC$ | P-val | FDR |
|---|---|---|---|
| **COL7A1** | 0.84 | 1.0983E-15 | 1.2411E-12 |
| **COL3A1** | 0.94 | 2.0792E-13 | 1.1748E-10 |
| **OGN** | 1.16 | 8.2686E-11 | 3.1145E-08 |
| **HIST1H4A** | 0.71 | 5.3619E-08 | 9.3092E-06 |
| **COL1A2** | 0.61 | 5.7668E-08 | 9.3092E-06 |
| **HSPA1B** | 0.78 | 1.131E-06 | 0.0001 |
| **HSPA1A** | 0.79 | 1.131E-06 | 0.0001 |
| **COL6A1** | 0.43 | 1.1842E-05 | 0.0001 |
| **H1F0** | 0.82 | 0.00002 | 0.0001 |
| **CPA3** | 1.81 | 0.00003 | 0.002 |
| **CTSG** | 1.12 | 0.00005 | 0.003 |
| **H3F3B** | 1.21 | 0.00008 | 0.004 |
| **COL1A1** | 0.39 | 0.0001 | 0.005 |
| **LUM** | 0.82 | 0.0001 | 0.006 |
| **ANXA5** | 0.57 | 0.0005 | 0.02 |
| **DPT** | 0.98 | 0.0008 | 0.02 |
| **PRELP** | 0.71 | 0.0008 | 0.02 |
| **APCS** | 0.52 | 0.0009 | 0.02 |
| **LMNB2** | 0.28 | 0.001 | 0.03 |
| **COL5A3** | 1.36 | 0.002 | 0.04 |
| **COL5A1** | 0.87 | 0.002 | 0.04 |
| **BCAM** | 0.87 | 0.003 | 0.05 |

**Table 4.7 Down-regulated proteins identified in the lobular compartment of pair of samples from participants included in RG1. $Log_2FC$= log fold change. P value ≤ 0.05. FDR= False discovery rate. N=3**

| PROTEIN NAMES | $LOG_2FC$ | P-VAL | FDR |
|---|---|---|---|
| **HSPA5** | -0.45 | 4.46E-10 | 1.2592E-07 |
| **CKAP4** | -0.8 | 7.9224E-09 | 1.7905E-06 |
| **EEF2** | -0.4 | 1.2611E-07 | 0.00002 |
| **AZGP1** | -1.56 | 3.8628E-07 | 0.00005 |
| **VCL** | -0.34 | 1.1773E-06 | 0.0001 |
| **DDX17** | -0.47 | 9.8467E-06 | 0.0009 |
| **CRABP2** | -0.79 | 0.00001 | 0.001 |
| **PRKDC** | -0.36 | 0.00003 | 0.002 |
| **UGDH** | -1.12 | 0.00003 | 0.002 |
| **IARS** | -0.52 | 0.00005 | 0.003 |
| **ITIH1** | -1.89 | 0.00005 | 0.003 |
| **YWHAE** | -0.61 | 0.00007 | 0.003 |
| **SERPINA3** | -1.21 | 0.00007 | 0.003 |
| **EIF4A1** | -1.91 | 0.0002 | 0.008 |
| **FGG** | -0.92 | 0.0002 | 0.008 |
| **SERPINA3** | -1.61 | 0.0003 | 0.01 |
| **EML4** | -1.04 | 0.0003 | 0.01 |
| **VCAN** | -2.23 | 0.0003 | 0.01 |
| **SLC25A5** | -0.51 | 0.0004 | 0.01 |
| **EEF1G** | -0.45 | 0.0004 | 0.01 |
| **CRABP1** | -1.51 | 0.0005 | 0.01 |
| **RPL34** | -0.61 | 0.0005 | 0.01 |
| **FN1** | -1.01 | 0.0006 | 0.01 |
| **PSMA7** | -0.62 | 0.0006 | 0.02 |
| **LAP3** | -0.61 | 0.0006 | 0.02 |
| **ASAH1** | -0.51 | 0.0007 | 0.02 |
| **LARS** | -0.59 | 0.0008 | 0.02 |
| **CCT7** | -0.52 | 0.0009 | 0.02 |
| **PDIA3** | -0.31 | 0.0009 | 0.02 |
| **LDHB** | -0.65 | 0.001 | 0.03 |
| **SERPINH1** | -1.1 | 0.001 | 0.03 |
| **IDH1** | -0.81 | 0.001 | 0.03 |
| **TF** | -0.44 | 0.002 | 0.03 |
| **DSC1** | -0.62 | 0.002 | 0.03 |
| **RPS25** | -0.41 | 0.002 | 0.04 |
| **FSCN1** | -0.72 | 0.002 | 0.04 |
| **TAGLN** | -0.42 | 0.002 | 0.04 |
| **HNRNPL** | -0.71 | 0.002 | 0.05 |
| **CFAP20** | -1.51 | 0.002 | 0.05 |
| **RCN1** | -1.12 | 0.002 | 0.05 |

### 4.2.7 Potential biomarkers associated with poor response to tamoxifen

In contrast to RG1, there were only 32 proteins differentially expressed in RG2, (Figure 4.12a; Tables 4.8-4.9). We noted that six proteins involved in ECM organisation tended to downregulate, however, this was only statistically significant for the COL14A1 protein. GO analysis further indicated that the ECM-receptor interaction pathway was reduced significantly by tamoxifen treatment in RG2, (Figure 4.12b).

(a)

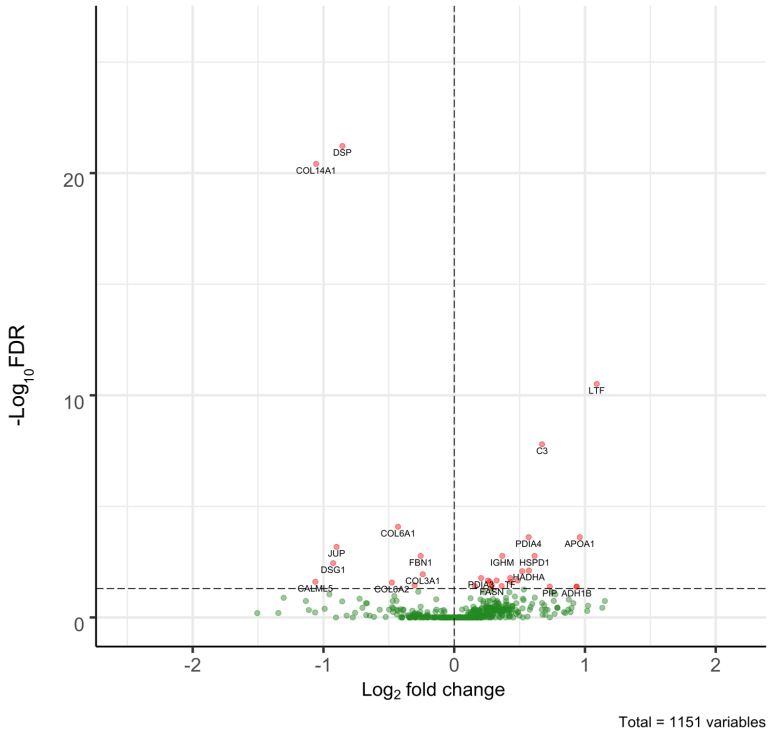


(b)

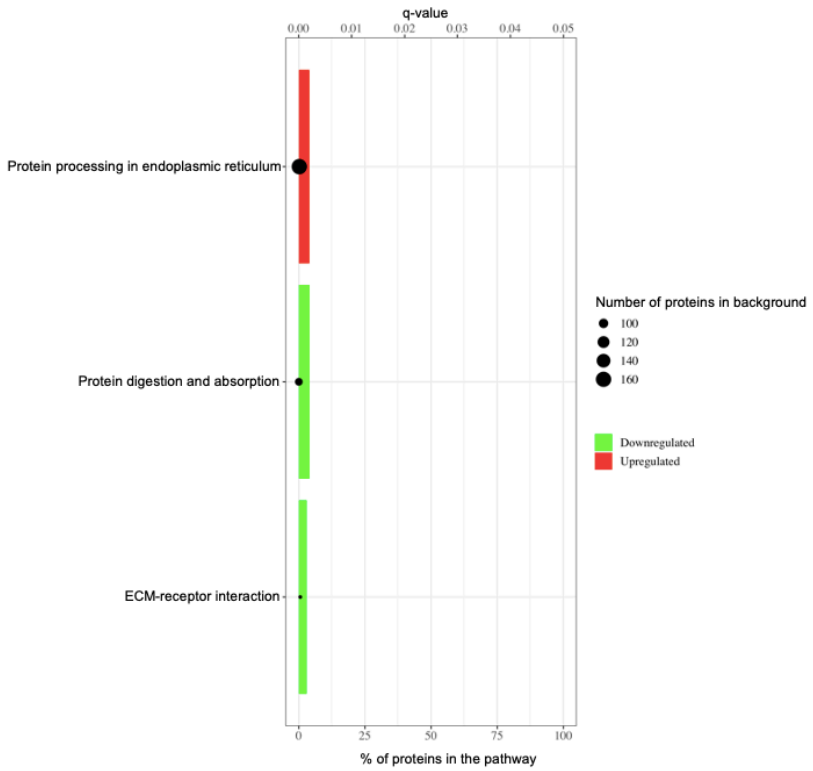


**Figure 4.12: Differentially expressed proteins in the lobular compartment of RG2 after TAM treatment.** A total of 1151 proteins were identified. 32 differentially expressed genes were identified. (a) Volcano plot generated using a -Log 10 (FDR) and fold change ≥2. Significantly differentially expressed proteins are labelled in red, where q value < 0.05. Proteins that pass the fold change cut-off, but not the q-value cut-off, are labelled in green. (b) Gene Ontology (GO) analysis of differentially expressed proteins. Bars in green represent the down-regulated proteins while bars in red represent the up-regulated proteins.

**Table 4.8 Up-regulated proteins identified in the lobular compartment of pairs of samples from participants included in RG2. $Log_2FC$= log fold change. P value ≤ 0.05. FDR= False discovery rate. N=3 pairs**

| PROTEIN NAMES | $LOG_2FC$ | P-VAL | FDR |
|---|---|---|---|
| **LTF** | 1.1 | 1.1719E-13 | 3.0879E-11 |
| **C3** | 0.71 | 7.6204E-11 | 1.6064E-08 |
| **PDIA4** | 0.57 | 0.000002 | 0.0002 |
| **APOA1** | 0.96 | 0.000002 | 0.0002 |
| **HSPD1** | 0.61 | 0.000002 | 0.002 |
| **IGHM** | 0.37 | 0.00002 | 0.002 |
| **HADHA** | 0.57 | 0.0001 | 0.008 |
| **APCS** | 0.52 | 0.0001 | 0.008 |
| **TF** | 0.43 | 0.0003 | 0.02 |
| **PDIA3** | 0.21 | 0.0003 | 0.02 |
| **VPS35** | 0.26 | 0.0004 | 0.02 |
| **TXNDC5** | 0.49 | 0.0004 | 0.02 |
| **TMEM43** | 0.32 | 0.0005 | 0.02 |
| **A2M** | 0.43 | 0.0006 | 0.02 |
| **LMNB2** | 0.27 | 0.0006 | 0.02 |
| **FASN** | 0.29 | 0.0001 | 0.04 |
| **SLC25A11** | 0.36 | 0.001 | 0.04 |
| **SPTAN1** | 0.16 | 0.001 | 0.04 |
| **HEL-S-117** | 0.94 | 0.001 | 0.04 |
| **PIP** | 0.73 | 0.001 | 0.04 |
| **RPN1** | 0.28 | 0.001 | 0.05 |

**Table 4.9 Down-regulated proteins identified in the lobular compartment of pair of samples from participants included in RG2. $Log_2FC$= log fold change. P value ≤ 0.05. FDR= False discovery rate. N=3**

| PROTEIN NAMES | $LOG_2FC$ | P-VAL | FDR |
|---|---|---|---|
| **DSP** | -0.85 | 1.1407E-24 | 6.0113E-22 |
| **COL6A1** | -0.43 | 4.7185E-07 | 0.00008 |
| **JUP** | -0.91 | 5.6875E-06 | 0.0007 |
| **FBN1** | -0.26 | 0.00002 | 0.002 |
| **DSG1** | -0.92 | 0.00004 | 0.004 |
| **COL14A1** | -1.21 | 0.0002 | 0.01 |
| **COL3A1** | -0.24 | 0.0002 | 0.01 |
| **CALML5** | -1.06 | 0.0006 | 0.02 |
| **COL6A2** | -0.48 | 0.0007 | 0.03 |
| **LAMC2** | -0.3 | 0.0009 | 0.04 |

### 4.2.8 Functional protein associated networks modified by tamoxifen therapy

To investigate the patterns of protein regulation in response to tamoxifen further we used STRING-DB and Ingenuity Pathway Analysis (IPA) approaches to assess functional protein networks. In RG1 samples, collagen and collagen associated proteins were upregulated within the lobular compartment, (Figure 4.13).

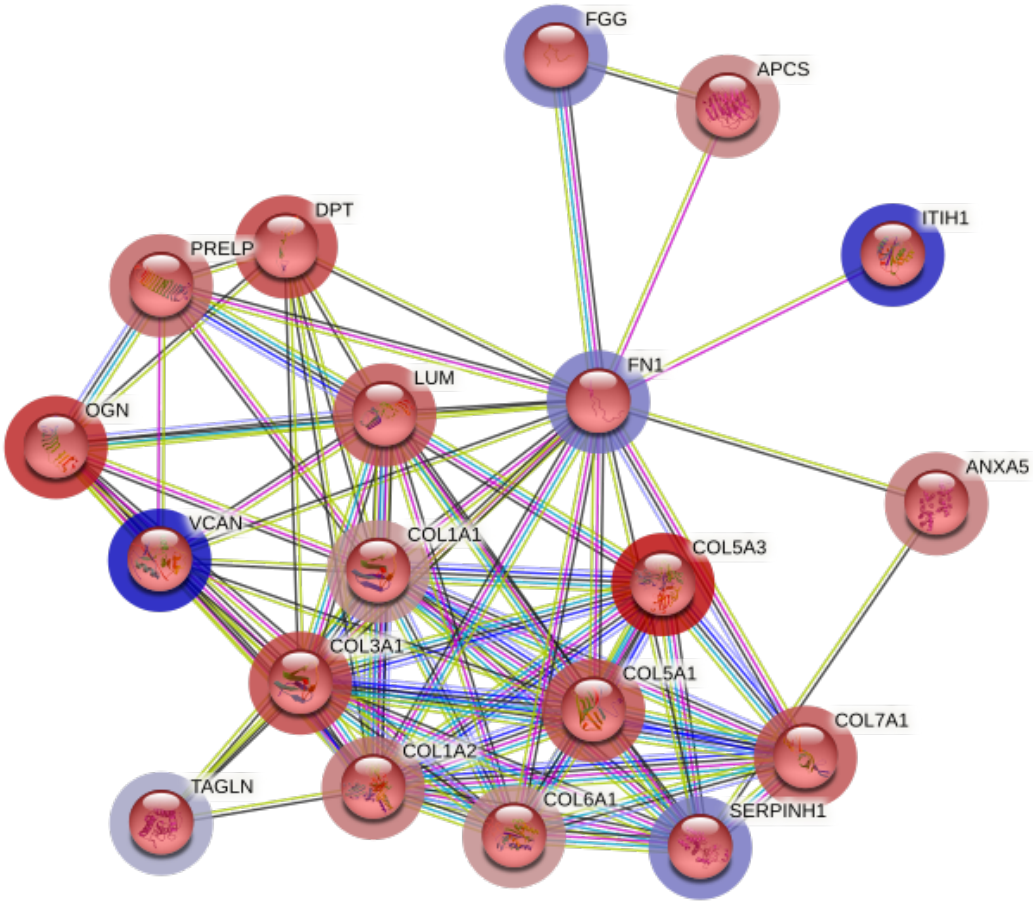


**Figure 4.13: Functional protein association networks within breast lobules in RG1.** Differentially expressed proteins were identified and their network connection investigated using STRING-DB.org. Red and blue halos indicate up- and down-regulation respectively. Collagen and collagen associated proteins are upregulated in the RG1.

In contrast in RG2 samples only 2 small networks were perturbed, (Figure 4.14). Intriguingly, and at least partially validating the RNAseq data proteins involved in the androgen receptor signalling pathways, including PIP and APOA1, were upregulated in RG2, (Figure 4.14b). Moreover, we found that lactotransferrin (LTF) expression by luminal cells was increased, which is associated with milk production and secretory molecules (Nguyen et al. 2018).

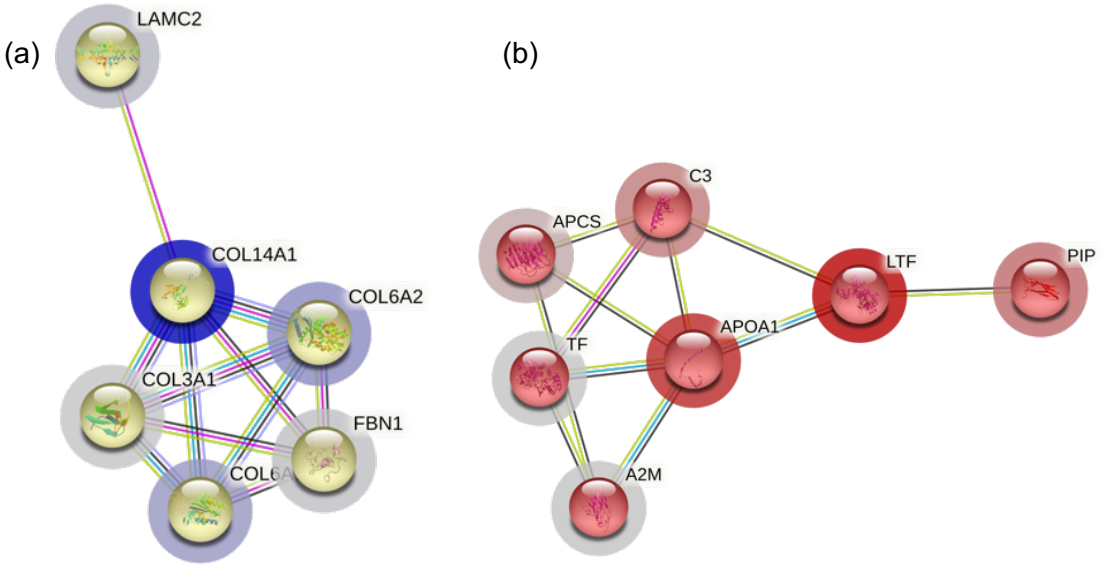


**Figure 4.14: Functional proteins association networks within RG2 lobules**. (a-b) Differentially expressed proteins were identified and their network connection investigated using STRING-DB.org. Red and blue halos indicate up- and down-regulation respectively.

Then, we aimed to determine pathways and proteins structures that were up and down regulated in the post-treatment samples versus the baseline. The Ingenuity Pathway Analysis (IPA) software was used to analyse the differently expressed proteins in RG1 and RG2, Figure 4.15 shows the affected pathways in each group by tamoxifen treatment. This analysis verifies the responses variations of participants within each group. The activity of steroid receptors ER and AR signalling pathway were downregulated in RG1 (z-score -3.024; -0.8 respectively), however both were upregulated in RG2 (z-score 2.746 and 1.134 respectively). The activity of EIF2 signalling was also downregulated in RG1 (z-score -3.703) and upregulated in RG2 (z-score 2.722). The wound healing signalling pathway, including collagen and collagen related proteins, was activated in RG1 and (z-score 1.333) and trended to increase in RG2 (z-score 0.06).

(a)

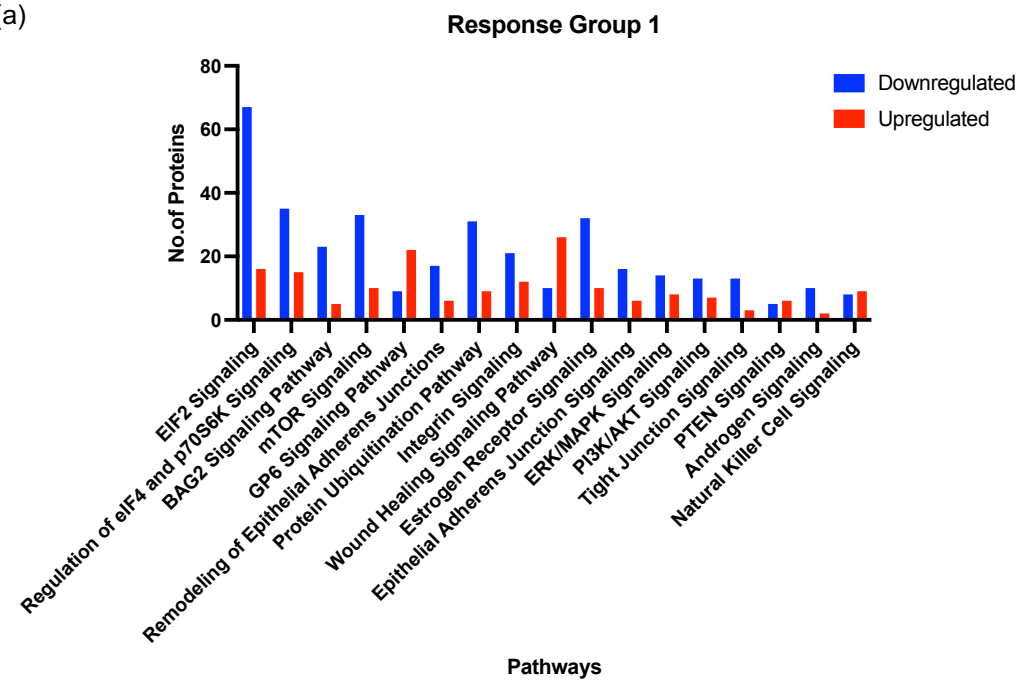


(b)

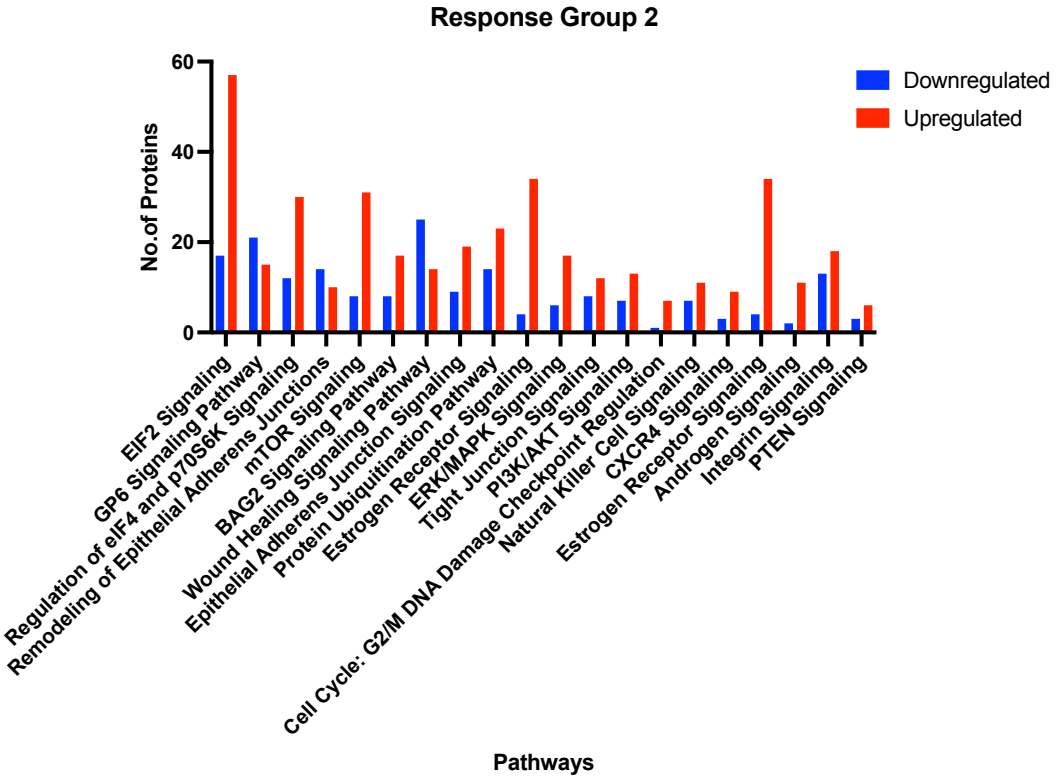


**Figure 4.15 Differentially regulated pathways in the different responsive groups as predicted by IPA approach.** (a): Response Group 1, (b) Response Group 2

## 4.3 Discussion

The purpose of this study was to identify potential signalling pathways that drive tamoxifen resistance. As tamoxifen is a SERM that has been shown to have agonistic effects in the body to produce some of its side effects, such as venous thrombosis and uterine cancer, we hypothesized that tamoxifen may also have agonistic effects in breast tissue in some women. As a first step, we established our RNAseq analysis with unsupervised analysis to determine how gene patterns overall respond to tamoxifen treatment in paired samples. Our preliminary findings show in the PCA that seven post treatment samples responded similarly, while BCPT05, BCPT07, and BCPT11 participants reacted differently, indicating that breast tissues in this cohort were responding in different ways to tamoxifen treatment. In addition, applying a variance stabilization paired wise distance analysis showed that paired sample from BCPT07 participants did not separate Using the differential expression PCA we were able to define two lead-groups of response characteristics for further evaluation. The low number of differentially expressed genes observed in our cohort might be explained by variability in response but also interpatient heterogeneity as we only found 54 differently expressed genes across all participants. As a result, we adapted a targeted approach to determine any differential response using gene set signatures. As tamoxifen binds to the ER, we hypothesized that the greatest effect in differential response characteristics may be seen in the HR+ luminal cells signatures. Tamoxifen did indeed impact the expression of genes normally expressed in HR+ luminal cells and we noted a separation of participants into two differential response groups.

Of particular interest the Ki67 expression data broadly agreed with the luminal ER+ epithelial cell signature data in dividing responders above and below the median change in Ki67 to the same RG1 and RG2 response groups. Samples in RG1 exhibited a reduction in proliferation, while participants in RG2 showed an increase in proliferation except for one participant (BCPT10).

54 genes showed differential regulation by tamoxifen therapy across all paired samples. Despite the fact that many of the genes regulated by tamoxifen are known to be involved in ER signalling, and have previously been shown to be down regulated by tamoxifen in a similar study, (Euhus et al. 2011), no discrete pathways were significantly enriched. This could be due to heterogeneity in baseline expression or the small sample size, but a differential response remains a possibility. Interestingly we noted that certain endocrine regulated genes such as, AGR2, *PRLR, PIP and AZGP1* were upregulated in *RG2. AGR2* and *PRLR* genes have been linked with tamoxifen resistance based on examination of breast cancer cell-lines (Elias et al. 2014; Wang and Wang 2021). While, androgen signalling has been demonstrated to regulate *PIP, AZGP1* and *KLK3* genes, (Hanamura et al. 2021), the higher expression of these genes in the breast suggests androgen signalling activity. The activity of AR signalling pathway has been linked to poor response to endocrine therapy, (Basile et al. 2017) and thus required a consideration of different therapeutic strategies.

The AR signaling pathway has been previously suggested to promote tamoxifen resistance in breast cancer, (De Amicis et al. 2010; Ciupek et al. 2015). One possibility is that AR interacts with ER to mediate tamoxifen resistance. In support of this, it has been previously shown that the presence

of tamoxifen can cause AR and ERα to physically interact and that their recruitment to ER-responsive gene promoters can drive transcription and promote cell cycle progression, (De Amicis et al. 2010). In their study De Amicis et al. reported that tamoxifen promotes AR transcriptional activity, which was suppressed by Casodex, an anti-androgen receptor drug, implying that AR expression promotes tamoxifen's agonistic activity. Their findings indicate that AR expression may play a role in hormone resistance as a novel mechanism, and thus it might be a potential clinical treatment target in human breast cancer and potentially a biomarker of inactivity for prevention.

Tamoxifen binds to ER, preventing estrogen hormone binding, which downregulates ER target gene expression. Normally, the net outcome of tamoxifen is a block in the G1 phase of the cell cycle, which prevents cell proliferation, (Criscitiello et al. 2011). In our investigations, we determined that better response of RG1 to tamoxifen could be based on lower Ki67 protein expression and changes in the acinar area.

In our transcriptomic analyses, we determined that tamoxifen treatment led to downregulation of genes normally enriched in proliferation in RG1. However, we determined that three proliferation-related genes, *MKI67, BUB1, MYBL2*, were upregulated in participants BCPT04, BCPT07 and BCPT11 from RG2. This finding corresponded with our immunohistochemical and morphometric data where Ki67 protein expression and the acinar area of these participants were increased.

To date, while effects of tamoxifen treatment on breast cancer proliferation have been reported, (Osborne et al. 1983; Zhang et al. 2003), it remains less

clear how tamoxifen resistance affects proliferation in high-risk participants and whether proliferation can serve as a robust biomarker of tamoxifen resistance in this setting. In our small trial cohort, we determined that expression of ER and PR were downregulated after tamoxifen treatment at both the gene expression and protein levels. Moreover, we determined that the expression of downstream *ESR1* genes, including *PGR* and *AREG,* were also down regulated and correlated positively with lower *ESR1* expression. Intriguingly, autocrine amphiregulin expression has been previously implicated in expansion of ER-negative breast cancer cells, (Peterson et al. 2015; Willmarth and Ethier 2006) However, its role in mediating breast cancer development and therapy resistance has received very little attention. Future work investigating the contributions of amphiregulin towards resistance against hormone therapy may shed much needed light on downstream mechanisms that confer resistance and elucidate new therapeutic targets.

Interestingly, our analyses indicated upregulation of the androgen receptor related gene *PIP* (encoding Prolactin-Induced Protein) in women in RG2.

Interestingly PIP (GCDFP-15) expression in nipple aspirates from non cancer bearing breasts was shown to increase with suppression of ovarian function and reduction in estrogen levels in one study (Harding et al. 2000). In breast cancers the expression of PIP is higher in tumours with better prognostic features and has been shown to be closely correlated to AR expression and the molecular apocrine subtype. Lower grade tumours (<0.0001) and negative nodal status (p=0.008) had higher rates of positive PIP expression (Darb-Esfahani et al. 2014). Therefore, it will be important to further characterize *PIP*

dynamics and its effects in this context of chemoprevention and normal tissue endocrine resistance.

In our proteomic analyses, we have uncovered proteins involved in ECM compositions. Fibrillar collagen trimerization, ECM organization, ECM-receptor interaction and focal adhesion pathways are upregulated within lobules. Moreover, tamoxifen significantly reduced the expression of FN1 (encoding fibronectin), proteins related to epithelial-stromal interaction, as well as tissue remodelling. This finding is in agreement with a previous study by Euhus et al., who similarly showed that tamoxifen reduces the expression of *SERPIN3,* (Euhus et al. 2011). In the previous chapter, we demonstrated that the acinar area and proliferation of epithelial cells were significantly diminished within the lobules. Although we used LCM to isolate breast lobules from the surrounding stroma, it is possible that we saw an increase in stromal signalling and collagen networks in RG1 due to the relative reduction in the epithelial compartment.

We also noted an elevation in the expression of ApoA1 and LTF proteins in RG2. According to Martin et al. (2015), ApoA1 is linked with 28% higher breast cancer risk, and they discovered that serum lipids to be an independent risk factor in women with high mammographic density, (Martin et al., 2015). Lactoferrin (LTF), an iron-binding glycoprotein, is an estrogen responsive gene whose expression is upregulated in the normal breast by estrogen, (Pentecost et al., 1987; Teng et al., 1986). Lactoferrin (LTF) presents in human breast milk and it is found in most of secretions from the exocrine gland and human uterine endometrium, (Walmer et al., 1992; Yanaihara et al., 2000).

As mentioned previously, tamoxifen behaves as an estrogen agonist in the endometrium leading to endometrial hyperplasia and endometrial carcinoma formation, (Wallach et al., 1996). Lactoferrin been shown to be estrogen responsive in both the breast and endometrium, (Park et al. 2005; Teng 2002) and its increased expression in the normal breast in RG2 suggests a possible estrogen agonist action in these women. Interestingly LTF itself has been shown to have mitogenic effects on normal and malignant human endometrial epithelial cells and its expression was stimulated by tamoxifen in human endometrial cancer cells, again suggesting agonism, (Albright et al., 2001).

ER activity is regulated by a family of transcriptional coregulators which either repress or stimulate downstream ERE transcription. The agonist effect of tamoxifen on breast tissue have been identified as one of the factors that develop tamoxifen resistance, (Graham et al., 2000). It is believed that the levels of transcripts encoding coactivators and corepressors might dictate the activity of tamoxifen on breast tissues. This suggest that the agonist effect of tamoxifen in RG2 may be explained by the relative levels of coactivators versus corepressors.

One notable finding in our analyses is that osteoglycin (*OGN*) expression had increased in RG1 in response to tamoxifen. In previous reports, it has been shown that OGN functions as a tumour suppressor and was downregulated in higher grades of breast cancers (Xu et al., 2019). As such, the observed increase in OGN in RG1 may suggest a regulatory role in mammary epithelial cell maintenance and the potential as a predictive biomarker.

By performing pathway analysis using Ingenuity Pathway Analysis (IPA), we confirmed a reduction in eukaryotic initiation factor 2 (eIF2) signalling in RG1, but an increase in RG2. The eIF2 signalling pathway has been reported to play an important role in regulating cellular homeostasis and cell growth, (Hao et al., 2020). Further, ERα has been shown to control eukaryotic translation initiation factor 3 subunit f (eIF3f) at both the transcriptional and translational levels via the mTORC1 pathway, (Cuesta et al., 2019). Moreover, decreased eIF3c can suppress proliferation and can lead to apoptosis via mTOR signalling. It is possible that, like the activity of eIF3f and eIF3c, the anti-estrogenic effects of tamoxifen could affect eIF2 signalling components, possibly also via mTOR. This may explain the observed decrease in epithelial cell proliferation and possibly, as a result, increased collagen components in the lobules.

Eigeliene et al. (2016) demonstrated that SERM-mediated mammary proliferation suppression is linked to the maintenance of the androgen receptor. In their study AR had an antiproliferative and E2-opposing activity at relatively high SERM concentrations in normal human breast tissue culture ex vivo. On AR-positive cell populations, the SERMs had an ER-agonist activity, (Eigeliene et al., 2016).

In summary, our findings suggest that alterations in ER signaling and AR signaling may serve as indicators and potential mechanisms of tamoxifen resistance in women at increased risk of breast cancer. The agonist effects of tamoxifen may drive resistance and could potentially be harnessed as dynamic biomarkers of tamoxifen activity. Ideally any changes seen in the breast tissue should be replicated in the blood to facilitate the development of more

acceptable predictive biomarkers. To this end serum proteomic analyses of the women in this study and a second cohort of 10 women have been undertaken and the results are eagerly awaited. Further longitudinal studies will then be required to prospectively test whether such changes in tissue proteomics truly represent accurate and reliable biomarkers of tamoxifen's preventive activity.

# Chapter 5

# Can *In vitro* Tissue Culture Systems Replicate *In vivo* response to Tamoxifen?

# 5 Can *In vitro* Tissue Culture Systems Replicate *In vivo* Response to Tamoxifen?

## 5.1 Introduction

Optimisation of normal intact breast tissue *in vitro* models may allow them to more closely mimic *in vivo* breast tissue characteristics and responses to therapy. Current *In vitro* models have variable degrees of complexity and can be classified into 2 dimensional or 3-dimensional cell cultures. The most complex models are useful for demonstrating cell-to-cell interaction and cell-to-matrix interaction. Accordingly, they can be used to study abnormalities or dysregulation involved in cancer formation and progression.

The first attempt to culture the intact mammary gland of pregnant rat in 1959 maintained tissue viability up to 6 days (Trowell et al., 1959). Afterwards, the organotypic human tissue slice technique was established in 1967 but it was considered unsuccessful, probably because large samples were used. Thick slices do not allow enough oxygen and nutrient to penetrate into deep tissue resulting in cell death (Matoska et al., 1967). Other investigators attempted to improve the culture technique by thinly slicing the tissue to be cultured, thus reducing the distance media required to travel by diffusion. Studies attempting to culture breast cancers suggested that slices of 200-300 μm were optimal for this culture system, as cells did not undergo necrosis and maintained their healthy status for at least seven days, (Holliday et al., 2013; Naipal et al., 2016). However, the fatty nature of normal breast tissue prevented sectioning to this thickness, (Holliday et al. 2013).

Eigeliene et al developed a method to optimize intact human mammary gland tissue culture with an air-fluid interface to investigate responses to hormones

*in vitro* (Eigeliene et al., 2006). Instead of culturing explant directly on the top of a plastic surface, a porous membrane was used that enabled nutrients, signalling molecules, growth factors, and test agents to penetrate inside the explant from its underside. The usage of the porous membrane was reported to minimise the limitation caused by the absence of the blood supply. The investigators placed tissue explants onto lens papers lying on stainless steel grids in Petri dishes and reported culture of normal mammary tissue samples for three weeks and demonstrate responses to steroid hormones and antiestrogens. However, limited data on changes from the baseline uncultured condition of the tissue were reported.

The attempt to maintain tissue culture over a long duration of time is important to study tissues in terms of morphology and function, and for drug sensitivity analyses. This could be achieved by the use of dynamic 3D approaches for culturing tissues, such as the Rotatory Cell Culture System (RCCS$^{TM}$, Synthecon Inc., Houston TX, USA), (Ferrarini et al., 2013). The bioreactor was invented in 1990 by Engineers Charles D. Anderson and Ray Schwarz of the North American Space Agency (NASA). This system applies novel microgravity technology aiming to replicate the weightlessness of space.

The bioreactor rotates horizontally, and the medium is enclosed in liquid, with no contact with the surrounding air. The 3D samples of tissue are kept in ‘free fall’ state which minimises turbulence and mechanical strain (shear) associated with impeller bioreactors (Tai et al., 2014). Meanwhile, nutrient exchange is thought to be enhanced due to the sample being constantly in motion, reviewed in (Lovett et al., 2009)

Chapter 5

In this chapter, we set out to evaluate human breast tissue slice culture under different *in vitro* culture conditions with the goal of identifying a system that most faithfully replicated the *in vivo* response to tamoxifen in women receiving preventive therapy. We used static culture in plastic and air fluid interface culture on insert and compared these to the novel rotatory culture system.

## 5.2 Results

### 5.2.1 Morphometric analysis

Normal breast samples were obtained from reduction mammoplasty and risk-reducing mastectomies and cultured under three different culture conditions. The static petri dish culture system (PD), the static plate with insert culture system (PI) and rotatory culture system (RCCS) were used in our investigation. Tissue fragments were cultured in serum free media (SF), FBS-supplemented media (FBS) and CSS-supplemented media (CSS). It is noteworthy that cryotome technique was initially used to prepare tissue samples of thin thickness. However, we also found that it was not possible to prepare thin slices of normal breast tissue, likely due to the high fat content of the samples, (Vandeweyer et al., 2002; Holliday et al., 2013). Therefore, we prepared the tissue fragments manually using a scalpel under sterile conditions. Experimental design was illustrated in (Figure 5.1).

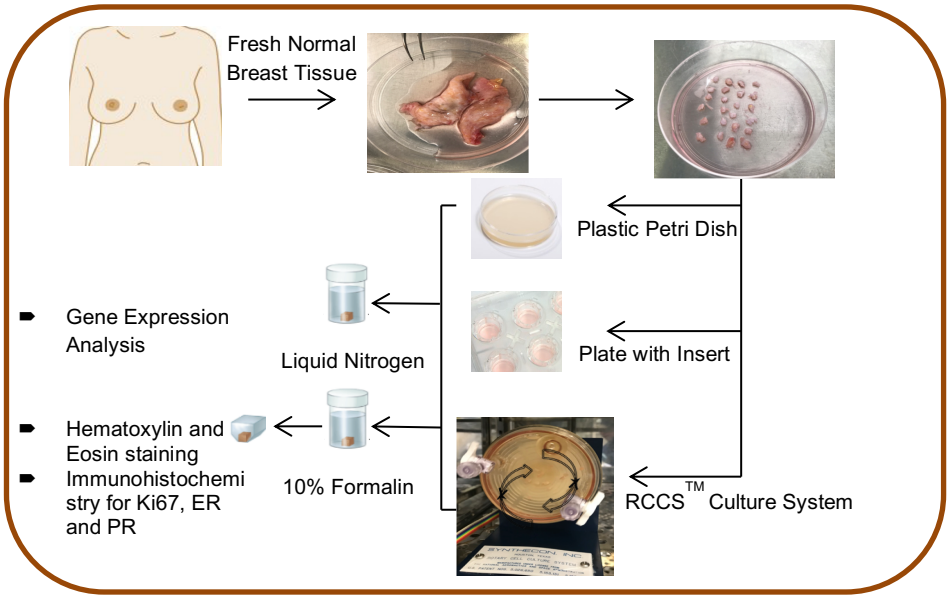


**Figure 5.1: Illustration of 3D tissue culture systems.** Fresh normal breast tissues were subjected to manual tissue slicing under sterile conditions. Excess fat tissue was discarded. Tissue slices of approximately 0.5mm$^3$ thickness were cultured in DMEM/F-12 medium (Gibco® life Technology™) supplemented with different serum constituents; 10µg/ml Insulin (Sigma Aldrich), 10µg/ml Hydrocortisone (Sigma Aldrich) and 5ng/ml Epidermal Growth Factor EGF (Sigma Aldrich) 1% penicillin-streptomycin, 1% Amphotericin B (Gibco® life Technology™), at 5 % $CO_2$ at 37°C and at atmospheric oxygen levels. Tissue slices were cultured in three different culture systems, plastic petri dish (PD), plate with insert (PI) and the dynamic 3D Rotatory Cell Culture System (RCCS) culture systems in a medium with different serum supplementation; medium alone (Serum Free; SF), 10% foetal bovine serum (FBS) supplemented media and 10% charcoal stripped-FBS (CSS) supplemented media. Medium was replaced every 2 days. Tissue slices were fixed in 10 % neutral buffered formalin for 24 hours at room temperature. Subsequently, tissue slices were embedded in paraffin and 4µm sections were generated for histological and immunohistochemical analysis.

Morphometric analysis demonstrated that the mean acinar area within the breast lobules increased significantly in the PD culture system from baseline to day 7, (Figure 5.2 i-a-; 5.2 ii-b; p= 0.0140) and then reduced thereafter at day 14, (p= 0.0174). The morphological lobular structure was significantly perturbed at day 21, (Figure 5.2, i-a, 5.2, ii-[c-d]). A similar increase in acinar area was observed in tissue cultured in the RCCS at day 7 (Figure 5.2, i-b, 5.2, ii-e; p <0.0001), with the mean area of acini reducing at day14, (p=0.0177), and then again at day 21 with apparent maintenance of morphological tissue structure (Figure 5.2 i-b; 5.2, ii-[f-g]). There was no significant difference in the acini area between samples at baseline and day 21 in samples cultured in the RCCS with FBS.

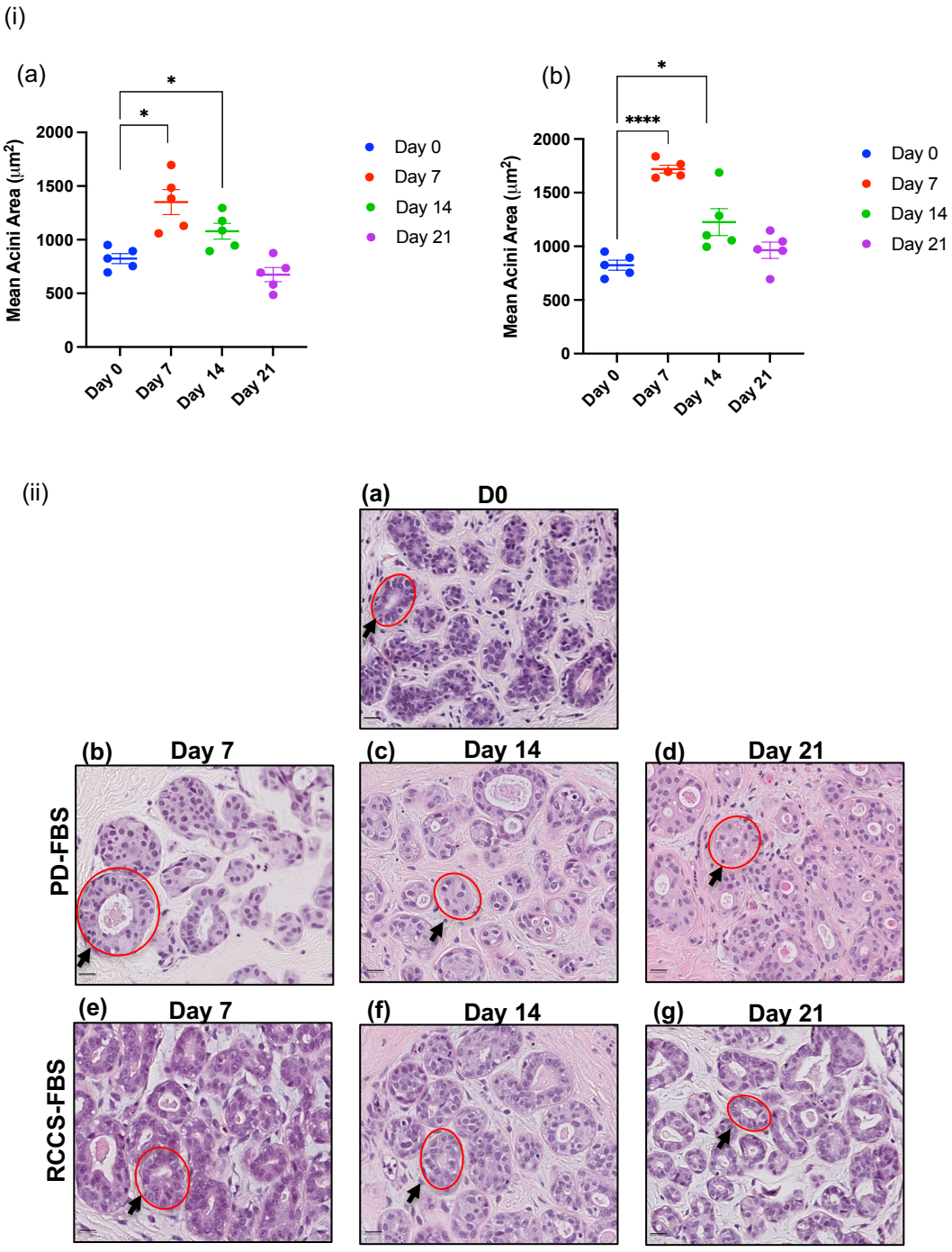


**Figure 5.2: Quantification of the mean acini area of normal breast tissues from healthy women cultured *in vitro* for 21 days**. (i) The mean acinar area (µm$^2$) within lobules in normal breast samples at Day 0, 7, 14 and 21 days in culture was measured. 5 lobules of the same size were chosen randomly from each sample included in the analysis. Tissue sections were stained with H&E staining and scanned using Aperio Digital pathology Scanner and digital images visualized by Aperio ImageScope for measurement. (ii) Representative images of acini at D0 (a), PD-FBS at day 7, 14, and 21; ii (b - d) and RCCS-FBS at day 7, 14 and 21 ii (e – g). Arrows point out the mean average of the acini area. The mean acini area in tissues cultured in PD-FBS and RCCS-FBS were determined and represented. Data in scatter plots represent values of individual samples from 5 different patients and mean ±SEM of PD-FBS in ii-a and RCCS-FBS. The statistical significance was determined using paired t-test. *p<0.05, ****p<0.0001. Scale bars are 50µm.

### 5.2.2 Proliferation assessment of *in vitro* tissue culture of normal breast tissue samples

To evaluate the cause of this increase in acinar area at day 7, we evaluated proliferation using Ki67 expression. Positive Ki67 expression was defined as a nuclear brown stain and the test score was measured as the number of positively stained epithelial cells divided by the total number of epithelial cells in acini and presented in percentage as shown in Figure 5.3-i. Breast samples obtained from 6 different patients were used for this analysis. The mean Ki67 of all samples at baseline was 3.6%±1.1. On day 7, Ki67 was increased in epithelial cells in tissue samples compared to day 0 in all culture systems. The percentage increased to approximately 30-40% in all culture systems and was not obviously impacted by the media constituents. Thereafter, Ki67 level decreased in all culture conditions to day 14 and then further to day 21. Ki67 had returned to baseline or below in all conditions apart from that cultured in FBS in the RCCS where Ki67 remained significantly raised over the baseline levels.

(i)

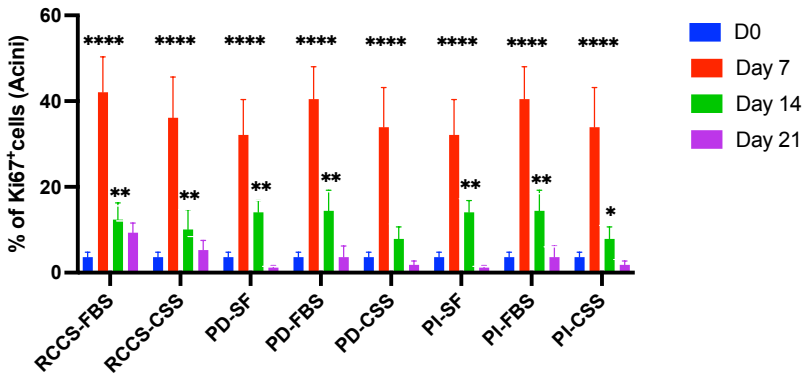


(ii)

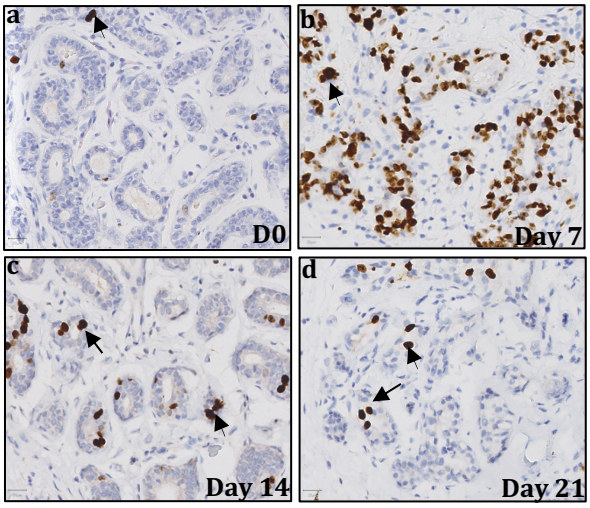


**Figure 5.3: The percentage of Ki67 positive cells and nuclear staining in normal breast tissue in three different culture conditions with different serum constituents at Day 0, 7, 14, and 21 days, respectively.** (i) Percentage of acinar epithelial cells positive for Ki67 expression as detected by immunohistochemical analysis. (ii) Representative images of tissue explants cultured in FBS supplemented media in RCCS and stained with Ki67 antibody at the (a) D0, (b) 7-,(c) 14-, and (d) 21-day, respectively. The statistical significance was determined using 2 way ANOVA. *p<0.05; **p<0.01 and ****p<0.001. Scale bars are 20μm. IHC was performed using an automatic approach (BenchMark Ultra, Ventana medical system 790-2223). Staining was done using UltraVIEW universal DAB detection kit. n=6 Data in (i) represents mean ± SEM.

### 5.2.3 Estrogen receptor expression of normal breast tissue cultured *in vitro*

ER expression was assessed to investigate whether hormonal receptors expression could be maintained by mammary epithelial cells during *in vitro* tissue culture. ER expression was determined by immunohistochemical staining. Positive staining was defined as a nuclear brown stain, and the percentage ER-positive cells of the total acinar epithelium calculated (Figure 5.4). ER protein was assessed on days 0,7,14 and 21 in samples obtained from six patients. The mean number of ER-positive cells was 37.3%±8.1 positive on day 0 (n=6). On day 7, the ER expression had reduced significantly in all culture systems. The decline in ER expression was least in tissue cultured in the RCCS, with maintenance of some ER expression at day 21 whereas this was almost completely lost in the other culture methods. There was some evidence that culture medium could support ER expression with serum free medium resulting in a more rapid loss of ER expression in the static culture conditions.

(i)

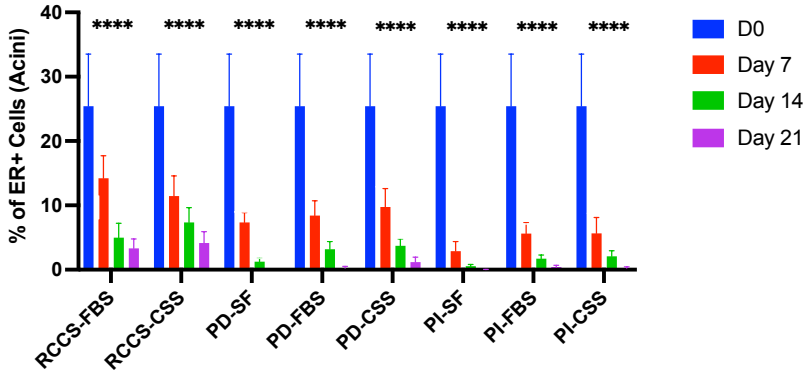


(ii)

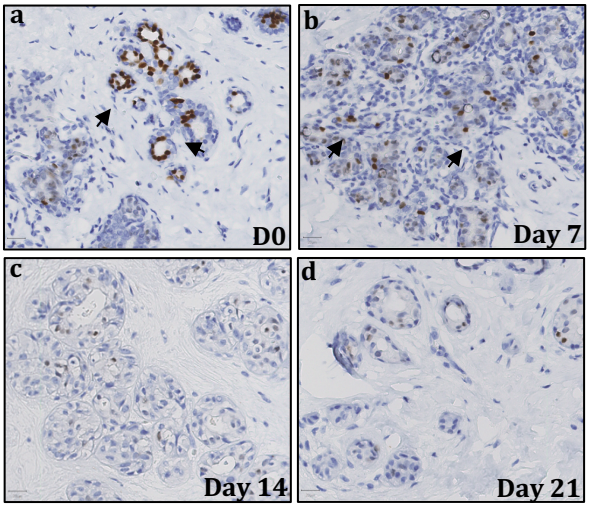


**Figure 5.4: The percentage of ER positive cells and nuclear staining of normal breast tissue slices cultured in three different culture conditions with different serum constituents at D0, 7, 14, and 21 days.** (i) Percentage of acinar epithelial cells positive for ER expression as detected by immunohistochemical analysis. (ii) Representative images of tissue explants cultured in FBS supplemented media in RCCS and stained with ER antibody at Day 0 (a), (b) 7,(c) 14, and (d) 21 days, respectively. The statistical significance was determined using 2 way ANOVA. ****p<0.0001. Scale bars are 20µm. IHC was performed using an automatic approach (BenchMark Ultra, Ventana medical system 790-2223). Staining was done using UltraVIEW universal DAB detection kit. n=6 Data in (i) represents mean ± SEM.

### 5.2.4 PR expression of *in vitro* tissue culture of normal breast tissue slices

PR was assessed by IHC to examine its expression level in normal breast tissue cultured in the 3 different culture methods. The assessment was obtained by immunohistochemical staining as shown in (Figure 5.5). At D0, the mean number of PR-positive cells across the six patient samples was 14.8%±8.9. In contrast to ER expression, in the presence of serum PR expression was either maintained or significantly increased at day 7 across all culture conditions. This increase was maintained until day 21 with the RCCS in the presence of FBS but not CSS and in all other conditions PR expression reduced to sub-baseline levels by day 14, with the exception of PD culture with FBS where the decline only became significant at 21 days.

(i)

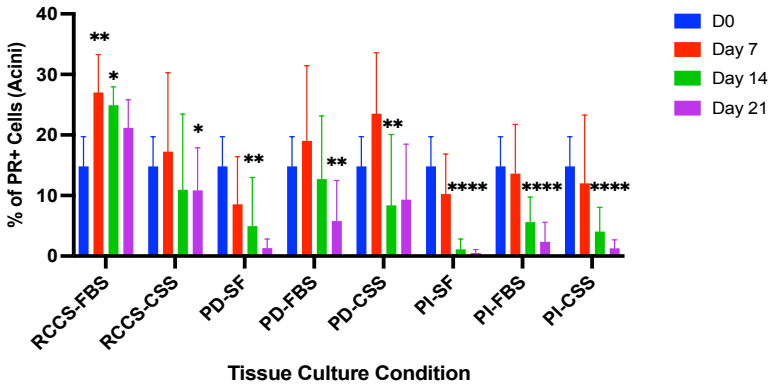


(ii)

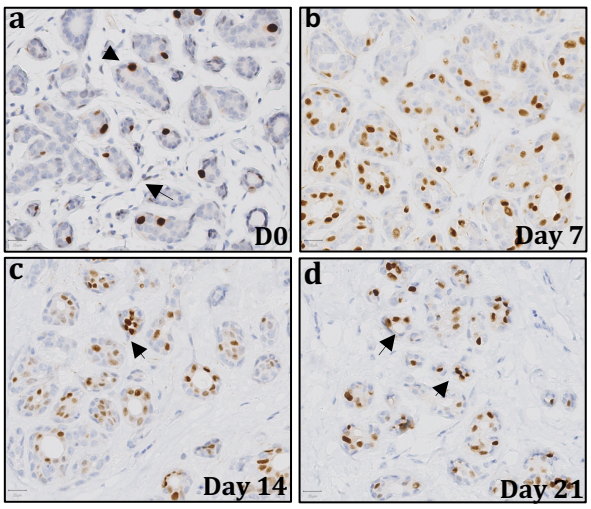


**Figure 5.5: The percentage of PR positive cells and nuclear staining of normal breast tissue slices cultured in 3 different culture conditions with different serum constituents at D0, 7, 14, and 21 days.** (i) Percentage of acinar epithelial cells positive for PR expression as detected by immunohistochemical analysis. (ii) Representative images of tissue explants cultured in FBS supplemented media in RCCS and stained with PR antibody at the (a) D0, (b) 7, (c) 14, and (d) 21 days, respectively. The statistical significance was determined using 2 way ANOVA *p<0.05, **p<0.01and ****p<0.0001. Scale bars are 20µm. IHC was performed using an automatic approach (BenchMark Ultra, Ventana medical system 790-2223). Staining was done using UltraVIEW universal DAB detection kit. n=6 Data in (i) represents mean ± SEM.

### 5.2.5 Gene Expression of normal breast tissue samples cultured *in vitro*

Even though we had demonstrated perseverance of relatively normal tissue architecture, ER and PR expression, in particular with the RCCS we were concerned that the large, early spike in proliferation may make all culture conditions non-representative of the in vivo situation. To examine this, we studied gene expression pattern for 5 different patients on day 0 (D0) and after one week (W1) of culture in RCCS and PD systems in either CSS or FBS using STAR RNA-seq reads aligner. Reads associated with genes were counted and the data was then run through differential gene expression analysis tool (DESeq2). DEseq2 normalizes read count data and then performs statistical analysis to investigate quantitative changes in gene expression levels within samples cultured in different culture systems and conditions. Overall, data showed that more than 18,000 genes were differentially expressed between (D0) samples and (W1) samples of the same patients. The heatmap illustrated below (Figure 5.6), shows the top 150 differentially expressed genes that were up or downregulated from baseline to W1 samples in all patients. The horizontal dendrogram displayed at the top of the heatmap represents a clear separation between (D0) and (W1) independently of the origin of tissues.

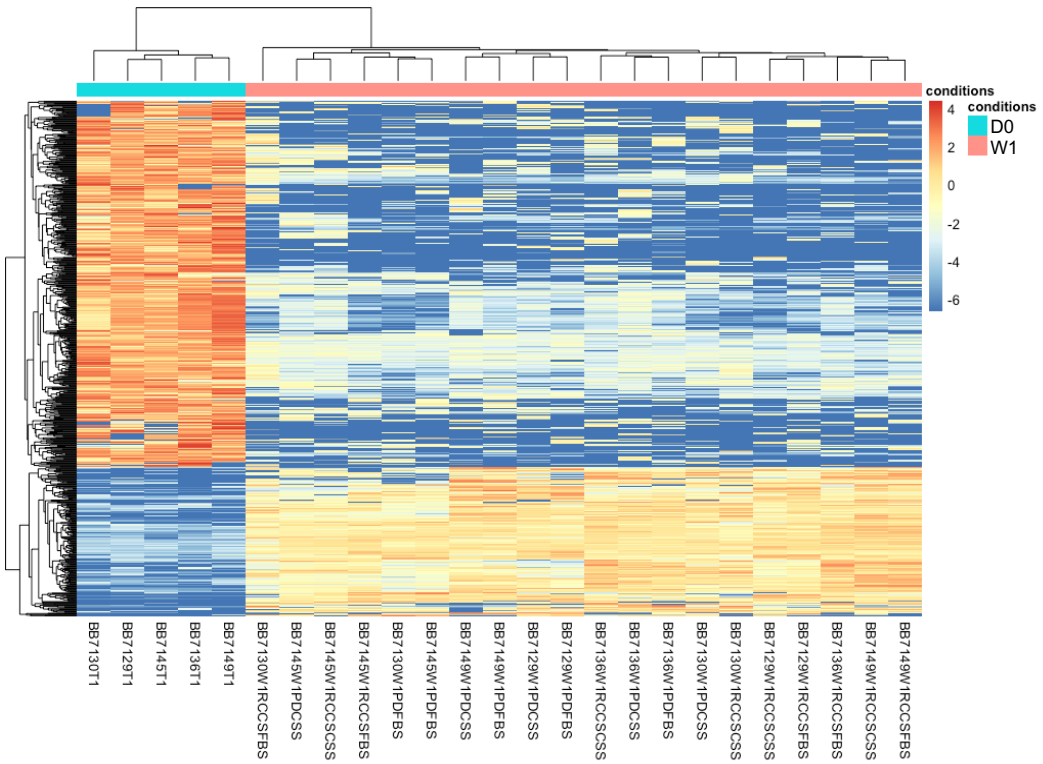


**Figure 5.6: Heatmap of top 150 significant differentially expressed genes in patients' samples cultured *in vitro* at D0 and week 1**. Samples from 5 different individuals; BB7129, BB7130, BB7136, BB7145, and BB7149, were cultured *in vitro* in static (PD) and rotatory (RCCS) systems and in two different conditions FBS-supplemented medium and CSS supplemented medium systems, and were collected at week 1. For clinical information refer to Table 2. Orange and Blue colors represent upregulated and downregulated genes, respectively.

Pathway enrichment analysis was performed using the differentially expressed genes to identify significant differences among different culture systems and to compare (D0) vs (W1). There were 6 gene set signatures related to the proliferation process with a positive enrichment score consistent with the increase in Ki67 by immunohistochemical analysis, (Table 5.1). Immune response pathways were not maintained during tissue culture; there were blood component-related genes such as haemoglobins and immunoglobulins that were down-regulated at W1 presumably due to haematopoietic and immune cell death in the culture conditions, at least in part due to loss of the vascular supply. DNA damage was also evident with two pathways indicating increased DNA strand or nucleotides abnormalities.

**Table 5.1: Pathway enrichment analysis for differentially expressed genes in patients' samples cultured *in vitro* at D0 and week 1. NES = Normalized enrichment score, Padj= adjusted P value. Size = number of genes included in each pathway.**

| Hallmark Name | NES | Padj | Size | Process Category |
|---|---|---|---|---|
| E2F TARGETS | 3.23 | 0.00 | 129 | Proliferation |
| G2M CHECKPOINT | 3.40 | 0.00 | 130 | Proliferation |
| MITOTIC_SPINDLE | 1.71 | 0.01 | 109 | Proliferation |
| MYC TARGETS V1 | 3.48 | 0.00 | 142 | Proliferation |
| MYC TARGETS V2 | 1.86 | 0.02 | 28 | Proliferation |
| P53 PATHWAY | 2.17 | 0.00 | 123 | Proliferation |
| ALLOGRAFT REJECTION | -2.95 | 0.00 | 131 | Immune |
| COAGULATION | 1.94 | 0.00 | 83 | Immune |
| INFLAMMATORY RESPONSE | -1.62 | 0.02 | 122 | Immune |
| INTERFERON ALPHA RESPONSE | -1.78 | 0.02 | 56 | Immune |
| DNA_REPAIR | 2.10 | 0.00 | 80 | DNA damage |
| UV_RESPONSE_UP | 1.72 | 0.01 | 90 | DNA damage |
| ESTROGEN_RESPONSE_LATE | 1.75 | 0.01 | 129 | Signalling |
| MTORC1 SIGNALING | 3.53 | 0.00 | 157 | Signalling |
| PI3K AKT MTOR SIGNALING | 1.59 | 0.05 | 60 | Signalling |
| TGF BETA SIGNALING | 2.01 | 0.01 | 31 | Signalling |
| TNFA SIGNALING VIA NFKB | -2.26 | 0.00 | 119 | Signalling |
| HYPOXIA | 2.86 | 0.00 | 130 | Pathway |
| PROTEIN_SECRETION | 1.97 | 0.00 | 57 | Pathway |
| REACTIVE_OXYGEN_SPECIES_PATHWAY | 2.03 | 0.01 | 35 | Pathway |
| UNFOLDED PROTEIN RESPONSE | 2.27 | 0.00 | 67 | Pathway |
| APICAL JUNCTION | 1.70 | 0.01 | 107 | Cellular Component |
| ANGIOGENESIS | 2.03 | 0.01 | 20 | Development |
| EPITHELIAL MESENCHYMAL TRANSITION | 2.55 | 0.00 | 137 | Development |
| CHOLESTEROL HOMEOSTASIS | 2.29 | 0.00 | 53 | Metabolic |
| GLYCOLYSIS | 3.75 | 0.00 | 138 | Metabolic |
| OXIDATIVE PHOSPHORYLATION | 2.68 | 0.00 | 120 | Metabolic |

A principal component analysis confirms this separation with 65% of the variance explained by PC1 (Figure 5.7-a). Analysis of only the W1 samples in a separate PCA (Figure 5.7b) shows that there is some evidence of clustering according to the culture condition. In particular, in all samples the RCCS FBS and CSS appear to cluster more closely to each other than the PD FBS and CSS samples.

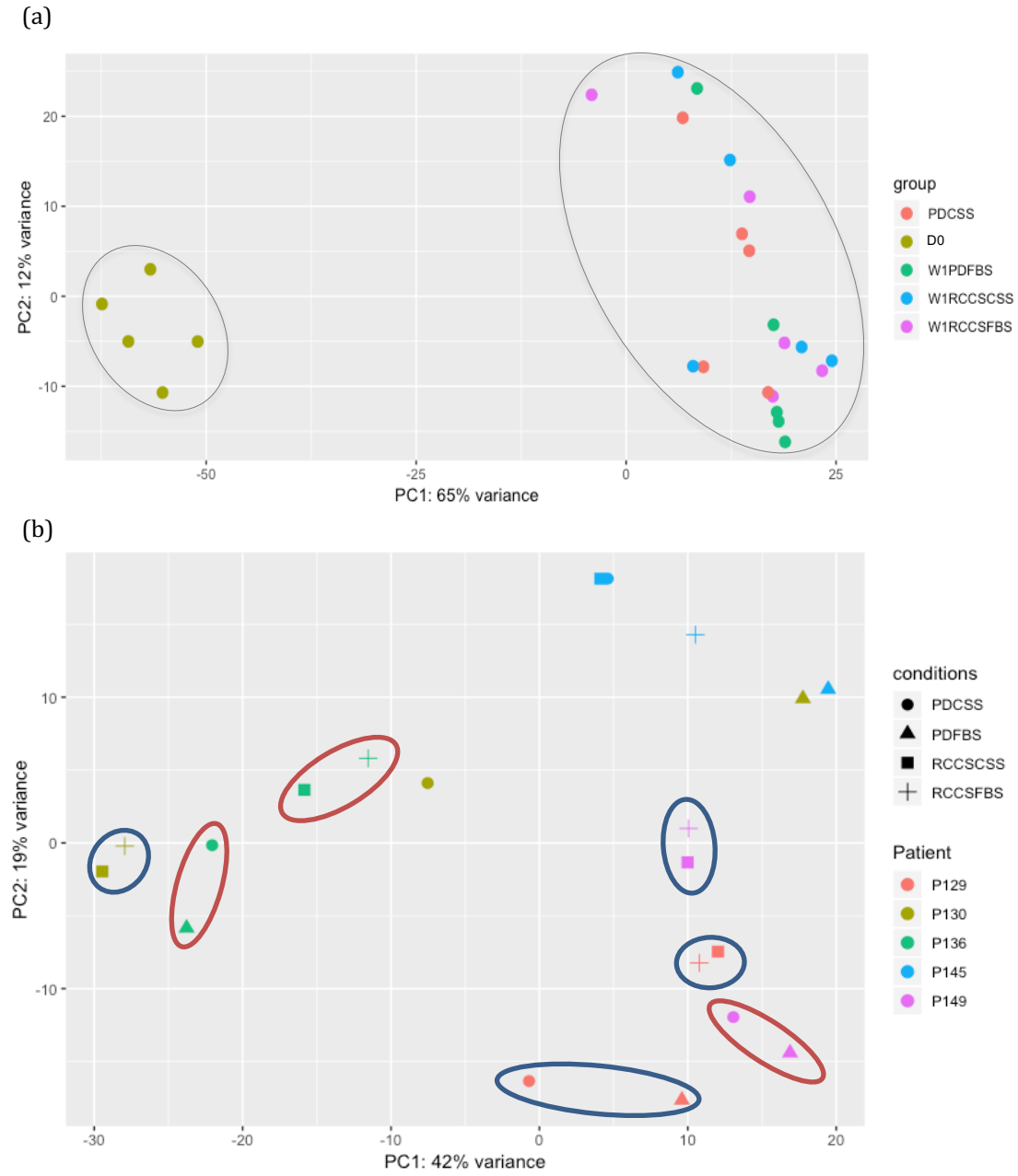


**Figure 5.7 Principal Component analysis.** (a) PCA diagram of cultured tissues at D0 and after one week of treatment (b) PCA of W1 samples. Clustered samples demonstrate the ability to retain transcriptional memory of their origin. STAR RNA read Aligner guide software was used to plot the diagrams. Square and plus icons represent rotatory culture system (enriched in blue) while circle and triangle represent static system (enriched in red).

### 5.2.6 Hydrogel culture system

In cooperation with Dr.Hannah Harrison, a member of Breast Biology group in Manchester university, we have investigated a hydrogel tissue culture system using intact normal breast tissue. We hypothesised that the use of a semi-solid support system might better maintain tissue characteristics.

#### 5.2.6.1 Acinar area was maintained in hydrogel culture system

Morphometric analysis was done to investigate the morphological features of normal breast tissue slices that have been cultured *in vitro* using hydrogel culture system for up to 7 days. The results demonstrated that the mean acinar area within lobules was not significantly increased over baseline values for at least seven days in culture, (Figure 5.8).

(i)

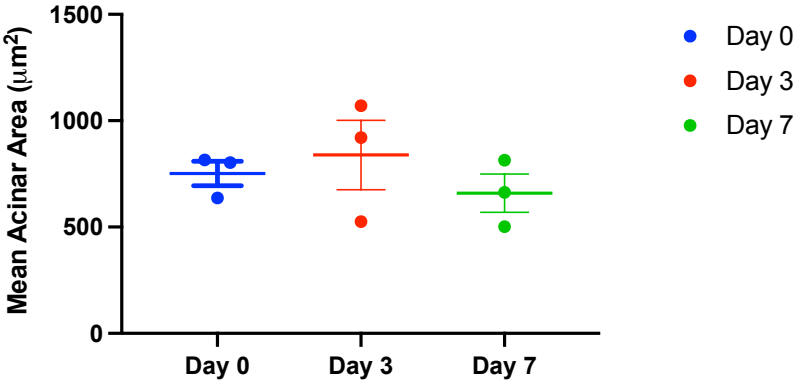


(ii)

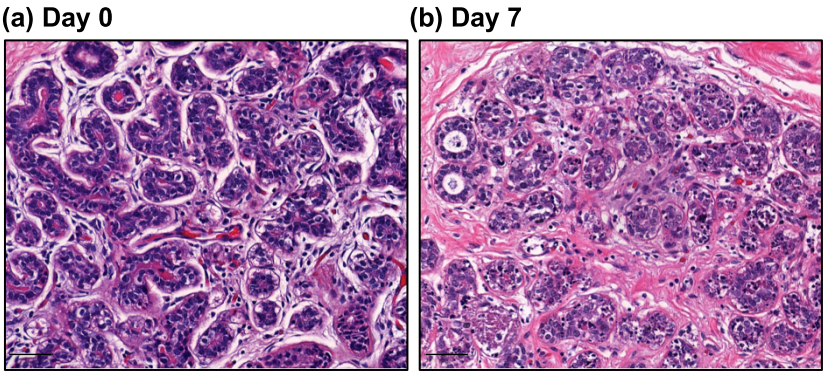


**Figure 5.8: Quantification of the mean average acini area of normal breast tissues from healthy women cultured *in vitro* for 7 days using hydrogel culture system**. Tissue sections were stained with H&E staining and scanned using Aperio Digital pathology Scanner and digital images visualized by Aperio ImageScope for measurement. (i) The mean acini area of breast tissues cultured in hydrogel were determined and represented. (ii) Representative images of acini at Day 0 (a) and Day 7 Scale bars are 50µm. Data in scatter blots represent mean average of acini area values of individual samples from 3 different patients and mean±SEM. The statistical significance was determined using 2 way ANOVA.

### 5.2.6.2 Ki67 expression

Samples obtained from 12 different women were cultured in hydrogel and proliferation assessed by Ki67 at baseline, day 3,7 and 14. During the first week of culture, the percentage of Ki67 positive cells increased by 1.41±0.2 and 1.7±0.2 fold on days 3 and 7 respectively, however, after 14 days of culture levels returned to baseline (Figure 5.9).

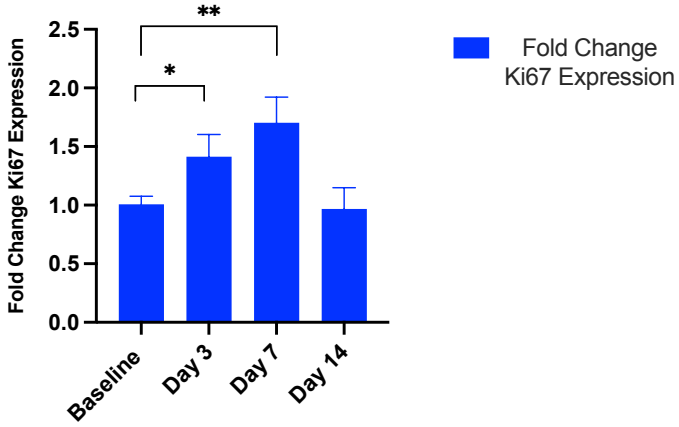


**Figure 5.9: Fold change of Ki67 positive cells in normal breast tissue slices cultured in the hydrogel with FBS and B27 constituents at D0, 3, 7, and 14 days.** The fold change of acinar epithelial cells positive for Ki67 expression as detected by immunohistochemical analysis. IHC was performed using automatic approach (BenchMark Ultra, Ventana medical system 790-2223). Staining was done using UltraVIEW universal DAB detection kit. n=12. The statistical significance was determined using 2 way ANOVA. Data in the graph represents mean ± SEM. *p<0.05, **p<0.01.

### 5.2.6.3 ER and PR expression

ER and PR expression was examined in the hydrogel culture system over 14 days culture period. A significant reduction in ER expression was seen after 3 days with further decline to day 14 (Figure 5.10a). There was a non-significant trend to reduced PR expression at day 3, however, PR expression was maintained throughout the culture period, (Figure 5.10b). There was no significant difference in PR expression when comparing baseline expression levels and any of the culture time points.

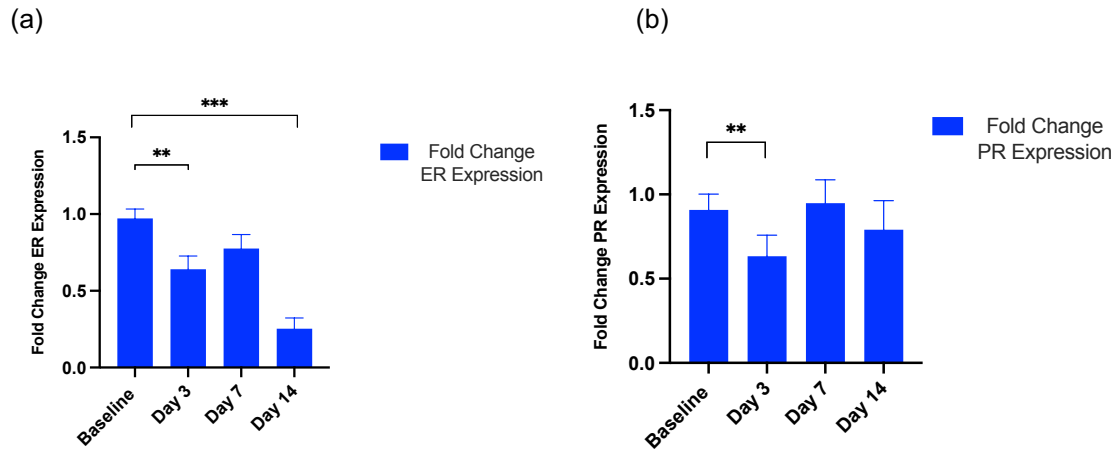


**Figure 5.10: Fold change of cells positive for ER and PR expression in normal breast tissue slices cultured in the hydrogel with FBS and B27 constituents at D0, 3, 7, and 14 days, respectively. (a)** The fold change of acinar epithelial cells positive for ER expression as detected by immunohistochemical analysis. (b) The fold change of acinar epithelial cells positive for PR expression as detected by immunohistochemical analysis, (n=12). IHC was performed using an automatic approach (BenchMark Ultra, Ventana medical system 790-2223). Staining was done using UltraVIEW universal DAB detection kit. n=15. The statistical significance was determined using 2 way ANOVA. Data in the graph represents mean ± SEM. **p<0.01, ***p< 0.001

## 5.3 Discussion

Optimizing 3D normal breast models *in vitro* might allow close mimicking of *in vivo* breast tissue characteristics maintaining cell-to-cell and cell-to-matrix interactions. In this chapter, we aimed to investigate 3D *in vitro* culture models of intact human breast tissue with the hope that we would be able to refine such models to test whether they recapitulated the in vivo responses seen in patients receiving preventive tamoxifen therapy. Several model systems using disaggregated cells of various lineages have been developed previously.

Nash et al. reported the development of a 3D *in vitro* model of normal breast that composed of three co-cultured cell lines. The culture was prepared from myoepithelial cells, fibroblasts and luminal epithelial cells isolated from breast reduction mammoplasty samples and cultured in collagen-1. The model was evaluated after 21 days and confirmed epithelial polarization with the formation of microstructures with lumens and basement membrane, (Nash et al., 2015). Marchese and Silva developed another 3D *in vitro* model for breast using breast epithelial MCF-12A cells cultured in reconstituted basement membrane matrix. These cells express ER and GPER proteins. The model resulted in the formation of acini with basement membrane and hollow lumen. The 3D culture retained this gland-like structure after 16 days albeit with 5 – 10% of the cells going into apoptosis. 17β-oestradiol deformed acini and filling of the acinar lumen in a dose-dependent manner, (Marchese et al., 2012). This disruptive effect of estrogen could be antagonised successfully using the ER antagonist fulvestrant. In another study, Carter and colleagues developed a 3D model of the human breast duct. For this purpose, myoepithelial and luminal cells were isolated from reduction mammoplasty specimens and cultured separately.

Thereafter, the cells were co-cultured in collagen gels and developed into spheroidal structures after 10 days, forming more complex structures after 21 days, (Carter et al., 2017). Despite these advances regarding the *in vitro* models, the reliability of these models to accurately represent the normal breast is still an open question, as *in vitro* system may have a certain limitations with regard to reproducing an *in vivo*-like microenvironment, (Nerger et al., 2019; Vidi et al., 2012)

In the current study, we used three models to investigate *in vitro* culture systems in the presence of serum-supplemented media using intact human breast tissues. Herein, we first investigated whether the morphology of tissues can be effectively maintained using static (the petri culture dish and the static plate with insert culture) and rotatory culture systems. It has been suggested that dynamic culture systems maintain cultured cells in a continuous flow of growth medium at least partially mimicking *in vivo* conditions, (Sacco et al. 2011).

Results from our study showed that the average acinar area increased by approximately 2-fold after 7 days in culture. The morphological analysis showed that the tissue appearance was disrupted after 7 days in culture with an increase in the acinar area. Glandular morphological feature was retained after 7 days. The normal breast structure appeared to be better maintained in the RCCS compared to static culture conditions. Although the morphology of the lobular structures at 2-3 weeks was maintained the increase in acinar area at day 7 was a concern. We thus conducted. immunohistochemical and transcriptomic analyses to further evaluate the models.

Immunohistochemical analysis for Ki67 and hormone receptors expression was performed to investigate whether normal breast tissue can maintain its physiological characteristics *in vitro*. Moreover, basal media and serum-supplemented media were used to examine different culture conditions. Foetal Bovine serum and charcoal striped serum were used in our culture systems to investigate whether hormones and growth factors contents would better maintain tissue explant physiology. Level of hormones and growth factors level in FBS-supplemented media were not measured. Epithelial cells proliferation was investigated at several time points using Ki67 expression as a proliferation marker. The baseline Ki67 of 3.6% is higher than others have reported for the normal breast epithelium. However, our samples were obtained from women at increased risk of breast cancer in whom Ki67 has previously been reported to be higher than those at normal risk, (Huh et al., 2016). Our data shows that there was a dramatic increase in epithelial proliferation at 7 days in all culture systems by approximately 10-fold followed but a tendency to reduced Ki67 levels thereafter, albeit levels were still above the D0 values at 21 days. These women had not received hormone replacement therapy for at least 6 months and as such one would expect their baseline Ki67 to be a median of approximately 1% from previously published studies, (Cheng et al., 2013; Harper-Wynne et al., 2002). To our knowledge there are no published data that report the change in epithelial cell proliferation from excision to organ culture *ex vivo.* In the study by Eigeliene et al. (2006), the lens paper culture system was used to culture pieces of normal breast tissue from postmenopausal women aged 48-66 years undergoing breast reduction surgery. The group used protocol for an *ex vivo* breast tissue culture system

prepared on lens paper on stainless steel grids, which serve as support and tissues holders. In that protocol, explants are cultured in DMEM/F12 medium supplemented with 10% dextran-charcoal stripped fetal calf serum. The explants were grown on lens paper that is slightly submerged from one end in the growth medium. The system provides controlled diffusion of the growth medium. This tissue culture approach allows easy replacement of the medium without disturbing the explants. The control Ki67 reported by Eigilene et al. after 7 days in culture, was 12-13% suggesting that their culture conditions also resulted in at least a 10-fold artefactual increase in proliferation, (Eigeliene et al., 2006). Furthermore, no significant decline in Ki67 was seen in day 14 controls with their approach.

Eigeliene et al. (2016) used human breast tissue explants on a lens paper culture system to test the effects of several SERMs (Ospemifene, Raloxifene, and Tamoxifen) on the breast tissue, (Eigeliene et al., 2016). ER expression was detected in approximately 20% of epithelial cells at 7 days in culture. Despite a similar increase in Ki67 expression as seen in our culture systems, the authors demonstrated that estrogen supplementation could increase proliferation and estrogen responsive gene expression *in vitro*, (Eigeliene et al., 2016) In addition they showed that the anti-estrogens fulvestrant and tamoxifen could antagonize the effects of estrogen suggesting that the ER was functional.

The same tissue culture model was used to evaluate the effects of hormonal therapy on the breast tissues from pre- and post-menopausal. Results showed that tissues from post-menopausal women are more sensitive to hormone therapy compared to pre-menopausal tissues. This observation was

expressed in the form of increased cyclin D1 and decreasing p27 expression in tissues obtained from postmenopausal women and not in pre-menopausal tissues, (Eigeliene et al., 2008). This argues in favor of detailed analyses, such as RNA sequencing, being needed to properly assess culture conditions. Although several studies reported the development of tissue culture approaches that can maintain normal breast tissue structure, there is little information provided in these studies about the gene expression profile of cultured tissues. Gene expression data evaluated by RNAseq showed important differences between the cultured tissues and the normal tissues *in vivo*. These differences can easily be missed when evaluating only the crude morphological structure of the tissues. Genetic analysis in our studies indicated the differential expression of 18,000 genes for samples from the same patient between D0 and W1.

We investigated the mechanisms that drive this proliferative activity through the assessment of gene expression profiles after one week of culture in both static and rotatory culture systems. Pathway enrichment analysis demonstrated multiple dysregulated pathways in all samples cultured *in vitro* and heatmaps and PCA clearly show that the cultured samples exhibit transcriptional profiles markedly different from the uncultured samples, snap frozen immediately after excision from the breast.

It is not clear what mediates the increase in proliferation and acinar area in vitro. We can speculate from our transcriptional data that the reduction in immune signalling may play a role as three immune pathways and one inflammatory pathway were significantly reduced through culture. The breast microenvironment is mainly composed of the ducts and stroma which includes

immune cells, fibroblasts, adipocytes, blood vessels and microbiome. Immune cells have a significant role in the development of breast cancer starting with immune surveillance in normal breast and progressing through primary and metastatic breast cancer, reviewed in (Goff et al., 2021).

The ductal cellular layer in the normal human breast contains the CD8+ and CD4+ T cells, B cells, dendritic cells, macrophages, natural killer cells (NK), and other immune cell subtypes, (Degnim et al., 2014). The epithelium layer depends on these immune cells for protection from exogenous and endogenous agents, as well as the breast cancer initiation and progression, (Degnim et al., 2014).

It has previously been shown that multiple immune cells are found in breast tissue and, in particular, are intimately related to lobular epithelial cells, reviewed by (Goff et al., 2021). If *in vitro* cell culture results in loss of such cellular interactions this could in turn result in dysregulated proliferation. To investigate this hypothesis, one could examine the breast tissue for cellular components such as macrophages and T lymphocytes and consider stimulating immune signalling pathways, for example with IFNa (T lymphocyte) or CSF (macrophage) to assess the impact on the proliferative response to culture. Such additions to the culture media could potentially enhance ex vivo breast tissue culture systems.

Maintenance of estrogen and progesterone receptors expression is a fundamental requirement for normal breast culture models that seek to test endocrine prevention approaches. In static culture systems, ER expression could not be maintained throughout the culture period while in the rotatory

culture system, ER expression was reduced significantly by 1.8-fold. Maintenance of ER expression has been previously reported in different cell culturing techniques.

In spite of the fact that static and rotatory culture systems presented with mostly typical morphology after 7 days in culture, a more detailed analysis showed an increased acinar area, Ki67 protein and proliferation pathways suggesting a systematic problem with the culture systems. Therefore, a fourth system, a hydrogel culture, was investigated. In the hydrogel culture system, DMEM media supplemented with B27$^{TM}$ and L-Glutamine was used. The present study showed that hydrogel culture system maintained normal breast characteristics better than rotatory and static culture systems for up to 14 days. In the hydrogel culture system, there was no significant difference in acinar area up to 7 days compared to D0. In comparison to static and rotatory culture systems, Ki67 expression was increased by only 1.7-fold at week one and no significant change in Ki67 expression was detected at week two.

Under our different culture conditions and systems, ER protein expression was better maintained in RCCS and hydrogel culture system and certainly at week 1 and 2. There was 0.2-fold reduction in ER expression in hydrogel after one week in culture. Furthermore, our data demonstrate that PR expression was maintained in petri dish, rotatory, and hydrogel culture systems up to day 14 suggesting an estrogenic signalling.

Even though we observed a reduction in ER protein expression, our gene expression data shows an increase in estrogen response signalling. This suggests that it is important to examine the effects of estrogen and tamoxifen

on the models to determine the biological implications of reduced ER expression. Low levels of ER expression can still simulate the effects of ER signalling on tissues.

The major challenge for developing 3D cultures is to recreate a microenvironment sufficiently close to the *in vivo* conditions to allow appropriate differentiation into phenotypically normal tissues. Development and optimization of 3D in vitro models requires precise comparison to *in vivo* tissues. An ECM-like hydrogel foundation and a suitable medium should be carefully picked, to provide conditions pertinent to the organ *in vivo*. Besides the morphology of the tissues, the genetic profile should be investigated to confirm the validity and accuracy of the tissue culture as a representation to the normal tissues *in vivo*.

For example, the use of biochambers maintained the expression of ER for up to 6 weeks *in vivo*. In this technique, breast cells were cultured in Matrigel supplemented with FGF-2 and then implanted in silicon chambers in the groin of SCID mice. Although this model maintained the characteristics of the cells, the use of mice for incubation does not make it an ideal model as it includes the cost and time requirements of *in vivo* models, (Chew et al., 2012).

Despite the different trials to prepare representative intact breast tissue *in vitro*, one of the major limitations remains to be the absence of a complex vascular system. This system is vital for oxygenation, nutrient diffusion, and waste removal. We tried preparing thin tissue slices of 200-300 μm to overcome limitations related to diffusion. However, this was not possible since breast tissue has a very fatty texture. Therefore, the cutting process was done

manually making the tissue thickness unknown, which may limit the diffusion of nutrients to the central portions of the tissue.

Accordingly, current in vitro culture systems without hydrogels have limitations, and organ tissue culture systems could not provide an alternative system to organoids or xenograft culture systems that have been used to investigate the impact of SERMs on normal breast explants, despite maintaining some hormonal responsiveness. The hydrogel system appears to restrain the significant increase in proliferation, indicating that it might be an effective model for further investigation, but additional optimization is required.

In conclusion, the present study demonstrates that culturing intact normal breast tissue poses significant challenges and requires further improvement of culture conditions to maintain original epithelial proliferation and hormone receptors expression. Our data shows that hydrogel culture system can maintain normal breast characteristics better than rotatory and static culture systems for up to 14 days. Overall, all four tested culture systems demonstrated nearly normal tissue morphology, however, more detailed tests revealed transcripyomics and proliferative changes that are of significant concern. For example, in rotatory and static culture systems the expression of the proliferation marker Ki67 was dramatically increased, and RNA sequencing revealed marked upregulation of proliferation-related genes.

# Chapter 6

# Discussion and Future Direction

# 6 Discussion and Future Directions

Breast cancer incidence continues to rise despite the role of mammography on reducing the mortality rate, (Sun et al., 2017). According to the latest statistics by GLOBOCAN on cancer incidence and mortality, breast cancer is the leading cancer worldwide. In women, breast cancer accounts for 24.5% and 15.5% of all cancer incidence and mortality respectively, (Sung et al., 2021).

BC development is a multi-step process involving different cell types, and various risk factors can increase the chances of developing the disease. To fully utilise the factors that contribute to an increased risk of breast cancer, these factors can be combined into risk estimation tools. There are available options including surgery, medication, and lifestyle adjustment for women at high risk to reduce their risk.

In the clinic, mammograms can be used to define the mammographic density (MD), which is an indication of the proportion of these cell types and amount of dense tissue within the entire breast, (Nazari et al., 2018). Women who exhibit higher MD typically harbour less adipose tissue, more epithelial and stromal cells and are placed at higher risk of developing breast cancers, (Nazari et al., 2018). Modification of this risk factor is a key goal of chemoprevention studies, (Boyd et al. 2009; McCormack et al., 2006; Ursin et al., 2003).

In healthy women, increased mammographic density was associated with a higher level of epithelium, stroma (collagen deposition), and immune cells than women with low mammographic density, (Huo et al. 2015). Selective estrogen

receptor modulators (SERMs) such as tamoxifen and raloxifene, as well as the aromatase inhibitors exemestane and anastrozole, are recommended for risk-reducing medications in international guidelines, (National Comprehensive Cancer Network. Breast cancer risk reduction 2020). All of them, however, have been demonstrated to lower the incidence of ER+ breast cancer but not breast mortality rates,

Studies have found that those women who received tamoxifen and who had a least 10% reduction in breast density experienced a 63% reduction in breast cancer risk, (Cuzick et al., 2011). For these patients, the risk is reduced not only during the five years of taking the medication, but also for at least 15 years after cessation. Accordingly, it is the treatment of choice for premenopausal women, as it grants prolonged benefits for more than 20 years after initiation of treatment. Cuzick et al (2015) reported that tamoxifen showed a continued reduction in the incidence of breast cancer; invasive ER-positive cancer, and ductal carcinoma in situ, (Cuzick et al. 2015).

Although the risk is relatively small, there is a reported risk that tamoxifen may develop endometrial cancer in postmenopausal women, (Nelson et al., 2013). Tamoxifen has an agonist effect in certain tissue in women's body (Fisher et al., 1998). It was reported by several studies that longer duration and higher doses of tamoxifen; 20 mg daily for prevention and 40 mg daily for breast cancer treatment, are linked with high risk of developing endometrial diseases by 3-4 fold (Bergman et al., 2000; Fisher et al., 1998). Adjusting the dose and delivery mode is a new approach for existing risk reducing medications to reduce the negative side effects. According to biomarker investigations, the 5 mg of tamoxifen daily is equivalent to 20 mg daily in reducing the progression

of breast cancer, indicating that low-dose tamoxifen might be effective as preventative dose, (DeCensi et al., 2003). In addition, a recent randomized experiment found that lowering the dose and duration of tamoxifen 5 mg daily for 3 years is equivalent to 20 mg daily for 5 years in breast cancer prevention with a fewer side effect, (DeCensi et al. 2019). According to De Lima, et al. (2003), low doses of tamoxifen did not significantly elevate oestradiol blood level, (De Lima et al. 2003). Meanwhile, our data presented an elevation in oestradiol levels after tamoxifen treatment, this finding agrees with a previous study which reported that tamoxifen treatment was associated with an elevation in oestradiol blood levels, (Bernardes et al., 1999). It has been suggested that tamoxifen may decrease breast cancer risk in a dose-dependent manner, (Bernardes et al. 1999; De Lima et al. 2003). The effect of tamoxifen either the 10 mg or 20 mg daily was investigated on normal breast tissue from premenopausal patients. Both doses significantly inhibit proliferating activity of lobular epithelium (Bernardes et al., 1999). Another study examined the impact of different doses of tamoxifen on normal breast tissue samples, the findings of this study reported that Ki67 labelling index expression was reduced in patients receiving 5, 10, or 20 mg/ day of tamoxifen after 50 days of treatment when compared to placebo group. They stated that lowering tamoxifen doses could lessen the negative side effects of tamoxifen when using for prevention of breast cancer, (de Lima et al., 2003).

Another selective estrogen receptor modulator is raloxifene which is only undergone trials in postmenopausal women. In the study of tamoxifen and raloxifene (STAR) trial, they compared raloxifene (60 mg daily for five years) with tamoxifen (20 mg daily for five years), the findings at the 81-month median

follow-up raloxifene was only 76% as effective at reducing ER+ breast cancer compared with tamoxifen. However, long term follow up is highly desirable for raloxifene as prevention as a long-term issue, (Vogel et al., 2010).

Aromatase inhibitors are more effective than either of these agents but can only be used in postmenopausal women as they are ineffective in women with functioning ovaries. Randomized controlled trials of the aromatase inhibitors exemestane and anastrozole have also shown that these medications can reduce the breast cancer risk by 60% at a median 2.5 years of follow- up and by 49% at a median 10.9 years of follow- up, respectively, (Cuzick et al., 2014, 2020; Goss et al., 2011).

Metformin, a diabetic medicine, appears to reduce the risk of cancer, and longer-term usage is associated with a reduced, adjusted odds ratio of 0.63 for developing breast cancer. Bisphosphonates have also been shown to minimize the risk of breast cancer. Retinoids are another class of medicine now being tested in breast cancer prevention studies. Evidence in preclinical studies employing retinoids fenretinide proceeded to a phase III preventive study in the late 1980s, (Bodmer et al., 2010)

In clinical studies, current preventative drugs could not lower ER- breast cancer in BRCA1 mutant carriers, accordingly, the breast cancer prevention in BCRA1 mutation carriers has been controversial. In a phase III randomized study, researchers will see if giving denosumab once every six months for five years reduces the risk of breast cancer in BRCA1 mutation carriers. Anti-progestins (synthetic progesterone) are also being studied for breast cancer prevention, (Phillips et al., 2013; Xu et al., 2015). Determining the appropriate

timing for all of these preventive agents will helps in providing preventive care before age of onset of women at high risk for breast cancer.

Tamoxifen resistance in women was reported and the mechanism of resistance is still unclear. Our main objective was to investigate the molecular mechanism of tamoxifen resistance in healthy women with high risk for breast cancer. Our primary endpoint was to determine the expression of the proliferation marker, Ki67 after tamoxifen treatment. Our finding indicated that Ki67 expression was reduced at protein and RNA levels. These results were validated by investigating the morphometric data that confirmed the reduction in the average acinar area within lobules is correlated with the reduction in Ki67 expression. Despite that we found a significant in Ki67 expression, some patients did not show a reduction and/or had an increase in Ki67 expression. So we needed different approach to group patients in our cohort into different responsive groups. To do this we selected different gene set signatures and generated heatmaps to visualize patients clustering. We found that according to hormone positive luminal cells, patients were grouped into two responsive groups that corresponding with Ki67 expression data. These two responsive groups show a reduction in ER related genes; however, *PRLR, PIP, AGR2*, *ANKRD30A, AZGP1* and *FOXA1* genes were upregulated in the group that did not show a reduction in Ki67 expression. We therefore hypothesized that tamoxifen resistance is promoted by the signalling activity of androgen receptor related pathway. Future work to better develop this hypothesis would be investigating the protein expression of biomarkers related to androgen receptor pathway using an IHC approach, validating the ‘omics’ approaches presented.

We next wanted to compare the effect of tamoxifen on the lobular compartments in both responsive groups by using LCM-SM approach. We showed that collagenous proteins were increased after tamoxifen treatment within the lobules in patients' samples who experienced a reduction in cell proliferation and average acinar area. We suggested that lobule had less epithelial cells and reduction in epithelial cells led to increase collagenous contents. We also found that these samples had significant reduction in PIP protein expression while there was an increase in the protein expression in the other group. As such, it will be interesting in future to map AR and ER genome-wide binding sites, which may provide insight into this phenomenon, as well as enable the development of new therapeutic targets and combinatorial chemopreventive therapies. Future investigation could be carried out on investigation the role of PIP on promoting epithelial cells proliferation. In the future, we could investigate whether androgen receptor related pathway activity in tamoxifen-resistant patients and whether available targeted therapy could enhance patients' responsiveness to tamoxifen treatment.

In chemoprevention clinical trials, the evaluation of the efficacy of preventive medications is critical in order to identify the responders and resistance patients to the treatment. By assessing Ki67 expression level, we were able to identify the effect of tamoxifen on normal breast tissue. Multiple studies have shown an interest in identifying the biomarkers to predict responsiveness. The nipple secretion protein level was evaluated in a preventive study using anti-estrogen preventive therapy. After 3 months of treatment, tamoxifen lowered pS2 and increased Apolipoprotein D (Apo D) levels, (Harding et al., 2000). It is important to mention that Apo D levels is suppressed by estrogen and

stimulated by androgen. These protein levels might be taken into account in our chemoprevention clinical trial of tamoxifen.

Our study had a small sample size for both RNA seq and proteomic analyses. An additional 10 women with paired biopsies have been recruited and analyses are ongoing to try and validate the findings presented here. Translation of these findings to predictive serum or plasma biomarkers will be vital. Avoidance of tamoxifen in women with an estrogen agonist signature in their breast tissue may save them the side effects of treatment. Furthermore, if there is truly an increase in ER negative BC with tamoxifen, as seen in meta-analysis of prevention trials, it is likely that this would be seen in women with such 'agonist' signatures. Predictive biomarkers are vital to enhance the safety of preventive tamoxifen and further investigation from this thesis hold promise in their identification.

References

Reference:


Abe, O. et al. 2011. “Relevance of Breast Cancer Hormone Receptors and Other Factors to the Efficacy of Adjuvant Tamoxifen: Patient-Level Meta-Analysis of Randomised Trials.” *The Lancet* 378(9793): 771–84. http://dx.doi.org/10.1016/S0140-6736(11)60993-8.

Abid, Abubakar, Martin J. Zhang, Vivek K. Bagaria, and James Zou. 2018. “Exploring Patterns Enriched in a Dataset with Contrastive Principal Component Analysis.” *Nature Communications* 9(1). http://dx.doi.org/10.1038/s41467-018-04608-8.

Albright, Craig D., and David G. Kaufman. 2001. “Lactoferrin: A Tamoxifen-Responsive Protein in Normal and Malignant Human Endometrial Cells in Culture.” *Experimental and Molecular Pathology* 70(2): 71–76.

Alonzo-Proulx, Olivier et al. 2015. “Reliability of Automated Breast Density Measurements.” *Radiology* 275(2): 366–76.

De Amicis, Francesca et al. 2010. “Androgen Receptor Overexpression Induces Tamoxifen Resistance in Human Breast Cancer Cells.” *Breast Cancer Research and Treatment* 121(1): 1–11.

Anbazhagan, Ramaswamy et al. 1998. “The Development of Epithelial Phenotypes in the Human Fetal and Infant Breast.” *The Journal of Pathology* 184(2): 197–206. https://onlinelibrary.wiley.com/doi/10.1002/(SICI)1096-9896(199802)184:2%3C197::AID-PATH992%3E3.0.CO;2-J.

Anthis, Nicholas J., and Marion H.E. Kavanaugh-Lynch. 2020. “The Global Challenge to Prevent Breast Cancer: Surfacing New Ideas to Accelerate Prevention Research.” *International Journal of Environmental Research and Public Health* 17(4).

Archer, Maddison et al. 2022. “Immune Regulation of Mammary Fibroblasts and the Impact of Mammographic Density.” : 1–24.

Asselin-Labat, Marie Liesse et al. 2007. “Gata-3 Is an Essential Regulator of Mammary-Gland Morphogenesis and Luminal-Cell Differentiation.” *Nature Cell Biology* 9(2): 201–9.

Astley, Susan M. et al. 2018. “A Comparison of Five Methods of Measuring Mammographic Density: A Case-Control Study.” *Breast Cancer Research* 20(1): 1–13.

Aydiner, Adnan, Abdullah Igci, and Atilla Siran, eds. 2016. *Breast Disease Diagnosis Ana Pathology*. 1st ed. Springer International Publishing.

Bach, Karsten et al. 2017. “Differentiation Dynamics of Mammary Epithelial Cells Revealed by Single-Cell RNA Sequencing.” *Nature Communications* 8(1).

Baker, Joseph C. et al. 2008. “ESR1 Promoter Hypermethylation Does Not Predict Atypia in RPFNA nor Persistent Atypia after 12 Months Tamoxifen

Chemoprevention." *Cancer Epidemiology Biomarkers and Prevention* 17(8): 1884–90.

Basile, Debora et al. 2017. "Androgen Receptor in Estrogen Receptor Positive Breast Cancer: Beyond Expression." *Cancer Treatment Reviews* 61: 15–22. https://linkinghub.elsevier.com/retrieve/pii/S0305737217301512.

Baylis, Françoise. 2020. "The Nf-Core Framework for Community-Curated Bioinformatics Piplines." *Nature Biotechnology* 38(3): 271.

Bergman, Liesbeth et al. 2000. "Risk and Prognosis of Endometrial Cancer after Tamoxifen for Breast Cancer." *The Lancet* 356(9233): 881–87. https://linkinghub.elsevier.com/retrieve/pii/S0140673600026775.

Bernardes, J.R.M. et al. 1999. "Effect of a Half Dose of Tamoxifen on Proliferative Activity in Normal Breast Tissue." *International Journal of Gynecology & Obstetrics* 67(1): 33–38. http://doi.wiley.com/10.1016/S0020-7292%2899%2900092-2.

Bernardo, Gina M. et al. 2010. "FOXA1 Is an Essential Determinant of ERα Expression and Mammary Ductal Morphogenesis." *Development* 137(12): 2045–54. https://journals.biologists.com/dev/article/137/12/2045/43755/FOXA1-is-an-essential-determinant-of-ER-expression.

Bodmer, Michael et al. 2010. "Long-Term Metformin Use Is Associated With Decreased Risk of Breast Cancer." *Diabetes Care* 33(6): 1304–8. https://diabetesjournals.org/care/article/33/6/1304/27526/Long-Term-Metformin-Use-Is-Associated-With.

Boyd, Norman et al. 2009. "Breast-Tissue Composition and Other Risk Factors for Breast Cancer in Young Women: A Cross-Sectional Study." *The Lancet Oncology* 10(6): 569–80. https://linkinghub.elsevier.com/retrieve/pii/S1470204509700786.

Boyd, Norman F. et al. 2002. "Heritability of Mammographic Density, A Risk Factor for Breast Cancer." *The New England Journal of Medicine* 347(12): 886–94.

———. 2005. "Mammographic Breast Density as an Intermediate Phenotype for Breast Cancer." *Lancet Oncology* 6(10): 798–808.

Boyd, Norman F, Lisa J Martin, Martin J Yaffe, and Salomon Minkin. 2011. "Mammographic Density and Breast Cancer Risk: Current Understanding and Future Prospects." *Breast Cancer Research* 13(6): 223. http://breast-cancer-research.biomedcentral.com/articles/10.1186/bcr2942.

Boyer, B., and E. Russ. 2014. "Anatomical-Radiological Correlations: Architectural Distortions." *Diagnostic and Interventional Imaging* 95(2): 134–40. https://linkinghub.elsevier.com/retrieve/pii/S2211568414000047.

Bray, Freddie et al. 2018. "Global Cancer Statistics 2018: GLOBOCAN Estimates of Incidence and Mortality Worldwide for 36 Cancers in 185

Countries.” *CA: A Cancer Journal for Clinicians* 68(6): 394–424.

Breindel, Jerrica L. et al. 2017. “Epigenetic Reprogramming of Lineage-Committed Human Mammary Epithelial Cells Requires DNMT3A and Loss of DOT1L.” *Stem Cell Reports* 9(3): 943–55. http://dx.doi.org/10.1016/j.stemcr.2017.06.019.

Brentnall, Adam R. et al. 2020. “Mammographic Density Change in a Cohort of Premenopausal Women Receiving Tamoxifen for Breast Cancer Prevention over 5 Years.” *Breast Cancer Research* 22(1): 1–10.

Briem, Eirikur et al. 2019. “Application of the D492 Cell Lines to Explore Breast Morphogenesis, EMT and Cancer Progression in 3D Culture.” *Journal of Mammary Gland Biology and Neoplasia* 24(2): 139–47. http://link.springer.com/10.1007/s10911-018-09424-w.

Brisken, Cathrin et al. 1998. “A Paracrine Role for the Epithelial Progesterone Receptor in Mammary Gland Development.” *Proceedings of the National Academy of Sciences of the United States of America* 95(9): 5076–81.

———. 2000. “Essential Function of Wnt-4 in Mammary Gland Development Downstream of Progesterone Signaling.” *Genes and Development* 14(6): 650–54.

———. 2002. “IGF-2 Is a Mediator of Prolactin-Induced Morphogenesis in the Breast.” *Developmental Cell* 3(6): 877–87. https://linkinghub.elsevier.com/retrieve/pii/S1534580702003659.

Brisken, Cathrin, and Bert O’Malley. 2010. “Hormone Action in the Mammary Gland.” *Cold Spring Harbor perspectives in biology* 2(12): a003178.

Brisken, Cathrin, and Renuga Devi Rajaram. 2006. “Alveolar and Lactogenic Differentiation.” *Journal of Mammary Gland Biology and Neoplasia* 11(3–4): 239–48.

Britt, K., A. Ashworth, and M. Smalley. 2007. “Pregnancy and the Risk of Breast Cancer.” *Endocrine Related Cancer* 14(4): 907–33. https://erc.bioscientifica.com/doi/10.1677/ERC-07-0137.

Britt, Kara L., Jack Cuzick, and Kelly Anne Phillips. 2020. “Key Steps for Effective Breast Cancer Prevention.” *Nature Reviews Cancer* 20(8): 417–36. http://dx.doi.org/10.1038/s41568-020-0266-x.

Byng, J. W. et al. 1994. “The Quantitative Analysis of Mammographic Densities.” *Physics in Medicine and Biology* 39(10): 1629–38.

Byrne, Annette T. et al. 2017. “Interrogating Open Issues in Cancer Precision Medicine with Patient-Derived Xenografts.” *Nature Reviews Cancer* 17(4): 254–68. http://www.nature.com/articles/nrc.2016.140.

Carter, Edward P. et al. 2017. “A 3D in Vitro Model of the Human Breast Duct: A Method to Unravel Myoepithelial-Luminal Interactions in the Progression of Breast Cancer.” *Breast Cancer Research* 19(1): 50. http://breast-cancer-

research.biomedcentral.com/articles/10.1186/s13058-017-0843-4.

Cheng, Guojun et al. 2013. “Effects of Short-Term Estradiol and Norethindrone Acetate Treatment on the Breasts of Normal Postmenopausal Women.” *Menopause (New York, N.Y.)* 20(5): 496–503. http://www.ncbi.nlm.nih.gov/pubmed/23615640.

Chew, G. L. et al. 2012. “High and Low Mammographic Density Human Breast Tissues Maintain Histological Differential in Murine Tissue Engineering Chambers.” *Breast Cancer Research and Treatment* 135(1): 177–87.

———. 2013. “Dynamic Changes in High and Low Mammographic Density Human Breast Tissues Maintained in Murine Tissue Engineering Chambers during Various Murine Peripartum States and over Time.” *Breast Cancer Research and Treatment* 140(2): 285–97.

———. 2014. “Effects of Tamoxifen and Oestrogen on Histology and Radiographic Density in High and Low Mammographic Density Human Breast Tissues Maintained in Murine Tissue Engineering Chambers.” *Breast Cancer Research and Treatment* 148(2): 303–14.

———. 2015. “Increased COX-2 Expression in Epithelial and Stromal Cells of High Mammographic Density Tissues and in a Xenograft Model of Mammographic Density.” *Breast Cancer Research and Treatment* 153(1): 89–99.

Ciarloni, Laura, Sonia Mallepell, and Cathrin Brisken. 2007. “Amphiregulin Is an Essential Mediator of Estrogen Receptor α Function in Mammary Gland Development.” *Proceedings of the National Academy of Sciences of the United States of America* 104(13): 5455–60.

Ciupek, Andrew et al. 2015. “Androgen Receptor Promotes Tamoxifen Agonist Activity by Activation of EGFR in ERα-Positive Breast Cancer.” *Breast Cancer Research and Treatment* 154(2): 225–37. http://link.springer.com/10.1007/s10549-015-3609-7.

Clarke, Robert B., Elizabeth Anderson, and Anthony Howell. 2004. “Steroid Receptors in Human Breast Cancer.” *Trends in Endocrinology & Metabolism* 15(7): 316–23. https://linkinghub.elsevier.com/retrieve/pii/S1043276004001523.

Clarke, Robert B., Christopher S Potten, Anthony Howell, and Elizabeth Anderson. 1997. “Dissociation between Steroid Receptor Expression and Cell Proliferation in the Human Breast.” : 4987–91.

Clarke, Robert B, Anthony Howell, Christopher S Potten, and Elizabeth Anderson. 1997. “Dissociation between Steroid Receptor Expression and Cell Proliferation in the Human Breast.” *Cancer Research* 57(22): 4987 LP – 4991. http://cancerres.aacrjournals.org/content/57/22/4987.abstract.

Claus, Elizabith B., Neil J. Rich, and W. Douglas Thomson. 1990. “AGE AT ONSET AS AN INDICATOR OF FAMILIAL RISK OF BREAST CANCER.” *American Journal of Epidemiology* 131(6): 961–72.

https://academic.oup.com/aje/article/109484/AGE.

Collaborative Group on Hormonal Factors in Breast Cancer. 2019. “Type and Timing of Menopausal Hormone Therapy and Breast Cancer Risk: Individual Participant Meta-Analysis of the Worldwide Epidemiological Evidence.” *The Lancet* 394(10204): 1159–68. https://linkinghub.elsevier.com/retrieve/pii/S014067361931709X.

Conneely, Orla M, Biserka Mulac-Jericevic, and John P Lydon. 2003. “Progesterone-Dependent Regulation of Female Reproductive Activity by Two Distinct Progesterone Receptor Isoforms.” *Steroids* 68(10–13): 771–78.

Cowin, Pamela, and John Wysolmerski. 2010. “Molecular Mechanisms Guiding Embryonic Mammary Gland Development.” *Cold Spring Harbor perspectives in biology* 2(6): a003251. http://www.ncbi.nlm.nih.gov/pubmed/2048486.

Crest, Anthony B., Erin J. Aiello, Melissa L. Anderson, and Diana S.M. Buist. 2006. “Varying Levels of Family History of Breast Cancer in Relation to Mammographic Breast Density (United States).” *Cancer Causes and Control* 17(6): 843–50.

Criscitiello, Carmen, Debora Fumagalli, Kamal S. Saini, and Sherene Loi. 2011. “Tamoxifen in Early-Stage Estrogen Receptorpositive Breast Cancer: Overview of Clinical Use and Molecular Biomarkers for Patient Selection.” *OncoTargets and Therapy* 4: 1–11.

Cronin-Fenton, Deirdre P, Per Damkier, and Timothy L Lash. 2014. “Metabolism and Transport of Tamoxifen in Relation to Its Effectiveness: New Perspectives on an Ongoing Controversy.” *Future oncology (London, England)* 10(1): 107–22. http://www.ncbi.nlm.nih.gov/pubmed/24328412.

Cuesta, Rafael, Adi Y. Berman, Anya Alayev, and Marina K. Holz. 2019. “Estrogen Receptor Promotes Protein Synthesis by Fine-Tuning the Expression of the Eukaryotic Translation Initiation Factor 3 Subunit f (EIF3f).” *Journal of Biological Chemistry* 294(7): 2267–78.

Cuzick, J. 2002. “First Results from the International Breast Cancer Intervention Study (IBIS-I): A Randomised Prevention Trial.” *The Lancet* 360(9336): 817–24. https://linkinghub.elsevier.com/retrieve/pii/S0140673602099622.

———. 2011. “Tamoxifen-Induced Reduction in Mammographic Density and Breast Cancer Risk Reduction: A Nested Case-Control Study.” *JNCI Journal of the National Cancer Institute* 103(9): 744–52. https://academic.oup.com/jnci/article-lookup/doi/10.1093/jnci/djr079.

Cuzick, Jack. 2005. “Aromatase Inhibitors for Breast Cancer Prevention.” *Journal of Clinical Oncology* 23(8): 1636–43.

Cuzick, Jack, Andrea DeCensi, et al. 2011. “Preventive Therapy for Breast

Cancer: A Consensus Statement." *The Lancet Oncology* 12(5): 496–503. http://dx.doi.org/10.1016/S1470-2045(11)70030-4.

Cuzick, Jack, Jane Warwick, et al. 2011. "Tamoxifen-Induced Reduction in Mammographic Density and Breast Cancer Risk Reduction: A Nested Case-Control Study." *Journal of the National Cancer Institute* 103(9): 744–52.

Cuzick, Jack et al. 2013. "Selective Oestrogen Receptor Modulators in Prevention of Breast Cancer: An Updated Meta-Analysis of Individual Participant Data." *The Lancet* 381(9880): 1827–34. http://dx.doi.org/10.1016/S0140-6736(13)60140-3.

———. 2014. "Anastrozole for Prevention of Breast Cancer in High-Risk Postmenopausal Women (IBIS-II): An International, Double-Blind, Randomised Placebo-Controlled Trial." *The Lancet* 383(9922): 1041–48. http://dx.doi.org/10.1016/S0140-6736(13)62292-8.

———. 2015. "Tamoxifen for Prevention of Breast Cancer: Extended Long-Term Follow-up of the IBIS-I Breast Cancer Prevention Trial." *The Lancet Oncology* 16(1): 67–75. http://dx.doi.org/10.1016/S1470-2045(14)71171-4.

———. 2020. "Use of Anastrozole for Breast Cancer Prevention (IBIS-II): Long-Term Results of a Randomised Controlled Trial." *The Lancet* 395(10218): 117–22. http://dx.doi.org/10.1016/S0140-6736(19)32955-1.

Dabelow, Adolf. 1957. "Die Milchdrüse." In , 277–485. http://link.springer.com/10.1007/978-3-662-25619-0_2.

Darb-Esfahani, Silvia et al. 2014. "Gross Cystic Disease Fluid Protein 15 (GCDFP-15) Expression in Breast Cancer Subtypes." *BMC cancer* 14: 546. http://www.ncbi.nlm.nih.gov/pubmed/25070172.

Decensi, Andrea et al. 2003. "A Randomized Trial of Low-Dose Tamoxifen on Breast Cancer Proliferation and Blood Estrogenic Biomarkers." *Journal of the National Cancer Institute* 95(11): 779–90. http://www.ncbi.nlm.nih.gov/pubmed/12783932.

DeCensi, Andrea et al. 2019. "Randomized Placebo Controlled Trial of Low-Dose Tamoxifen to Prevent Local and Contralateral Recurrence in Breast Intraepithelial Neoplasia." *Journal of Clinical Oncology* 37(19): 1629–37. https://ascopubs.org/doi/10.1200/JCO.18.01779.

Degnim, Amy C. et al. 2014. "Immune Cell Quantitation in Normal Breast Tissue Lobules with and without Lobulitis." *Breast Cancer Research and Treatment* 144(3): 539–49.

Deome, K. B., L. J. Faulkin, Howard A. Bern, and Phyllis B. Blair. 1959. "Development of Mammary Tumors from Hyperplastic Alveolar Nodules Transplanted into Gland-Free Mammary Fat Pads of Female C3H Mice." *Cancer Research* 19(5): 515.

Dhawan, Andrew et al. 2016. "Mathematical Modelling of Phenotypic Plasticity

and Conversion to a Stem-Cell State under Hypoxia." *Scientific Reports* 6(June 2015): 1–10.

Eigeliene, Natalija et al. 2016. "Effects of Ospemifene, a Novel Selective Estrogen-Receptor Modulator, on Human Breast Tissue Ex Vivo." *Menopause* 23(7): 719–30.

Eigeliene, Natalija, Risto Erkkola, and Pirkko Härkönen. 2016. "Comparison of the Effects of the Selective Estrogen Receptor Modulators Ospemifene, Raloxifene, and Tamoxifen on Breast Tissue in Ex Vivo Culture." In , 327–36. http://link.springer.com/10.1007/978-1-4939-3127-9_25.

Eigeliene, Natalija, Pirkko Härkönen, and Risto Erkkola. 2006. "Effects of Estradiol and Medroxyprogesterone Acetate on Morphology, Proliferation and Apoptosis of Human Breast Tissue in Organ Cultures." *BMC Cancer* 6.

———. 2008. "Effects of Estradiol and Medroxyprogesterone Acetate on Expression of the Cell Cycle Proteins Cyclin D1, P21 and P27 in Cultured Human Breast Tissues." *Cell Cycle* 7(1): 71–80. http://www.tandfonline.com/doi/abs/10.4161/cc.7.1.5102.

Eng, Amanda et al. 2014. "Digital Mammographic Density and Breast Cancer Risk: A Case --- Control Study of Six Alternative Density Assessment Methods." *Breast Cancer Research* 16(5): 439, 1–12.

Euhus, David et al. 2011. "Tamoxifen Downregulates Ets Oncogene Family Members ETV4 and ETV5 in Benign Breast Tissue: Implications for Durable Risk Reduction." *Cancer Prevention Research* 4(11): 1852–62.

Evans, D. G.R. et al. 2004. "A New Scoring System for the Chances of Identifying a BRCA1/2 Mutation Outperforms Existing Models Including BRCAPRO." *Journal of Medical Genetics* 41(6): 474–80.

Fan, Cheng et al. 2006. "Concordance among Gene-Expression–Based Predictors for Breast Cancer." *New England Journal of Medicine* 355(6): 560–69. http://www.nejm.org/doi/abs/10.1056/NEJMoa052933.

Feng, Qin, and Bert W. O'Malley. 2014. "Nuclear Receptor Modulation - Role of Coregulators in Selective Estrogen Receptor Modulator (SERM) Actions." *Steroids* 90: 39–43. http://dx.doi.org/10.1016/j.steroids.2014.06.008.

Feng, Y., D. Manka, K.-U. Wagner, and S. A. Khan. 2007. "Estrogen Receptor-Expression in the Mammary Epithelium Is Required for Ductal and Alveolar Morphogenesis in Mice." *Proceedings of the National Academy of Sciences* 104(37): 14718–23. http://www.pnas.org/cgi/doi/10.1073/pnas.0706933104.

Ferlay, Jacques et al. 2021. "Cancer Statistics for the Year 2020: An Overview." *International Journal of Cancer* 149(4): 778–89.

Ferrarini, Marina et al. 2013. "Ex-Vivo Dynamic 3-D Culture of Human Tissues in the RCCS™ Bioreactor Allows the Study of Multiple Myeloma Biology

and Response to Therapy.” *PLoS ONE*.

Fisher, B et al. 1986. “Adjuvant Chemotherapy with and without Tamoxifen in the Treatment of Primary Breast Cancer: 5-Year Results from the National Surgical Adjuvant Breast and Bowel Project Trial.” *Journal of clinical oncology : official journal of the American Society of Clinical Oncology* 4(4): 459–71. http://www.ncbi.nlm.nih.gov/pubmed/2856857.

Fisher, Bernard et al. 1998. “Tamoxifen for Prevention of Breast Cancer: Report of the National Surgical Adjuvant Breast and Bowel Project P-1 Study and Other National Surgical Adjuvant Breast and Bowel Project Investigators.” 90(18): 1371–88.

Frederiksen, Hanne et al. 2020. “Sex-Specific Estrogen Levels and Reference Intervals from Infancy to Late Adulthood Determined by LC-MS/MS.” *Journal of Clinical Endocrinology and Metabolism* 105(3): 754–68.

Freedman, Andrew N. et al. 2003. “Estimates of the Number of U.S. Women Who Could Benefit from Tamoxifen for Breast Cancer Chemoprevention.” *Journal of the National Cancer Institute* 95(7): 526–32.

Gadkar-Sable, Sushama et al. 2005. “Progesterone Receptors: Various Forms and Functions in Reproductive Tissues.” *Front Biosci* 10(2118): 30.

Gaudet, Mia M. et al. 2011. “Risk Factors by Molecular Subtypes of Breast Cancer across a Population-Based Study of Women 56 Years or Younger.” *Breast Cancer Research and Treatment* 130(2): 587–97.

Ghosh, Karthik et al. 2012. “Tissue Composition of Mammographically Dense and Non-Dense Breast Tissue.” *Breast Cancer Research and Treatment* 131(1): 267–75. http://link.springer.com/10.1007/s10549-011-1727-4.

Ghoussaini, Maya et al. 2012. “Genome-Wide Association Analysis Identifies Three New Breast Cancer Susceptibility Loci.” *Nature Genetics* 44(3): 312–18.

Gilmore, Andrew P, Thomas W Owens, Fiona M Foster, and Jennefer Lindsay. 2009. “How Adhesion Signals Reach a Mitochondrial Conclusion--ECM Regulation of Apoptosis.” *Current opinion in cell biology* 21(5): 654–61. http://www.ncbi.nlm.nih.gov/pubmed/19570669.

Ginsburg, O. M., L. J. Martin, and N. F. Boyd. 2008. “Mammographic Density, Lobular Involution, and Risk of Breast Cancer.” *British Journal of Cancer* 99(9): 1369–74.

Gjerde, J et al. 2008. “Effects of CYP2D6 and SULT1A1 Genotypes Including SULT1A1 Gene Copy Number on Tamoxifen Metabolism.” *Annals of oncology : official journal of the European Society for Medical Oncology* 19(1): 56–61. http://www.ncbi.nlm.nih.gov/pubmed/17947222.

Goeminne, Ludger J. E. et al. 2020. “MSqRob Takes the Missing Hurdle: Uniting Intensity- and Count-Based Proteomics.” *Analytical Chemistry* 92(9): 6278–87. https://pubs.acs.org/doi/10.1021/acs.analchem.9b04375.

References

Goeminne, LudgerJ.E., Kris Gevaert, and Lieven Clement. 2016. “Peptide-Level Robust Ridge Regression Improves Estimation, Sensitivity, and Specificity in Data-Dependent Quantitative Label-Free Shotgun Proteomics.” *Molecular & Cellular Proteomics* 15(2): 657–68. https://linkinghub.elsevier.com/retrieve/pii/S153594762033694X.

Goff, Stephanie L., and David N. Danforth. 2021. “The Role of Immune Cells in Breast Tissue and Immunotherapy for the Treatment of Breast Cancer.” *Clinical Breast Cancer* 21(1): e63–73. https://doi.org/10.1016/j.clbc.2020.06.011.

Goss, Paul E. et al. 2011. “Exemestane for Breast-Cancer Prevention in Postmenopausal Women.” *New England Journal of Medicine* 364(25): 2381–91. http://www.nejm.org/doi/10.1056/NEJMoa1103507.

Graham, J. Dinny et al. 2000. “Nuclear Receptor Conformation, Coregulators, and Tamoxifen-Resistant Breast Cancer.” *Steroids* 65(10–11): 579–84.

Graham, J Dinny, and Christine L Clarke. 1997. “Physiological Action of Progesterone in Target Tissues.” *Endocrine reviews* 18(4): 502–19.

Green, Kelly A., and Jason S. Carroll. 2007. “Oestrogen-Receptor-Mediated Transcription and the Influence of Co-Factors and Chromatin State.” *Nature Reviews Cancer* 7(9): 713–22.

Greendale, G.A. et al. 2003. “Postmenopausal Hormone Therapy and Change in Mammographic Density.” *J.Natl.Cancer Inst.* 95(0027-8874 (Print)): 30–37.

Groom, G. V., and K. Griffiths. 1976. “Effect of The Anti-Oestrogen Tamoxifen on Plasma Levels of Luteinizing Hormone, Follicle-Stimulating Hormone, Prolacin, Oestradiol and Progesterone in Normal Pre-Menopausal Women.” *Journal of Endocrinology* 70(3): 421–28. https://joe.bioscientifica.com/view/journals/joe/70/3/joe_70_3_009.xml.

Hamburger, Anne, and Sydney E. Salmon. 1977. “Primary Bioassay of Human Myeloma Stem Cells.” *Journal of Clinical Investigation* 60(4): 846–54. http://www.jci.org/articles/view/108839.

Hao, Peiqi et al. 2020. “Eukaryotic Translation Initiation Factors as Promising Targets in Cancer Therapy.” *Cell Communication and Signaling* 18(1): 1–20.

Harding, C et al. 2000. “Hormonally-Regulated Proteins in Breast Secretions Are Markers of Target Organ Sensitivity.” *British Journal of Cancer* 82(2): 354–60. http://www.nature.com/doifinder/10.1054/bjoc.1999.0926.

Harper-Wynne, Catherine et al. 2002. “Effects of the Aromatase Inhibitor Letrozole on Normal Breast Epithelial Cell Proliferation and Metabolic Indices in Postmenopausal Women: A Pilot Study for Breast Cancer Prevention.” *Cancer Epidemiology Biomarkers and Prevention* 11(7): 614–21.

Harrison, Rose G., M. J. Greenman, Franklin P. Mall, and C. M. Jackson. 1907.

"Observations of the Living Developing Nerve Fiber." *The Anatomical Record* 1(5): 116–28. http://doi.wiley.com/10.1002/ar.1090010503.

Harvey, H. A., A. Lipton, and D. S. White. 1982. "A Crossover Comparison of Tamoxifen and Aminoglutethimide in Advanced Breast Cancer." *Proceedings of the American Society of Clinical Oncology* Vol. 1(August): 3451–54.

Harvey, Jennifer A. et al. 2008. "Histologic Changes in the Breast with Menopausal Hormone Therapy Use." *Menopause* 15(1): 67–73. https://journals.lww.com/00042192-200815010-00013.

Hattar, Rhonda et al. 2009. "Tamoxifen Induces Pleiotrophic Changes in Mammary Stroma Resulting in Extracellular Matrix That Suppresses Transformed Phenotypes." *Breast Cancer Research* 11(1): 1–16.

Hein, S. M. et al. 2016. "Luminal Epithelial Cells within the Mammary Gland Can Produce Basal Cells upon Oncogenic Stress." *Oncogene* 35(11): 1461–67.

Hofseth, Lorne J. et al. 1999. "Hormone Replacement Therapy with Estrogen or Estrogen plus Medroxyprogesterone Acetate Is Associated with Increased Epithelial Proliferation in the Normal Postmenopausal Breast." *Journal of Clinical Endocrinology and Metabolism* 84(12): 4559–65.

Holliday, D. L. et al. 2013. "The Practicalities of Using Tissue Slices as Preclinical Organotypic Breast Cancer Models." *Journal of Clinical Pathology*.

Holm, Johanna et al. 2017. "Assessment of Breast Cancer Risk Factors Reveals Subtype Heterogeneity." *Cancer Research* 77(13): 3708–17.

Horwitz, Kathryn B., Jeffrey A. Smith, Phillip B. Jewett, and Kathryn B. Horwitz. 1992. "Heterogeneity of Progesterone Receptor Content and Remodeling by Tamoxifen Characterize Subpopulations of Cultured Human Breast Cancer Cells: Analysis by Quantitative Dual Parameter Flow Cytometry." *Cancer Research* 52(3): 593–602.

Hovey, Russell C., Josephine F. Trott, and Barbara K. Vonderhaar. 2002. "Establishing a Framework for the Functional Mammary Gland: From Endocrinology to Morphology." *Journal of Mammary Gland Biology and Neoplasia* 7(1): 17–38.

Howard, B A, and B A Gusterson. 2000. "Human Breast Development." *Journal of mammary gland biology and neoplasia* 5(2): 119–37. http://www.ncbi.nlm.nih.gov/pubmed/11149569.

Howell, Anthony et al. 2014. "Risk Determination and Prevention of Breast Cancer." *Breast Cancer Research* 16(5): 446. http://breast-cancer-research.biomedcentral.com/articles/10.1186/s13058-014-0446-2.

Howlin, Jillian, Jean McBryan, and Finian Martin. 2006. "Pubertal Mammary Gland Development: Insights from Mouse Models." *Journal of Mammary Gland Biology and Neoplasia* 11(3–4): 283–97.

Hughes, E S. 1950. “The Development of the Mammary Gland: Arris and Gale Lecture, Delivered at the Royal College of Surgeons of England on 25th October, 1949.” *Annals of the Royal College of Surgeons of England* 6(2): 99–119. http://www.ncbi.nlm.nih.gov/pubmed/19309885.

Huh, Sung Jin et al. 2016. “The Proliferative Activity of Mammary Epithelial Cells in Normal Tissue Predicts Breast Cancer Risk in Premenopausal Women.” *Cancer Research* 76(7): 1926–34.

Huo, Cecilia W. et al. 2015. “High Mammographic Density Is Associated with an Increase in Stromal Collagen and Immune Cells within the Mammary Epithelium.” *Breast Cancer Research* 17(1): 1–20. http://dx.doi.org/10.1186/s13058-015-0592-1.

Hurd, Cliff et al. 1995. “Hormonal Regulation of the P53 Tumor Suppressor Protein in T47D Human Breast Carcinoma Cell Line.” *Journal of Biological Chemistry* 270(48): 28507–10.

Huss, Fredrik R.M., and Gunnar Kratz. 2001. “Mammary Epithelial Cell and Adipocyte Co-Culture in a 3-D Matrix: The First Step towards Tissue-Engineered Human Breast Tissue.” *Cells Tissues Organs* 169(4): 361–67. https://www.karger.com/Article/FullText/47903.

Infante, Marco et al. 2019. “RANKL/RANK/OPG System beyond Bone Remodeling: Involvement in Breast Cancer and Clinical Perspectives.” *Journal of Experimental and Clinical Cancer Research* 38(1): 1–18.

Ingelman-Sundberg, M. 2005. “Genetic Polymorphisms of Cytochrome P450 2D6 (CYP2D6): Clinical Consequences, Evolutionary Aspects and Functional Diversity.” *The pharmacogenomics journal* 5(1): 6–13. http://www.ncbi.nlm.nih.gov/pubmed/15492763.

Johansson, I et al. 1994. “Genetic Analysis of the Chinese Cytochrome P4502D Locus: Characterization of Variant CYP2D6 Genes Present in Subjects with Diminished Capacity for Debrisoquine Hydroxylation.” *Molecular pharmacology* 46(3): 452–59. http://www.ncbi.nlm.nih.gov/pubmed/7935325.

Jones, Stacey et al. 2021. “Identification of Factors That Influence the Decision to Take Chemoprevention in Patients with a Significant Family History of Breast Cancer: Results from a Patient Questionnaire Survey.” *Breast Cancer Research and Treatment* 187(1): 207–13. https://doi.org/10.1007/s10549-020-06046-x.

Jung, Younghun et al. 2020. “CXCL12γ Induces Human Prostate and Mammary Gland Development.” *The Prostate* 80(13): 1145–56. https://onlinelibrary.wiley.com/doi/10.1002/pros.24043.

Kanaya, Noriko et al. 2019. “Single-Cell RNA-Sequencing Analysis of Estrogen- and Endocrine-Disrupting Chemical-Induced Reorganization of Mouse Mammary Gland.” *Communications Biology* 2(1): 1–15. http://dx.doi.org/10.1038/s42003-019-0618-9.

References

Kaprio, J., A. Alanko, and L. Kivisaari. 1987. “Mammogrpahic Patterns in Twin Pairs Discordant for Breast Cancer.” *British Journal of Radiology* 60(713): 459–62.

Keller, Patricia J. et al. 2012. “Defining the Cellular Precursors to Human Breast Cancer.” *Proceedings of the National Academy of Sciences of the United States of America* 109(8): 2772–77.

Van Keymeulen, Alexandra et al. 2011. “Distinct Stem Cells Contribute to Mammary Gland Development and Maintenance.” *Nature* 479(7372): 189–93.

———. 2015. “Reactivation of Multipotency by Oncogenic PIK3CA Induces Breast Tumour Heterogeneity.” *Nature* 525(7567): 119–23.

Kiechl, Stefan et al. 2017. “Aberrant Regulation of RANKL/OPG in Women at High Risk of Developing Breast Cancer.” *Oncotarget* 8(3): 3811–25.

Kim, Hyun-Ah et al. 2020. “Adding Ovarian Suppression to Tamoxifen for Premenopausal Breast Cancer: A Randomized Phase III Trial.” *Journal of Clinical Oncology* 38(5): 434–43. https://ascopubs.org/doi/10.1200/JCO.19.00126.

Koren, Shany et al. 2015. “PIK3CAH1047R Induces Multipotency and Multi-Lineage Mammary Tumours.” *Nature* 525(7567): 114–18.

Krishnamurthy, Sudha, and Jacques E. Nör. 2013. “Orosphere Assay: A Method for Propagation of Head and Neck Cancer Stem Cells.” *Head & Neck* 35(7): 1015–21. https://onlinelibrary.wiley.com/doi/10.1002/hed.23076.

Kurpios, Natasza A. et al. 2009. “The Pea3 Ets Transcription Factor Regulates Differentiation of Multipotent Progenitor Cells during Mammary Gland Development.” *Developmental Biology* 325(1): 106–21. http://dx.doi.org/10.1016/j.ydbio.2008.09.033.

Lazarus, Philip, Andrea S Blevins-Primeau, Yan Zheng, and Dongxiao Sun. 2009. “Potential Role of UGT Pharmacogenetics in Cancer Treatment and Prevention: Focus on Tamoxifen.” *Annals of the New York Academy of Sciences* 1155: 99–111. http://www.ncbi.nlm.nih.gov/pubmed/19250197.

Lee, Genee Y, Paraic A Kenny, Eva H Lee, and Mina J Bissell. 2007. “Three-Dimensional Culture Models of Normal and Malignant Breast Epithelial Cells.” *Nature Methods*.

Leonhardt, Susan A, Viroj Boonyaratanakornkit, and Dean P Edwards. 2003. “Progesterone Receptor Transcription and Non-Transcription Signaling Mechanisms.” *Steroids* 68(10–13): 761–70.

Levin, Ellis R. 2005. “Integration of the Extranuclear and Nuclear Actions of Estrogen.” *Molecular endocrinology* 19(8): 1951–59.

Li, Christopher I. et al. 2013. “Reproductive Factors and Risk of Estrogen Receptor Positive, Triple-Negative, and HER2-Neu Overexpressing

Breast Cancer among Women 20-44 Years of Age." *Breast Cancer Research and Treatment* 137(2): 579–87.

Li, Sijie et al. 2010. "Immunocytochemical Localization of Sex Steroid Hormone Receptors in Normal Human Mammary Gland." *Journal of Histochemistry and Cytochemistry* 58(6): 509–15.

Li, Tong et al. 2005. "The Association of Measured Breast Tissue Characteristics with Mammographic Density and Other Risk Factors for Breast Cancer The Association of Measured Breast Tissue Characteristics with Mammographic Density and Other Risk Factors for Breast Cancer." 14(February): 343–49.

Lim, Elgene et al. 2009. "Aberrant Luminal Progenitors as the Candidate Target Population for Basal Tumor Development in BRCA1 Mutation Carriers." *Nature Medicine* 15(8): 907–13. http://www.nature.com/doifinder/10.1038/nm.2000.

Lim, Young Chai, Zeruesenay Desta, David A Flockhart, and Todd C Skaar. 2005. "Endoxifen (4-Hydroxy-N-Desmethyl-Tamoxifen) Has Anti-Estrogenic Effects in Breast Cancer Cells with Potency Similar to 4-Hydroxy-Tamoxifen." *Cancer chemotherapy and pharmacology* 55(5): 471–78. http://www.ncbi.nlm.nih.gov/pubmed/15685451.

de Lima, G.R. et al. 2003. "Effects of Low Dose Tamoxifen on Normal Breast Tissue from Premenopausal Women." *European Journal of Cancer* 39(7): 891–98. https://linkinghub.elsevier.com/retrieve/pii/S0959804902005300.

Lindström, Sara et al. 2014. "Genome-Wide Association Study Identifies Multiple Loci Associated with Both Mammographic Density and Breast Cancer Risk." *Nature Communications* 5.

Lovett, Michael, Kyongbum Lee, Aurelie Edwards, and David L. Kaplan. 2009. "Vascularization Strategies for Tissue Engineering." *Tissue Engineering Part B: Reviews* 15(3): 353–70. https://www.liebertpub.com/doi/10.1089/ten.teb.2009.0085.

Lydon, J. P. et al. 1995. "Mice Lacking Progesterone Receptor Exhibit Pleiotropic Reproductive Abnormalities." *Genes and Development* 9(18): 2266–78.

Lyons, Traci R., Pepper J. Schedin, and Virginia F. Borges. 2009. "Pregnancy and Breast Cancer: When They Collide." *Journal of Mammary Gland Biology and Neoplasia* 14(2): 87–98. http://link.springer.com/10.1007/s10911-009-9119-7.

Macias, Hector, and Lindsay Hinck. 2013. "Mammary Gland Development." *Wiley Interdisciplinary Reviews: Developmental Biology* 1(4): 533–57.

Madeddu, Clelia et al. 2014. "Ovarian Hyperstimulation in Premenopausal Women during Adjuvant Tamoxifen Treatment for Endocrine-Dependent Breast Cancer: A Report of Two Cases." *Oncology Letters* 8(3): 1279–82.

References

Mallepell, Sonia, Andrée Krust, Pierre Chambon, and Cathrin Brisken. 2006. "Paracrine Signaling through the Epithelial Estrogen Receptor Alpha Is Required for Proliferation and Morphogenesis in the Mammary Gland." *Proceedings of the National Academy of Sciences of the United States of America* 103(7): 2196–2201. http://www.ncbi.nlm.nih.gov/pubmed/16452162.

Maller, O. et al. 2013. "Collagen Architecture in Pregnancy-Induced Protection from Breast Cancer." *Journal of Cell Science* 126(18): 4108–10. http://jcs.biologists.org/cgi/doi/10.1242/jcs.121590.

Marchese, Stephanie, and Elisabete Silva. 2012. "Disruption of 3D MCF-12A Breast Cell Cultures by Estrogens – An In Vitro Model for ER-Mediated Changes Indicative of Hormonal Carcinogenesis" ed. Irina Agoulnik. *PLoS ONE* 7(10): e45767. https://dx.plos.org/10.1371/journal.pone.0045767.

Martin, Lisa J. et al. 2015. "Serum Lipids, Lipoproteins, and Risk of Breast Cancer: A Nested Case-Control Study Using Multiple Time Points." *Journal of the National Cancer Institute* 107(5): 1–9.

Masood, Shahla. 1992. "Estrogen and Progesterone Receptors in Cytology: A Comprehensive Review." *Diagnostic Cytopathology* 8(5): 475–91. https://onlinelibrary.wiley.com/doi/10.1002/dc.2840080508.

Masters, J R W, J O Drife, and J J Scarisbrick. 1977. "Cyclic Variation of DNA Synthesis in Human Breast Epithelium." *Journal of the National Cancer Institute* 58(5): 1263–65.

Matoska, J, and F Stricker. 1967. "Following Human Tumours in Primary Organ Culture." *Neoplasma* 14(5): 507–19. http://www.ncbi.nlm.nih.gov/pubmed/5583355.

McConnell, James C. et al. 2016. "Increased Peri-Ductal Collagen Micro-Organization May Contribute to Raised Mammographic Density." *Breast Cancer Research* 18(1): 1–17. http://dx.doi.org/10.1186/s13058-015-0664-2.

McCormack, Valerie A., and Isabel Dos Santos Silva. 2006. "Breast Density and Parenchymal Patterns as Markers of Breast Cancer Risk: A Meta-Analysis." *Cancer Epidemiology Biomarkers and Prevention* 15(6): 1159–69.

Meadows, A.L. et al. 2008. "Metabolic and Morphological Differences between Rapidly Proliferating Cancerous and Normal Breast Epithelial Cells." *Biotechnology Progress* 24(2): 334–41. http://doi.wiley.com/10.1021/bp070301d.

Mehasseb, Mohamed Khairy et al. 2011. "Estrogen and Progesterone Receptor Isoform Distribution through the Menstrual Cycle in Uteri with and without Adenomyosis." *Fertility and sterility* 95(7): 2228–35.

Meng, Peng et al. 2019. "Propagation of Functional Estrogen Receptor Positive Normal Human Breast Cells in 3D Cultures." *Breast Cancer*

*Research and Treatment* 176(1): 131–40. http://link.springer.com/10.1007/s10549-019-05229-5.

Michowitz, Moshe, Shlomo Noy, Noam Lazebnik, and David Aladjem. 1985. "Bilateral Breast Cancer." *Journal of Surgical Oncology* 30(2): 109–12. https://onlinelibrary.wiley.com/doi/10.1002/jso.2930300210.

Mihm, M., S. Gangooly, and S. Muttukrishna. 2011. "The Normal Menstrual Cycle in Women." *Animal Reproduction Science* 124(3–4): 229–36. http://dx.doi.org/10.1016/j.anireprosci.2010.08.030.

Milanese, Tia R. et al. 2006. "Age-Related Lobular Involution and Risk of Breast Cancer." *JNCI: Journal of the National Cancer Institute* 98(22): 1600–1607. http://academic.oup.com/jnci/article/98/22/1600/2521878/AgeRelated-Lobular-Involution-and-Risk-of-Breast.

Mohammadi, Hamid, and Erik Sahai. 2018. "Mechanisms and Impact of Altered Tumour Mechanics." *Nature Cell Biology* 20(7): 766–74. https://doi.org/10.1038/s41556-018-0131-2.

Molyneux, Gemma et al. 2010. "BRCA1 Basal-like Breast Cancers Originate from Luminal Epithelial Progenitors and Not from Basal Stem Cells." *Cell Stem Cell* 7(3): 403–17. http://dx.doi.org/10.1016/j.stem.2010.07.010.

Moran, Olivia et al. 2018. "Serum Osteoprotegerin Levels and Mammographic Density among High-Risk Women." *Cancer Causes and Control* 29(6): 507–17. http://dx.doi.org/10.1007/s10552-018-1035-y.

Munne, Pauliina M. et al. 2021. "Compressive Stress-Mediated P38 Activation Required for ERα + Phenotype in Breast Cancer." *Nature Communications* 12(1): 1–17.

Musgrove, E A et al. 1993. "Growth Factor, Steroid, and Steroid Antagonist Regulation of Cyclin Gene Expression Associated with Changes in T-47D Human Breast Cancer Cell Cycle Progression." *Molecular and cellular biology* 13(6): 3577–87.

Musgrove, Elizabeth A, C S Lee, and ROBERT L Sutherland. 1991. "Progestins Both Stimulate and Inhibit Breast Cancer Cell Cycle Progression While Increasing Expression of Transforming Growth Factor Alpha, Epidermal Growth Factor Receptor, c-Fos, and c-Myc Genes." *Molecular and cellular biology* 11(10): 5032–43.

Naipal, Kishan A.T. et al. 2016. "Tumor Slice Culture System to Assess Drug Response of Primary Breast Cancer." *BMC Cancer* 16(1): 78. http://www.biomedcentral.com/1471-2407/16/78.

Nash, Claire E. et al. 2015. "Development and Characterisation of a 3D Multi-Cellular in Vitro Model of Normal Human Breast: A Tool for Cancer Initiation Studies." *Oncotarget* 6(15): 13731–41. https://www.oncotarget.com/lookup/doi/10.18632/oncotarget.3803.

"National Comprehensive Cancer Network. Breast Cancer Risk Reduction."

2020. *National Comprehensive Cancer Network Clinical Parctise Guidelines in Oncology*: 1–59. http://breast-cancer-research.biomedcentral.com/articles/10.1186/s13058-017-0826-5.

Nazarali, Safia A., and Steven A. Narod. 2014. "Tamoxifen for Women at High Risk of Breast Cancer." *Breast Cancer: Targets and Therapy* 6: 29–36.

Nazari, Shayan Shaghayeq, and Pinku Mukherjee. 2018. "An Overview of Mammographic Density and Its Association with Breast Cancer." *Breast Cancer* 25(3): 259–67. https://doi.org/10.1007/s12282-018-0857-5.

Nelson, Heidi D., M.E. Beth Smith, Jessica C. Griffin, and Rongwei Fu. 2013. "Use of Medications to Reduce Risk for Primary Breast Cancer: A Systematic Review for the U.S. Preventive Services Task Force." *Annals of Internal Medicine* 158(8): 604. http://annals.org/article.aspx?doi=10.7326/0003-4819-158-8-201304160-00005.

Nerger, Bryan A., and Celeste M. Nelson. 2019. "3D Culture Models for Studying Branching Morphogenesis in the Mammary Gland and Mammalian Lung." *Biomaterials* 198: 135–45. https://linkinghub.elsevier.com/retrieve/pii/S0142961218306033.

Nguyen, Quy H. et al. 2018. "Profiling Human Breast Epithelial Cells Using Single Cell RNA Sequencing Identifies Cell Diversity." *Nature Communications* 9(1): 1–12.

NICE Guidelines committee. 2019. "Familial Breast Cancer : Classification , Care and Managing Breast Cancer and Related Risks in People with a Family History of Breast Cancer." *National institute for Health and Care Excellence. UK* (June 2013): 47. https://www.nice.org.uk/guidance/cg164.

Niemeier, Leo A. et al. 2010. "Androgen Receptor in Breast Cancer: Expression in Estrogen Receptor-Positive Tumors and in Estrogen Receptor-Negative Tumors with Apocrine Differentiation." *Modern Pathology* 23(2): 205–12.

Oakes, Samantha R. et al. 2008. "The Ets Transcription Factor Elf5 Specifies Mammary Alveolar Cell Fate." *Genes and Development* 22(5): 581–86.

Oh, Hannah et al. 2016. "Expression of Estrogen Receptor, Progesterone Receptor, and Ki67 in Normal Breast Tissue in Relation to Subsequent Risk of Breast Cancer." *npj Breast Cancer* 2(1): 2015–17.

Okamoto, Yoshinori, and Shinya Shibutani. 2019. "Development of Novel and Safer Anti-Breast Cancer Agents, SS1020 and SS5020, Based on a Fundamental Carcinogenic Research." *Genes and Environment* 41(1): 1–6.

Osborne, C K, D H Boldt, G M Clark, and J M Trent. 1983. "Effects of Tamoxifen on Human Breast Cancer Cell Cycle Kinetics: Accumulation of Cells in Early G1 Phase." *Cancer research* 43(8): 3583–85.

http://www.ncbi.nlm.nih.gov/pubmed/6861130.

Oscarson, M, M Hidestrand, I Johansson, and M Ingelman-Sundberg. 1997. "A Combination of Mutations in the CYP2D6*17 (CYP2D6Z) Allele Causes Alterations in Enzyme Function." *Molecular pharmacology* 52(6): 1034–40. http://www.ncbi.nlm.nih.gov/pubmed/9415713.

Osin, P P et al. 1998. "Breast Development Gives Insights into Breast Disease." *Histopathology* 33(3): 275–83. https://onlinelibrary.wiley.com/doi/abs/10.1046/j.1365-2559.1998.00479.x.

Pampaloni, Francesco, Emmanuel G. Reynaud, and Ernst H. K. Stelzer. 2007. "The Third Dimension Bridges the Gap between Cell Culture and Live Tissue." *Nature Reviews Molecular Cell Biology* 8(10): 839–45. http://www.nature.com/doifinder/10.1038/nrm2236.

Pankratz, V. S. et al. 2015. "Predicting the Risk of Mild Cognitive Impairment in the Mayo Clinic Study of Aging." *Neurology* 84(14): 1433–42. http://www.neurology.org/cgi/doi/10.1212/WNL.0000000000001437.

Park, Seong-Eun et al. 2005. "Genetic Deletion of the Repressor of Estrogen Receptor Activity (REA) Enhances the Response to Estrogen in Target Tissues in Vivo." *Molecular and cellular biology* 25(5): 1989–99. http://www.ncbi.nlm.nih.gov/pubmed/15713652.

Parks, R. M., M. G. M. Derks, E. Bastiaannet, and K. L. Cheung. 2018. "Breast Cancer Epidemiology." In *Breast Cancer Management for Surgeons*, Cham: Springer International Publishing, 19–29. http://link.springer.com/10.1007/978-3-319-56673-3_3.

Pavlacky, Jiri, and Jan Polak. 2020. "Technical Feasibility and Physiological Relevance of Hypoxic Cell Culture Models." *Frontiers in Endocrinology* 11. https://www.frontiersin.org/article/10.3389/fendo.2020.00057/full.

Pelissier Vatter, Fanny A. et al. 2018. "High-Dimensional Phenotyping Identifies Age-Emergent Cells in Human Mammary Epithelia." *Cell Reports* 23(4): 1205–19. https://linkinghub.elsevier.com/retrieve/pii/S221112471830490X.

Pentecost, B T, and C T Teng. 1987. "Lactotransferrin Is the Major Estrogen Inducible Protein of Mouse Uterine Secretions." *The Journal of biological chemistry* 262(21): 10134–39. http://www.ncbi.nlm.nih.gov/pubmed/3611056.

Petersen, O W, P E Høyer, and B van Deurs. 1987. "Frequency and Distribution of Estrogen Receptor-Positive Cells in Normal, Nonlactating Human Breast Tissue." *Cancer research* 47(21): 5748–51. http://www.ncbi.nlm.nih.gov/pubmed/3664479.

Peterson, Esther A. et al. 2015. "Amphiregulin Is a Critical Downstream Effector of Estrogen Signaling in ERα-Positive Breast Cancer." *Cancer Research* 75(22): 4830–38.

Phillips, Kelly-Anne et al. 2013. “Tamoxifen and Risk of Contralateral Breast Cancer for BRCA1 and BRCA2 Mutation Carriers.” *Journal of clinical oncology : official journal of the American Society of Clinical Oncology* 31(25): 3091–99. http://www.ncbi.nlm.nih.gov/pubmed/23918944.

Piva, Marco et al. 2014. “Sox2 Promotes Tamoxifen Resistance in Breast Cancer Cells.” *EMBO Molecular Medicine* 6(1): 66–79.

Poole, Elizabeth M. et al. 2011. “Body Size in Early Life and Adult Levels of Insulin-like Growth Factor 1 and Insulin-like Growth Factor Binding Protein 3.” *American Journal of Epidemiology* 174(6): 642–51.

Pradhan-Bhatt, Swati et al. 2014. “A Novel in Vivo Model for Evaluating Functional Restoration of a Tissue-Engineered Salivary Gland.” *The Laryngoscope* 124(2): 456–61. https://onlinelibrary.wiley.com/doi/10.1002/lary.24297.

Prat, Aleix, and Charles M. Perou. 2011. “Deconstructing the Molecular Portraits of Breast Cancer.” *Molecular Oncology* 5(1): 5–23.

Pritchard, K. I. 2001. “Hormone Replacement in Women with a History of Breast Cancer.” *The Oncologist* 6(4): 353–62. http://theoncologist.alphamedpress.org/cgi/doi/10.1634/theoncologist.6-4-353.

Qu, Qing et al. 2015. “USP2 Promotes Cell Migration and Invasion in Triple Negative Breast Cancer Cell Lines.” *Tumor Biology* 36(7): 5415–23. http://link.springer.com/10.1007/s13277-015-3207-7.

Qureshi, Rehana et al. 2020. “The Major Pre-and Postmenopausal Estrogens Play Opposing Roles in Obesity-Driven Mammary Inflammation and Breast Cancer Development.” *Cell metabolism* 31(6): 1154–72.

Raffo, Diego et al. 2013. “Tamoxifen Selects for Breast Cancer Cells with Mammosphere Forming Capacity and Increased Growth Rate.” *Breast Cancer Research and Treatment* 142(3): 537–48.

Rajaram, Renuga Devi, and Cathrin Brisken. 2012. “Paracrine Signaling by Progesterone.” *Molecular and Cellular Endocrinology* 357(1–2): 80–90. http://dx.doi.org/10.1016/j.mce.2011.09.018.

Ramakrishnan, Rathi et al. 2004. “Normal Breast Lobular Architecture in Breast Biopsy Samples from Breast Cancer Cases and Benign Disease Controls.” *Breast cancer research and treatment* 86(3): 259–68. http://www.ncbi.nlm.nih.gov/pubmed/15567942.

Ramakrishnan, Rathi, Seema A. Khan, and Sunil Badve. 2002. “Morphological Changes in Breast Tissue with Menstrual Cycle.” *Modern Pathology* 15(12): 1348–56. http://www.nature.com/doifinder/10.1097/01.MP.0000039566.20817.46.

Rios, Anne C., Nai Yang Fu, Geoffrey J. Lindeman, and Jane E. Visvader. 2014. “In Situ Identification of Bipotent Stem Cells in the Mammary Gland.” *Nature* 506(7488): 322–27.

Rosen, Jeffrey M., and Kevin Roarty. 2014. “Paracrine Signaling in Mammary Gland Development: What Can We Learn about Intratumoral Heterogeneity?” *Breast Cancer Research* 16(1): 1–6.

Ross, R K, A Paganini-Hill, P C Wan, and M C Pike. 2000. “Effect of Hormone Replacement Therapy on Breast Cancer Risk: Estrogen versus Estrogen plus Progestin.” *Journal of the National Cancer Institute* 92(4): 328–32. http://www.ncbi.nlm.nih.gov/pubmed/10675382.

Ruggeri, Bruce A., Faye Camp, and Sheila Miknyoczki. 2014. “Animal Models of Disease: Pre-Clinical Animal Models of Cancer and Their Applications and Utility in Drug Discovery.” *Biochemical Pharmacology* 87(1): 150–61. http://dx.doi.org/10.1016/j.bcp.2013.06.020.

Russo, J., X. Ao, C. Grill, and I.H. Russo. 1999. “Pattern of Distribution of Cells Positive for Estrogen Receptor α and Progesterone Receptor in Relation to Proliferating Cells in the Mammary Gland.” *Breast Cancer Research and Treatment* 53(3): 217–27. http://link.springer.com/10.1023/A:1006186719322.

Russo, Jose, and Irma H. Russo. 2004. “Development of the Human Breast.” *Maturitas* 49(1): 2–15.

Sacco, Riccardo, Paola Causin, Paolo Zunino, and Manuela T Raimondi. 2011. “A Multiphysics/Multiscale 2D Numerical Simulation of Scaffold-Based Cartilage Regeneration under Interstitial Perfusion in a Bioreactor.” *Biomechanics and Modeling in Mechanobiology* 10(4): 577–89. http://www.ncbi.nlm.nih.gov/pubmed/20865436.

Saladores, P et al. 2015. “Tamoxifen Metabolism Predicts Drug Concentrations and Outcome in Premenopausal Patients with Early Breast Cancer.” *The pharmacogenomics journal* 15(1): 84–94. http://www.ncbi.nlm.nih.gov/pubmed/25091503.

Schultz, Jennifer R, Larry N Petz, and Ann M Nardulli. 2003. “Estrogen Receptor Alpha and Sp1 Regulate Progesterone Receptor Gene Expression.” *Molecular and cellular endocrinology* 201(1–2): 165–75. http://www.ncbi.nlm.nih.gov/pubmed/12706304.

Shang, Yongfeng, and Myles Brown. 2002. “Molecular Determinants for the Tissue Specificity of SERMs.” *Science (New York, N.Y.)* 295(5564): 2465–68. http://www.ncbi.nlm.nih.gov/pubmed/11923541.

Shaw, Frances L. et al. 2012. “A Detailed Mammosphere Assay Protocol for the Quantification of Breast Stem Cell Activity.” *Journal of Mammary Gland Biology and Neoplasia* 17(2): 111–17. http://link.springer.com/10.1007/s10911-012-9255-3.

Shaw, Jacqueline A et al. 2002. “Oestrogen Receptors Alpha and Beta Differ in Normal Human Breast and Breast Carcinomas.” *The Journal of Pathology* 198(4): 450–57. https://onlinelibrary.wiley.com/doi/10.1002/path.1230.

Shehata, Mona et al. 2012. “Phenotypic and Functional Characterisation of the Luminal Cell Hierarchy of the Mammary Gland.” *Breast Cancer Research* 14(5): 1–19.

Shiah, Yu Jia et al. 2015. “A Progesterone-CXCR4 Axis Controls Mammary Progenitor Cell Fate in the Adult Gland.” *Stem Cell Reports* 4(3): 313–22. http://dx.doi.org/10.1016/j.stemcr.2015.01.011.

Shoker, Balvinder S et al. 1999. “Estrogen Receptor-Positive Proliferating Cells in the Normal and Precancerous Breast.” *The American journal of pathology* 155(6): 1811–15.

Simões, Bruno M. et al. 2011. “Effects of Estrogen on the Proportion of Stem Cells in the Breast.” *Breast Cancer Research and Treatment* 129(1): 23–35.

Sleeman, Katherine E. et al. 2007. “Dissociation of Estrogen Receptor Expression and in Vivo Stem Cell Activity in the Mammary Gland.” *Journal of Cell Biology* 176(1): 19–26.

Sodunke, T et al. 2007. “Micropatterns of Matrigel for Three-Dimensional Epithelial Cultures.” *Biomaterials* 28(27): 4006–16. https://linkinghub.elsevier.com/retrieve/pii/S0142961207004152.

Sorlie, T et al. 2001. “Gene Expression Patterns of Breast Carcinomas Distinguish Tumor Subclasses with Clinical Implications.” *Proceedings of the National Academy of Sciences of the United States of America* 98(19): 10869–74. http://www.ncbi.nlm.nih.gov/entrez/query.fcgi?cmd=Retrieve&db=PubMed&dopt=Citation&list_uids=11553815%5Cnhttp://www.ncbi.nlm.nih.gov/pmc/articles/PMC58566/pdf/pq010869.pdf.

Sternlicht, Mark D. 2005. “Key Stages in Mammary Gland Development: The Cues That Regulate Ductal Branching Morphogenesis.” *Breast Cancer Research* 8(1): 201. http://breast-cancer-research.biomedcentral.com/articles/10.1186/bcr1368.

Stone, Jennifer et al. 2006. “The Heritability of Mammographically Dense and Nondense Breast Tissue.” *Cancer Epidemiology Biomarkers and Prevention* 15(4): 612–17.

———. 2007. “Mammographic Density and Candidate Gene Variants: A Twins and Sisters Study.” *Cancer Epidemiology Biomarkers and Prevention* 16(7): 1479–84.

Streuli, Charles H. 2016. “Integrins as Architects of Cell Behavior.” *Molecular Biology of the Cell* 27(19): 2885–88.

Sun, Yi Sheng et al. 2017. “Risk Factors and Preventions of Breast Cancer.” *International Journal of Biological Sciences* 13(11): 1387–97.

Sung, Hyuna et al. 2021. “Global Cancer Statistics 2020: GLOBOCAN Estimates of Incidence and Mortality Worldwide for 36 Cancers in 185 Countries.” *CA: A Cancer Journal for Clinicians* 71(3): 209–49.

Tai, Joseph et al. 2014. “Antiproliferation Activity of Devil’s Club (Oplopanax Horridus) and Anticancer Agents on Human Pancreatic Cancer Multicellular Spheroids.” *Phytomedicine* 21(4): 506–14. http://www.ncbi.nlm.nih.gov/pubmed/24215675.

Teng, C. T. 2002. “Lactoferrin Gene Expression Is Estrogen Responsive in Human and Rhesus Monkey Endometrium.” *Molecular Human Reproduction* 8(1): 58–67. https://academic.oup.com/molehr/article-lookup/doi/10.1093/molehr/8.1.58.

Teng, C T et al. 1986. “Purification and Properties of an Oestrogen-Stimulated Mouse Uterine Glycoprotein (Approx. 70 KDa).” *The Biochemical journal* 240(2): 413–22. http://www.ncbi.nlm.nih.gov/pubmed/3814091.

Tharmapalan, Pirashaanthy, Mathepan Mahendralingam, Hal K Berman, and Rama Khokha. 2019. “Mammary Stem Cells and Progenitors: Targeting the Roots of Breast Cancer for Prevention.” *The EMBO Journal* 38(14): 1–19.

Tobon, Hector, and Hernando Salazar. 1975. “Ultrastructure of the Human Mammary Gland. II. Postpartum Lactogenesis.” *The Journal of Clinical Endocrinology & Metabolism* 40(5): 834–44. https://academic.oup.com/jcem/article-lookup/doi/10.1210/jcem-40-5-834.

Tomasek, James J. et al. 2002. “Myofibroblasts and Mechano: Regulation of Connective Tissue Remodelling.” *Nature Reviews Molecular Cell Biology* 3(5): 349–63.

DI Tommaso, Paolo et al. 2017. “Nextflow Enables Reproducible Computational Workflows.” *Nature Biotechnology* 35(4): 316–19.

Den Tonkelaar, I., P. H M Peeters, and P. A H Van Noord. 2004. “Increase in Breast Size after Menopause: Prevalence and Determinants.” *Maturitas* 48(1): 51–57.

Torre, Lindsey A., Rebecca L. Siegel, Elizabeth M. Ward, and Ahmedin Jemal. 2016. “Global Cancer Incidence and Mortality Rates and Trends - An Update.” *Cancer Epidemiology Biomarkers and Prevention* 25(1): 16–27.

Trowell, OA. 1959. “The Culture of Mature Organs in a Systhetic Medium.” *Cell Research* 147: 118–47.

Twigger, Alecia-Jane et al. 2020. “Transcriptional Changes in the Mammary Gland during Lactation Revealed by Single Cell Sequencing of Cells from Human Milk.” *bioRxiv*: 2020.11.06.371443. http://biorxiv.org/content/early/2020/11/27/2020.11.06.371443.abstract.

Tyanova, Stefka, Tikira Temu, and Juergen Cox. 2016. “The MaxQuant Computational Platform for Mass Spectrometry-Based Shotgun Proteomics.” *Nature Protocols* 11(12): 2301–19.

Uebersax, Lorenz et al. 2006. “Effect of Scaffold Design on Bone Morphology In Vitro.” *Tissue Engineering* 12(12): 3417–29.

https://www.liebertpub.com/doi/10.1089/ten.2006.12.3417.

Ursin, Giske et al. 2003. “Mammographic Density and Breast Cancer in Three Ethnic Groups.” *Cancer Epidemiology Biomarkers and Prevention* 12(4): 332–38.

———. 2009. “The Relative Importance of Genetics and Environment on Mammographic Density.” *Cancer Epidemiology Biomarkers and Prevention* 18(1): 102–12.

Vandeweyer, Eric, and Dina Hertens. 2002. “Quantification of Glands and Fat in Breast Tissue: An Experimental Determination.” *Annals of anatomy = Anatomischer Anzeiger : official organ of the Anatomische Gesellschaft* 184(2): 181–84. http://www.ncbi.nlm.nih.gov/pubmed/11936199.

Viale, Giuseppe et al. 2008. “Prognostic and Predictive Value of Centrally Reviewed Ki-67 Labeling Index in Postmenopausal Women with Endocrine-Responsive Breast Cancer: Results from Breast International Group Trial 1-98 Comparing Adjuvant Tamoxifen with Letrozole.” *Journal of Clinical Oncology* 26(34): 5569–75.

Vidi, Pierre-Alexandre, Mina J. Bissell, and Sophie A. Lelièvre. 2012. “Three-Dimensional Culture of Human Breast Epithelial Cells: The How and the Why.” In *Epithelial Cell Culture Protocols*, Humana Press, 193–219. http://link.springer.com/10.1007/978-1-62703-125-7_13.

Visvader, J E, and G H Smith. 2011. “Murine Mammary Epithelial Stem Cells: Discovery, Function, and Current Status.” *Cold Spring Harb. Perspect. Biol.* 3: a004879.

Visvader, Jane E., and John Stingl. 2014. “Mammary Stem Cells and the Differentiation Hierarchy: Current Status and Perspectives.” *Genes and Development* 28(11): 1143–58.

Vogel, Victor G et al. 2010. “Update of the National Surgical Adjuvant Breast and Bowel Project Study of Tamoxifen and Raloxifene (STAR) P-2 Trial: Preventing Breast Cancer.” *Cancer prevention research (Philadelphia, Pa.)* 3(6): 696–706. http://www.ncbi.nlm.nih.gov/pubmed/20404000.

de Vries Schultink, Aurelia H.M. et al. 2015. “Effects of Pharmacogenetics on the Pharmacokinetics and Pharmacodynamics of Tamoxifen.” *Clinical Pharmacokinetics* 54(8): 797–810.

Wallach, Edward E. et al. 1996. “The Effects of Tamoxifen Treatment on the Endometrium.” *Fertility and Sterility* 65(6): 1083–89. https://linkinghub.elsevier.com/retrieve/pii/S0015028216583186.

Walmer, D K, M A Wrona, C L Hughes, and K G Nelson. 1992. “Lactoferrin Expression in the Mouse Reproductive Tract during the Natural Estrous Cycle: Correlation with Circulating Estradiol and Progesterone.” *Endocrinology* 131(3): 1458–66. https://academic.oup.com/endo/article-lookup/doi/10.1210/endo.131.3.1505477.

Wang, Hua et al. 2016. “BRCA1/FANCD2/BRG1-Driven DNA Repair

Stabilizes the Differentiation State of Human Mammary Epithelial Cells." *Molecular Cell* 63(2): 277–92. http://dx.doi.org/10.1016/j.molcel.2016.05.038.

Wang, Xiuli et al. 2010. "A Complex 3D Human Tissue Culture System Based on Mammary Stromal Cells and Silk Scaffolds for Modeling Breast Morphogenesis and Function." *Biomaterials* 31(14): 3920–29. https://linkinghub.elsevier.com/retrieve/pii/S0142961210001663.

Weiss, Linda K et al. 2002. "Hormone Replacement Therapy Regimens and Breast Cancer Risk(1)." *Obstetrics and gynecology* 100(6): 1148–58. http://www.ncbi.nlm.nih.gov/pubmed/12468157.

Willmarth, Nicole E., and Stephen P. Ethier. 2006. "Autocrine and Juxtacrine Effects of Amphiregulin on the Proliferative, Invasive, and Migratory Properties of Normal and Neoplastic Human Mammary Epithelial Cells." *Journal of Biological Chemistry* 281(49): 37728–37. http://dx.doi.org/10.1074/jbc.M606532200.

Woodward, Emma R., Elke M. Van Veen, and D. Gareth Evans. 2021. "From BRCA1 to Polygenic Risk Scores: Mutation-Associated Risks in Breast Cancer-Related Genes." *Breast Care* 16(3): 202–13.

Work, M. E. et al. 2014. "Reproductive Risk Factors and Oestrogen/Progesterone Receptor-Negative Breast Cancer in the Breast Cancer Family Registry." *British Journal of Cancer* 110(5): 1367–77. http://dx.doi.org/10.1038/bjc.2013.807.

Wuidart, Aline et al. 2016. "Quantitative Lineage Tracing Strategies to Resolve Multipotency in Tissue-Specific Stem Cells." *Genes and Development* 30(11): 1261–77.

Xu, Lingyun et al. 2015. "Tamoxifen and Risk of Contralateral Breast Cancer among Women with Inherited Mutations in BRCA1 and BRCA2: A Meta-Analysis." *Breast cancer (Tokyo, Japan)* 22(4): 327–34. http://www.ncbi.nlm.nih.gov/pubmed/26022977.

Xu, Tao et al. 2019. "Osteoglycin (OGN) Inhibits Cell Proliferation and Invasiveness in Breast Cancer via PI3K/Akt/MTOR Signaling Pathway." *OncoTargets and Therapy* 12: 10639–50.

Yanaihara, Atsushi, Yoshiro Toma, Hiroshi Saito, and Takumi Yanaihara. 2000. "Cell Proliferation Effect of Lactoferrin in Human Endometrial Stroma Cells." *MHR: Basic science of reproductive medicine* 6(5): 469–73. https://academic.oup.com/molehr/article-lookup/doi/10.1093/molehr/6.5.469.

Yu, Ji Hoon et al. 2013. "Breast Diseases during Pregnancy and Lactation." *Obstetrics & Gynecology Science* 56(3): 143. https://synapse.koreamed.org/DOIx.php?id=10.5468/ogs.2013.56.3.143.

Zhang, B., Daoda Chen, Guobin Wang, and Yihua Wu. 2003. "Effects of Estradiol and Tamoxifen on Proliferation of Human Breast Cancer Cells

and Human Endometrial Cells." *Journal of Huazhong University of Science and Technology. Medical sciences = Hua zhong ke ji da xue xue bao. Yi xue Ying De wen ban = Huazhong keji daxue xuebao. Yixue Yingdewen ban* 23(3): 283–85.

Zhu, Jieqing, Gaofeng Xiong, Christine Trinkle, and Ren Xu. 2014. "Integrated Extracellular Matrix Signaling in Mammary Gland Development and Breast Cancer Progression." *Histology and Histopathology* 29(9): 1083–92.

Zhu, Wenting, and M Nelson. 2013. "Adipose and Mammary Epithelial Tissue Engineering." *Breast* (September): 1–6.

Ziv, Elad, John Shepherd, and Karla Kerlikowske. 2003. "BRIEF Mammographic Breast of Breast Cancer Women in the San Francisco Mam-." *Journal of the National Cancer Institute* 95(7): 2–4.